AD_____

Award Number: DAMD17-97-1-7068

TITLE: Amphiphysin and Breast Cancer

PRINCIPAL INVESTIGATOR: Pietro DeCamilli, M.D.

CONTRACTING ORGANIZATION: Yale University School of Medicine
New Haven, Connecticut 06520-8047

REPORT DATE: October 1999

TYPE OF REPORT: Final

PREPARED FOR: U.S. Army Medical Research and Materiel Command
Fort Detrick, Maryland 21702-5012

REPORT DOCUMENTATION PAGE | OMB No. 074-0188

1. AGENCY USE ONLY (Leave blank)	2. REPORT DATE	3. REPORT TYPE AND DATES COVERED
	October 1999	Final (1-Oct-97 - 30-Sep-99)

4. TITLE AND SUBTITLE
Amphiphysin and Breast Cancer

5. FUNDING NUMBERS
DAMD17-97-1-7068

6. AUTHOR(S)
Pietro DeCamilli, M.D.

7. PERFORMING ORGANIZATION NAME(S) AND ADDRESS(ES)
Yale University School of Medicine
New Haven, Connecticut 06520-8047

E-MAIL:
pietrodecamilli@yale.edu

8. PERFORMING ORGANIZATION REPORT NUMBER

9. SPONSORING / MONITORING AGENCY NAME(S) AND ADDRESS(ES)
U.S. Army Medical Research and Materiel Command
Fort Detrick, Maryland 21702-5012

10. SPONSORING / MONITORING AGENCY REPORT NUMBER

11. SUPPLEMENTARY NOTES
This report contains colored photos

12a. DISTRIBUTION / AVAILABILITY STATEMENT
Approved for public release; distribution unlimited

12b. DISTRIBUTION CODE

13. ABSTRACT ***(Maximum 200 Words)***

Amphiphysin I is a 128 kD nerve terminal protein with a role in clathrin mediated endocytosis, actin function and intracellular signaling. Amphiphysin was first identified as an autoantigen by our laboratory in breast cancer patients with the neurological disease Stiff-man syndrome. We have tested a large case load of patients with neurological disease for autoantibodies by immunocytochemistry and Western blotting. Thirteen patients have tested positive for amphiphysin autoantibodies and cancer. In two cases, the autoantibodies were discovered before the cancer, prompting a search for occult neoplasia. We tested breast tumors for the presence of amphiphysin by RT-PCR and Western blotting. We cloned an alternatively spliced isoform of amphiphysin I from a breast cancer cell line and demonstrated low level expression in several non-neuronal tissues and enhanced expression in several breast cancers. We have also found that amphiphysin interacts with members of the cyclin dependent kinase gene family and may be involved in cell cycle control. Finally, we have produced an amphiphysin knock-out mouse and are currently analyzing the phenotype.

14. SUBJECT TERMS
Breast Cancer

15. NUMBER OF PAGES
116

16. PRICE CODE

17. SECURITY CLASSIFICATION OF REPORT	18. SECURITY CLASSIFICATION OF THIS PAGE	19. SECURITY CLASSIFICATION OF ABSTRACT	20. LIMITATION OF ABSTRACT
Unclassified	Unclassified	Unclassified	unlimited

FOREWORD

Opinions, interpretations, conclusions and recommendations are those of the author and are not necessarily endorsed by the U.S. Army.

___ Where copyrighted material is quoted, permission has been obtained to use such material.

___ Where material from documents designated for limited distribution is quoted, permission has been obtained to use the material.

___ Citations of commercial organizations and trade names in this report do not constitute an official Department of Army endorsement or approval of the products or services of these organizations.

X_ In conducting research using animals, the investigator(s) adhered to the "Guide for the Care and Use of Laboratory Animals," prepared by the Committee on Care and use of Laboratory Animals of the Institute of Laboratory Resources, national Research Council (NIH Publication No. 86-23, Revised 1985).

X_ For the protection of human subjects, the investigator(s) adhered to policies of applicable Federal Law 45 CFR 46.

X_ In conducting research utilizing recombinant DNA technology, the investigator(s) adhered to current guidelines promulgated by the National Institutes of Health.

X_ In the conduct of research utilizing recombinant DNA, the investigator(s) adhered to the NIH Guidelines for Research Involving Recombinant DNA Molecules.

X_ In the conduct of research involving hazardous organisms, the investigator(s) adhered to the CDC-NIH Guide for Biosafety in Microbiological and Biomedical Laboratories.

1/25/2000 Pietro De Camilli
Date PIETRO DE CAMILLI PI - Signature

TABLE OF CONTENTS

INTRODUCTION

Breast cancer is a relatively common disease that is estimated to affect 1 in 10 women at some point during life (Seidman, H., et al., *CA Cancer J.*, 35(1):36-56, 1985). Among the many women who suffer from breast cancer, a small number also suffer from autoimmune conditions related to the cancer. Stiff Man Syndrome (SMS) is a rare neurological disorder characterized by progressive rigidity of the body musculature with superimposed painful spasms. (Lorish, T.R., et al., *Mayo Clin. Proc.* 64:629-636, 1989). Work from our laboratory has demonstrated that SMS and a variety of other related conditions can be autoimmune diseases associated with breast cancer (Folli, F., et. al. *New Engl. J. Med.* 328:546-551, 1993). We have identified the synaptic protein amphiphysin as a major target of autoantibodies in patients with SMS and breast cancer. Amphiphysin is implicated in the cellular prcesses of clathrin mediated endocytosis (Shupliakov, O., et al., *Science*. 276:259-63, 1997), actin function (Mundigl, O., et al., *J. Neurosci.* 18: 93-103, 1997) and intracellular signaling (Pawson, T., *Nature*. 373: 573-80, 1995, Leprince, C., et al., *J. Biol. Chem.* 272: 15101-15105, 1997, Sakamuro, D., et al., *Nature Genet.* 14: 69-77. 1997). The goal of this project is to explore the relationship between breast cancer, autoimmunity to amphiphysin and neurological disease. During the period of study supported by the U.S. Army Medical Research and Material Command, we have made progress in the understanding the function of the protein amphiphysin and how it may contribute to the biology of cancer. It is our hope that this progress will lead to better understanding of the cellular processes that lead to cancer, and aid in early detection of breast cancer, at least in a subpopulation of patients.

BODY

We have proceeded according to the plan outlined in the original grant application. This report will be organized around the tasks indicated in the Statement of Work (SOW) in the applications which were as follows:

Year 1

1. Collect and screen a large population of breast cancer tissues and cell lines for the expression of amphiphysin or amphiphysin-108.

2. Collect and screen a large population of breast cancer patients for autoantibodies against amphiphysin.

*3. Characterize amphiphysin-108 by peptide mapping, RNAse protection assay and FISH.

4. Construct a cDNA library from HS578T cell line and screening by nucleic acid hybridization or antibodies.

*5. Protein microsequencing of 108 kD band.

Year 2

(Continue 1 and 2 above)

*3. Study the oncogenic potential of amphiphysin or amphiphysin-108 (focus forming assay, soft agar growth).

*4. Production of transgenic mice for amphiphysin or amphiphysin-108 (minigene construct, pronuclear microinjection, PCR and/or Southern blotting screening, begin the characterization of transgenic mice for copy number and expression).

Year 3
(Complete 1 and 2 from year 1)

*3. Complete the study for the oncogenic potential of amphiphysin or amphiphysin-108 (tumorogenicity assay in nude mice).

*4. Complete the study on transgenic mice for amphiphysin or amphiphysin-108 (complete the characterization of transgenic mice for the appearance of mammary tumors in the different expression classes).

This Statement of Work was modified based on:
a. the deletion of a third year of support
b. new data that became available during the time of the allocation
Those tasks that were modified are indicated with an asterisk (*) above and were modified as detailed below.

Collect and screen a large population of breast cancer tissues and cell lines for the expression of amphiphysin or amphiphysin-108.

We have extensively searched for the presence of amphiphysin protein family members expressed in human and rat tissues. In a preliminary screening, we had not detected amphiphysin in normal tissue using Western blot, Northern blot, and immunofluorescence of cultured cells and tissues (De Camilli, P., et al., *J. Exp. Med.* 178: 2219-2223, 1993) However, we subsequently found high level expression of amphiphysin I by Western blotting breast cancer tissue of a patient affected by a neurological autoimmune paraneoplastic syndrome. This amphiphysin I immunoactivity migrated as two major isoforms on SDS-PAGE gels. One of them had the same electrophorectic mobility of brain amphiphysin I. The other had a faster mobility with an apparent molecular weight of about 108 kDa. These data suggested that the cancer tissue of paraneoplastic patients may ectopically express amphiphysin. Second, they also raised the possibility that such tissue may express an abnormal form of amphiphysin. In an effort to characterize the expression of amphiphysin in breast tissue in more detail, we improved our detection technique and screen a number of breast cancer cell lines by Western blot. We found that two breast cancer cell lines expressed amphiphysin I with a molecular weight of 108 kD. In the meantime, we generated a battery of high affinity monoclonal antibodies and used these antibodies to further improve our detection of amphiphysin I expression in breast tissue. Using these antibodies, we were able to detect that low levels of the 108 kDa isoform of amphiphysin I are expressed by normal human

breast tissue. In addition, we found that the expression level of amphiphysin I is enhanced in a number of breast cancer tissues (Floyd, S., et al., *Molecular Medicine* 4(1):29-39, 1998). We draw two conclusions from these data: The first is that amphiphysin I is expressed at low levels in normal breast tissue, and has an increased level of expression in a variety of neoplastic tissues. This suggests a potential link between increased cell proliferation and the function of amphiphysin I isoforms. The second is that neurological autoimmune conditions most likely result from the abnormal expression of amphiphysin in cancer tissue. Thus, as proposed for other paraneoplastic autoimmune neurological conditions, it is the expression of a neuronal antigen in the cancer tissue that triggers the neurological condition.

Collect and screen a large population of breast cancer patients for autoantibodies against amphiphysin.

We have continued to screen a large case load of over 800 patients with neurological syndromes for the presence of autoantibodies directed against neuronal proteins. In the time period of the grant award, we have identified thirteen new cases of amphiphysin autoimmunity associated with cancer. In some instances, neurological symptoms preceded the detection of breast cancer. During the period of the award, we have identified anti-amphiphysin antibodies in two patients with neurological disease before the detection of a tumor. The identification of the autoantibodies prompted an extensive search for occult malignancy, and in both cases, a breast tumor was subsequently found.

Construct a cDNA library from HS578T cell line and screening by nucleic acid hybridization or antibodies.

In order to characterize this amphiphysin I isoform, we generated a cDNA library from the human breast cancer cell line HS578T. We then cloned amphiphysin I from this cDNA library and found that the 108 kDa amphiphysin I isoform represents an alternative splice variant of the typical neuronal amphiphysin which is different in molecular weight because of the lack of a 42 amino acid insert. Using RT-PCR, we were able to determine that several non-neuronal tissues, including normal human breast tissue and several breast tumors expressed this splice isoform (Floyd, S., et al., *Molecular Medicine* 4(1):29-39, 1998). The cloning of the splice isoform from the cDNA library and demonstration that it encodes the 108 kD protein seen in breast tumors and breast cancer cell lines eliminated the need to carry out tasks 3 (Characterize amphiphysin-108 by peptide mapping, RNAse protection assay and FISH) and 5 (Protein microsequencing of 108 kD band) of Year 1.

Study the oncogenic potential of amphiphysin or amphiphysin-108 (focus forming assay, soft agar growth)

As of today we have not obtained conclusive data concerning a potential role of amphiphysin in the control of cell proliferation. Overexpression in a variety of cell lines did not cause an obvious increase in the proliferation of these cells. The fact that expression of amphiphysin did not have a detectable affect on the proliferation of cells

made studies such as soft agar growth, tumorogenicity in nude mice and transgenic animals unlikely to yield a useful result. Data from study of amphiphysin homologues in yeast led us to a new line of investigation. The yeast homologue of amphiphysin, RVS167, is phosphorylated by the PHO85 kinase, an enzyme implicated in the regulation of cell entry into a stationary growth phase after exposure to starvation conditions (Lee, J., et al., *Curr Biol* 8(24):1310-21, 1998). PHO85 belongs to the cyclin dependent kinase family of proteins. These proteins play a major role in the control of cell cycle progression and cell proliferation control. We hypothesized that genes of the amphiphysin family might interact with these cell cycle control genes in mammalian cells, and that this interaction might give clues to a role for amphiphysin in cell proliferation control. We further hypothesized that abnormal function of amphiphysin might interfere with normal cell cycle progression and therefore lead to cancer. Since cdk5 is a mammalian homologue of PHO85, we have investigated the interaction of amphiphysin I with the cdk5 kinase complex. We have found that indeed amphiphysin binds to and is phosphorylated by the cdk5 kinase complex (figures 1-5). We are currently investigating the physiological function of this reaction.

Production of transgenic mice for amphiphysin or amphiphysin-108 (minigene construct, pronuclear microinjection, PCR and/or Southern blotting screening, begin the characterization of transgenic mice for copy number and expression).

As detailed above, the lack of a direct proliferative affect of amphiphysin expression in cell lines made the production of transgenic mice over expressing amphiphysin an unfeasible experiment. In order to better explore the potential role of amphiphysin in mammary tumorogenesis, we modified this task to produce mice in which the expression of amphiphysin I is destroyed by germ line homologous recombination. We have succeeded in producing a line of mice in which amphiphysin I is not expressed (fig. 6-7). We have begun the characterization of this mouse line. To date, the mice are born normally and live to 7-9 weeks when they suddenly die. We are investigating the cause of this sudden death, and screening the mice closely for the appearance of any abnormal mammary tissue.

KEY RESEARCH ACCOMPLISHMENTS

-Amphiphysin I is expressed at low levels outside the nervous system
-Normal breast tissue expresses low levels of amphiphysin I
-Amphiphysin I is overexpressed in some breast tumors and breast cancer cell lines
-A splice variant of amphiphysin I missing a 42 amino acid insert is the predominant isoform of amphiphysin that is expressed outside the nervous system.
-Amphiphysin I interacts with and is phosphorylated by the cdk5 kinase complex
-Mice that lack expression of amphiphysin I apparently develop normally until age 7-9 weeks when they suddenly die.

REPORTABLE OUTCOMES

Publications:
(Reprints attached in **APPENDIX A**)

1. Solimena M, Dirkx R, Bulter M, Hermel JM, Guernaccia J, Marek K, David C, and De Camilli P. Stiff-man syndrome and glutamic acid decarboxylase: an updated view. GABA: Receptor, transporter and metabolism. Basel, Switzerland: Birkhauser Verlag, 1996.

2. Butler MH, David C, Ochoa G, Freyberg Z, Daniell L, Grabs D, Cremona O, De Camilli P. Amphiphysin II (SH3P9; BIN1), a member of the amphihpysin/Rvs family, is concentrated in the cortical cytomatrix of axon initial segments and nodes of Ranvier in brain and around T tubules in skeletal muscle. J. Cell Biology 1997;137:1355-1367.

3. Floyd S, Butler MH, Cremona O, David C, Freyberg Z, Zhang X, Solimena M, Tokunaga A, Ishizu H, Tsutsui K, and De Camilli P. Expression of amphiphysin I, an autoantigen of paraneoplastic neurological syndromes, in breast cancer. Molecular Medicine 1998;4:29-39.

4. Floyd S and De Camilli P. Endocytosis proteins and cancer: a potential link? Trends in Cell Biology 1998;8:299-301.

5. Rosin L, De Camilli P, Butler MH, Solimena M, Schmitt HP, Morgenthaler N, Meinck HM. Stiff-man syndrome in a woman with breast cancer. Neurology 1998;50:94-98.

6. Saiz A, Dalmau J, Butler MH, Chen Q, Delattre JY, De Camilli P, Graus F. Anti-amphiphysin I antibodies in patients with paraneoplastic neurological disorders associated with small cell lung carcinoma. J. Neurol. Neurosurg. Psychiatry 1999;66:214-217.

7. Ferracci F, Fassetta G, Butler MH, Floyd S, Solimena M, and De Camilli P. A novel antineuronal antibody in a motor neuron syndrome associated with breast cancer. Neurology 1999;53:852-855.

8. Schmierer K, Valdueza JM, Bender A, De Camilli P, David C, Solimena M and Zschenderlein R. Atypical stiff-person syndrome with spinal MRI findings, amphiphysin autoantibodies, and immunosuppression. Neurology 1998;51:250-252.

9. Ringstad N, Gad H, Low P, Di Paolo G, Brodin L, Shupliakov O, and De Camilli P. Endophilin/SH3P4 is required for the transition from early to late stages in clathrin-mediated synaptic vesicle endocytosis. Neuron 1999;24:143-154.

10. Takei K, Slepnev V, Haucke V, and De Camilli P. Functional partnership between amphiphysin and dynamin in clathrin-mediated endocytosis. Nature Cell Biol. 1999;1:33-39.

11. Chen H, Fre S, Slepnev VI, Capua MR, Takei K, Butler MH, De Fiore PP, and De Camilli, P. Epsin is an EH-domain-binding protein implicated in clathrin-mediated endocytosis. Nature 1998;394:793-797.

12. Takei K, Haucke V, Slepnev V, Farsad K, Salazar M, Chen H, and De Camilli P. Generation of Coated intermediates of clathrin-mediated endocytosis on protein-free liposomes. Cell 1999;94:131-141.

Meeting Abstracts
(Copies included in **APPENDIX A**)

American Society for Cell Biology 37th Annual Meeting, 1997

Keystone Symposium: Specificity in Signal Transduction & Oncogene Networks in Signal Transduction, 1999

Degrees Obtained

Ph.D. expected May, 2000, Niels Ringstad

Ph.D. expected May, 2000, Hong Chen

Ph.D. expected May, 2000, Gian-Carlo Ochoa

CONCLUSIONS

Breast cancer is a major health problem for millions of women annually. For a small subset of these patients, autoimmune neurological disease further complicates the clinical picture. Work from our laboratory has identified the protein amphiphysin I as an autoantigen in paraneoplastic autoimmune neurological syndromes associated with breast cancer. We have determined that this protein is overexpressed in some breast tumors, and that this leads to autoimmune response in some patients. Based on preliminary data concerning interaction with key cell cycle regulatory genes, we believe that amphiphysin may play a role in the biology of cancer through interaction with the set of genes that control cell proliferation. We have generated knock-out mice that lack amphiphysin and appear to develop normally until early adulthood (7-9 weeks), when they suddenly die. Future studies of these mice and of cell lines derived from them will further our understanding of the function of amphiphysin and hopefully shed light on the specific role amphiphysin may play in the development of cancer and the steps that lead to autoimmune response in some patients.

REFERENCES

Seidman, H., et al., *CA Cancer J.*, 35(1):36-56, 1985.

Lorish, T.R., et al., *Mayo Clin. Proc.* 64:629-636, 1989.

Folli, F., et. al., *New Engl. J. Med.* 328:546-551, 1993.

De Camilli, P., et al., *J. Exp. Med.* 178: 2219-2223, 1993.

Floyd, S., et al., *Molecular Medicine* 4(1):29-39, 1998.

Lee, J., et al., *Curr Biol* 8(24):1310-21, 1998.

Mundigl, O., et al., *J. Neurosci.* 18: 93-103, 1997.

Shupliakov, O., et al., *Science*. 276:259-63, 1997

Pawson, T., *Nature*. 373: 573-80, 1995.

Leprince, C., et al., *J. Biol. Chem.* 272: 15101-15105, 1997.

Sakamuro, D., et al., *Nature Genet.* 14: 69-77. 1997.

APPENDIX A

Publication Reprints

Meeting Abstract Copies

GABA: Receptors, Transporters and Metabolism
ed. by C. Tanaka & N.G. Bowery

STIFF-MAN SYNDROME AND GLUTAMIC ACID DECARBOXYLASE: AN UPDATED VIEW.

M. Solimena*, R. Dirkx*, M. Butler‡, J.-M. Hermel*, J. Guernaccia$^{\Delta}$, K. Marek$^{\Delta}$, C. David‡ and P. De Camilli‡.

*Department of Internal Medicine, Section of Endocrinology, ‡ Department of Cell Biology and the Howard Hughes Medical Institute, Department of Neurology$^{\Delta}$, Yale University School of Medicine, New Haven, CT 06510.

Summary: Evidence collected during the last decade suggests that Stiff-Man syndrome (SMS), a neuromuscular disorder characterized by continuous rigidity of the body musculature, results from an autoimmune impairment of inhibitory neurons controlling motor neuron activity. The dominant autoantigen is glutamic acid decarboxylase (GAD), the enzyme responsible for the synthesis of GABA. In this chapter, we summarize some of the relevant features of SMS and GAD, with an emphasis on the contribution of our group to this field.

Clinical Features of Stiff-Man Syndrome

Stiff-man syndrome (SMS) is a rare disease of the central nervous system characterized by muscle rigidity and painful spasms of limbs, trunk and abdominal muscles (1-5). The disease develops in adulthood and affects mostly women. SMS resembles a chronic form of tetanus, but trismus does not occur. Electromyography shows persistent motor unit activity which is, however, indistinguishable electrophysiologically from normal voluntary muscle activity except that patients are not able to relax. Rigidity and spasms result from the simultaneous activation of agonist and antagonist muscles, caused by the continuous firing of α-motor neurons. An imbalance between noradrenergic and GABA-ergic pathways involved in the control of muscle tone may be at the origin of the disease (5). Most patients respond to pharmacological treatments with high doses of drugs which potentiate the action of GABA, such as benzodiazepines, baclofen or sodium valproate. These pharmacological treatments, however, do not affect the slowly progressive course of the disease. Patients may be eventually bedridden and respiratory failure or sudden death has been reported (7). Neuropathological studies of SMS have been meager, and, when available, have shown no specific abnormalities. In a few cases, however, evidence of a perivascular lymphocytic infiltration has been observed. Because of its rarity, of the subjective nature of the symptoms and the lack of confirmatory laboratory tests, SMS often remained undiagnosed for a

long period of time. In many cases, SMS patients are erroneously diagnosed as hysteric (8). Depression, dysphoria, unusual personality traits and paroxysmal fear when crossing a free space unaided are common in SMS patients, even beyond what one may expect as a natural reaction to the difficulties of living with this unusual syndrome (5, 4, 9).

Evidence for an Autoimmune Pathogenesis of Stiff-man Syndrome

Increasing evidence suggests that at least in the majority of cases SMS has an autoimmune pathogenesis (10, 11). Key observations in support of this hypothesis include:

- presence of high titer autoantibodies directed against presynaptic antigens [glutamic acid decarboxylase (GAD), amphiphysin] in the serum (12-16).
- presence of anti-GAD or anti-amphiphysin autoantibodies in the patients' cerebrospinal fluid at concentrations which suggest their production within the central nervous system (12-14).
- frequent occurence of oligoclonal IgG in the cerebrospinal fluid, a general indication of IgG production within the central nervous system (12-14).
- high prevalence of organ specific-autoimmune diseases among SMS patients positive for anti-GAD autoantibodies and their relatives (4, 12, 13).
- presence of breast cancer among SMS patients positive for anti-amphiphysin autoantibodies (paraneoplastic SMS) suggesting an autoimmune paraneoplastic pathogenesis in theses cases (14-16).
- frequent and sometimes dramatic improvement of the symptoms following different immunotherapies including plasmapheresis, steroids, and intravenous immunoglobulins (17-19).

We still do not know, however, the precise role of autoimmunity against GAD or amphiphysin in the pathogenesis of SMS and why these proteins are such prominent autoantigens. Strikingly, both antigens are cytosolic proteins associated with the cytosolic surface of synaptic vesicles (20, 21), the organelles responsible for secretion of non-peptide neurotransmitters, such as GABA. Because of the intracellular localization of GAD and amphiphysin, it is unlikely that anti-GAD or anti-amphiphysin autoantibodies are directly pathogenic. SMS may be caused, for example, by autoantibodies directed against yet to be identified neuronal surface autoantigen(s), including intrinsic membrane protein(s) of synaptic vesicles which interacts with GAD and/or amphiphysin at their cytoplasmic side. Such autoantigen(s) would be accessible to circulating autoantibodies.

This hypothesis is based on the observation that in most autoimmune diseases autoimmunity is directed against a macromolecular complex, rather than against a single antigen.

Classification of SMS Based on Immunological Responses

In our laboratories, we screened the sera of more than 600 neurological patients by immunocytochemistry and western blotting for autoantibodies directed against brain antigens. In a recent survey, 90 of these patients, many of whom at one time were diagnosed as hysteric, fulfilled the stringent clinical criteria for the diagnosis of SMS established by Lorish and coworkers (3). According to the presence of autoantibodies directed against neuronal antigens, these 90 patients can be classified in three distinct groups (Table I).

Group I: (~50% of SMS patients) is characterized by the presence of anti-GAD autoantibodies in the serum and in the cerebrospinal fluid (10, fig. 1). Seventy percent of patients in this group are also affected by other autoimmune diseases (such as hypothyroidism, hyperthyroidism, pernicious anemia, vitiligo), and primarily IDDM (46% of the cases). Some of the patients suffer from depression and dysphoria and paroxysmal fear when crossing a free-space unaided (9). Finally, five (~10%) of these patients suffer from epilepsy.

SMS patients	Autoantibodies	Associated Disorders	Prognosis
46 [M:12; F:34]	Anti-GAD	Autoimmune disorders: 71% Insulin-dependent diabetes mellitus: 46% Epilepsy: 10% Psychiatric disorders: 17%	Chronic; slowly progressive; in some cases partial improvement after immunotheraphy
5 [M:0; F: 5]	Anti-Amphiphysin	Breast cancer : 100%	Partial improvement after cancer removal
39 [M:15; F:24]	Not detected	Autoimmune diseases: 30% Insulin-dependent diabetes mellitus: 8% Epilepsy: 5% Psychiatric disorders: 5%	Chronic; slowly progressive; in some cases partial improvement after immunotheraphy

Table I. Classification of SMS patients according to clinical features and presence of autoantibodies.

Group II: (~5% of SMS patients) is characterized by the presence of autoantibodies directed against amphiphysin (14-16). Amphiphysin is a neuron specific protein which is highly concentrated in nerve terminals (14, 15, 21) and with a putative role in endocytosis for synaptic vesicles (16, 22) None of these five SMS patients have anti-GAD autoantibodies and all suffer from breast cancer. In two of these five patients, the search for an occult breast cancer was

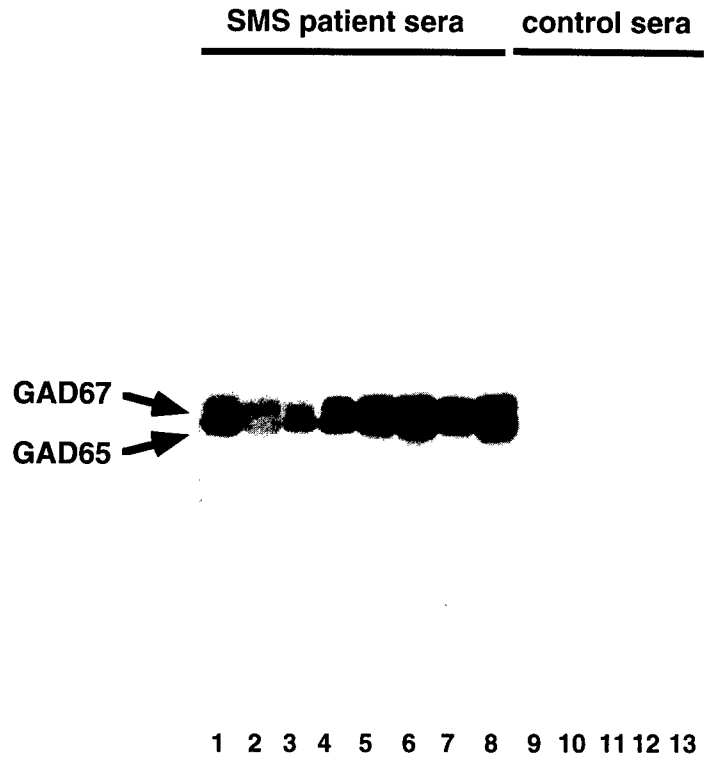

Fig. 1. Presence of anti-GAD autoantibodies in the serum of Stiff-Man syndrome patients. Stiff-Man syndrome patient's and control subject's sera were used for immunoprecipitation from rat brain Triton-X100 extracts. Immunoprecipitates were separated by SDS-gel electrophoresis, transferred on nitrocellulose, and immunoblotted by alkaline phosphatase with an anti-GAD rabbit antiserum. Autoantibodies of SMS patients immunoprecipitated both GAD65 and GAD67 (lanes 1–8), whereas neither GAD65 or GAD67 were detected in immunoprecipitates of control subject's sera (lanes 9–13).

prompted by our previous detection of anti-amphiphysin autoantibodies in the patient serum. In 4 cases (one patient could not undergo surgery) removal of breast cancer resulted in a drastic improvement of the neurological symptoms. This observation suggests that SMS has a paraneoplastic origin in these patients. It also suggests that rigidity is caused by a functional impairment rather than a destructive process of neurons controlling muscle tone.

Group III: (~45% of SMS patients) is characterized by SMS patients with no evident autoantibodies directed against neuronal antigens (14, 23). Despite the lack of autoantibodies detectable by standard assays, some of these patients suffer from autoimmune diseases, psychiatric disorders, and epilepsy. Therefore, it is possible that similar mechanisms may lead to the pathogenesis of SMS in patients of group I and III.

General Properties of GAD, the Dominant Autoantigen of SMS

GAD is a cytosolic protein represented by two isoforms of 65 (GAD65) and 67 (GAD67) kD, respectively (24). GAD65 and GAD67 are the products of two distinct genes (20), each of which has been cloned in several species. Both GAD65 and GAD67, bind piridoxal phosphate (PLP), are enzymatically active (25, 26) and are expressed in GABA-ergic neurons (27-30) and pancreatic

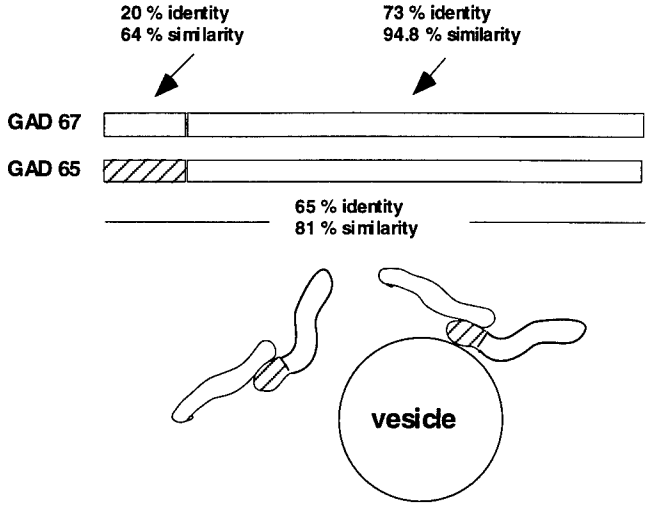

Fig. 2. Schematic representation of GAD67 and GAD65 homologous regions. Percentages of identities and similarities refer to rat GAD 67 and GAD65. Association of GAD67 with membranes involves its interaction with the N-terminal region of GAD65.

ß-cells (31) although their level of expression varies according to the cell type and the species (30, 32, 33).Each isoform is highly conserved during evolution with >95% identity among human, rat and mouse. Overall, GAD65 and GAD67 are very similar to each other (65% identity in humans), but are significantly divergent in their NH2-terminal regions (Fig. 2). The NH2-terminal region of GAD65, but not of GAD67, is palmitoylated and contains information for its association with membranes (34, 35).

SMS Autoantibodies Primarily Recognize the C- and N-terminal Regions of GAD65

With few exceptions anti-GAD autoantibodies of SMS patients can be revealed by immunocytochemistry and western blotting, as well as by immunoprecipitation and ELISA. All SMS patients develop autoantibodies directed against both GAD isoforms, but, preferentially, against GAD65 (23, 36). More specifically, GAD65 is the only isoform recognized by SMS anti-GAD autoantibodies in western blots (36). The dominant epitope of GAD65 recognized by virtually all group I SMS sera is a conformational epitope resistant to SDS denaturation contained within the last 110 amino acids (a.a. 475-485) of GAD65 (epitope SMS 1) (36). Interestingly, this region is the most conserved between the two GAD isoforms, yet the epitope SMS 1 is only present in GAD65. Deletion of a few amino acids at either side of this region of GAD65 results in the nearly complete loss of immunoreactivity. The C-terminal region of GAD65 is also the primary target of anti-GAD65 autoantibodies of IDDM patients (37-39) and contains the early NOD T-cell GAD65 determinants (40). Almost all SMS patients in group I have, in addition, autoantibodies directed against the N-terminal region (amino acids 1-95) of GAD65 (epitope SMS 2) (36, 41). This is the region of GAD65 responsible for its association with membrane compartments (fig. 3). Differently from SMS, IDDM anti-GAD65 autoantibodies do not generally recognize the epitopes SMS 1 or SMS 2 (39). This data suggests that different clinical conditions may correlate with different patterns of humoral autoimmunity (36).

Association of GAD with Synaptic Vesicles and Synaptic-like Microvesicles

Previous immunocytochemical studies with antisera which recognize both GAD isoforms had indicated that GAD is concentrated in nerve terminals of GABA-ergic neurons (27, 42) and in pancreatic ß-cells and in the Golgi complex region of both cells (27, 35, 43). The development of antibodies specifically directed against either GAD65 or GAD67 made it possible to address the

cellular and intracellular localization of each isoform. Both GAD isoforms are present in the presynaptic terminals of the majority of GABA-ergic neurons, with a relative enrichment of GAD65 compared to GAD67 (28, 30). Double immunostaining on rat pancreatic sections with anti-glucagon and anti-somatostatin antibodies indicate that GAD67, like GAD65, is only expressed in ß-cells (30). Most ß-cells express high levels of GAD65 and very low levels of GAD67, but a few ß-cells are strongly positive for GAD67 and do not contain detectable levels of GAD65 (30). The physiological significance of the heterogeneous expression of the two GAD isoforms in ß-cells remains to be established.

Immunogold electron microscopy for GAD in rat synaptosomes and pancreatic islets demonstrated that a pool of GAD is localized in close proximity to synaptic vesicles and synaptic-like microvesicles in GABA-ergic neurons and pancreatic ß-cells, respectively (20) (Fig. 2). Synaptic vesicles are concentrated at neuronal presynaptic terminals and are responsible for the storage and secretion of non-peptide neurotransmitter molecules including GABA. Upon depolarization of the nerve terminal, synaptic vesicles fuse with the plasma membrane and release their neurotransmitter content. ß-cell synaptic-like microvesicles, similarly to synaptic vesicles of GABA-ergic neurons, have a GABA-specific transport activity, suggesting that these vesicles may be responsible for the paracrine secretion of GABA from ß-cells. Association of GAD with the cytoplasmic surface of synaptic vesicles and synaptic-like microvesicles may provide a mechanism for the rapid uptake of the newly synthesized GABA into synaptic vesicles (44). The association of GAD, and primarily of GAD65, with these organelles is most likely mediated via its binding to a synaptic vesicle membrane protein. The hypothesis that protein-protein interaction is responsible for the anchoring of GAD65 to synaptic vesicles and synaptic-like microvesicles is supported by the evidence that palmitoylation of GAD65 is not required for its association to membranes (34, 35).

Molecular mechanisms in GAD membrane interaction

The nature of the interaction of GAD with membranes was investigated by transfection of GAD65 and GAD67 in CHO and COS cells (fig. 4) (45). In these cells, which lack synaptic vesicles and synaptic-like microvesicles, GAD65 was found to be selectively targeted to the Golgi complex region. Conversely, GAD67 was evenly distributed in the cell cytosol of transfected fibroblasts, compatible with GAD67 being mostly a soluble protein. Accordingly, upon subcellular fractionation of CHO cells transfected independently with GAD65 and GAD67, approximately 40-50% of GAD65 was recovered in the high speed pellet partitioned in the detergent phase after Triton X-114 extraction, whereas virtually all GAD67 was recovered in the high speed supernatant

and in the Triton X-114 aqueous phase. Using a variety of chimeric constructs, we found that a.a. 1-83 of GAD65 contain information required for the targeting of the remaining portion of the GAD molecule (i.e. the region highly similar between GAD65 and GAD67) to the region of the Golgi apparatus (fig. 4) (45). The same GAD65 domain is also sufficient to target to the Golgi complex region a GAD-unrelated protein (ß-galactosidase) (32) (fig.4). It appears, therefore, that a.a. 1-83

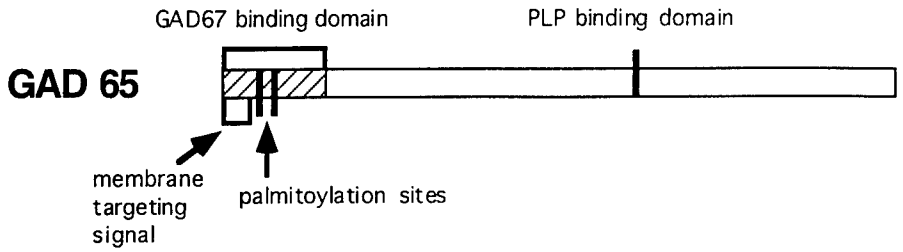

Fig. 3. Schematic representations of the domains of GAD65.

of GAD65 contains information which is necessary and sufficient to target GAD65 and other cytosolic proteins to the Golgi complex area.

It had been proposed that palmitoylation on cysteine residue(s) at the NH2-terminal region of GAD65 is responsible for anchoring GAD65 to membranes (46). Amino acids 1-83 of GAD65 contain six cysteines at position 30, 45, 73, 75, 80, 82. Following transfection of CHO cells with GAD65 constructs in which, individually or simultaneously, each of these six cysteines was replaced by a serine residue, it was found that every Cys-mutated GAD65 protein, including the GAD65 in which all six cysteines had been mutagenized (GAD65S1-6) (fig.4), was still primarily localized in the Golgi complex region (35). Upon subcellular fractionation, GAD65S1-6 was recovered in the high speed pellet, further indicating its ability to interact with subcellular particles. A chimeric GAD65-GAD67 protein in which a.a. 1-29 of GAD67 were replaced by a.a. 1-27 of GAD65 was also targeted to the Golgi complex area (fig. 4). The region of GAD65 corresponding to a.a. 1-27 does not contain any cysteine residues. These findings, which are in agreement with those reported by Shi and coworkers, 1994 (34), exclude the possibility that palmitoylation of GAD65 is directly responsible for the targeting of the protein to membrane organelles. However, both GAD65S1-6 and GAD65(1-27)/GAD67 retained some hydrophobic properties, as demonstrated by their partial recovery in the Triton X-114 detergent phase. These results support the hypothesis that the NH2-terminal domain of GAD65 may undergo a second hydrophobic post-translation modification (46), yet to be characterized. Conversely, replacement of a.a. 1-27 of

GAD65 with a.a 1-29 of GAD67 generated a protein [GAD67(1-29)/GAD65] which, similarly, to GAD67, was homogeneously distributed in the cytosol (fig. 4). The GAD67(1-29)/GAD65 protein was recovered only in the high speed supernatant and in the Triton X-114 aqueous phase. This data suggests that targeting to the Golgi complex region is required for the protein to undergo hydrophobic post-translational modifications, such as palmitoylation. While palmitoylation may stabilize the anchoring of GAD65 to membranes, other mechanisms such as protein-protein interactions are likely to account for the association of GAD65 to specific intracellular compartments (35, 45).

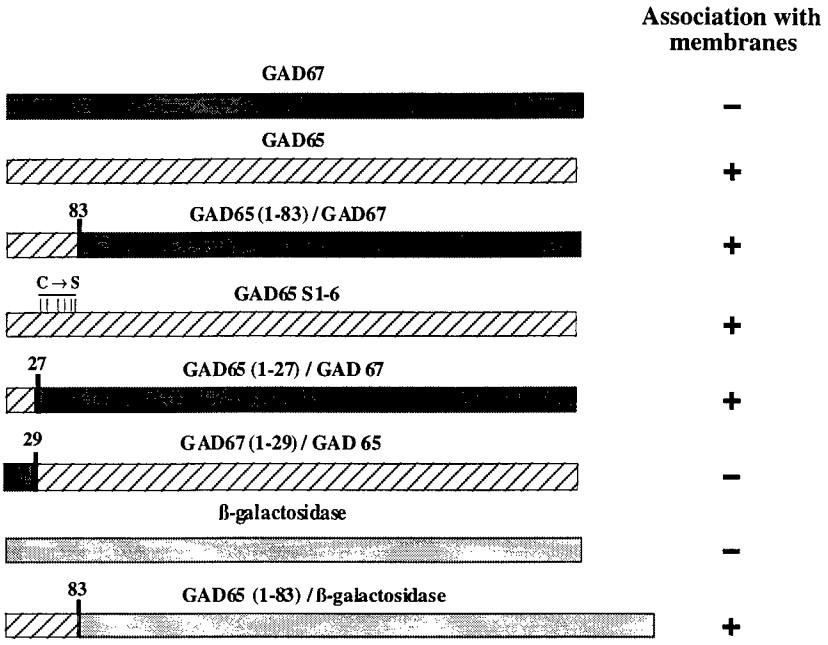

Fig. 4. Ability of various GAD constructs to interact with membranes in transfected fibroblasts.

GAD65 and GAD67 Form a Heterodimeric Complex *In Vivo*.

GAD67 from transfected cells is recovered in the high speed supernatant only and in the Triton X-114 aqueous phase (45, 46). In contrast, a considerable pool of rat brain GAD67 sediments together with GAD65 in pellet fractions (30, 47). Furthermore, immunoprecipitation and affinity purification of brain GAD65 with a monoclonal antibody which selectively recognizes GAD65 results in the co-purification of GAD67, despite the complete lack of cross-reactivity of this

antibody with GAD67 (36, 47). It was suggested, therefore, that GAD65 and GAD67 form heterodimers, both as cytosolic proteins as well as in association to membrane compartments (47). Consistent with this hypothesis, a pool of GAD67 colocalizes with GAD65 in the Golgi complex region of neurons and pancreatic ß-cells, both of which express GAD65 and GAD67. Similarly, co-expression of GAD65 and GAD67 in CHO cells results in targeting of GAD67 to the Golgi complex region (30) and co-immunoprecipitation of the two proteins. To establish which domain of GAD65 interacts with GAD67, GAD65(1-83)/ß-galactosidase and GAD67 constructs were co-transfected in CHO cells and their distribution analyzed by immunocytochemistry (30). GAD67 and GAD65(1-83)/ß-galactosidase fusion protein colocalized in the Golgi complex region, indicating that the domain encompassing a.a 1-83 of GAD65 is directly responsible for the association of GAD65 with GAD67 (fig. 2 and 3). Additional data indicates that palmitoylation of GAD65 is not required for its association with GAD67.

Concluding Remarks

SMS is a very disabling disease, which is often misdiagnosed. The detection of anti-GAD autoantibodies in SMS patients has provided a useful tool for the diagnosis of this disease. This discovery, in addition, has led to the identification of GAD65 as the 64kD autoantigen of IDDM and therefore to the discovery that GAD autoimmunity plays a key role in the pathogenesis of IDDM (13, 48).

Acknowledgments. This work was partially supported by NIH grants AI30248, DK43078 and a McKnight Research Project Award to PDC, by a Juvenile Diabetes Foundation International Career Development Award and NIH pilot grant DK-45735 to MS, by a traveling fellowship from the Association Française contre les Myopathies to J-MH and by a U.S. Army Medical Research Postdoctoral Fellowship to CD.

References

1. Moersch FP, Woltman HW. Progressive and fluctuating muscular rigidity and spasm (stiff-man syndrome): report of a case and some observation in 13 other cases. Mayo Clin. Proc. 1956; 31: 421-427.

2. Layzer RB. Stiff-man syndrome: an autoimmune disease? N. Engl. J. Med. 1988; 318: 1060 -1063.

3. Lorish TR, Thorsteinsson G, Howard FM. Stiff-man syndrome updated. Mayo Clin Proc. 1989; 64: 629-636.

4. Blum P, Jankovic J. Stiff-Person syndrome: an autoimmune disease. Mov. Dis. 1991; 6: 12-20.

5. McEvoy KM. Stiff-Man syndrome. Mayo Clin. Proc. 1991; 66: 300-304.

6. Meinck HM, Ricker K, Conrad B. The stiff-man syndrome: new pathophysiological aspects from abnormal exteroceptive reflexes and ther response to clorimipramine clonidine and tizanidine. J. Neurol. Neurosurg. Psychiatry 1984; 47: 280-287.

7. Mitsumoto H, Schwartzman MJ, Estes ML, Chou SM, La Franchise EF, De Camilli P, and Solimena M. Sudden death and paroxysmal autonomic dysfunction in stiff-man syndrome. J. Neurol. 1991; 238: 91-96.

8. Tarsey D, and Miyawaki EK. Stiff-man syndrome. Report of a case. Arch. Int. Med. 1994; 154: 1285-1288.

9. Meinck HM, Ricker K, Hulser PJ, Schmid E, Pfeiffer J, and Solimena M. Stiff-man syndrome: clinical and laboratory findings in eight patients. J. Neurol. 1994; 241: 157-166.

10. Solimena M, Butler M, and De Camilli P. GAD, diabetes and stiff-man syndrome: some progress and more questions. J. Endocrin. Invest. 1994a; 17: 509-520.

11. McEvoy KM and Lennon VA. 1994. Stiff-man syndrome: clinical aspects and anti-islet cell antibodies as a disease marker. In: Motor Unit Hyperactivity States. RB Layzer, editor. New York: Raven Press 1994: 45-51.

12. Solimena M, Folli F, Denis-Donini S, Comi GC, Pozza G, De Camilli P, and Vicari AM. Autoantibodies to glutamic acid decarboxylase in a patient with Stiff-Man syndrome epilepsy and type I diabetes mellitus. N. Engl. J. Med. 1988; 318: 1012-1020.

13. Solimena M, Folli F, Aparisi R, Pozza G, and De Camilli P. Autoantibodies to GABAergic neurons and pancreatic beta cells in Stiff-Man syndrome. N. Engl. J. Med. 1990; 322: 1555-1560.

14. Folli F, Solimena M, Cofiell R, Austoni M, Tallini G, Fassetta G, Bates D, Cartlidge N, Bottazzo GF, Piccolo G, and De Camilli P. Autoantibodies to a 128 kd synaptic protein in Stiff-Man syndrome with breast cancer. N. Engl. J. Med. 1993; 328: 546-551.

15. De Camilli P,Thomas A, Cofiell R, Folli F, Lichte B, Piccolo G, Meinck H-M, Austoni M, Fassetta G, Bottazzo GF, Bates D, Cartlidge N, Solimena M, and Kilimann MW. The synaptic vesicle-associated protein amphiphysin is the autoantigen of Stiff-Man syndrome with breast cancer. J. Exp. Med. 1993; 178: 2219-2223.

16. David C, Solimena M, and De Camilli P. Autoimmunity to Stiff-man syndrome with breast cancer is targeted to the C-terminal region of human amphiphysin, a protein homologous to the yeast protein, Rvs167 and Rvs161. FEBS Letter 1994; 351: 73-79.

17. Vicari AM, Folli F, Pozza G, Comi GC, Comola M, Canal N, Besana C, Borri A, Tresoldi M, Solimena M, and De Camilli P. Plasmapheresis in the treatment of stiff-man syndrome. N. Engl. J. Med. 1989; 320 :1499.

18. Piccolo G, Cosi V, Zandrini C, Moglia A. Steroid-responsive and dependent stiff-man syndrome: a clinical and electrophysiological study of two cases. Ital. J. Neurol Sci. 1988; 9 : 559-66.

19. Karlson EW, Sudarsky L, Ruderman E, Pierson S, Scott M, and Helfgott SM. Treatment of stiff-man syndrome with intravenous immune globulin. Arthritis Rheum 1994; 37: 915-8.

20. Reetz A, Solimena M, Matteoli M, Folli F, Takei K, and De Camilli P. GABA and pancreatic ß-cells: colocalization of glutamic acid decarboxylase (GAD) and GABA with synaptic-like microvesicles suggests their role in GABA storage and secretion. EMBO J. 1991; 10: 1275-1284.

21. Lichte B, Veh RW, Meyer HE, and Kilimann MW. Amphiphysin, a novel protein associated with synaptic vesicles. EMBO J. 1992; 11: 2521-2530.

22. David, C., McPherson, P.S., Cho, Y., Solimena, M., and De Camilli, P. Amphiphysin, a nerve terminal protein similar to yeast RVS161 and RVS167, binds dynamin and P145 via its SH3 domain. 1994. 34th meeting of the American Society for Cell Biology

23. Solimena M, and De Camilli P. Autoimmunity to glutamic acid decarboxylase (GAD) in Stiff-Man syndrome and insulin-dependent diabetes mellitus. TINS 1991; 14: 452-457.

24. Erlander MG, Tillakaratne NJK, Feldblum S, Patel N, and Tobin AJ. Two genes encode distinct glutamate decarboxylases. Neuron 1991; 7: 91-100.

25. Erlander MG, and Tobin AJ. The structural and functional heterogeneity of glutamic acid decarboxylase: a review. Neurochem. Res. 1991; 16: 215-226.

26. Martin DL, Martin SB, Wu SJ and Espina N. Regulatory properties of brain glutamate decarboxylase (GAD): the apoenzyme of GAD is present principally as the smaller of two molecular forms of GAD in brain. J. Neurosci. 1991, 11: 2725-2731.

27. Mugnaini E, and Oertel WH. An atlas of the distribution of GABAergic neurons and terminals in the rat CNS as revealed by GAD immunohistochemistry. In: Handbook of Chemical Neuroanatomy Vol. 4: GABA and Neuropeptides in the CNS Part I. A. Bjorklund and T. Hökfelt, editors. Amsterdam: Elsevier Science Publishers B.V. 1985: 436-608.

28. Kaufman DL, Houser CR, and Tobin AJ. Two forms of the GABA synthetic enzume glutamate decarboxylase have distinct intraneuronal distributions and cofactor interactions. J. Neurochem. 1991; 56: 720-723.

29. Esclapez M, Tillakaratne NJK, Kaufman DL, Tobin AJ, and Houser CR. Comparative localization of two forms of glutamic acid decarboxylase and their mRNAs in rat brain supports the concept of functional differences between the forms. J. Neurosci 1994; 14: 1834-1855.

30. Dirkx R., Thomas A., Li L., Lernmark Å., Sherwin R., De Camilli P., and Solimena M. Targeting of GAD67 to membranes via heterodimeric interaction with the N-terminal region of GAD65. J. Biol. Chem. 1994; 270: 2241-2246.

31. Vincent SR, Hökfelt T, Wu JY, Elde RP, Morgan LM, and Kimmel JR. Immunohistochemical studies of the GABA system in the pancreas. Neuroendocrin. 1983; 36: 197-204.

32. Faulkner-Jones BE, Cram DS, Kun J, and Harrison LC. Localization and quantitation of expression of two glutamate decarboxylase genes in pancreatic ß-cells and other peripheral tissues of mouse and rat. Endocrinol. 1993; 133: 2962-2972.

33. Kim J, Richter W, Aanstoot H-J, Shi Y, Fu Q, Rajotte R, Warnock G, and Bækkeskov S. Differential expression of GAD65 and GAD67 in human rat and mouse pancreatic islets. Diabetes 1993; 42: 1799-1808.

34. Shi Y, Veit B, and Bækkeskov S. Amino acid residues 24-31 but not palmitoylation of cysteins 30 and 45 are required for membrane anchoring of glutamic acid decarboxylase GAD65. J. Cell Biol. 1994;124: 927-934.

35. Solimena M, Dirkx R, Radzynski M, Mundigl O, and De Camilli P. A signal located within amino acids 1-27 of GAD65 is required for its targeting to the Golgi complex region. J. Cell Biol. 1994b, 126: 331-41.

36. Butler M, Solimena M, Dirkx R, Hayday A, and De Camilli P. Identification of a dominant epitope of glutamic acid decarboxylase (GAD65) recognized by autoantibodies in Stiff-Man syndrome. J. Exp. Med. 1993; 178: 2097-2106.

37. Kaufman DL, Erlander MG, Claire-Salzler M, Atkinson MA, Maclaren NK, and Tobin AJ. Autoimmunity to two forms of glutamate decarboxylase in insulin dependent diabetes mellitus. J. Clin. Invest. 1992; 89: 283-292.

38. Mauch L, Seissler J, Haubruck H, Cook NJ, Abney CC, Berthold H, Wirbelauer C, Liedvogel B, Scherbaum WA, and Northemann W. Baculovirus-mediated expression of human 65 kDa and 67 kDa glutamic acid decarboxylases in SF9 insect cells and their relevance in diagnosis of insulin-dependent diabetes mellitus. J. Biochem 1993; 113: 699-704.

39. Richter W, Shi Y, and Bækkeskov S. Autoreactive epitopes defined by diabetes-association human monoclonal antibodies are localizaed in the middle and C-terminal domains of the smaller form of glutamate decarboxylase. Proc. Natl. Acad. Sci. USA 1993; 90: 2832-2836.

40. Kaufman DL, Clare-Salzer M, Tian J, Forsthuber T, Ting GSP, Robinson P, Atkinson MA, Sercarz EE, Tobin AJ, and Lehmann PV. Spontaneous loss of T-cell tolerance to glutamic acid decarboxylase in murine insulin-dependent diabetes. Nature 1993; 366: 69-72.

41. Kim J, Namchuk M, Bugawan T, Fu Q, Jaffe M, Shi Y, Aanstoot HJ, Turck CW, Erlich H, Lennon V, and Baekkeskov S. Higher autoantibody levels and recognition of a linear NH2-terminal epitope in the autoantigen GAD65, distinguish stiff-man syndrome from insulin-dependent diabetes mellitus. J. Exp. Med. 1994; 180:595-606.

42. McLaughlin BJ, Barber R, Saito K, Roberts E, Wu JY. Immunocytochemical localization of glutamate decarboxylase in rat spinal cord. J. Comp. Neurol. 1975; 164: 305-321.

43. Sorenson RL, Garry DG, and Brelje TC. Structural and functional considerations of GABA in islets of Langerhans ß-cells and nerves. Diabetes 1991; 41: 1365-1374.

44. Thomas-Reetz A, Hell JW, During MJ, Walch-Solimena C, Jahn R, and De Camilli P. A γ-aminobutyric acid transporter driven by a proton pump is present in synaptic-like microvesicles of pancreatic ß cells. Proc. Natl. Acad. Sci. USA 1993; 90: 5317-5321.

Amphiphysin II (SH3P9; BIN1), a Member of the Amphiphysin/Rvs Family, Is Concentrated in the Cortical Cytomatrix of Axon Initial Segments and Nodes of Ranvier in Brain and around T Tubules in Skeletal Muscle

Margaret Husta Butler, Carol David, Gian-Carlo Ochoa, Zachary Freyberg, Laurie Daniell, Detlev Grabs, Ottavio Cremona, and Pietro De Camilli

Department of Cell Biology and Howard Hughes Medical Institute, Yale University School of Medicine, New Haven, Connecticut 06510

Abstract. Amphiphysin (amphiphysin I), a dominant autoantigen in paraneoplastic Stiff-man syndrome, is a neuronal protein highly concentrated in nerve terminals, where it has a putative role in endocytosis. The yeast homologue of amphiphysin, Rvs167, has pleiotropic functions, including a role in endocytosis and in actin dynamics, suggesting that amphiphysin may also be implicated in the function of the presynaptic actin cytoskeleton. We report here the characterization of a second mammalian amphiphysin gene, amphiphysin II (SH3P9; BIN1), which encodes products primarily expressed in skeletal muscle and brain, as differentially spliced isoforms. In skeletal muscle, amphiphysin II is concentrated around T tubules, while in brain it is concentrated in the cytomatrix beneath the plasmamembrane of axon initial segments and nodes of Ranvier. In both these locations, amphiphysin II is colocalized with splice variants of ankyrin3 ($ankyrin_G$), a component of the actin cytomatrix. In the same regions, the presence of clathrin has been reported. These findings support the hypothesis that, even in mammalian cells, amphiphysin/Rvs family members have a role both in endocytosis and in actin function and suggest that distinct amphiphysin isoforms contribute to define distinct domains of the cortical cytoplasm. Since amphiphysin II (BIN1) was reported to interact with Myc, it may also be implicated in a signaling pathway linking the cortical cytoplasm to nuclear function.

Amphiphysin I, a human autoantigen in Stiff-man syndrome associated with breast cancer (De Camilli et al., 1993; Folli et al., 1993), is a neuronal protein highly concentrated in the cortical cytomatrix of nerve terminals where it has a putative role in synaptic vesicle endocytosis (Lichte et al., 1992; David et al., 1994, 1996; Shupliakov et al., 1997). It comprises an NH_2-terminal region, which is predicted to form coiled coil structures, a COOH-terminal SH3 domain, and a proline-rich linker region between these two domains that is poorly conserved evolutionarily (David et al., 1994). Biochemical studies, complemented by colocalization and coimmunoprecipitation experiments, have strongly suggested that the two main physiological ligands for the SH3 domain of amphiphysin I are the GTPase dynamin I (David et al., 1996; Grabs et al., 1997) and the inositol–5-phosphatase synaptojanin (McPherson et al., 1996). Dynamin I participates in synaptic vesicle recycling via its critical role in the fission of clathrin-coated vesicles from the nerve terminal plasmalemma (Kosaka and Ikeda, 1983; Koenig and Ikeda, 1989; Shpetner and Vallee, 1989; Takei et al., 1995), and synaptojanin is thought to function in a closely related step (McPherson et al., 1996). In addition, amphiphysin I interacts in vitro, via a region distinct from its SH3 domain, with the appendage domain of the α subunit of the clathrin adaptor AP2 (Wang et al., 1995; David et al., 1996). It has, therefore, been suggested that one of the functions of amphiphysin I is to recruit dynamin I and synaptojanin at the clathrin coat of synaptic vesicles (David et al., 1996). Consistent with this hypothesis, disruption of amphiphysin SH3 domain interactions in living nerve terminals produces a potent block of synaptic vesicle endocytosis at the stage of deeply invaginated clathrin coated pits (Shupliakov et al., 1997).

M.H. Butler and C. David contributed equally to this work.

Please address all correspondence to Pietro De Camilli, Department of Cell Biology and HHMI, Yale University School of Medicine, 295 Congress Avenue, New Haven, CT 06510. Tel.: (203) 737-4465; Fax: (203) 737-1762; E-mail: pietro.decamilli@yale.edu

Detlev Grabs' current address is Institut für Anatomie and Spezielle Embryologie, Universität Fribourg, 1 Rue Gockel, CH-1700 Fribourg, Switzerland.

Ottavio Cremona's permanent address is Department of Medical Sciences, II Faculty of Medicine, University of Torino, Via Solaroli 17, 21100 Novara, Italy.

Amphiphysin I shares substantial primary sequence similarity and a similar domain structure, with the yeast protein Rvs167. Furthermore, the NH_2-terminal portion of both proteins is similar to the yeast protein Rvs161 (Bauer et al., 1993; David et al., 1994; Sivadon et al., 1995). Mutations in either *RVS161* or *RVS167* block receptor-mediated and fluid phase endocytosis in yeast, strongly supporting a role of the Amphiphysin/Rvs family in endocytic processes (Munn et al., 1995). In addition, *RVS161* and *RVS167* mutants also exhibit defects in the function of the actin cytoskeleton, in agreement with the general link between actin and endocytosis that has emerged from yeast studies (Munn et al., 1995; Sivadon et al., 1995). A corresponding link between amphiphysin I and the function of the actin cytoskeleton has been suggested by studies in cultured hippocampal neurons (Mundigl O., C. Ochoa, C. David, A.K. Kabanov, and P. De Camilli. *Mol. Biol. Cell (Suppl.).* 7:84*a.*). Finally, *rvs* mutants impair the ability of yeast cells to enter stationary phase upon exposure to nutrient starvation (reduced viability upon starvation) suggesting an indirect role of the *RVS* genes in controlling cell proliferation (Crouzet et al., 1991; David et al., 1994).

Amphiphysin I is expressed at a high concentration in brain and testis, at a lower concentration in neuroendocrine tissues (De Camilli et al., 1993; Folli et al., 1993; Lichte et al., 1992), and at only much lower levels in most other tissues (Butler, M.H., S. Floyd, and P. De Camilli, unpublished results). We have characterized here the product of a second amphiphysin gene, which we refer to as amphiphysin II. Amphiphysin II is localized primarily in specialized regions of the cortical cytoplasm of axons and muscle cells. These observations add further evidence for a general connection between proteins of the amphiphysin/Rvs family and the function of the cortical cell cytoskeleton.

Materials and Methods

Antibodies

The following affinity purified rabbit polyclonal antibodies were generated in our laboratory. CD5 antibodies specific for amphiphysin I (raised against a GST-fusion protein comprising the full length amphiphysin I protein [David et al., 1994]); CD7 and CD8 antibodies specific for amphiphysin II (raised against a GST-fusion protein comprising the last 68 amino acids of amphiphysin II; in this region, the amino acid identity between amphiphysin I and II is 55%); CD9 antibodies directed against both amphiphysin I and II (raised against a synthetic peptide corresponding to amino acids 26 to 40 of amphiphysin I, which is 100% conserved in amphiphysin II). A mouse polyclonal serum specific for amphiphysin I was raised against the polyhistidine-tagged full length amphiphysin I protein (David et al., 1996). Rabbit polyclonal antibodies directed against synaptojanin were previously described (McPherson et al., 1996). DG1 antibodies specific for dynamin I were generated against a dynamin I GST-fusion protein lacking the proline-rich domain. Antibodies directed against desmin, MAP2, and myelin basic protein (MBP) were purchased from Immunon (Pittsburgh, PA), Boehringer Mannheim Corp. (Indianapolis, IN), and Sternberger Monoclonals (Baltimore, MD), respectively. Polyclonal anti-ankyrin3 antibodies and anti-glut4 antibodies were kind gifts of J. Morrow (Yale University, New Haven, CT; Devarajan et al., 1996) and D. James (University of Queensland, Australia), respectively. A monoclonal anti-clathrin antibody (X22) was a kind gift of F. Brodsky (University of California, San Francisco, CA; Brodsky, 1985). A mouse monoclonal antibody (GAD6) against glutamic acid decarboxylase (GAD) was a kind gift of D. Gottlieb (Washington University, St. Louis, MO; Chang and Gottlieb, 1988).

DNA Cloning

By searching the database for amphiphysin I homologues, a sequence of 289 bp was identified from a human muscle library with 76% identity to the COOH-terminal region of human amphiphysin I. (These sequence data are available from Genbank/EMBL/DDBJ under accession Z24784.) A probe corresponding to the first 251 bp of this sequence was amplified by PCR (forward primer 5′-cccaagcacgactacacggc-3′; reverse primer 5′-ggaggaggtgttcttcacacgc-3′) from a human skeletal muscle cDNA library constructed in λZAPII phage (Stratagene, La Jolla, CA). The probe was then radioactively labeled by primer-direct labeling (Bogue et al., 1994) and used to screen 2×10^6 plaques of the same library. The two longest clones isolated by the screen (clones 17-42 and 12-1A) were partially characterized by restriction mapping and found to overlap extensively. Both clones were fully sequenced, and clone 17-42 was found to encode a nearly full length protein, missing only three amino acids at its COOH-terminal end. Subsequent searches of the database revealed additional expressed sequence tag (EST) sequences from a human infant brain library that were identical to portions of our clone 17-42. Clones 24660, 30686, and 27466 (Genbank/EMBL/DDBJ T80281, R18250 and R12992, respectively) were obtained through the IMAGE Consortium (Research Genetics Inc., Huntsville, AL) and fully sequenced. A human brain cDNA library constructed in λgt11 (Clontech, Palo Alto, CA) was then screened with a 220-bp probe amplified by PCR (forward primer 5′-cttggggagggtggccccg-3′; reverse primer 5′-agcaagctcaaccagaacc-3′) and labeled by primer-direct labeling. 26 positive plaques out of 1×10^6 were identified, and the two longest clones (clone 11 and clone 19) were fully sequenced. These clones were identical to the IMAGE cDNA clones mentioned above, except for some additional alternative splicings (see Fig. 1 *B*). Since none of the clones isolated encoded an entire reading frame, the full length clones were assembled as follows starting from the two longest clones. Clone 17/12 (see Fig. 1 *C*) was assembled from clone 17-42 by replacing its COOH terminus with that of clone 12-1A using the SapI restriction site. Clone 17/19 (see Fig. 1 *C*) was assembled from clone 19 (Genbank/EMBL/DDBJ U87558) by replacing its NH_2-terminal region with that of clone 17-42 at the unique restriction site BsaAI. Nucleotide sequences were analyzed by Blast and Fasta and aligned by Bestfit and Pileup (Genetics Computer Group, Madison, WI). Chromatograms from sequencing analysis were assembled by Seqman (DNASTAR, Inc., Madison, WI). Coiled coil structure identification was performed using Coils 2.2 (Lupas, 1996).

Northern Blot Analysis

Northern blot analysis of amphiphysin II expression was performed on a human multiple tissue RNA filter (Clontech) containing 2 μg of Poly A+ RNA on each lane. The full length amphiphysin II cDNA (clone 17/12) and an oligonucleotide of 120 bp corresponding to amino acid 351–390 of the contiguous sequence shown in Fig. 1 *A*, were labeled by random priming (Boehringer Mannheim Corp.; 2×10^6 cpm/ml) and hybridized at 42°C in 50% formamide, 6× SSC, 0.1% SDS, 2× Denhardt's, 100 μg/ml salmon sperm DNA. An actin probe was used as a control to assess gel loading. Filters were washed twice for 20 min at high stringent conditions in 0.2× SSC, 0.1% SDS at 50°C.

Cell Transfection

COS-7 cells were transiently transfected with cDNAs corresponding to either clone 17/12 or clone 17/19 (see Fig. 1 *C*). The two cDNAs were subcloned in pcDNA3 (Invitrogen, San Diego, CA) and then purified with a Maxiprep kit (Qiagen, Chatsworth, CA). COS-7 cells (American Type Culture Collection, Rockville, MD) were transfected with lipofectamine (GIBCO BRL, Gaithersburg, MD), according to standard procedures (Chen and Okayama, 1987). Triton X-100 extracts of transfected cells and untransfected COS-7 cells were harvested after 24 h and analyzed by SDS-PAGE and Western blotting.

Immunocytochemistry

Light microscopy. Rat brains were fixed and frozen sectioned as described (De Camilli et al., 1983). Small fragments of rat soleus skeletal muscle were incubated in relaxing media (100 mM Hepes, 100 mM potassium propionate, 3 mM MgCl, 5 mM EGTA, 15 mM phosphocreatine, 2 mM NaATP; Kaufman et al., 1990) at room temperature for 10 min. Muscles were then stretched, fixed in 4% paraformaldehyde/0.1 M phosphate buffer, pH 7.4, and semithin sectioned (0.5 mm) on an ultramicrotome (Ultracut FCS; Reichert, Vienna, Austria). Rat muscle and brain sections were stained

for indirect immunofluorescence according to De Camilli et al. (1983). Pictures were recorded on black and white films (T-MAX 100; Kodak, Rochester, NY) with a microscope (Axiophot; Zeiss Inc., Thornwood, NY) equipped for epifluorescence microscopy.

Electron microscopy. Small pieces of rat soleus skeletal muscle were rapidly excised and fixed by immersion in 4% paraformaldehyde in 0.12 M sodium phosphate buffer, pH 7.4. The samples were then infiltrated with polyvinylpyrrolidone/sucrose for 2 h. Ultrathin frozen sections were cut

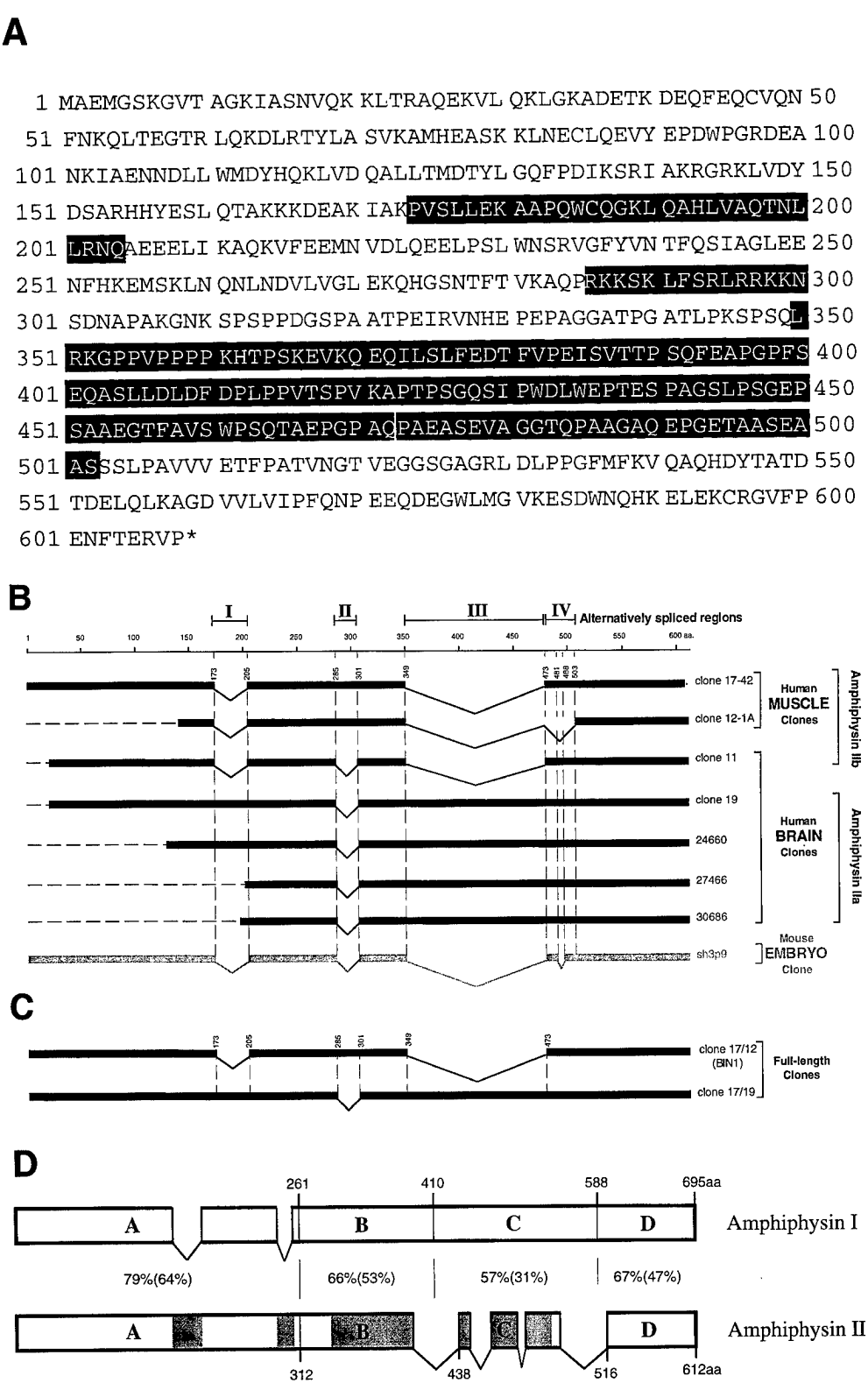

Figure 1. (*A*) Human amphiphysin II contiguous sequence obtained from a Pileup analysis of the human clones shown in *B*. Alternatively spliced regions are depicted by shaded amino acid residues. (*B*) Schematic representation of the human amphiphysin II clones analyzed in this study and of the mouse homologue of amphiphysin II previously reported (Sparks et al., 1996). The calibration bar (*top*) indicates number of amino acid residues. Alternatively spliced regions are indicated by roman numerals (I–IV). (*C*) Schematic representation of full length amphiphysin II clones assembled from clones 17-42 and 12-1A and from clones 19 and 17-42, respectively. Clone 17/12 is identical to the recently reported BIN1 clone with the exception of a K→E difference at position 434 of BIN1 and the corresponding position 591 of the contiguous sequence shown in Fig. 1 *A* (Sakamuro et al., 1996). (*D*) Domain diagram of human amphiphysins I and II showing the homology between the two genes. The boundaries of the A–D domains are delineated by amino acid numbers. A–D domains were previously defined as follows based on comparisons among human and chicken amphiphysin I and yeast Rvs proteins (David et al., 1994). The A, B, and D domains are the regions most highly conserved between chicken and human amphiphysin, while the C domain is poorly conserved. The A domain, within the A and B region, is defined by the yeast proteins Rvs161, which comprises this domain only. The percent similarity and identity (in parenthesis) for each domain is given. The shaded areas in the amphiphysin II gene represent the alternatively spliced regions outlined in Fig. 1 *B*.

onto an ultramicrotome (Reichert) with FCS attachment and immediately processed for immunogold labeling (10-nm gold) as previously described (Keller et al., 1984; Tokuyasu et al., 1989).

Miscellaneous Procedures

SDS-PAGE and Western blotting were performed essentially as described by Laemmli (1970) and Towbin et al. (1979), respectively. Immunoreactive bands were detected by either alkaline phosphatase conjugated secondary antibodies (Bio Rad, Hercules, CA) or ^{125}I-protein A (10^5 cpm/ml; Dupont/NEN, Boston, MA).

Results

Cloning of Amphiphysin II

Human adult skeletal muscle and brain cDNA libraries were screened with probes corresponding to human partial cDNA sequences present in the database with significant homology to human amphiphysin I. Four clones identified by this screening (muscle clones 17-42 and 12-1A and brain clones 11 and 19) and three human infant brain clones (clones 24660, 27466, and 30686) obtained from the IMAGE Consortium were fully sequenced.

A comparative analysis of all these clones suggests that they are derived by alternative splicing from a single gene. The products of this gene will be collectively referred to as amphiphysin II, because of their strong sequence similarity to amphiphysin I. The contiguous amino acid sequence derived from the analysis of the individual human clones is shown in Fig. 1 *A*. Fig. 1 *B* is a schematic alignment of the human clones with a mouse sequence (SH3P9) that represents the murine homologue of amphiphysin II and which was obtained during a screen for SH3 domain-containing proteins (Sparks et al., 1996). The partial clones depicted in Fig. 1 *B* were used to assemble the full length clones 17/12 and 17/19, as shown in Fig. 1 *C* (see Materials and Methods). These full length clones correspond to two alternative splicing variants of amphiphysin II. Clone 17/12 is identical to BIN1 (with the exception of a single amino acid; see Fig. 1 *C*, *legend*), a protein recently identified in a two hybrid screen for MYC-interacting proteins (Sakamuro et al., 1996).

The percentages of similarity and identity between the contiguous sequence of human amphiphysin II (as defined by Fig. 1 *A*) and human amphiphysin I (David et al., 1994) are 71 and 55%, respectively. Fig. 1 *D* shows a schematic alignment of the two sequences, as well as the boundaries of the A–D domains as defined previously on the basis of blocks of similarity between the Rvs yeast proteins and human and chicken amphiphysins (David et al., 1994; Fig. 1, *legend*).

Note that alternatively spliced fragments I and II (Fig. 1 *B*) of amphiphysin II coincide with gaps in the amphi-

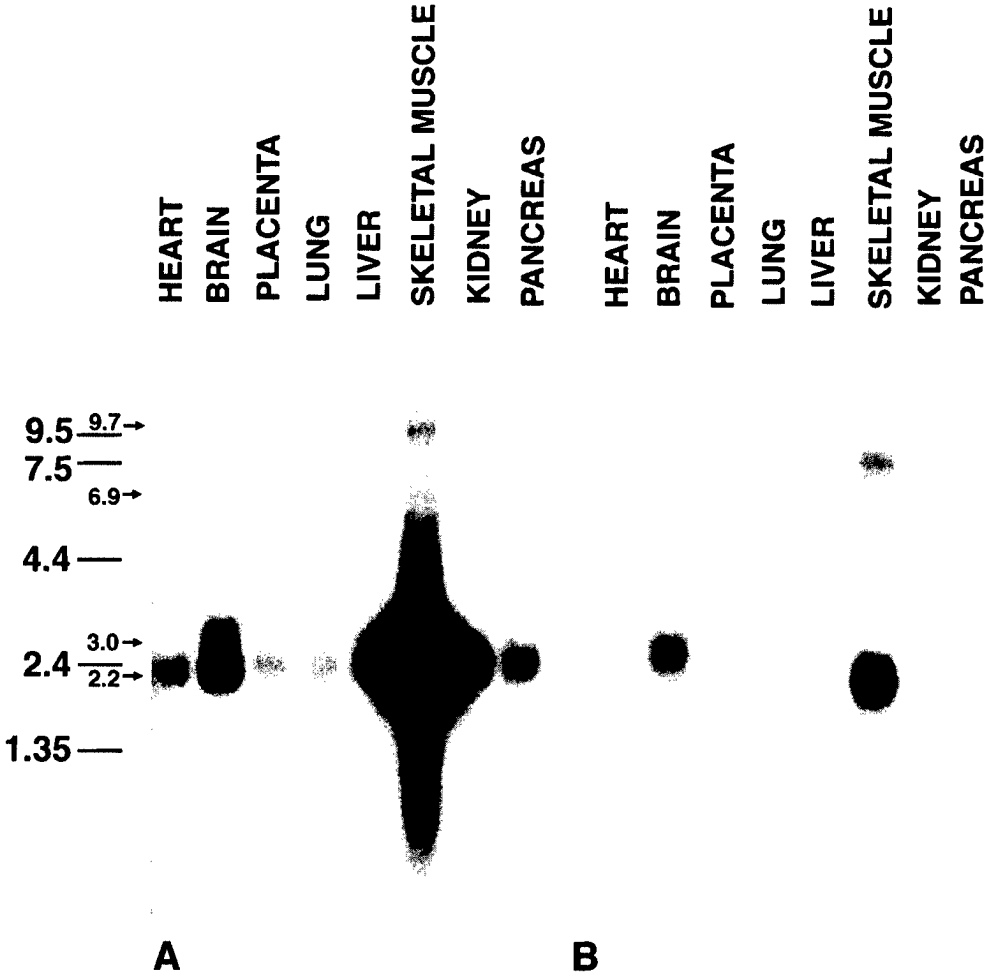

Figure 2. Northern blot analysis of human tissues demonstrating patterns of expression of amphiphysin II mRNAs. Two identical blots containing Poly(A+) RNA from a variety of tissues were probed with clone 17/12 (*A*) and a probe corresponding to alternatively spliced segment III (*B*). Note the different labeling patterns produced by the two probes. Amphiphysin II is expressed primarily in skeletal muscle and brain. Numbers at left indicate molecular weights (kb).

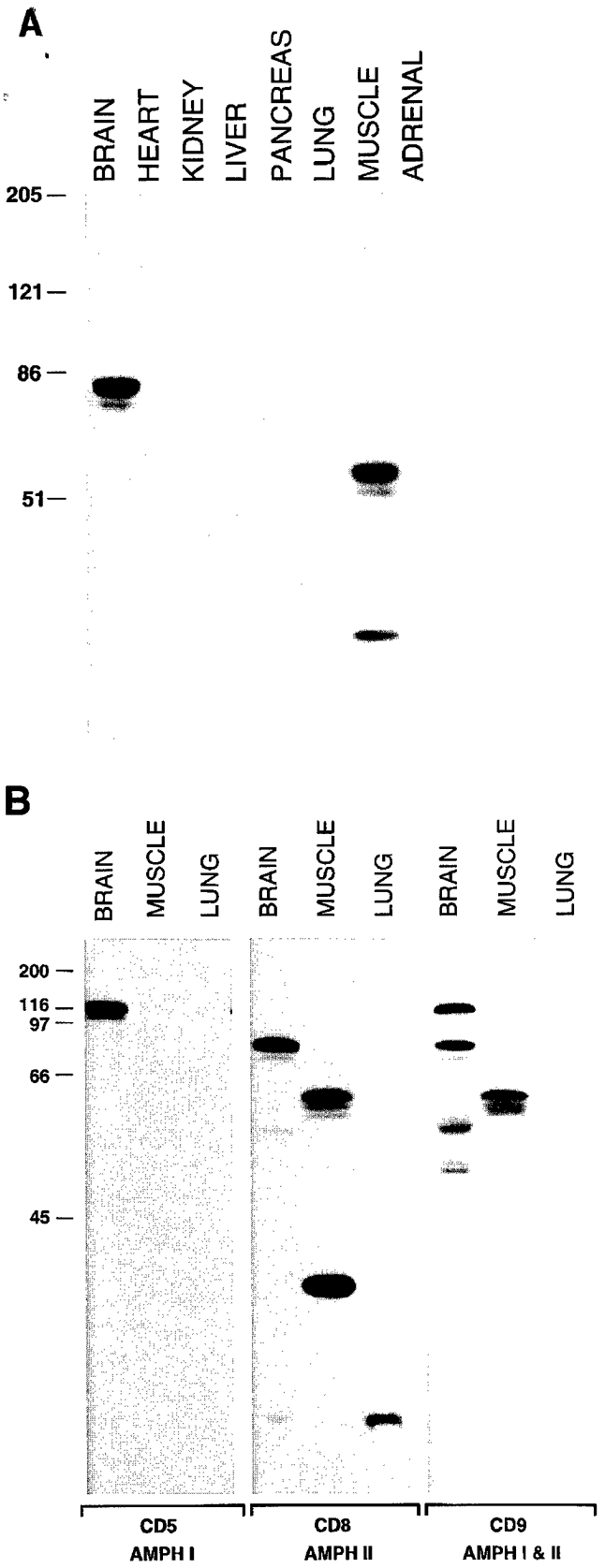

Figure 3. (*A*) Tissue distribution of amphiphysin II as demonstrated by Western blotting. Amphiphysin II is expressed primarily in brain and skeletal muscle. Equal protein amounts of post nuclear supernatants prepared from rat tissues were loaded in each lane and probed with the CD8 polyclonal rabbit serum specific for amphiphysin II. Bound antibodies were detected by ^{125}I-protein A. (*B*) Comparison of amphiphysin I and amphiphysin II expression in rat brain, skeletal muscle, and lung. Extracts of the three tissues were probed with an antibody specific for amphiphysin I (CD5), for amphiphysin II (CD8), and with an antibody that recognizes both amphiphysin I and II (CD9). Bound antibodies were detected by ^{125}I-protein A. The low molecular weight bands labeled by the CD8 antibody are not visible in the brain and lung lanes of Fig. 3 *A* because they had migrated at the gel front. Numbers at left indicate molecular weights (kD).

physin I sequence, raising the possibility that even the amphiphysin I gene may undergo a similar alternative splicing in this region.

Amphiphysin II Is Primarily Expressed in Brain and Muscle

Northern blot analysis of different tissues with the full length amphiphysin II cDNA (clone 17/12) revealed that skeletal muscle is, by far, the major site of expression of this gene (Fig. 2 *A*). A major band centered at 2.2 kb was present in this tissue. The same band was present at much lower levels in brain and at an even lower concentration in several other tissues (Fig. 2 *A*). Several minor transcripts were also visible, including a band of 3 kb in brain. Since the putative alternatively spliced sequence III was only detected in brain clones (Fig. 1 *B*), we probed a blot identical to that of Fig. 2 *A* with constructs generated by PCR and corresponding either to this entire sequence (Fig. 1 *A*, amino acids 350–472) or to its 5′ portion (Fig. 1 *A*, amino acids 350–390). Both probes produced an identical pattern (Fig. 2 *B* and data not shown) and labeled bands with similar mobility as those labeled by the full length probe (clone 17/12) but with different relative intensities. The most striking difference is a strong labeling of the 3-kb band in brain and the weaker labeling of transcripts migrating at the 2.2-kb region. These observations confirm the preferential inclusion of splice segment III in brain amphiphysin II. No cross-reactivity with amphiphysin I mRNA (major transcript at 4.5 kb [David et al., 1994]) was observed in the high stringency conditions at which the Northern blot analysis was performed.

To determine the electrophoretic mobility and the tissue distribution of amphiphysin II, two rabbit antibodies (CD7 and CD8) were raised against the COOH-terminal 68 amino acids of amphiphysin II and tested by Western blotting against a variety of tissues (Fig. 3 *A* and data not shown). These antibodies specifically recognized very strongly a cluster of bands around 85 kD in brain and around 60 kD in skeletal muscle (Fig. 3 *A*) and did not react with amphiphysin I. Bands of similar molecular weight were seen in other tissues (primarily lung) only after very prolonged autoradiographic exposures (not shown). In these long exposures, the 85-kD band was also detectable in skeletal muscle in agreement with the Northern blot data of Fig. 2 *B*. In addition, a prominent band of 35 kD was visible in skeletal muscle (Fig. 3 *A*). As seen by a comparison of Figs. 2 and 3 *A*, there is a discrepancy between overall levels of amphiphysin II proteins and amphiphysin II mRNAs detected in muscle and brain. This discrepancy

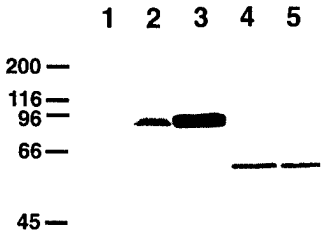

Figure 4. Comparison of the electrophoretic mobility of amphiphysin II expressed in COS-7 cells with the electrophoretic mobilities of muscle and brain amphiphysin II. Triton X-100 extracts of tissues and COS-7 cells were probed by Western blotting with the amphiphysin II specific antibody, CD7. Lanes are as follows: *1*, control untransfected COS-7 cells; *2*, rat brain; *3*, COS-7 cells transfected with clone 17/19; *4*, COS-7 cells transfected with clone 17/12; *5*, skeletal muscle. Immunoreactive bands were detected by using alkaline phosphatase-conjugated anti–rabbit IgG. Numbers at left indicate molecular weights (kD).

may be partially explained by a less efficient extractability of amphiphysin II from skeletal muscle. Alternatively, it may be due to the occurrence of major differences in amphiphysin II mRNA translation efficiency and/or in protein turnover in the two tissues.

To corroborate the identification of the brain and muscle bands as amphiphysin II, a distinct antiserum (CD9) was raised against a 15-mer peptide corresponding to amino acids 26–40 of amphiphysin I, which is identical to the corresponding region of amphiphysin II. This antibody recognized both the 128-kD brain amphiphysin I band (as the CD5 antibody does) and the bands immunoreactive with the amphiphysin II-specific antibody CD8 (Fig. 3 *B*). The CD9 antibody also recognized a few other bands in brain, suggesting the existence of additional amphiphysin isoforms. The CD7/CD8-immunoreactive 35-kD protein band of skeletal muscle was not recognized by the CD9 antibody and may therefore represent a variant of amphiphysin II that does not include its NH_2-terminal domain. (Henceforth, we will refer to the brain 85- and muscle 60-kD bands as amphiphysin IIa and IIb, respectively.)

Both amphiphysin IIa and IIb were recognized by antibodies directed against either NH_2-terminal (CD 9) or COOH-terminal (CD7 and CD8) epitopes. Their different mobility suggests therefore internal alternative splicing. Most likely, this difference reflects the presence of splice fragment III (127 amino acids) in amphiphysin IIa. This

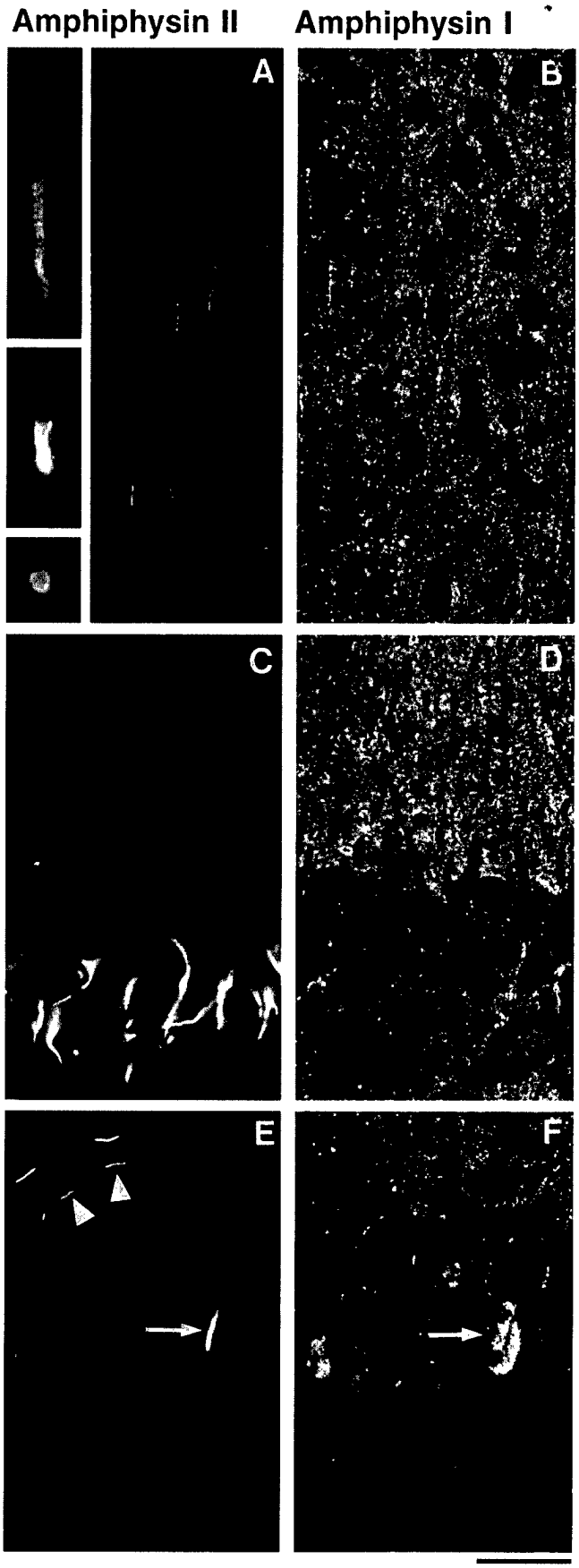

Figure 5. Comparison of the localization of amphiphysin I (mouse polyclonal serum) and amphiphysin II (rabbit antibody CD8) in rat brain. Double immunofluorescence micrographs. In all fields, amphiphysin I immunoreactivity (*B*, *D*, and *F*) has a typical nerve terminal pattern represented by small puncta throughout the gray matter. Amphiphysin II (*A*, *C*, and *E*) is primarily localized at initial axon segments. (*A* and *B*) cerebral cortex. The inset of A shows high power views of two longitudinal sections and one transverse section of initial axon segments. Note the concentration of immunoreactivity in the cortical region of the cytoplasm. (*C* and *D*) CA1 region of the hippocampus demonstrating in *C* the initial axon segments of pyramidal neurons visible in *D* as negative images. (*E* and *F*) Cerebellar cortex. Arrows point to the amphiphysin II positive initial segment of a Purkinje cell axon, which is surrounded by amphiphysin I positive nerve terminals of basket cells. Arrowheads in *E* point to initial axon segments of stellate cells. Bar, 63 μm; inset, 126 μm.

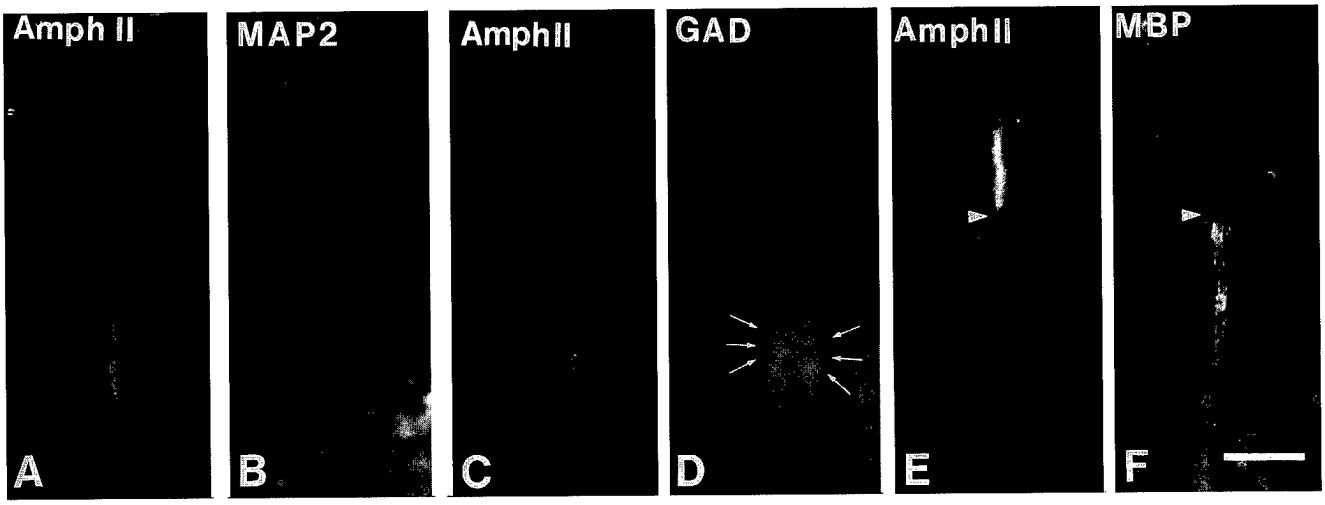

Figure 6. Double immunofluorescence micrographs demonstrating the selective localization of amphiphysin II at axon initial segments. (*A* and *B*) Amphiphysin II-MAP2 immunostaining demonstrating the emergence of the amphiphysin II positive segment from the Purkinje cell body. (*C* and *D*) Amphiphysin II-GAD immunostaining demonstrating that the immunoreactive region of the axon corresponds to its region enclosed by the GABAnergic nerve terminals (*arrows*) of basket cells. (*E* and *F*) Amphiphysin II-myelin basic protein immunostaining demonstrating that amphiphysin II immunostaining terminates abruptly (*arrowhead*) at the site where the myelin sheath begins. Bar, 126 μm.

hypothesis was supported by the transfection of COS-7 cells with clones 17/12 and 17/19. Amphiphysin II immunoreactivity induced by these transfections comigrated with amphiphysin IIa and IIb, respectively (Fig. 4). The difference of ~25 kD between amphiphysin IIa and IIb is more than the difference expected by the inclusion of 127 amino acids. However, it was previously shown that amphiphysin I has an aberrant mobility in SDS-PAGE, migrating significantly slower (~128 kD) than predicted by its amino acid sequence (76 kD; Lichte et al., 1992; David et al., 1994). This aberrant mobility is primarily due to a region (David et al., 1994) that strikingly corresponds to the alternatively spliced region III in amphiphysin II.

To determine whether the SH3 domains of amphiphysin I and II have similar properties, we carried out parallel affinity-purification experiments of brain extracts on GST fusion proteins comprising either one of the two SH3 domains. Both amphiphysin SH3 domains were equally effective in binding dynamin I, but the SH3 domain of amphiphysin II bound synaptojanin less effectively (not shown). Thus, amphiphysin I and amphiphysin II's SH3 domains have similar but not identical binding properties.

Localization of Amphiphysin II in the Nervous System

Considering their significant primary sequence similarity, amphiphysin I and II may have overlapping functions in brain. Therefore, we investigated whether these two proteins have a similar subcellular distribution by double immunofluorescence of rat brain frozen sections. Fig. 5 shows a comparison of the localization of amphiphysin I and II in three different gray matter regions of the brain: the cerebral cortex, the hippocampus, and the cerebellum. In all regions, amphiphysin I immunoreactivity (Fig. 5, *B*, *D*, and *F*) has the punctate distribution typical of nerve terminal staining. In contrast, amphiphysin II immunoreactivity occurs in the shape of short segments emerging from neuronal perikarya (Fig. 5, *A*, *C*, and *E*). In each region, the site of emergence of these processes and their shape is consistent with their identification as axon initial segments (Peters et al., 1991). High magnification views indicate that amphiphysin II is strictly confined to the cortical cytoplasm (Fig. 5 *A*, *insets*).

The specific localization of amphiphysin II at axon initial segments is further demonstrated in the high power views of cerebellar sections double stained for amphiphysin II and other protein markers (Fig. 6). Labeling for MAP2, a marker of perikarya and dendrites (De Camilli et al., 1984), demonstrates the origin of the amphiphysin II positive process from a small indentation at the basal pole of the cell (Fig. 6, *A* and *B*). Staining for glutamic acid decarboxylase, a marker of basket cell nerve terminals (Mugnaini and Oertel, 1985), shows that the amphiphysin II-positive region of the axon coincides with its unmyelinated portion innervated by basket cells (Fig. 6, *C* and *D*). Labeling for myelin basic protein illustrates the sharp boundary between the amphiphysin II-positive portion of the axon and its myelinated portion (Fig. 6, *E* and *F*).

In addition to axon initial segments, amphiphysin II immunoreactivity was also observed in spots sparsely distributed in the gray matter (which contains axons as well as neuronal perikarya and dendrites) and more densely packed in the white matter (which contains axon tracts only). These spots are illustrated in Fig. 7, *A* and *B*, which show brain regions double stained for amphiphysin II and myelin basic protein. At high power, these immunoreactive structures appear as bright rings overlapping with axonal profiles (Fig. 7 *C*), very similar to the rings of amphiphysin II immunoreactivity visible at axon initial segments. The distribution of these structures and their fine morphology allows their identification as nodes of Ranvier (Peters et al., 1991).

The presence of amphiphysin II in the cortical region of both axon initial segments and nodes of Ranvier is consis-

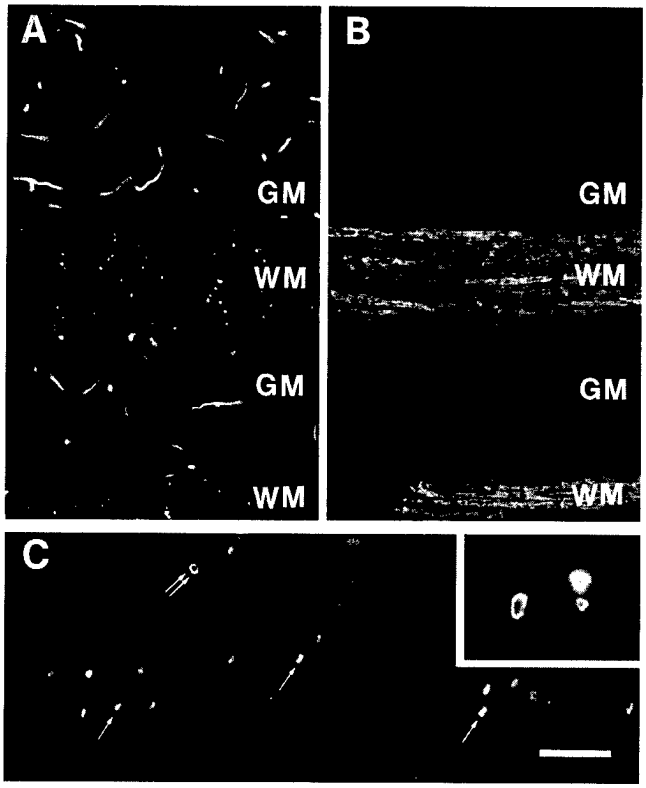

Figure 7. Localization of amphiphysin II at nodes of Ranvier. (*A* and *B*) Double immunofluorescence for amphiphysin II and myelin basic protein. Field shown is from the forebrain including two longitudinally sectioned white matter tracts. (*A*) Amphiphysin II positive axon initial segments are visible in the gray matter (*GM*). Small spots of amphiphysin II immunoreactivity visible on white matter tracts (*WM*) represent nodes of Ranvier. (*C*) White matter region in the brain stem demonstrating front (*double arrows*) and side (*single arrows*) views of nodes of Ranvier. The inset shows at high power a bundle of cross-sectioned axons demonstrating the localization of amphiphysin II in the cortical cytoplasm of nodes of Ranvier. Bar: (*A* and *B*) 27 μm; inset, 135 μm.

tent with the functional and structural similarity of these two axonal portions (Waxman and Quick, 1978). An identical localization at both sites was previously reported for a neuron-specific isoform of ankyrin3 (ankryin$_G$; Kapfhamer et al., 1995; Kordeli et al., 1995).

Localization of Amphiphysin II in Skeletal Muscle

The light microscopic localization of amphiphysin II in skeletal muscle is illustrated in Fig. 8. Amphiphysin II immunoreactivity appears as transverse striations along the muscle fiber (Fig. 8 *A*). These striations are within the I band, as shown by counterstaining of actin by fluorescent phalloidin (Fig. 8, *B* and *C*), and they flank the Z line, as shown by counterstaining for desmin (Fig. 8, *D* and *E*). The amphiphysin II stripes are similar to the stripes of ankyrin3 (ankyrin$_G$) immunoreactivity (Fig. 8, *F* and *G*, as shown by double staining of ankyrin3 and actin). Ankyrin3 was previously shown to be concentrated along plasmalemmal T tubules (Flucher et al., 1990). Accordingly, the localization of amphiphysin II was also very similar to that of triadin, a marker of T tubules (Guo et al., 1994; data not shown). Immunoreactivity for clathrin heavy chain (monoclonal antibody X22), which was previously shown to be concentrated in muscle at I bands (Muñoz et al., 1995*a*,*b*), formed stripes comprised between the amphiphysin II striations and the Z line, as shown by double staining of amphiphysin II and clathrin (Fig. 8, *H* and *I*). The glucose transporter, glut4, a protein that is internalized at least partially via clathrin coated vesicles (Garippa et al., 1996; Robinson et al., 1996), is also localized in proximity of T tubules (Muñoz et al., 1995*a*). Glut4 immunoreactivity is centered around the M line, as shown by double labeling with anti-glut4 and anti-clathrin antibodies (Fig. 8, *J* and *K*).

The localization of amphiphysin II was further investigated by immunogold labeling of ultrathin frozen sections and found to be localized in correspondence with T tubules (Fig. 9, *B* and *D*). The specificity of this labeling was confirmed by labeling similar sections for desmin. As expected, desmin immunoreactivity was concentrated along the Z line and absent from the T system (Fig. 9, *A* and *C*).

Cytoplasmic Localization of Amphiphysin II in Transfected Cells

Neither in brain nor in muscle (Figs. 5–8) was amphiphysin II found to have a nuclear localization. This was in contrast to the nuclear localization of this protein (BIN1) reported by Sakamuro et al. (1996) in transfected HepG2 cells. We examined, therefore, the localization of amphiphysin IIa and IIb in transfected COS-7 cells as well as in HepG2 cells transfected with the same clone (17/12, and under the same experimental conditions) used by Sakamuro et al. (1996). In all cases the protein was primarily localized in the cytosol (Fig. 10 and data not shown).

Discussion

We report here the characterization of an amphiphysin gene (amphiphysin II) that is primarily, but not exclusively, expressed in brain and skeletal muscle. The gene undergoes extensive alternative splicing. Amphiphysin II is substantially similar in amino acid sequence and domain structure to amphiphysin I. The strongest similarity is present in the A domain, which is predicted to form coiled coil structures (Sivadon et al., 1995), and in the D domain, which contains the SH3 domain (David et al., 1994). Domain A is characteristic of all proteins of the amphiphysin/Rvs family identified so far, including the yeast protein Rvs161, which is composed of the A domain only (David et al., 1994; Sivadon et al., 1995). Due to these similarities, the two amphiphysins are likely to have homologous functions. However, their different cellular and subcellular localizations clearly indicate that their functions are not overlapping.

In brain, amphiphysin I is concentrated in the cortical cytoplasm of nerve terminals where it participates in synaptic vesicle endocytosis (David et al., 1996; Shupliakov et al., 1997). In contrast, amphiphysin II is concentrated in axon initial segments and nodes of Ranvier. The occurrence of clathrin coated pits and clathrin coated invaginations has been reported to occur more frequently at initial segments and nodes of Ranvier than at other locations along the ax-

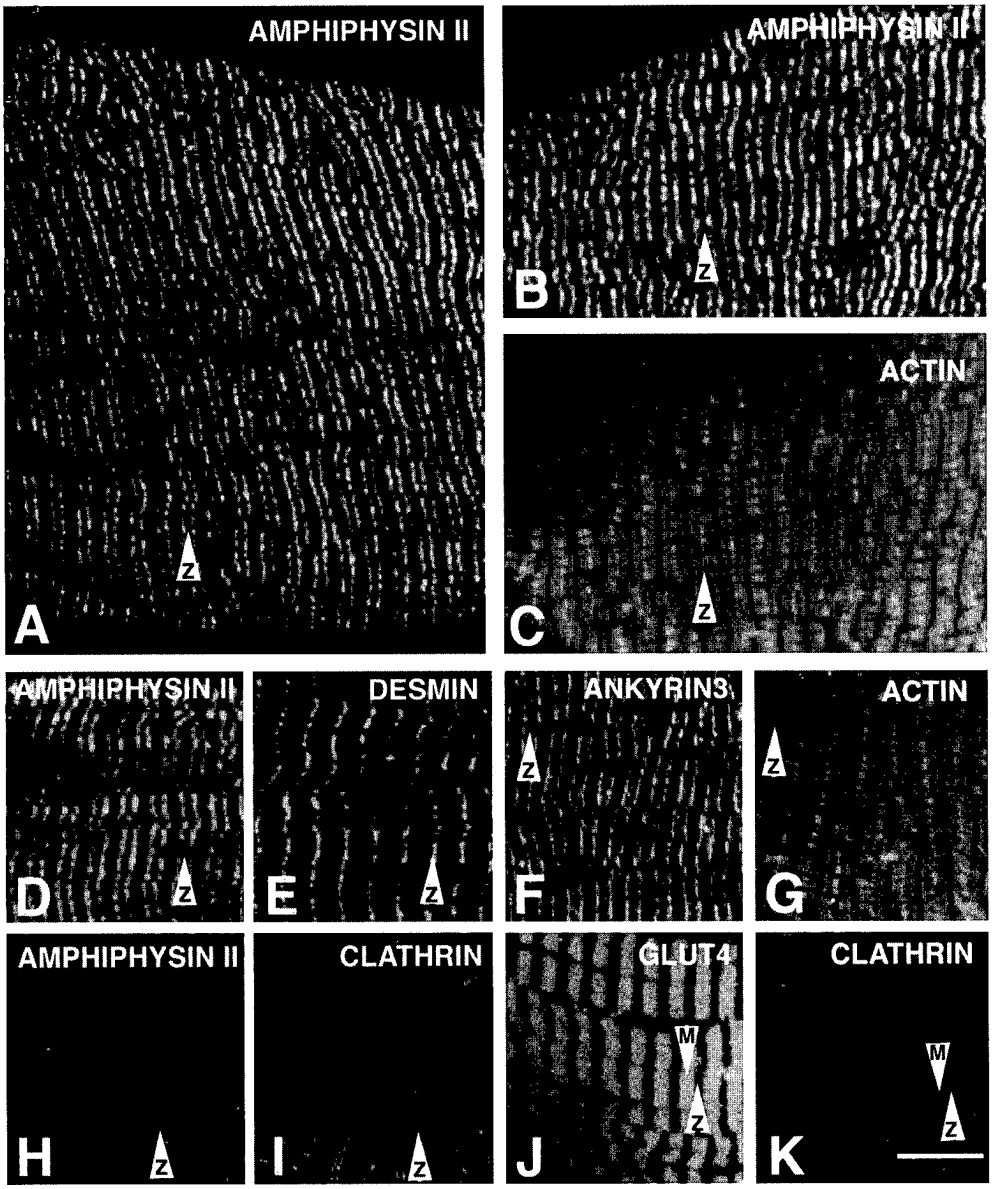

Figure 8. Immunofluorescence localization of amphiphysin II and other proteins of the sarcomere in skeletal muscle. Immunofluorescence of semithin frozen sections. Amphiphysin II immunoreactivity (*A*, *B*, *D*, and *H*) forms transverse bands that flank the Z line. *B–K* show pairs of double-fluorescence micrographs. (*B* and *C*) Amphiphysin II and actin (phalloidin staining); (*D* and *E*) amphiphysin II and desmin, a marker of the Z line; (*F* and *G*) ankyrin (ankyrin3) and actin; (*H* and *I*) amphiphysin II and clathrin heavy chain (antibody X22); (*J* and *K*) glut4 and clathrin. Arrows equal Z and M lines, as indicated. Bar, 7.9 μm.

onal surface, with the exception of nerve terminals (Karlsson, 1967; Campos-Ortega et al., 1968; Conradi, 1969). Thus, an involvement of amphiphysin II in endocytosis is plausible. However, it is unlikely that the high and specific concentration of amphiphysin II present at these sites may be simply related to endocytosis.

A characteristic feature of the cortical cytoplasm at initial segments and nodes of Ranvier is the presence of a dense matrix underlying the plasmalemma (Palay et al., 1968; Conradi, 1969; Waxman and Quick, 1978). This submembranous cytoskeleton may participate in mediating the local enrichment of special adhesion molecules (members of the neurofascin/L1 family; Shiga and Oppenheim, 1991) and of proteins required for the generation and propagation of action potentials, such as Na^+ channels (Srinivasan et al., 1988; Waxman and Ritchie, 1993), Na^+/K^+ ATPase (Nelson and Veshnock, 1987; Waxman and Ritchie, 1993), and Na^+/Ca^{2+} exchangers (Waxman and Ritchie, 1993). The only unique component of this specialized cortical cytomatrix identified so far is a neuron-specific isoform of ankyrin3 ($ankyrin_G$; Kordeli et al., 1995). Neuronal amphiphysin II may be a second component of this matrix. As in the case of amphiphysin II, the isoform of ankyrin expressed at axon initial segments and nodes of Ranvier is generated by alternative splicing of a gene (ankyrin3) that is widely expressed outside the nervous system, and at particularly high concentrations in skeletal muscle (Kordeli et al., 1995).

In skeletal muscle, amphiphysin II is concentrated around the plasmalemma of T tubules, and even here, it colocalizes with ankyrin3, previously shown to be a component of the submembranous cytoskeleton of T tubules (Flucher et al., 1990). Like axon initial segments and nodes of Ranvier, T tubules are enriched in proteins responsible for controlling ion permeability and transport (Lau et al., 1979; Flucher et al., 1990) and a specialized cytomatrix around the T tubules, including both amphiphysin II and ankyrin3, may help to define the composition and function of these plasmalemmal domains (Flucher et al., 1990). T tubules are not typically regarded as sites specialized for endocytosis. However, there is evidence that

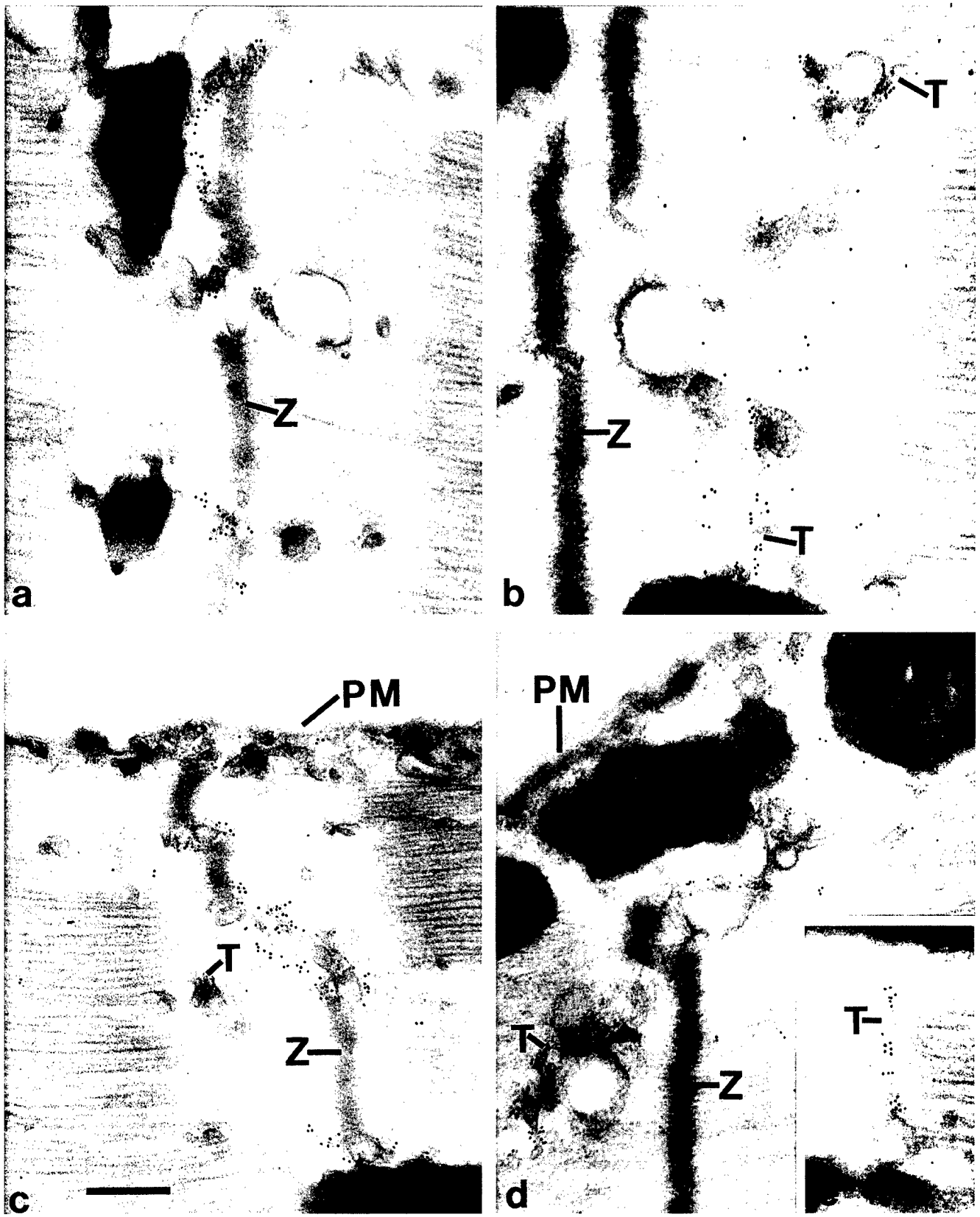

Figure 9. Comparison of the localizations of desmin and amphiphysin II in skeletal muscle by electron microscopy immunocytochemistry. Ultrathin frozen sections were labeled by immunogold for desmin (*A* and *C*) and amphiphysin II (*B*, *D* and *E*). Desmin immunoreactivity is localized on a network of filamentous structures that are in register with Z lines. Amphiphysin is selectively localized at the T system and is present on T tubules (*E*). *Z*, Z lines; *T*, T tubules; *PM*, plasmalemma. Bar: (*A*, *B*, and *E*) 300 nm; (*C* and *D*) 378 nm.

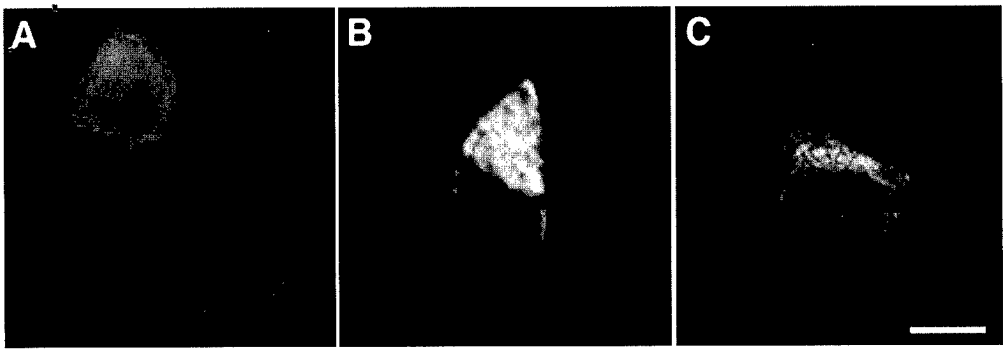

Figure 10. Immunofluorescence localization of amphiphysin II in transfected cells. (*A*) COS-7 cells transfected with clone 17-12 and examined by conventional epifluorescence light microscopy. (*B* and *C*) HepG2 cells transfected with clone 17/12 and examined by confocal microscopy. The slight fluorescence visible in *A* over the nuclei is out of the nuclei focal plane. Bar, (*A*) 12.6 μm; (*B* and *C*) 9.0 μm.

clathrin-mediated endocytosis may occur at this region. First, clathrin immunoreactivity (detected by monoclonal antibody X22) is present in proximity of T tubules as previously reported (Kaufman et al., 1990) and further confirmed by this study. This clathrin heavy chain is likely to correspond to the skeletal muscle specific clathrin recently described by several groups (Gong et al., 1996; Kedra et al., 1996; Lindsay et al., 1996; Sirotkin et al., 1996). Second, the glut4 transporter, which undergoes regulated surface exposure in response to insulin (Wang et al., 1996) and is internalized at least in part via clathrin coated vesicles (Garippa et al., 1996; Robinson et al., 1996), is concentrated along the T system and surrounding vesicles (Slot et al., 1991; Muñoz et al., 1995*a*,*b*).

In yeast, mutations in either the *Rvs161* and/or the *RVS167* genes produce both endocytosis defects and defects in the function of the peripheral actin cytoskeleton, including abnormal polarity, uneven cell size and morphology, and delocalization of actin patches (Munn et al., 1995; Sivadon et al., 1995). The COOH-terminal region of Rvs167 was identified in a two hybrid screen for actin binding proteins (Amberg et al., 1995). More generally, yeast studies have demonstrated an important role of the actin cytoskeleton in endocytosis, thus raising the possibility that effects of *RVS* mutations on endocytosis and the peripheral cytoskeleton may be interrelated (Munn and Riezman, 1994; Amberg et al., 1995; Munn et al., 1995).

Our present demonstration that amphiphysin II is localized in the cortical cytomatrix of specialized regions of axons and muscle is consistent with the role of the *RVS* genes in actin function. A dual role in endocytosis and in the dynamics of the peripheral cytoskeleton may be a general characteristic of amphiphysin/Rvs family proteins. The strong implication of amphiphysin I in synaptic vesicle endocytosis may reflect the unique specialization of the presynaptic actin cytomatrix for this function.

An additional phenotype produced by mutations in the *RVS* genes is reduced viability upon starvation, a phenotype displayed by an inability of the cell to enter in stationary phase under these conditions (Crouzet et al., 1991; Bauer et al., 1993). Since amphiphysin I was shown to be an autoantigen in breast cancer (De Camilli et al., 1993; David et al., 1994, 1996), it was speculated (David et al., 1994) that proteins of the amphiphysin/Rvs family, like other proteins of the cortical cell cytomatrix that can act as tumor suppressors (Rubinfeld et al., 1993; Tsukita et al., 1993), may be directly implicated in cancer.

While this study was in progress, sequences of amphiphysin II isoforms were independently published in the context of two studies. A first study reported the identification of mouse muscle amphiphysin II during a search for novel SH3-containing proteins (Sparks et al., 1996). This protein (SH3P9) was not further characterized. A second study identified a fragment of murine amphiphysin II in a yeast two hybrid screen for MYC binding proteins (Sakamuro et al., 1996). The authors of this study went on to isolate a human amphiphysin II isoform, BIN1, which is identical to our clone 17/12, and to demonstrate that this protein is localized in the nucleus and has the properties of a tumor suppressor gene. These findings are consistent with the presence of a nuclear localization sequence in BIN1 (Sakamuro et al., 1996), which we show here to be encoded by splice fragment II (Fig. 1 *B*). In our study, however, we do not have any evidence for a nuclear localization of amphiphysin II in adult muscle or brain. Our results, therefore, argue for a primary function of amphiphysin II in the cytoplasm, although they clearly do not exclude that amphiphysin II may shuttle from the cytoplasm to the nucleus and that it may function in a signaling pathway from the cell periphery to the nucleus. It was shown previously that proteins of the submembranous cytoskeleton (e.g., the tight junction protein ZO1 [Gottardi et al., 1996]) have a nuclear localization under certain conditions. Thus, the possibility that amphiphysin II may participate in nuclear events and even be concentrated in the nucleus under certain functional states cannot be ruled out.

In conclusion, we suggest that amphiphysin/Rvs proteins may play a general role in the physiology of the peripheral cytoskeleton which underlies the plasmalemma. Different isoforms, generated either by distinct genes or by alternative splicing of the same genes, may serve to adapt this general role to specific functions of specialized cell surface domains. Given the central importance of the subplasmalemmal cytomatrix in a variety of cellular processes, including vesicular trafficking to and from the plasmalemma, generation of regional heterogeneity of plasmalemma, signal transduction, and regulation of cell–cell interaction, the components of this matrix are likely to have pleiotropic functions. Further studies of amphiphysin family members may not only reveal new aspects of the function of the peripheral cytoskeleton and endocytosis, but also help elucidate a novel signaling pathway from the cell surface to the nucleus. The reported connection between amphiphysin I autoimmunity and cancer (Folli et al., 1993; De

Camilli et al., 1993) suggests that these studies may be of relevance to the biology of at least some forms of human cancer.

We thank Corinne Leprince for discussing unpublished data.

This study was supported by grants from the Donaghue Foundation, the Human Frontier Science Program Organization, and the National Institutes of Health (CA46128) to P. De Camilli. D. Grabs was a recipient of a Deutscher Akademischer Austauschdienst fellowship, C. David of a United States Army Medical Research and Development Command fellowship, and O. Cremona of Telethon and Human Frontier Science Program Organization long-term fellowships.

Received for publication 9 December 1996 and in revised form 21 April 1997.

References

Amberg, D.C., E. Basart, and D. Botstein. 1995. Defining protein interactions with yeast actin in vivo. *Nat. Struct. Biol.* 2:28–35.

Bauer, F., M. Urdaci, M. Aigle, and M. Crouzet. 1993. Alteration of a yeast SH3 protein leads to conditional viability with defects in cytoskeletal and budding patterns. *Mol. Cell. Biol.* 13:5070–5084.

Bogue, C.W., I. Gross, H. Vasavada, D.W. Dynia, C.M. Wilson, and H.D. Jacobs. 1994. Identification of Hox genes in newborn lung and effects of gestational age and retinoic acid on their expression. *Am. J. Physiol.* 266:L448–454.

Brodsky, F.M. 1985. Clathrin structure characterized with monoclonal antibodies. I. Analysis of multiple antigenic sites. *J. Cell Biol.* 101:2047–2054.

Campos-Ortega, J.A., P. Glees, and V. Neuhoff. 1968. Ultrastructural analysis of individual layers in the lateral geniculate body of the monkey. *Z. Zellforsch. Mikrosk. Anat.* 87:82–100.

Chang, Y.C., and D.I. Gottlieb. 1988. Characterization of the proteins purified with monoclonal antibodies to glutamic acid decarboxylase. *J. Neurosci.* 8: 2123–2130.

Chen, C., and H. Okayama. 1987. High-efficiency transformation of mammalian cells by plasmid DNA. *Mol. Cell. Biol.* 7:2745–2752.

Conradi, S. 1969. Observations on the ultrastructure of the axon hillock and initial axon segment of lumbosacral motoneurons in the cat. *Acta. Physiol. Scand. Suppl.* 332:65–84.

Crouzet, M., M. Urdaci, L. Dulau, and M. Aigle. 1991. Yeast mutant affected for viability upon nutrient starvation: characterization and cloning of the RVS161 gene. *Yeast.* 7:727–743.

David, C., M. Solimena, and P. De Camilli. 1994. Autoimmunity in stiff-Man syndrome with breast cancer is targeted to the C-terminal region of human amphiphysin, a protein similar to the yeast proteins, Rvs167 and Rvs161. *FEBS (Fed. Eur. Biochem. Soc.) Letts.* 351:73–79.

David, C., P.S. McPherson, O. Mundigl, and P. De Camilli. 1996. A role of amphiphysin in synaptic vesicle endocytosis suggested by its binding to dynamin in nerve terminals. *Proc. Natl. Acad. Sci. USA.* 93:331–335.

De Camilli, P., R. Cameron, and P. Greengard. 1983. Synapsin I (protein I), a nerve terminal-specific phosphoprotein. I. Its general distribution in synapses of the central and peripheral nervous system demonstrated by immunofluorescence in frozen and plastic sections. *J. Cell Biol.* 96:1337–1354.

De Camilli, P., P.E. Miller, F. Navone, W.E. Theurkauf, and R.B. Vallee. 1984. Distribution of microtubule-associated protein 2 in the nervous system of the rat studied by immunofluorescence. *Neuroscience.* 11:817–846.

De Camilli, P., A. Thomas, R. Cofiell, F. Folli, B. Lichte, G. Piccolo, H.M. Meinck, M. Austoni, G. Fassetta, G.F. Bottazzo, et al. 1993. The synaptic vesicle-associated protein amphiphysin is the 128-kD autoantigen of Stiff-Man syndrome with breast cancer. *J. Exp. Med.* 178:2219–2223.

Devarajan, P., P.R. Stabach, A.S. Mann, T. Ardito, M. Kashgarian, and J.S. Morrow. 1996. Identification of a small cytoplasmic ankyrin (AnkG119) in the kidney and muscle that binds β I σ spectrin and associates with the Golgi apparatus. *J. Cell Biol.* 133:819–830.

Flucher, B.E., M.E. Morton, S.C. Froehner, and M.P. Daniels. 1990. Localization of the α1 and α2 subunits of the dihydropyridine receptor and ankyrin in skeletal muscle triads. *Neuron.* 5:339–351.

Folli, F., M. Solimena, R. Cofiell, M. Austoni, G. Tallini, G. Fassetta, D. Bates, N. Cartlidge, G.F. Bottazzo, G. Piccolo, et al. 1993. Autoantibodies to a 128-kd synaptic protein in three women with the Stiff-Man syndrome and breast cancer. *New Engl. J. Med.* 328:546–551.

Garippa, R.J., A. Johnson, J. Park, R.L. Petrush, and T.E. McGraw. 1996. The carboxyl terminus of GLUT4 contains a serine-leucine-leucine sequence that functions as a potent internalization motif in Chinese hamster ovary cells. *J. Biol. Chem.* 271:20660–20668.

Gong, W., B.S. Emanuel, J. Collins, D.H. Kim, Z. Wang, F. Chen, G. Zhang, B. Roe, and M.L. Budarf. 1996. A transcription map of the DiGeorge and velocardio-facial syndrome minimal critical region on 22q11. *Hum. Mol. Genet.* 5:789–800.

Gottardi, C.J., M. Arpin, A.S. Fanning, and D. Louvard. 1996. The junction-associated protein, zonula occludens-1, localizes to the nucleus before the maturation and during the remodeling of cell-cell contacts. *Proc. Natl. Acad. Sci. USA.* 93:10779–10784.

Grabs D, V. Slepnev, Z. Songyang, C. David, M. Lynch, L.C. Cantley, and P. De Camilli. 1997. The SH3 domain of amphiphysin binds the proline rich domain of dynamin at a single site which defines a new SH3 binding consensus sequence. *J. Biol. Chem.* 272:13419–13425.

Guo, W., A.O. Jorgensen, and K.P. Campbell. 1994. Characterization and ultrastructural localization of a novel 90-kDa protein unique to skeletal muscle junctional sarcoplasmic reticulum. *J. Biol. Chem.* 269:28359–28365.

Kapfhamer, D., D.E. Miller, S. Lambert, V. Bennett, T.W. Glover, and M. Burmeister. 1995. Chromosomal localization of the ankyrinG gene (ANK3/Ank3) to human 10q21 and mouse 10. *Genomics.* 27:189–191.

Karlsson, U.L. 1967. Three-dimensional studies of neurons in the lateral geniculate nucleus of the rat. III. Specialized neuronal contacts in the neuropile. *J. Ultrastruct. Res.* 17:137–157.

Kaufman, S.J., D. Bielser, and R.F. Foster. 1990. Localization of anti-clathrin antibody in the sarcomere and sensitivity of myofibril structure to chloroquine suggest a role for clathrin in myofibril assembly. *Exp. Cell Res.* 191: 227–238.

Kedra, C., M. Peyrard, I. Fransson, J.E. Collins, I. Dunham, B.A. Roe, and J.P. Dumanski. 1996. Characterization of a second human clathrin heavy chain polypeptide gene (*CLH-22*) from chromosome 22q11. *Hum. Mol. Genet.* 5: 625–631.

Keller, G.A., K.T. Tokuyasu, A.H. Dutton, and S.J. Singer. 1984. An improved procedure for immunoelectron microscopy: ultrathin plastic embedding of immunolabeled ultrathin frozen sections. *Proc. Natl. Acad. Sci. USA.* 81: 5744–5747.

Koenig, J.H., and K. Ikeda. 1989. Disappearance and reformation of synaptic vesicle membrane upon transmitter release observed under reversible blockage of membrane retrieval. *J. Neurosci.* 9:3844–3860.

Kordeli, E., S. Lambert, and V. Bennett. 1995. AnkyrinG. A new ankyrin gene with neural-specific isoforms localized at the axonal initial segment and node of Ranvier. *J. Biol. Chem.* 270:2352–2359.

Kosaka, T., and K. Ikeda. 1983. Possible temperature-dependent blockage of synaptic vesicle recycling induced by a single gene mutation in Drosophila. *J. Neurobiol.* 14:207–225.

Laemmli, U.K. 1970. Cleavage of structural proteins during the assembly of the head of bacteriophage T4. *Nature (Lond.).* 227:680–685.

Lau, H.Y., A.H. Caswell, H. Garcia, and L. Letelier. 1979. Ouabain binding and coupling sodium, potassium and chloride transport in isolated transverse tubules from skeletal muscle. *J. Gen. Physiol.* 74:335–349.

Lichte, B., R.W. Veh, H.E. Meyer, and M.W. Kilimann. 1992. Amphiphysin, a novel protein associated with synaptic vesicles. *EMBO (Eur. Mol. Biol. Organ.) J.* 11:2521–2530.

Lindsay, E.A., P. Rizzu, R. Antonacci, V. Jurecic, J. Delmas-Mata, C.C. Lee, U.J. Kim, P.J. Scambler, and A. Baldini. 1996. A transcription map in the CATCH22 critical region: identification, mapping, and ordering of four novel transcripts expressed in heart. *Genomics.* 32:104–112.

Lupas, A. 1996. Prediction and analysis of coiled-coil structures. *Methods Enzymol.* 266:513–525.

McPherson, P.S., K. Takei, S.L. Schmid, and P. De Camilli. 1994. p145, a major Grb2-binding protein in brain, is co-localized with dynamin in nerve terminals where it undergoes activity-dependent dephosphorylation. *J. Biol. Chem.* 269:30132–30139.

McPherson, P.S., E.P. Garcia, V.I. Slepnev, C. David, X.M. Zhang, D. Grabs, W.S. Sossin, R. Bauerfeind, Y. Nemoto, and P. De Camilli. 1996. A presynaptic inositol-5-phosphatase. *Nature (Lond.).* 379:353–357.

Mugnaini, E., and W.H. Oertel. 1985. An atlas of the distribution of GABAnergic neurons and terminals in the rat CNS as revealed by GAD immunocytochemistry. *In* Handbook of Chemical Neuroanatomy. Vol 4: GABA and Neuropeptides in the CNS. A. Bjorklund and T. Hokfelt, editors. Elsevier Science Publishers, Amsterdam, The Netherlands. 436–608.

Munn, A.L., and H. Riezman. 1994. Endocytosis is required for the growth of vacuolar H(+)-ATPase-defective yeast: identification of six new END genes. *J. Cell Biol.* 127:373–386.

Munn, A.L., B.J. Stevenson, M.I. Geli, and H. Riezman. 1995. end5, end6, and end7: mutations that cause actin delocalization and block the internalization step of endocytosis in Saccharomyces cerevisiae. *Mol. Biol. Cell.* 6:1721–1742.

Muñoz, P., M. Rosemblatt, X. Testar, M. Palacin, G. Thoidis, P.F. Pilch, and A. Zorzano. 1995*a*. The T-tubule is a cell-surface target for insulin-regulated recycling of membrane proteins in skeletal muscle. *Biochem. J.* 307:393–400.

Muñoz, P., M. Rosemblatt, X. Testar, M. Palacin, and A. Zorzano. 1995*b*. Isolation and characterization of distinct domains of sarcolemma and T-tubules from rat skeletal muscle. *Biochem. J.* 307:273–280.

Nelson, W.J., and P.J. Veshnock. 1987. Ankyrin binding to (Na+ + K+)ATPase and implications for the organization of membrane domains in polarized cells. *Nature (Lond.).* 328:533–536.

Palay, S.L., C. Sotelo, A. Peters, and P.M. Orkand. 1968. The axon hillock and the initial segment. *J. Cell Biol.* 38:193–201.

Peters, A., S. Palay, and H. Webster. 1991. The axon. *In* The Fine Structure of the Nervous System. A. Peters, S.L. Palay, and H. Webster, editors. Oxford University Press, New York. 101–137.

Robinson, L.J., S. Pang, D.S. Harris, J. Heuser, and D.E. James. 1996. Translocation of the glucose transporter (GLUT4) to the cell surface in permeabi-

lized 3T3-L1 adipocytes: effects of ATP, insulin, and GTP gamma S and localization of GLUT4 to clathrin lattices. *J. Cell Biol.* 117:1181–1196.

Rubinfeld, B., B. Souza, I. Albert, O. Muller, S.H. Chamberlain, F.R. Masiarz, S. Munemitsu, and P. Polakis. 1993. Association of the APC gene product with β-catenin. *Science (Wash. DC).* 262:1731–1734.

Sakamuro, D., K.J. Elliott, R. Wechsler-Reya, and G.C. Prendergast. 1996. BIN1 is a novel MYC-interacting protein with features of a tumour suppressor. *Nat. Gen.* 14:69–76.

Shiga, T., and M.W. Oppenheim. 1991. Immunolocalization studies of putative guidance molecules used by axons and growth cones of intersegemental interneurons in the chick embryo spinal cord. *J. Comp. Neurol.* 310:234–252.

Shpetner, H.S., and R.B. Vallee. 1989. Identification of dynamin, a novel mechanochemical enzyme that mediates interactions between microtubules. *Cell.* 59:421–432.

Shupliakov, O., P. Low, D. Grabs, H. Gad, H. Chen, C. David, K. Takei, P. De Camilli, and L. Brodin. 1997. Synaptic vesicle endocytosis impaired by disruption of dynamin-SH3 domain interactions. *Science (Wash. DC).* 276:259–263.

Sirotkin, H., B. Morrow, R. DasGupta, R. Goldberg, S.R. Patanjali, G. Shi, L. Cannizzaro, R. Shprintzen, S. Weissman, and R. Kucherlapati. 1996. Isolation of a new clathrin heavy chain gene with muscle-specific expression from the region commonly deleted in the velo-cardio-facial syndrome. *Human Mol. Genet.* 5:617–624.

Sivadon, P., F. Bauer, M. Aigle, and M. Crouzet. 1995. Actin cytoskeleton and budding pattern are altered in the yeast rvs161 mutant: The Rvs161 protein shares common domains with the brain protein amphiphysin. *Mol. Gen. Genet.* 246:485–495.

Slot, J.W., H.J. Geuze, S. Gigengack, D.E. James, and G.E. Lienhard. 1991. Translocation of the glucose transporter GLUT4 in cardiac myocytes of the rat. *Proc. Natl. Acad. Sci. USA.* 88:7815–7819.

Sparks, A.B., N.G. Hoffman, S.J. McConnell, D.M. Fowlkes, and B.K. Kay. 1996. Cloning of ligand targets: systemic isolation of SH3 domain-containing proteins. *Nat. Biotechnol.* 14:741–744.

Srinivasan, Y., L. Elmer, J. Davis, V. Bennett, and K. Angelides. 1988. Ankyrin and spectrin associate with voltage-dependent sodium channels in brain. *Nature (Lond.).* 333:177–180.

Takei, K., P.S. McPherson, S.L. Schmid, and P. De Camilli. 1995. Tubular membrane invaginations coated by dynamin rings are induced by GTP-γ S in nerve terminals. *Nature (Lond.).* 374:186–190.

Tokuyasu, K.T. 1989. Use of poly(vinylpyrrolidone) and poly(vinyl alcohol) for cryoultramicrotomy. *Histochem. J.* 21:163–171.

Towbin, H., T. Staehelin, and J. Gordon. 1979. Electrophoretic transfer of proteins from polyacrylamide gels to nitrocellulose sheets: procedure and some applications. *Proc. Natl. Acad. Sci. USA.* 76:4350–4354.

Tsukita, S., M. Itoh, A. Nagafuchi, S. Yonemura, and S. Tsukita. 1993. Submembranous junctional plaque proteins include potential tumor suppressor molecules. *J. Cell Biol.* 123:1049–1053.

Wang, L.H., T.C. Südhof, and R.G.W. Anderson. 1995. The appendage domain of α-adaptin is a high affinity binding site for dynamin. *J. Biol. Chem.* 270: 10079–10083.

Wang, W., P.A. Hansen, B.A. Marshall, J.O. Holloszy, and M. Mueckler. 1996. Insulin unmasks a COOH-terminal glut4 epitope and increases glucose transport across T-tubules in skeletal muscle. *J. Cell Biol.* 135:415–430.

Waxman, S.G., and D.C. Quick. 1978. Intra-axonal ferric ion-ferrocyanaide staining of nodes of Ranvier and initial segments in central myelinated fibers. *Brain Res.* 144:1–10.

Waxman, S.G., and J.M. Ritchie. 1993. Molecular dissection of the myelinated axon. *Ann. Neurol.* 33:121–136.

Molecular Medicine 4: 29-39, 1998

Molecular Medicine

Expression of Amphiphysin I, an Autoantigen of Paraneoplastic Neurological Syndromes, in Breast Cancer

Scott Floyd,[1] Margaret Husta Butler,[1] Ottavio Cremona,[1] Carol David,[1] Zachary Freyberg,[1] Xiaomei Zhang,[1] Michele Solimena,[2] Akira Tokunaga,[3] Hideki Ishizu,[4] Kimiko Tsutsui,[3] and Pietro De Camilli[1]

[1]Howard Hughes Medical Institute, Department of Cell Biology and [2]Department of Medicine, Yale University School of Medicine, New Haven, Connecticut, U.S.A.
[3]Third Department of Anatomy and [4]Department of Neuropsychiatry, Okayama University Medical School, Okayama, Japan

Communicated by V. T. Marchesi. Accepted November 24, 1997.

Abstract

Amphiphysin I is a 128 kD protein highly concentrated in nerve terminals, where it has a putative role in endocytosis. It is a dominant autoantigen in patients with stiff-man syndrome associated with breast cancer, as well as in other paraneoplastic autoimmune neurological disorders. To elucidate the connection between amphiphysin I autoimmunity and cancer, we investigated its expression in breast cancer tissue. We report that amphiphysin I was expressed as two isoforms of 128 and 108 kD in the breast cancer of a patient with anti-amphiphysin I antibodies and paraneoplastic sensory neuronopathy. Amphiphysin I was also detectable at variable levels in several other human breast cancer tissues and cell lines and at low levels in normal mammary tissue and a variety of other non-neuronal tissues. The predominant amphiphysin I isoform expressed outside the brain in humans is the 108 kD isoform which represents an alternatively spliced variant of neuronal amphiphysin I missing a 42 amino acid insert. Our study suggests a link between amphiphysin I expression in cancer and amphiphysin I autoimmunity. The enhanced expression of amphiphysin I in some forms of cancer supports the hypothesis that amphiphysin family members may play a role in the biology of cancer cells.

Introduction

Amphiphysin I is an SH3 domain–containing protein expressed at high levels in the nervous system (1,2). It is concentrated in axon terminals where it has a putative role in synaptic vesicle endocytosis (2–4) and growth cone dynamics (5). Outside the nervous system, it was reported to have a restricted distribution (1,6).

Address correspondence and reprint requests to: Dr. Pietro De Camilli, Department of Cell Biology, Howard Hughes Medical Institute, 295 Congress Ave., New Haven, CT 06510, U.S.A. Phone: (203) 737-4465; Fax: (203) 737-1762; E-mail: pietro.decamilli@yale.edu

Amphiphysin I has been identified as an autoantigen in human neurological paraneoplastic autoimmune diseases, often in association with breast cancer (6–9). The proposed scenario for these paraneoplastic syndromes is that (*i*) neoplastic transformation of a non-neuronal tissue results in ectopic expression of a neuronal protein in that tissue, and (*ii*) ectopic expression leads to anti-nervous system autoimmunity and neurological disease (10,11). Autoantigen expression in cancer has been reported in many cases (10,11), and it is possible that autoantigen expression may be involved in the biology of cancer.

Studies on members of the amphiphysin family have suggested a relationship between this protein family and the regulation of cell proliferation. Two proteins sharing blocks of homology with amphiphysin, Rvs161 and Rvs167, are present in *Saccaromyces cerevisiae* (12–15). The *RVS* (*r*educed *v*iability upon *s*tarvation) phenotype, which led to the identification of genes encoding these proteins, suggests the loss of regulatory feedback between availability of nutrients in the medium and growth (12,13). A homologue of amphiphysin I, amphiphysin II, has recently been described in mammalian cells. Amphiphysin II undergoes extensive alternative splicing, resulting in multiple isoforms with different tissue and subcellular distributions (16–22). One of these isoforms, BIN1, was reported to interact with the MYC proto-oncogene and to act as a negative regulator of cell proliferation (17). Another isoform was found to interact with the proto-oncogene cABL (23). It is therefore of interest to characterize amphiphysin I expression in cancer cells.

We show here that amphiphysin I is more widely expressed in non-neuronal tissues than previously reported, although its concentration in non-neuronal tissues is much lower than in brain. We also demonstrate enhanced expression of amphiphysin I isoforms in several breast cancer tissues and cell lines, including the tissue of a patient with paraneoplastic sensory neuronopathy.

Materials and Methods

Antibodies

Rabbit polyclonal antibodies directed against amphiphysin I (CD5) (14), amphiphysin I and II (CD9) (19), synaptojanin (24), dynamin (25), synapsin I (26), and synaptophysin (27) were previously described. Anti-vimentin monoclonal antibodies were obtained from Boehringer-Mannheim. Human anti-amphiphysin I positive sera from paraneoplastic patients were previously described (6,7). Mouse monoclonal antibodies were generated as described (28,29) using full-length His-tagged human amphiphysin I as the immunogen. Initial screening of hybrid clones was performed by Western blotting. The strongest 28 clones were selected and analyzed for their reactivity with amphiphysin I fragments expressed as GST fusion proteins in the pGEX-2T vector (Pharmacia) as previously described (14) (see also Fig. 4). The reactivity of the individual clones was as follows: Fragment 1: clones AI1, AI2, AI6, AI7, AI8, AI9, AI17, AI18, AI19, AI20, AI21, AI22, AI23; Fragment 2: clones AI15, AI16, AI24, AI25, AI26; Fragments 2 and 3: clones AI11, AI12, AI13, AI27, AI28; Fragment 3: clone AI14; Fragment 4: clone AI5; Fragment 5; clones AI3, AI4, AI10.

Human and Rat Tissues

Breast tissue from Patient 692 was collected at surgery and immediately quick-frozen in liquid N_2. Other frozen human tissues were obtained from the Critical Technologies Service at Yale University and from the National Breast Cancer Tissue Resource of the San Antonio SPORE (Specialized Program of Research Excellence). Fresh rat tissues were obtained from euthanized animals and quick-frozen in liquid N_2. Tissues were pulverized under liquid N_2 and solubilized (4 μl/mg tissue) in buffer A (150 mM NaCl, 10 mM Hepes (pH 7.5), 2% SDS, plus 4 μg/ml each of pepstatin, aprotinin, leupeptin, and phenylmethylsulfonyl fluoride).

Cell Culture and Affinity Chromatography

Human breast cell lines Hs578T, Hs578Bst, MCF7, MBA-MD-453, MDA-MB-231, SK-BR3, and MCF10 were either purchased from the American Type Culture Collection or obtained from Dr. David Stern (Yale University) and maintained as described earlier (30). Protein extracts for SH3 affinity-chromatography were prepared by lysing cells at 4°C in buffer A in which 2% SDS had been replaced with 2% Triton ×100 at 4°C. The extract was then clarified at 100,000 × *g* for 30 min. Affinity-chromatography of the extract on GST and GST fusion proteins comprising the proline-rich domain of human dynamin I (DynPRD 751-848) or a truncated form of this domain missing the amphiphysin I binding site (DynPRD 751-832) was performed as described earlier (25).

cDNA Cloning

Total RNA was extracted from approximately 10^{10} Hs578T cells using the guanidinium thiocyanate method (31) and a random and oligo dT primed cDNA library in λZAPII phage vector was constructed (Stratagene custom library service). A probe corresponding to bp 1573–2163 of the human brain amphiphysin I sequence (accession #U07616) (15) was constructed by polymerase chain reaction (PCR) from the human amphiphysin I complete cDNA using primers (forward) 5′-CTGCCGGGGAAGGAGTAAGTTT-3′

and (reverse) 5′-CCTAATCTAAGCGTCGGGTGA AGT-3′. This probe was radioactively labeled by primer direct labeling (32) and used to screen 1×10^6 plaques of the custom library. Five positive clones were identified (clones 1.4, 3.3, 3.4, 16.1, 16.3). Clone 3.4 was sequenced with an ABI automatic sequencer (Keck Biotechnology Foundation, Yale University) and found to contain a full-length coding sequence and untranslated 5′ and 3′ regions (accession #AF034996).

RT-PCR

Total RNA was extracted from either approximately 10^{10} Hs578T cells or 100–300 mg of human tissue (obtained from the Yale Critical Technology service) using the guanidinium method (31). The extracted total RNA was then reverse transcribed using Superscript II reverse transcriptase (Gibco), treated with RNAse, and purified with Glass Max columns (Gibco), and the resulting cDNA was amplified by PCR using overlapping primers designed to span the length of amphiphysin I. The primer sequences were as follows and were located in the following positions of the human amphiphysin I complete cDNA (accession # U07616) (15): #1 Forward 5′-TATGGGCGGGAAGATGTGAAAATG-3′ bp 1573–1594, Reverse 5′-CGGGAGACGCAGGTGC TAATGTAT-3′ bp 2163–2140; #2 Forward 5′-CCAGCACGGCCTCGGTCAC-3′ bp 936–954, Reverse 5′-TCTGTGGGTGGAGCCTGTT-3′ bp 1394–1371; #3 Forward 5′-AGCCGGCTTCTGGT GGTTCATT-3′ bp 1252–1273, Reverse 5′-CGCG TCCTCGGTGGTCTCC-3′ bp 1790–1772; #4 Forward 5′-CTGCCGGGGAAGGAGTAAGTTT-3′ bp 1573–1594, Reverse 5′-CCTAATCTAAGCGTCG GGTGAAGT-3′ bp 2163–2140; #5 Forward 5′-ATGGGCGGGAAGATGTGAAAATGG-3′ bp 343–366, Reverse 5′-TCTGTGGGTGGAGCCTGTT-3′ bp 1375–1357; #6 Forward 5′-TCACCCCGACA AAGGAACT-3′ bp 1000–1018, Reverse 5′-TAA AAACCCCGTAACTGAGC-3′ bp 2205–2186. Standard PCR techniques were employed. Amplified bands were analyzed by 1% agarose gel electrophoresis and ethidium bromide staining. Bands showing a molecular weight different from the predicted were purified from the gel and directly sequenced as above.

In Vitro Translation

cDNA clones in the Bluescript vector (Stratagene) were transcribed and translated in vitro using the TnT Coupled Reticulocyte Lysate system (Promega). One microgram of DNA was included in each reaction. A 5-μl aliquot of this reaction was then analyzed by Western blot.

Miscellaneous Procedures

Proteins were assayed by the BCA method (Pierce Pharmaceuticals). SDS-PAGE and Western blotting were carried out according to the method of Laemmli (33) and Towbin et al. (34), respectively.

Results

Amphiphysin I Autoimmunity in a Patient with Breast Cancer and Sensory Neuronopathy

A search for the presence of autoantibodies in a 44-year-old female patient with breast cancer and paraneoplastic sensory neuronopathy (Patient 692) led to the identification of high-titer anti-amphiphysin I antibodies in her serum and cerebrospinal fluid. The clinical history of this patient will be described in more detail in a separate case report (K. Tsutsui, unpublished observations). The amphiphysin I band was the only band recognized in rat or human brain by both the serum and the cerebrospinal fluid of the patient (Fig. 1 and data not shown). Autoantibodies of this patient did not recognize amphiphysin II in Western blots, as shown by a comparison with the labeling pattern produced by the CD9 rabbit serum (19) which recognizes both amphiphysin I and II (Fig. 1A). The autoantibodies of the patient were directed primarily against the COOH terminal region of the amphiphysin I (Fig. 1B), which is in agreement with results obtained previously with other paraneoplastic patients (ref. 14 and data not shown). We note that, whereas all sera of paraneoplastic patients have in common their reactivity with the COOH-terminal region of amphiphysin I, (ref. 14 and this study), this is not the immunodominant portion of the molecule as revealed by epitope mapping of a panel of 30 mouse monoclonal antibodies (data not shown and see Materials Methods), which suggests that the autoimmune response to amphiphysin I is not simply an exaggerated response to an immunodominant epitope.

Amphiphysin I Expression in Breast Cancer Tissue of Patient 692

A sample of cancer tissue from Patient 692 was obtained at surgery and analyzed for the expression of amphiphysin I immunoreactivity by

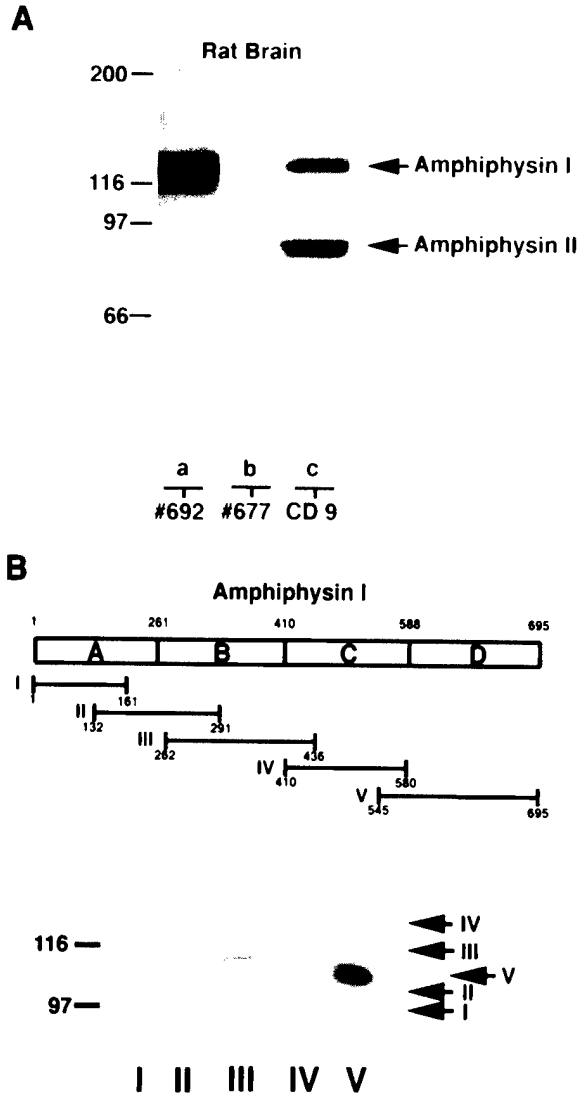

Fig. 1. Identification of anti-amphiphysin I autoimmunity in the serum of a patient with paraneoplastic sensory neuronopathy (Patient 692). (A) Total rat brain homogenate was analyzed by Western blotting with the following sera: (a) serum of the patient, (b) serum of a normal control patient, (c) rabbit serum CD9 that recognizes amphiphysin I and II (19). (B) The epitope specificity of the autoantibodies from Patient 692 was mapped by Western blot using GST fragments corresponding to the overlapping fragments of amphiphysin I depicted. Most autoantibodies reacted with fragment V, with a weaker response to fragment III. Electrophoretic mobility of the fragments is indicated at right.

Western blotting. A rabbit antiserum raised against recombinant human amphiphysin I (14) recognized two protein bands at 128 and 108 kD in the cancer tissue (Fig. 2). The 128 kD band precisely comigrated with neuronal amphiphysin I (Fig. 2). The 108 kD band was recognized by all anti-amphiphysin I antibodies tested, including the serum of Patient 692 and monoclonal antibodies reacting with five different fragments spanning the entire length of the protein (Fig. 4 and data not shown). Thus the 108 kD band (a doublet in many gels) is immunologically indistinguishable from the 128 kD amphiphysin I band and most likely represents an amphiphysin I isoform. None of several anti-amphiphysin II antibodies tested reacted with the 108 kD band, demonstrating that this band is not an amphiphysin II isoform (not shown).

Amphiphysin I Expression in Mammary Tissue and Cell Lines

Amphiphysin I immunoreactivity had not been detected previously in mammary tissue (7,8). The detection of amphiphysin I in the breast tissue of Patient 692 prompted us to reinvestigate its expression in other specimens of normal and neoplastic human mammary tissue. We searched for amphiphysin I immunoreactivity in 6 cell lines derived from neoplastic human mammary tissue and 2 cell lines derived from histologically normal tissue. One of the cancer cell lines, Hs578T (30), expressed high levels of the 108 kD amphiphysin I immunoreactive band (Fig. 3A,B). This band was recognized by polyclonal antibodies directed against amphiphysin I (Fig. 3) as well as by monoclonal antibodies directed against the five distinct regions of the protein (Fig. 4, lanes c). Lower levels of the 108 kD band were detected in the cell line Hs578Bst, which was derived from histologically normal tissue outside the margin of the cancer from which the cell line Hs578T was derived (30) (Fig. 3A). Other cell lines expressed amphiphysin I only at the limit of detectability. Neither the cancer tissue of Patient 692 nor the Hs578T cell line expressed elevated levels of synaptojanin I, dynamin I, and synapsin I, which suggests that the presence of amphiphysin I in the cell line and tissues was not due to neuroendocrine differentiation (Fig. 3C and data not shown). The expression of amphiphysin I in breast cell lines rules out the possibility that amphiphysin I expression in mammary tissue can be attributed to the presence of peripheral nerves.

We also searched for amphiphysin I immunoreactivity in normal and neoplastic human mammary tissues. We detected amphiphysin I in all tissues examined, which included 14 histologically normal breast tissues, 40 ductal, and 10 nonductal breast adenocarcinomas (Figs. 5, 6,

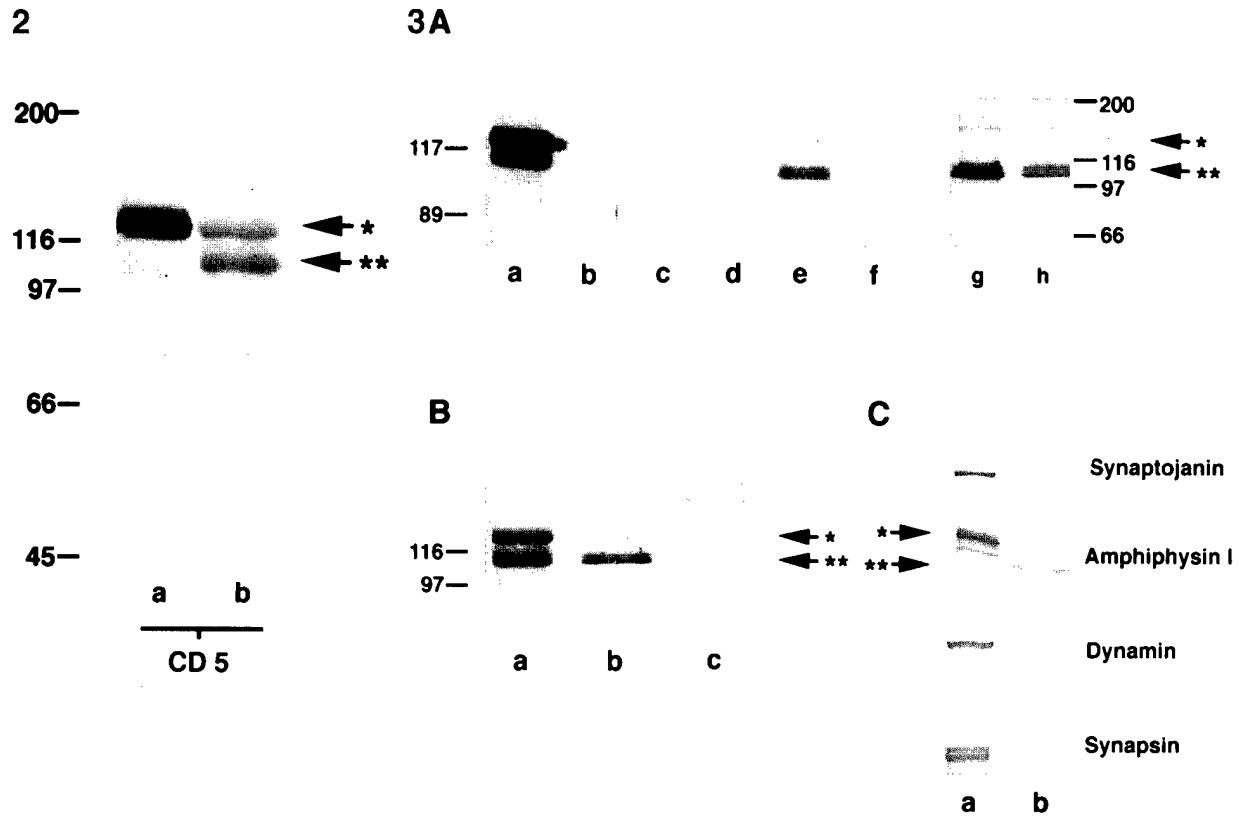

Fig. 2. Detection of amphiphysin I immunoreactivity in the cancer tissue of Patient 692. Total homogenates of human brain (a) and of the cancer tissue from Patient 692 (b) were analyzed by Western blotting using the anti-amphiphysin I rabbit serum CD5 as a probe. Brain contained a single 128 kD amphiphysin I immunoreactive band (one asterisk), whereas the cancer tissue contained both this band and a lower immunoreactive band of about 108 kD (two asterisks). Total protein loading was as follows: a, 100 μg; b, 35 μg.

Fig. 3. Expression of amphiphysin I immunoreactivity in human cell lines derived from normal and neoplastic breast tissue. (A) Total protein homogenates of human brain (10 μg) or of human cell lines (20 μg) were probed by Western blotting with the rabbit anti-amphiphysin I antiserum CD5. Lanes are as follows: (a) rat brain; (b) MDA-MB-453 breast cancer cell line; (c) MCF7 breast cancer cell line; (d) MDA-MB-231 breast cancer cell line; (e) Hs578T breast cancer cell line; (f) SK-BR3 breast cancer cell line; (g) Hs578T cell line; (h) Hs578Bst breast tissue cell line. (B) Western blotting with the CD5 antiserum of (a) the cancer tissue of Patient 692, (b) the Hs578T cell line, and (c) a normal breast tissue cell line (MCF-10A) demonstrating the identical electrophoretic mobility of the 108 kD bands in the cell line and in the cancer tissue. (C) Total homogenates of (a) rat brain and of (b) the cell line Hs578T probed by Western blotting with antibodies directed against the neuronal proteins indicated. Ten micrograms of rat brain and 20 μg of cell extract were loaded in a and b, respectively. One and two asterisks point to the 128 and the 108 kD bands, respectively.

and data not shown). However, levels of amphiphysin I were generally higher in cancer than in normal mammary tissue. Figure 5 compares the distribution of amphiphysin I immunoreactivity in overexposed Western blots of the breast cancer cell line Hs578T (lane b), a human primary breast tumor sample (lane c), and five normal breast tissues samples (lanes d–h). Note that both the 128 and the 108 kD bands are visible in all normal tissues whereas cancer tissues express predominantly the 108 kD band.

Figure 6A shows an additional comparison of the breast cancer cell line Hs578T (lane b), three normal mammary tissue samples (lanes c–e), and nine breast cancer tissue samples (lanes f–n). In this blot, the small amount of amphiphysin I present in normal tissues is undetectable, while enhanced, although variable levels of immunoreactivity are visible in all cancer tissues. Lane g contains the same cancer tissue as in lane c of Fig. 5 and serves therefore as an internal calibration of the two figures. Lane n in Fig. 6 contains

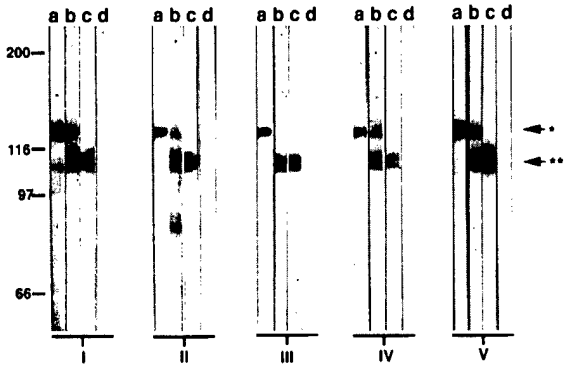

Fig. 4. Reactivity of the breast cancer tissue of Patient 692 and of the cell line Hs578T with 5 monoclonal antibodies directed against 5 distinct regions of amphiphysin I. Total homogenate proteins (30 μg for lanes a and 300 μg for the other lanes) were reacted by Western blotting with monoclonal antibodies directed against each of the 5 amphiphysin I fragments depicted in Fig. 1B. Lanes are as follows: (a) human brain; (b) cancer tissue of Patient 692; (c) cell line Hs578T; and (d) cell line MCF7. In these blots, the upper (128 kD, one asterisk) and lower (108 kD, two asterisks) amphiphysin I immunoreactive bands appear as doublets.

the cancer tissue of Patient 692 and is the only lane where both the 108 and the 128 kD bands are visible. Figure 6B shows the lower portion of the blot shown in Fig. 6A probed with anti-vimentin antibodies to control for protein loading.

Amphiphysin I Expression in Non-neuronal Tissues

The identification of amphiphysin I immunoreactive bands in normal mammary tissue prompted us to reinvestigate the tissue distribution of amphiphysin I, which thus far was thought to be very restricted (1,6). Monoclonal

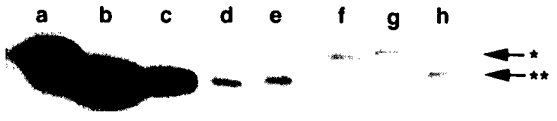

Fig. 5. Amphiphysin I is present in human mammary tissues. Total protein homogenates of (a) human brain (10 μg), (b) human breast cancer cell line Hs578T (100 μg), (c) primary human breast tumor (100 μg), and (d–h) normal human mammary tissues (100 μg each) were probed by Western blotting using a monoclonal antibody directed against domain V (see Fig. 1B) of amphiphysin I. One and two asterisks correspond to the 128 and 108 kD amphiphysin I immunoreactive bands, respectively.

antibodies directed against either the COOH terminal region (Fig. 7) or the NH2-terminal region (not shown) of amphiphysin I revealed its expression in all tissues tested. The highest level of expression outside the brain was found in testis as previously reported (6), with only very low levels of expression in other tissues. In several human non-neuronal tissues, the 108 kD band was the predominant band, while amphiphysin I had a similar mobility in neuronal and non-neuronal tissues of the rat.

Characterization of the 108 kD Amphiphysin I Immunoreactive band

The Hs578T cell line was used for a further analysis of the 108 kD band. Its strong immunological similarity to the 128 kD band (see above) suggested that it may represent a truncated form of neuronal amphiphysin I. Yet, a rabbit anti-serum (CD9) directed against amino acids 26–40 of amphiphysin I reacted with this band (not shown), which argues against an N-terminal deletion. Likewise, the 108 kD protein could be affinity purified by a GST fusion protein comprising the proline-rich region dynamin (Fig. 8), which is known to bind to the COOH-terminal SH3 domain of amphiphysin (25), demonstrating the presence of a functional SH3 domain. Thus, a COOH-terminal truncation is unlikely. To determine whether the 108 kD isoform corresponds to an internal deletion of neuronal amphiphysin I, we cloned amphiphysin I from the Hs578T cell line.

A cDNA library of the Hs578T cell line was constructed and screened with an amphiphysin I–specific probe. Nucleotide sequencing of clone 3.4 isolated from the library (accession #AF034996) revealed an open reading frame identical in sequence to that of neuronal amphiphysin I (accession #U07616) (14), except for a 126 base pair deletion corresponding to bases 1383–1508 of the coding sequence (Fig. 9). Similar results were obtained when overlapping regions of the entire coding sequence of amphiphysin I were amplified from total RNA of the Hs578T cell line by a series of RT-PCR reactions (not shown). The 126 base pair deletion predicts a corresponding deletion of 42 amino acids, which is less than expected for the electrophoretic difference between the 128 and 108 kD bands. However, amphiphysin I (128 kD isoform) is known to have an aberrantly low electrophoretic mobility (1) and the 42 amino acid deletion lies within the sequence previously

Fig. 6. Enhanced expression levels of amphiphysin I in neoplastic human mammary tissues. (A) Total protein homogenate of (a) human brain (10 μg), (b) Hs578T cell line (100 μg), (c–e) normal human mammary tissues (100 μg each), (d–m) human primary human breast tumors (100 μg each), and (n) breast tumor from Patient 692 (75 μg) was probed by Western blotting with an anti-amphiphysin I monoclonal antibody. For reference, the same samples in Fig. 5, lanes c and d appear in Fig. 6, lanes g and c, respectively. (B) The same blot as in B was probed with ^{125}I-labeled protein A and a monoclonal antibody directed against the intermediate filament protein vimentin (arrowhead) to control for total protein loading. One and two asterisks correspond to the 128 and 108 kD amphiphysin I immunoreactive bands, respectively.

found to be responsible for this low mobility (14,19). In addition, in vitro translation and Western blot analysis of clone 3.4 with this 126 base pair deletion showed an electophoretic mobility identical to that of the 108 kD isoform from the Hs578T cell line (Fig 10). Two of the breast cancers shown to overexpress amphiphysin I (Fig. 6) were also tested by RT-PCR and found to contain an identical 126 base pair deletion.

We next investigated whether an amphiphysin I mRNA with a similar deletion is present in normal human tissues, thus accounting for the 108 kD isoform present in these tissues. RT-PCR reactions performed on normal human heart, kidney, and mammary tissues revealed bands with a molecular weight identical to that seen in the Hs578T cell line. These bands were sequenced and found to contain the same 126 base

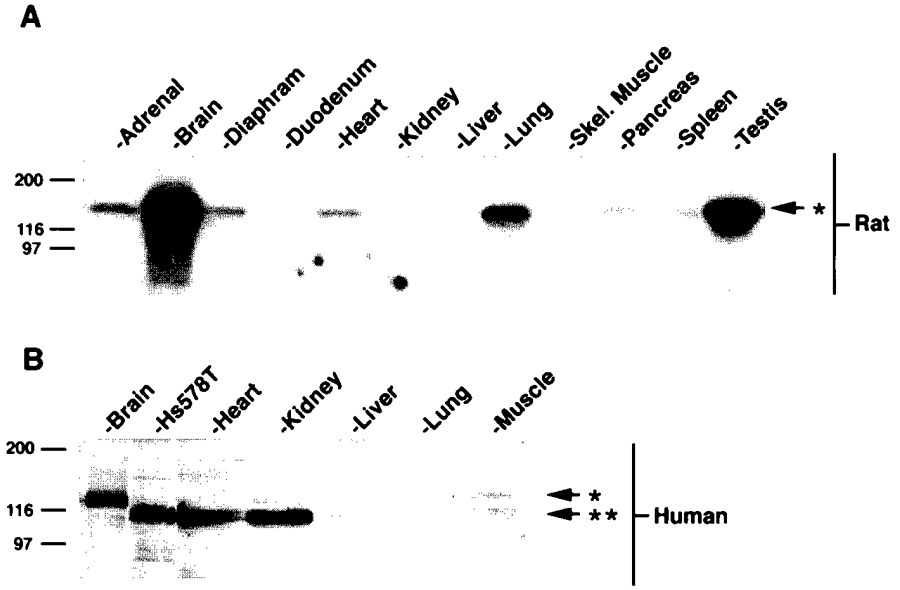

Fig. 7. Expression of amphiphysin I immunoreactivity in normal rat and human tissues. Total proteins of tissue homogenates were loaded in each lane and probed with monoclonal antibodies directed against domain V of amphiphysin I (see Fig. 3). Protein loaded was as follows: (A) rat tissues, 100 μg/lane; (B) human tissues, 10 μg of brain homogenate, 100 μg of the breast cancer cell line Hs578T, and 100 μg of all other tissue homogenates. One and two asterisks point to the 128 and 108 kD bands, respectively.

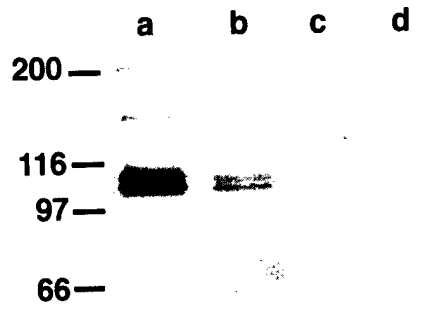

Fig. 8. The 108 kD amphiphysin I band contains a functional SH3 domain. Affinity-chromatography of a Triton X-100 extract from the Hs578T cell line was performed using GST-fusion proteins. The following material was probed by Western blotting with monoclonal antibodies directed against amphiphysin I: (a) starting extract; (b) material affinity purified on the full-length proline-rich domain of dynamin I; (c) material affinity purified on a truncated proline-rich domain of dynamin I missing the amphiphysin I binding site (construct DynPRD 751-832 of ref. 22); (d) material affinity purified on GST alone.

pair deletion. Most likely, this deletion is the result of an alternative splicing event. We note that a homologous region undergoes alternative splicing in amphiphysin II (18–21).

Discussion

Amphiphysin I was implicated as the key autoantigen in stiff-man syndrome associated with breast cancer (6,7) and subsequently as an autoantigen in other paraneoplastic disorders of the central nervous system (8,9). These disorders generally consist of various presentations of encephalomyelitis and the type of cancer varies, although in many cases, it is breast cancer (M. Solimena, M. Butler, J. Dalmau [New York], F. Graus [Barcelona, Spain], J. Honnorat [Lyon, France], J. C. Antoine [Saint-Etienne, France], and P. Sillevis-Smitt [Rotterdam, The Netherlands], unpublished observations). One of the proposed mechanisms for the pathogenesis of these conditions is that cancer cells of the affected patients express a protein that is normally expressed only in the immunoprivileged environment of the central nervous system (10,11,35). Expression of the amphiphysin I protein, however, has not been detected thus far in breast cancer (7,8). Here we report high-level expression of amphiphysin I isoforms in the breast cancer tissue of a patient with high-titer anti-amphiphysin I autoantibodies and paraneoplastic sensory neuronopathy. These findings are consistent with a cause–effect relationship between abnormal expression of amphiphysin I in cancer and neurological disease, although the exact pathogenic mechanism remains to be elucidated. Since both amphiphysin I isoforms present in the cancer of the paraneoplastic patient are found in a variety of non-neuronal tissues, low-level amphiphysin I expression outside the brain seems insufficient to trigger autoimmunity. The trigger to anti-amphiphysin I autoimmunity could be enhanced expression of the antigen in the context of an inflammatory autoimmune reaction against the

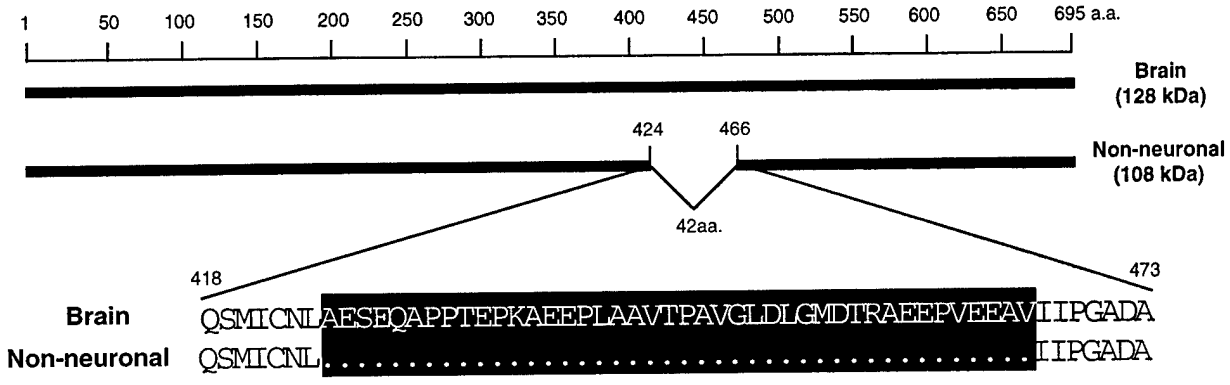

Fig. 9. Sequence comparison of amphiphysin I clone 3.4 from Hs578T cell line and human brain amphiphysin I. The schematic drawing illustrates the amino acid differences between the human brain isoform of amphiphysin I and the isoform encoded by clone 3.4 from a cDNA library of the Hs578T breast cancer cell line. This 42 amino acid deletion was also detectable by RT-PCR in normal human kidney, heart, and mammary tissues, as well as in at least two of the breast cancers with high-level amphiphysin I immunoreactivity in Fig. 6 above.

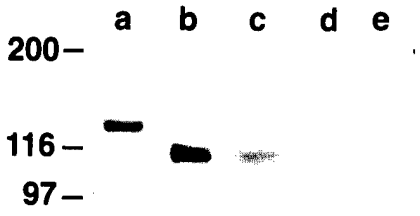

Fig. 10. In vitro transcription/translation of amphiphysin I clone 3.4. The following material was probed by Western blotting with a COOH-terminal directed anti-amphiphysin I monoclonal antibody: (a) human brain total protein homogenate; (b) Hs578T cell line total protein homogenate; (c) in vitro transcribed/translated product of clone 3.4; (d) in vitro transcribed/translated product of the luciferin cDNA; and (e) the product of an in vitro transcription/translation reaction in which no DNA was included.

tumor. Other predisposing factors, such as a specific HLA phenotype, may play a role in the development of autoimmunity. It is of interest that the breast cancer tissue of the patient with autoimmunity differed from the other cancer tissues we have examined in that it had higher levels of both the 128 kD and 108 kD amphiphysin I band.

A previous study has detected amphiphysin I mRNA in 5 of 14 breast cancer tissues by RT-PCR (8). However, considering our present identification of amphiphysin I expression in normal mammary tissue, it is the overexpression of the protein, rather than ectopic expression in mammary tissue, that seems characteristic of some breast cancers. That amphiphysin I mRNA was detected in 5 of 14 breast cancers in the previous study may reflect this overexpression as well (8). Both amphiphysin I and amphiphysin I mRNA had been detected in some small-cell lung carcinomas (8). The relationship between amphiphysin I expression and neoplastic growth in these latter tissues is unclear, as small-cell lung tumors have neuroendocrine properties and express significant levels of several neuronal proteins (36,37).

The enhanced expression of amphiphysin I isoforms in some cancers may be an epiphenomenon of neoplastic transformation. On the other hand, the possibility that amphiphysin I may be more closely linked to neoplastic transformation should be considered. As previously proposed (14), a relationship of the amphiphysin protein family to the control of cell proliferation is suggested by yeast studies. Mutations of the two yeast genes that encode proteins with homology to amphiphysin I, the *RVS161* and *RVS167* genes, produce a phenotype characterized by *r*educed *v*iability upon *s*tarvation (12,13) in addition to defects in endocytosis, cell polarity, and actin function (15,38). Reduced viability upon starvation can be explained by the inability of yeast cells to stop growing when exposed to unfavorable growth conditions and it suggests impairment of growth regulatory mechanisms. A similar phenotype is produced by mutations in the yeast homologue of the *ras* oncogene (12,13).

Abnormal amphiphysin I expression may affect cell proliferation in mammalian cells through several mechanisms. Proteins of the amphiphysin family are thought to have pleotropic functions including roles in endocytosis (2,3,21,38), actin function (5,13,15,23,39) and cell growth control (17,23). As a protein implicated in clathrin-mediated endocytosis, amphiphysin I may modulate signaling of growth factor receptors by regulating their internalization (3,21,40). Alternatively, it may affect signal transduction from the cell surface by actions on the actin cytoskeleton (5,38) or on protein–protein interaction cascades mediated through its SH3 domain (23,41). Finally, a more direct potential role of amphiphysin family members in the regulation of cell proliferation is suggested by the identification of amphiphysin II isoforms as either MYC-interacting proteins with some properties of a tumor suppressor (17) or as cABL-interacting proteins (23). The finding that amphiphysin I is overexpressed, rather than underexpressed, in some cancers, is in contrast to a putative role of amphiphysin family members as negative regulators of cell growth. However, amphiphysin I overexpression, or the overexpression of a specific isoform, may have a dominant negative role. Amphiphysin I forms heterodimers with amphiphysin II (ref. 21 and our unpublished observations) and it was reported that over expression of amphiphysin I, but not concomitant overexpression of both amphiphysin I and II, has a dominant negative affect on clathrin-mediated endocytosis (21).

Irrespective of whether amphiphysin I expression in cancer cells is an event that lies upstream or downstream of neoplastic transformation, enhanced amphiphysin I–expression in some cancers and its implication in autoimmune paraneoplastic disease predict that further studies of this protein may aid in understanding important human diseases.

Acknowledgments

We thank D. Stern (Yale), A. Perkins (Yale), and K. Tsutsui (Okayama, Japan) for discussion and J. Honnorat (Lyon, France), J. C. Antoine (Saint-Etienne, France), P. Sillevis-Smitt (Rotterdam, The Netherlands), K. Schmierer (Berlin, Germany), and J. Dalmau (New York) for discussing their patients with us. We thank L. Gutierez and C. Howe (Yale) and C. R. Wenger (University of Texas Health Science Center at San Antonio) for help in obtaining human tissues. Some of the material used for this study was provided through the Yale Critical Technologies Service (Dr. C. Howe, Director), and through the National Breast Cancer Tissue Resource of the San Antonio SPORE (Specialized Program of Research Excellence). This work was supported in part by grants from the Human Frontier Science Program and NIH (CA46128 and NS36251) to P. D. C., by fellowships from Telethon and the Human Frontier Science Program to O. C., by a fellowship from the United States Army Medical Research and Development Command to C. D., by Grants-in-Aid for Scientific Research from the Ministry of Education, Science, Sports and Culture of Japan to K. T., and by NIH grant (P50 CA58183) to the National Breast Cancer Tissue Resource of the San Antonio SPORE.

References

1. Lichte B, Veh RW, Meyer HE, Kilimann MW. (1992) Amphiphysin, a novel protein associated with synaptic vesicles. *EMBO J.* **11:** 2521–2530.
2. David C, McPherson PS, Mundigl O, De Camilli P. (1996) A role of amphiphysin in synaptic vesicle endocytosis suggested by its binding to dynamin in nerve terminals. *Proc. Natl. Acad. Sci. U.S.A.* **93:** 331–335.
3. Shupliakov O, Low P, Grabs D, Gad H, Chen H, David C, Takei K, De Camilli P, Brodin L. (1997) Synaptic vesicle endocytosis impaired by disruption of dynamin-SH3 domain interactions. *Science* **276:** 259–263.
4. Cremona O, De Camilli P. (1997) Synaptic vesicle endocytosis. *Curr. Opin. Neurobiol.* **7:** 323–330.
5. Mundigl O, Ochoa G, David C, Slepnev V, Kabanov A, De Camilli P. (1997) Amphiphysin I antisense oligonucleotides inhibit neurite outgrowth in cultured hippocampal neurons. *J. Neurosci.* **18:** 93–103.
6. De Camilli P, Thomas A, Cofiell R, Folli F, Lichte B, Piccolo G, Meinck H, M, Austoni M, Fassetta G, Bottazzo G, Bates D, Cartlidge N, Solimena M, Kiliman MW. (1993) The synaptic vesicle-associated protein amphiphysin is the 128-kD autoantigen of Stiff-Man syndrome with breast cancer. *J. Exp. Med.* **178:** 2219–2223.
7. Folli F, Solimena M, Cofiell R, Austoni M, Tallini G, Fassetta G, Bates D, Cartlidge N, Bottazzo GF, Piccolo G, et al. (1993) Autoantibodies to a 128-kd synaptic protein in three women with the stiff-man syndrome and breast cancer. *N. Engl. J. Med.* **328:** 546–551.
8. Dropcho EJ. (1996) Antiamphiphysin antibodies with small-cell lung carcinoma and paraneoplastic encephalomyelitis. *Ann. Neurol.* **39:** 659–667.
9. Lennon VA, Manley HA, Kim K, Parisi JE, Kilimann MW, Benarroch EE. (1997) Amphiphysin autoantibodies: A paraneoplastic serological marker of breast and lung cancer–related encephalomyeloradiculoneuritides but not classical stiff-man syndrome. *Neurology* **48:** A434.
10. Posner JB, Dalmau JO. (1997) Paraneoplastic syndromes affecting the central nervous system. *Annu. Rev. Med.* **48:** 157–166.
11. Darnell RB. (1996) Onconeural antigens and the paraneoplastic neurologic disorders: At the intersection of cancer, immunity, and the brain. *Proc. Natl. Acad. Sci. U.S.A.* **93:** 4529–4536.
12. Crouzet M, Urdaci M, Dulau L, Aigle M. (1991) Yeast mutant affected for viability upon nutrient starvation: Characterization and cloning of the RVS161 gene. *Yeast* **7:** 727–743.
13. Bauer F, Urdaci M, Aigle M, Crouzet M. (1993) Alteration of a yeast SH3 protein leads to conditional viability with defects in cytoskeletal and budding patterns. *Mol. Cell. Biol.* **13:** 5070–5084.
14. David C, Solimena M, De Camilli P. (1994) Autoimmunity in Stiff-Man syndrome with breast cancer is targeted to the C-terminal region of human amphiphysin, a protein similar to the yeast proteins, Rvs167 and Rvs161. *FEBS Lett.* **351:** 73–79.
15. Sivadon P, Bauer F, Aigle M, Crouzet M. (1995) Actin cytoskeleton and budding pattern are altered in the yeast rvs161 mutant: The Rvs161 protein shares common domains with the brain protein amphiphysin. *Mol. Gen. Genet.* **246:** 485–495.
16. Sparks AB, Hoffman NJ, McConnell SJ, Fowlkes DM, Kay BK. (1996) Cloning of ligand targets: Systemic isolation of SH3 domain–containing proteins. *Nature Biotech.* **14:** 741–744.
17. Sakamuro D, Elliott KJ, Wechsler-Reya R, Prendergast GC. (1996) BIN1 is a novel MYC-interacting protein with features of a tumour suppressor. *Nature Genet.* **14:** 69–77.
18. Leprince C, Romero R, Cussac D, Vayssiere B, Berger R, Tavitian A, Camonis JH. (1997) A new member of the amphiphysin family connecting endocytosis and signal transuction pathways. *J. Biol. Chem.* **272:** 15101–15105.
19. Butler MH, David C, Ochoa GC, Freyberg Z, Daniell L, Grabs D, Cremona O, De Camilli P. (1997) Amphiphysin II (SH3P9; BIN1), a member of the amphiphysin/RVS family, is localized in the

cortical cytomatrix of axon initial segments and nodes of Ranvier in brain and around T-tubules in skeletal muscle. *J. Cell Biol.* **137:** 1355–1367.

20. Tsutsui K, Maeda Y, Tsutsui K, Seki S, Tokunaga A. (1997) cDNA cloning of a novel amphiphysin isoform and tissue-specific expression of its multiple splice variants. *Biochem. Biophys. Res. Commun.* **236:** 178–83.
21. Wigge P, Kohler K, Vallis Y, Doyle CA, Owen D, Hunt SP, McMahon HT. (1997) Amphiphysin heterodimers: potential role in clathrin-mediated endocytosis. *Mol. Biol. Cell* **8:** 2003–2015.
22. Ramjaun AR, Micheva KD, Bouchelet I, McPherson PS. (1997) Identification and characterization of a nerve terminal–enriched amphiphysin isoform. *J. Biol. Chem.* **272:** 16700–16706.
23. Kadlec L, Pendergast AM. (1997) The amphiphysin-like protein 1 (ALP1) interacts functionally with the cABL tyrosine kinase and may play a role in cytoskeletal regulation [In Process Citation]. *Proc. Natl. Acad. Sci. U.S.A.* **94:** 12390–12395.
24. McPherson PS, Garcia EP, Slepnev VI, David C, Zhang XM, Grabs D, Sossin WS, Bauerfeind R, Nemoto Y, De Camilli P. (1996) A presynaptic inositol-5-phosphatase. *Nature* **379:** 353–357.
25. Grabs D, Slepnev VI, Songyang Z, David C, Lynch M, Cantley LC, De Camilli P. (1997) The SH3 domain of amphiphysin binds the proline-rich domain of dynamin at a single site that defines a new SH3 binding consensus sequence. *J. Biol. Chem.* **272:** 13419–13425.
26. De Camilli P, Cameron R, Greengard P. (1983) Synapsin I (protein I) a nerve terminal specific phosphoprotein. Its general distribution in synapses of the central and peripheral nervous system demonstrated by immunofluorescence in froxen and plastic sections. *J. Cell Biol.* **96:** 1337–1354.
27. Navone F, Jahn R, Di Gioia G, Stukenbrok H, Greengard P, De Camilli P. (1986) Protein p38: An integral membrane protein specific for small vesicles of neurons and neuroendocrine cells. *J. Cell Biol.* **103:** 2511–2527.
28. Jahn R, Schiebler W, Ouimet C, Greengard P. (1985) A 38,000-dalton membrane protein (p38) present in synaptic vesicles. *Proc. Natl. Acad. Sci. U.S.A.* **82:** 4137–4141.
29. Kohler G, Milstein C. (1975) Continuous cultures of fused cells secreting antibody of predefined specificity. *Nature* **256:** 495–497.
30. Hackett AJ, Smith HS, Springer EL, Owens RB, Nelson-Rees WA, Riggs JL, Gardner MB. (1977) Two syngeneic cell lines from human breast tissue: the aneuploid mammary epithelial (Hs578T) and the diploid myoepithelial (Hs578Bst) cell lines. *J. Natl. Cancer Inst.* **58:** 1795–806.
31. Chirgwin JM, Przybyla AE, MacDonald RJ, Rutter WJ. (1979) Isolation of biologically active ribonucleic acid from sources enriched in ribonuclease. *Biochemistry* **18:** 5294–5299.
32. Bogue CW, Gross I, Vasavada H, Dynia DW, Wilson CM, Jacobs HC. (1994) Identification of *Hox* genes in newborn lung and effects of gestational age and retinoic acid on their expression. *Am. J. Physiol.* **266:** L448–454.
33. Laemmli UK. (1970) Cleavage of structural proteins during the assembly of the head of bacteriophage T4. *Nature* **227:** 680–685.
34. Towbin H, Staehelin T, Gordon J. (1979) Electrophoretic transfer of proteins from polyacrylamide gels to nitrocellulose sheets: Procedure and some applications. *Proc. Natl. Acad. Sci. U.S.A.* **76:** 4350–4354.
35. Dalmau J, Graus F, Cheung NK, Rosenblum MK, Ho A, Canete A, Delattre JY, Thompson SJ, Posner JB. (1995) Major histocompatibility proteins, anti-Hu antibodies, and paraneoplastic encephalomyelitis in neuroblastoma and small cell lung cancer. *Cancer* **75:** 99–109.
36. Wiedenmann B, Huttner WB. (1989) Synaptophysin and chromogranins/secretogranins—Widespread constituents of distinct types of neuroendocrine vesicles and new tools in tumor diagnosis. *Virchows Arch. B Cell. Pathol. Incl. Mol. Pathol.* **58:** 95–121.
37. Williams CL. (1997) Basic science of small cell lung cancer. *Chest Surg. Clin. North Am.* **7:** 1–19.
38. Bauerfeind R, Takei K, De Camilli P. (1997) Amphiphysin I is associated with coated endocytic intermediates and undergoes stimulation-dependent dephosphorylation in nerve terminals. *J. Biol. Chem.* **272:** 30984–30992.
39. Munn AL, Stevenson BJ, Geli MI, Riezman H. (1995) end5, end6, and end7: Mutations that cause actin delocalization and block the internalization step of endocytosis in *Saccharomyces cerevisiae*. *Mol. Biol. Cell* **6:** 1721–1742.
40. Vieira AV, Lamaze C, Schmid SL. (1996) Control of EGF receptor signaling by clathrin-mediated endocytosis. *Science* **274:** 2086–2089.
41. Pawson T. (1995) Protein modules and signalling networks. *Nature* **373:** 573–580.

Trends in Cell Biology

Elsevier Trends Journals
68 Hills Road
Cambridge
UK CB2 1LA
Tel +44 1223 315961
Fax +44 1223 321410

Endocytosis proteins and cancer: a potential link?

Scott Floyd and Pietro De Camilli

Recent studies have shown that a variety of proteins participate with clathrin and clathrin adaptors in receptor-mediated endocytosis. The genes encoding some of these proteins are targets of chromosomal rearrangements in human haematopoietic malignancies. In addition, abnormal expression or mutation of some endocytosis proteins has been reported in human cancers. This article discusses these observations and elaborates the potential mechanisms by which the abnormal expression of endocytosis proteins might participate in the biology of cancer.

Clathrin-mediated endocytosis is a process by which cells internalize selected components of the plasmalemma[1]. Cells use this endocytic mechanism for diverse functions. For example, clathrin-coated vesicles mediate the clearance from the cell surface of receptor-bound hormones and growth factors, control the regulated internalization of channels and transporters, participate in the recycling of synaptic vesicles in nerve terminals and are implicated in cell invasion by a variety of pathogens. Formation of an endocytic clathrin-coated vesicle starts with the binding and oligomerization of AP-2 clathrin adaptors at the cytoplasmic surface of the plasmalemma and is followed by the recruitment of clathrin triskelia, the invagination of the coated membrane patch and, eventually, the fission of the coated bud to generate a free vesicle (for reviews, see Refs 1–3). In addition to AP-2 and clathrin, several accessory proteins have been implicated in this process (for review, see Ref. 4). Figure 1 illustrates these proteins and some of their interactions in a schematic fashion. A potential link between several of these proteins and cancer has emerged recently.

Chromosomal translocations in leukaemias

Three human genes encoding endocytosis-related proteins depicted in the figure and in Table 1 are involved in chromosomal translocations in haematopoietic malignancies. The human *AF-1p* gene encodes an orthologue of murine Eps15, which can induce transformation when overexpressed in NIH 3T3 cells[5]. AF-1p is fused to the *ALL1/HRX* gene (also referred to as *MLL* and *HTRX1*) in two human myeloid leukaemias[6]. The resulting t(1;11)(p32;q23) chromosomal translocation generates an expressed fusion protein comprising the N-terminal domain of ALL1/HRX fused in frame to the C-terminal region of AF-1p. The *EEN* gene, which encodes human SH3p8, was identified at the t(11;19)(q23;p13) translocation in a case of acute myeloid leukaemia[7]. This translocation results in an expressed fusion protein that contains the N-terminal domain of ALL1/HRX fused to the C-terminal domain of SH3p8. The *CALM* gene, which encodes a non-neuronal form of the AP180 protein, is the target of the t(10;11)(p13;q14) translocation in the U937 human cell line. As a consequence of the rearrangement, the N-terminal portion of *CALM* is fused to the *AF-10* gene[8], which had previously been identified as a fusion partner of *ALL1/HRX* in acute lymphoblastic[9] and myeloid leukaemia[10]. The U937 cell line was derived from a patient with diffuse histiocytic lymphoma, and an identical translocation has been identified subsequently in four patients, all with different haematological malignancies[11]. The *CALM–AF-10* translocation results in an expressed fusion protein comprising the almost full-length CALM protein with the last four amino acids replaced with amino acids 81–1027 of the AF-10 protein. In all three cases, the domain of the endocytosis protein that is expressed as a result of the translocation is functionally important (i.e. the SH3 domain of SH3p8, the EH domain of EPS15 and the inositol-phosphate-binding domain of CALM).

In two of these translocations, endocytosis proteins are fused with *ALL1/HRX*, a gene that has been mapped to chromosome 11q23 (Ref. 12). Abnormalities of this region have been identified in approximately 10% of acute lymphoblastic leukaemias and 5% of acute myeloid leukaemias (reviewed in Ref. 13). The *ALL1/HRX* gene has similarity to the transcription factor trithorax in *Drosophila* and has a role in haematopoiesis. In addition to translocations involving this region, the *ALL1/HRX* gene is partially duplicated in frame in some acute leukaemias[14]. However, several lines of evidence point to the importance of translocation partners of *ALL1/HRX* in leukaemogenesis. At least 12 different translocation partners have been identified for *ALL1/HRX*[15]. All of these translocation partners result in expressed fusion proteins, usually with a well-conserved portion of the ALL1/HRX N-terminal region fused to a large C-terminal region of the fusion partner. Although there is little sequence homology among the ALL1/HRX fusion partners, transgenic mouse studies have demonstrated that disruption of the *ALL1/HRX* gene or fusion with a non-leukaemic partner protein is insufficient to induce leukaemogenesis, whereas combination of *ALL1/HRX* with a known leukaemia fusion partner not only produces haematopoietic malignancy but also influences leukaemic type[16]. The identification of the *CALM–AF-10* translocation in a lymphoma cell line also suggests that these fusion partners have effects on cell proliferation that are independent of *ALL1/HRX*[8].

The authors are in the Howard Hughes Medical Institute and Dept of Cell Biology, Yale University School of Medicine, 295 Congress Ave., New Haven, CT 06510, USA. E-mail: pietro.decamilli@yale.edu

0962-8924/98/$19.00
PII: S0962-8924(98)01316-6

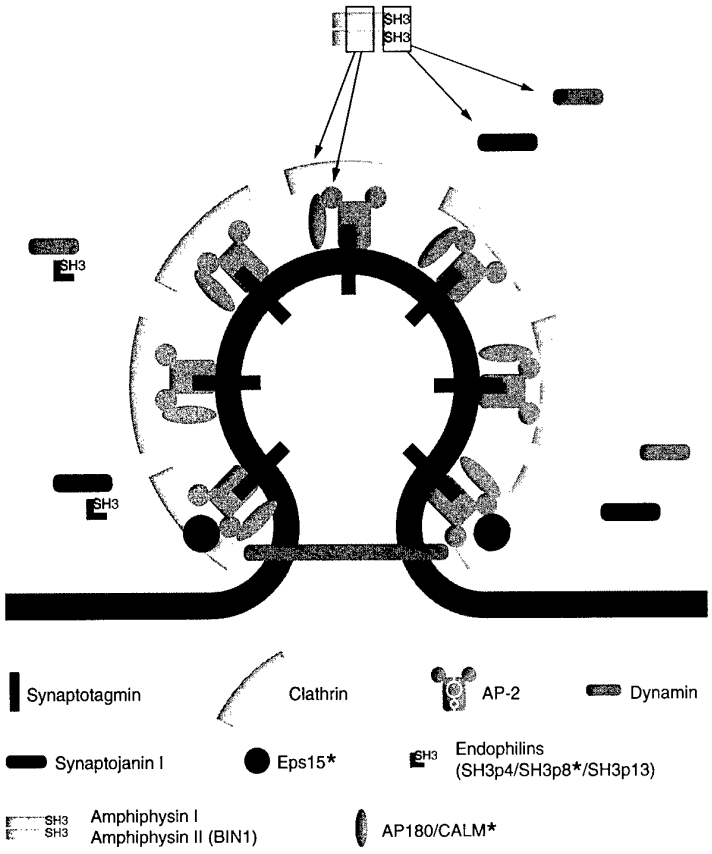

FIGURE 1

Schematic representation of proteins implicated in clathrin-mediated endocytosis. The clathrin adaptors AP-2 and AP180 are thought to act as linkers between clathrin and the membrane. Synaptotagmin is proposed to be a major binding site for AP-2 in the membrane. Dynamin forms rings at the neck of the coated pit and participates in the fission reaction. Amphiphysin, which binds to dynamin and synaptojanin I through its Src-homology 3 (SH3) domain and to clathrin/AP-2 through a distinct domain, might couple dynamin recruitment to clathrin coat formation. The precise function of synaptojanin I, Eps15 and the SH3p4/SH3p8/SH3p13 protein family (endophilins) in endocytosis remains unclear. (*Translocated in leukaemia.)

Other connections of endocytosis genes to cancer

Besides gene translocations, other connections between endocytosis proteins and human cancer have emerged. Amphiphysin I is a human paraneoplastic autoantigen that is overexpressed in a subset of breast cancers. In a small number of cancer patients, it triggers an autoimmune response leading to autoimmune neurological diseases[17–20]. A splice variant of amphiphysin II, BIN1, is a Myc-binding protein with properties of a tumour suppressor and is underexpressed in a variety of human cancer tissues[21]. Another amphiphysin II splice form binds to and enhances the transforming ability of the protooncogene c-Abl[22]. The amphiphysins are the mammalian homologues of the yeast Rvs161/End6 and Rvs167 proteins[23,24]. The pleiotropic phenotype induced by disruption of the yeast genes encoding these proteins includes reduced viability upon starvation, which has been interpreted as an inability of the cells to arrest cell proliferation when exposed to unfavourable growth conditions. Mutation of the yeast *RAS* genes produces a similar phenotype[23]. The Rvs161–Rvs167 dimer binds to the yeast cyclin-dependent kinase Pho85 and is a substrate for its kinase activity (J. Lee, K. Colwill and B. Andrews, pers. commun.). Another recently identified link between the endocytic pathway and cancer is represented by the properties of the *TSC2* gene, mutations in which are responsible for benign and malignant tumours characteristic of tuberous sclerosis[25]. The product of this gene, tuberin, appears to be a biochemical and functional partner of Rab5, a GTPase implicated in the early endocytic pathway[26,27]. A member of the β-adaptin gene family has also been linked to human malignancy. A deletion of chromosome 22q12 common in meningioma contains the *BAM22* gene, which has homology to the β subunit of the clathrin adaptors AP1 and AP2[28].

Possible mechanisms

These observations are unlikely to have a simple explanation, and a role for abnormal expression of endocytosis proteins in oncogenesis remains to be demonstrated. However, mutation or altered expression of endocytosis proteins could affect the control of cell proliferation by several potential mechanisms. Impaired endocytosis might enhance cell replication by prolonging signalling by growth-factor receptors. This possibility is supported by the demonstration that cells expressing either internalization-defective epidermal growth factor (EGF) receptors or a dominant–negative dynamin mutant display an enhanced proliferative response to EGF[28,29]. All the endocytosis proteins illustrated in Fig. 1 and Table 1 interact either directly or indirectly with signalling proteins (reviewed in Ref. 4). Their abnormal functioning could therefore also interfere with signalling cascades controlling cell proliferation[30]. In addition, there are several connections between endocytosis proteins and the cortical actin cytoskeleton[24,31,32], and abnormal flow of information from the cell cortex to the nucleus appears to underlie the function of several tumour-suppressor genes[33,34]. Finally, fusion proteins of putative transcription factors, such as ALL1/HRX and AF-10, with fragments of endocytosis proteins encoding targeting domains might result in the mistargeting of these factors and, therefore, in their abnormal function[35]. Irrespective of whether each of the observations summarized here has a direct link to oncogenesis, they point to the importance of exploring further the potential role of endocytosis genes in human cancer.

References

1 Pearse, B. M. and Robinson, M. S. (1990) *Annu. Rev. Cell Biol.* 6, 151–171
2 Kirchhausen, T., Bonifacino, J. S. and Riezman, H. (1997) *Curr. Opin. Cell Biol.* 9, 488–495
3 Schmid, S. L. (1997) *Annu. Rev. Biochem.* 66, 511–548
4 Cremona, O. and De Camilli, P. (1997) *Curr. Opin. Neurobiol.* 7, 323–330
5 Fazioli, F. *et al.* (1993) *Mol. Cell. Biol.* 13, 5814–5828
6 Bernard, O. A. *et al.* (1994) *Oncogene* 9, 1039–1045

TABLE 1 – ENDOCYTOSIS PROTEINS AND THEIR INVOLVEMENT IN CANCER

Endocytosis protein	Known interactions	Connection to cancer
Synaptotagmin	Binds to AP-2; putative role in coat recruitment[a]	
Clathrin	Binds to AP-2[b,c], AP180[d], central region of amphiphysin[e,f]	
AP-2	Heterotetramer; member of a family of clathrin adaptors; interacts with clathrin, AP180, phosphoinositides, synaptotagmin and cytoplasmic tail of receptors, amphiphysin and Eps15[a,c,g–j]	
Dynamin	GTPase; binds to SH3 domain of amphiphysin I, II and SH3p4/SH3p8/SH3p13 (endophilins) through proline-rich domain[e,k,l]	
Synaptojanin I	Inositol 5-phosphatase; colocalizes with dynamin; physiological interactor for the SH3 domain of amphiphysin and the SH3p4/SH3p8/SH3p13 (endophilin) family[l–n]	
Eps15 (AF-1p)	Target of EGF receptor phosphorylation[o]; binds to AP-2 and the 170-kDa isoform of synaptojanin I[l,p,q]	Translocated in leukaemia[r]
SH3p4/SH3p8/SH3p13 (endophilin I, II and III) EEN = human SH3p8	Bind to dynamin and synaptojanin I through their SH3 domain[l,n]	EEN translocated in one case of leukaemia[s]
Amphiphysin I and II	Bind to dynamin and synaptojanin I through their SH3 domains[e,k,t,u]; bind to clathrin and AP-2 through their central domain[e,f,v]; form heterodimers[w]; amphiphysin II binds to c-Myc[x] and c-Abl[y]	Amphiphysin I is an autoantigen in paraneoplastic conditions[z–bb] and is overexpressed in a subset of breast cancers[bb,cc]; amphiphysin II is reduced or absent in several solid tumours[x]
AP180 (CALM = non neuronal AP180 isoform)	Binds to clathrin, AP-2, inositol polyphosphates and phosphoinositides[d,g,dd]	Translocated in lymphoma and several forms of leukaemia[ee,ff]

[a]Zhang, J. Z. *et al.* (1994) *Cell* 78, 751–760; [b]Kirchhausen, T., Bonifacino, J. S. and Riezman, H. (1997) *Curr. Opin. Cell Biol.* 9, 488–495; [c]Robinson, M. S. (1994) *Curr. Opin. Cell Biol.* 6, 538–544; [d]Ye, W. and Lafer, E. M. (1995) *J. Biol. Chem.* 270, 10933–10939; [e]Ramjaun, A. R. *et al.* (1997) *J. Biol. Chem.* 272, 16700–16706; [f]McMahon, H. T., Wigge, P. and Smith, C. (1997) *FEBS Lett.* 413, 319–322; [g]Wang, L. H., Sudhof, T. C. and Anderson, R. G. (1995) *J. Biol. Chem.* 270, 10079–10083; [h]Gaidarov, I. *et al.* (1996) *J. Biol. Chem.* 271, 20922–20929; [i]Benmerah, A. *et al.* (1996) *J. Biol. Chem.* 271, 12111–12116; [j]Iannolo, G. *et al.* (1997) *Cancer Res.* 57, 240–245; [k]David, C. *et al.* (1996) *Proc. Natl. Acad. Sci. U. S. A.* 93, 331–335; [l]Ringstad, N., Nemoto, Y. and de Camilli, P. (1997) *Proc. Natl. Acad. Sci. U. S. A.* 94, 8569–8574; [m]McPherson, P. S. *et al.* (1996) *Nature* 379, 353–357; [n]de Heuvel, E. *et al.* (1997) *J. Biol. Chem.* 272, 8710–8716; [o]Fazioli, F. *et al.* (1993) *Mol. Cell. Biol.* 13, 5814–5828; [p]Haffner, C. *et al.* (1997) *FEBS Lett.* 419, 175–180; [q]Carbone, R. *et al.* (1997) *Cancer Res.* 57, 5498–5504; [r]Bernard, O. A. *et al.* (1994) *Oncogene* 9, 1039–1045; [s]So, C. W. *et al.* (1997) *Proc. Natl. Acad. Sci. U. S. A.* 94, 2563–2568; [t]Grabs, D. *et al.* (1997) *J. Biol. Chem.* 272, 13419–13425; [u]Butler, M. H. *et al.* (1997) *J. Cell Biol.* 137, 1355–1367; [v]Wang, L. H., Südhof, T. C. and Anderson, R. G. W. (1995) *J. Biol. Chem.* 270, 10079–10083; [w]Wigge, P. *et al.* (1997) *Mol. Biol. Cell* 8, 2003–2015; [x]Sakamuro, D. *et al.* (1996) *Nat. Genet.* 14, 69–77; [y]Kadlec, L. and Pendergast, A. M. (1997) *Proc. Natl. Acad. Sci. U. S. A.* 94, 12390–12395; [z]Folli, F. *et al.* (1993) *New Engl. J. Med.* 328, 546–551; [aa]de Camilli, P. *et al.* (1993) *J. Exp. Med.* 178, 2219–2223; [bb]Dropcho, E. J. (1996) *Ann. Neurol.* 39, 659–667; [cc]Floyd, S. R. *et al.* (1998) *Mol. Med.* 4, 29–39; [dd]Ye, W. *et al.* (1995) *J. Biol. Chem.* 270, 1564–1568; [ee]Dreyling, M. H. *et al.* (1996) *Proc. Natl. Acad. Sci. U. S. A.* 93, 4804–4809; [ff]Kobayashi, H. *et al.* (1997) *Genes Chromosomes Cancer* 20, 253–259. Abbreviations: AP, adaptor protein; EGF, epidermal growth factor; SH3, Src-homology 3

7 So, C. W. *et al.* (1997) *Proc. Natl. Acad. Sci. U. S. A.* 94, 2563–2568
8 Dreyling, M. H. *et al.* (1996) *Proc. Natl. Acad. Sci. U. S. A.* 93, 4804–4809
9 Djabali, M. *et al.* (1992) *Nat. Genet.* 2, 113–118
10 Iida, S. *et al.* (1993) *Oncogene* 8, 3085–3092
11 Kobayashi, H. *et al.* (1997) *Genes Chromosomes Cancer* 20, 253–259
12 Ziemin-van der Poel, S. *et al.* (1991) *Proc. Natl. Acad. Sci. U. S. A.* 88, 10735–10739
13 Bernard, O. A. and Berger, R. (1995) *Genes Chromosomes Cancer* 13, 75–85
14 Schichman, S. A. *et al.* (1994) *Proc. Natl. Acad. Sci. U. S. A.* 91, 6236–6239
15 Rubnitz, J. E., Behm, F. G. and Downing, J. R. (1996) *Leukemia* 10, 74–82
16 Corral, J. *et al.* (1996) *Cell* 85, 853–861
17 Floyd, S. R. *et al.* (1998) *Mol. Med. Today* 4, 29–39
18 Dropcho, E. J. (1996) *Ann. Neurol.* 39, 659–667
19 Folli, F. *et al.* (1993) *New Engl. J. Med.* 328, 546–551
20 De Camilli, P. *et al.* (1993) *J. Exp. Med.* 178, 2219–2223
21 Sakamuro, D. *et al.* (1996) *Nat. Genet.* 14, 69–77
22 Kadlec, L. and Pendergast, A. M. (1997) *Proc. Natl. Acad. Sci. U. S. A.* 94, 12390–12395
23 Crouzet, M. *et al.* (1991) *Yeast* 7, 727–743
24 Munn, A. L. *et al.* (1995) *Mol. Biol. Cell* 6, 1721–1742
25 (1993) *Cell* 75, 1305–1315
26 Xiao, G. H. *et al.* (1997) *J. Biol. Chem.* 272, 6097–6100
27 McLauchlan, H. *et al.* (1998) *Curr. Biol.* 8, 34–45
28 Peyrard, M. *et al.* (1994) *Hum. Mol. Genet.* 3, 1393–1399
29 Vieira, A. V., Lamaze, C. and Schmid, S. L. (1996) *Science* 274, 2086–2089
30 Pawson, T. (1995) *Nature* 373, 573–580
31 Lamaze, C. *et al.* (1996) *Nature* 382, 177–179
32 Geli, M. I. and Riezman, H. (1996) *Science* 272, 533–535
33 Barth, A. I. *et al.* (1997) *J. Cell Biol.* 136, 693–706
34 Tsukita, S. *et al.* (1993) *J. Cell Biol.* 123, 1049–1053
35 Rogaia, D. *et al.* (1997) *Cancer Res.* 57, 799–802

Acknowledgements

We thank Neils Ringstad, Ottavio Cremona, Margaret H. Butler, Michele Solimena and Brenda Andrews for discussion about this article.

Stiff-man syndrome in a woman with breast cancer

An uncommon central nervous system paraneoplastic syndrome

L. Rosin, MD; P. DeCamilli, MD; M. Butler, MD; M. Solimena, MD; H.-P. Schmitt, MD; N. Morgenthaler, MD; and H.-M. Meinck, MD

Article abstract—We report a patient who developed stiff-man syndrome, including disabling shoulder subluxation and wrist ankylosis, in association with breast cancer. Immunologic investigations disclosed autoimmunity directed against not only glutamic acid decarboxylase but also amphiphysin, a 128-kd protein located in the presynaptic compartment of neurons. The patient improved after surgery and corticosteroid treatment and has been stable for nearly 4 years on only anti-estrogenics. The triad of stiff-man syndrome, breast cancer, and autoantibodies against amphiphysin identifies a new autoimmune paraneoplastic syndrome of the CNS.

NEUROLOGY 1998;50:94–98

Stiff-man syndrome (SMS) is a rare CNS disease characterized by progressive fluctuating rigidity and superimposed spasms. Rigidity predominantly affects the trunk muscles. Spasms may occur spontaneously but are often precipitated by unexpected noise, sudden movements, or emotional upset. Muscle tone becomes normal and spasms disappear during sleep. In most cases, the neurologic examination lacks major pathologic signs. Neuroimaging does not show specific alterations but may help to exclude symptomatic cases.[1-4] The pathogenesis of SMS is unclear. However, two observations are compatible with an autoimmune etiology[5]: autoantibodies against glutamic acid decarboxylase (GAD), the enzyme responsible for the synthesis of the inhibitory neurotransmitter γ-aminobutyric acid (GABA), are present in 60% of patients with SMS, and insulin-dependent diabetes mellitus and other organ-specific autoimmune diseases are frequently found in these cases. Observation of SMS in patients with a variety of malignant tumors suggests a paraneoplastic nature of SMS in these cases.[4,6-11]

We report a patient who presented with SMS that was initially misdiagnosed as a psychogenic movement disorder associated with breast cancer. Biochemical investigations helped to establish the autoimmune paraneoplastic nature of the disease. Earlier reports included some of the data.[12,13]

Case report. This 59-year-old woman presented in July 1992 with a 2-month history of progressive aching and stiffness of the shoulder and arm muscles that began on the right side, then spread to the left. Later on mild spasms of shoulder and arm muscles occurred. At approximately the same time she noticed a small nodular mass in her left breast. Because her symptoms were preceded by serious personal and professional problems and her neurologic status was otherwise normal, a psychogenic origin was assumed. She was subsequently hospitalized for psychotherapy (see reference 12). However, rigidity of the shoulders, arms, and back progressed, and severe spasms developed spontaneously as well as during voluntary or passive movement. Spasms were so violent that subluxation of the shoulders and ankylosis of the wrists resulted.

On second admission in October 1992, she presented with painfully fixed subluxation of the shoulders, adduction of the arms, and maximum flexion of the elbows and wrists. The hands were permanently deformed in an S shape, and the fingers appeared flaccid and paralyzed because of mechanical constraints (figure 1A). The arms were covered by subcutaneous hematomas caused by the spasms. Spasms occurred spontaneously or in response to either active or passive movement of the arms or hands. Weak cutaneous, but not acoustic, stimuli also precipitated the spasms. This prohibited examination of muscular strength and deep tendon reflexes in the arms, but sensory functions appeared normal. Neurologic examination of the cranial nerves was normal as were muscular strength and tone as well as deep tendon and cutaneous reflexes of the

From the Department of Neurology (Drs. Rosin and Meinck), University of Heidelberg, Heidelberg, Germany; Department of Cell Biology and Howard Hughes Medical Institute (Drs. DeCamilli and Butler) and Department of Internal Medicine, Section of Endocrinology (Dr. Solimena), Yale University, New Haven, CT; Department of Neuropathology (Dr. Schmitt), University of Heidelberg, Heidelberg, Germany; and Department of Medicine III (Dr. Morgenthaler), University of Leipzig, Leipzig, Germany.

Supported by the Volkswagenstiftung and the Heidelberg Medical Research Council.

Received July 30, 1996. Accepted in final form July 22, 1997.

Address correspondence and reprint requests to Prof. Dr. Hans-Michael Meinck, Neurologische Universitätsklinik, Im Neuenheimerfeld 400, D 69120 Heidelberg, Germany.

Figure 1. (A) The patient 3 months after onset of symptoms with severe muscle rigidity and painful spasms, subluxation of the shoulders, fixed posture of the arms and hands, and widespread subcutaneous hematomas on both arms. (B) The patient 1 month after breast surgery.

lower body; no hyperlordosis was observed. Oral clonazepam effectively suppressed the spasms, but failed to reduce rigid immobility of the shoulders and arms even at high doses (up to 24 mg/d) or if the patient was comedicated with baclofen (100 mg/d). Repeat examination during general anesthesia and relaxation, immediately before breast surgery, disclosed severe restriction of passive joint movements—maximum shoulder abduction was limited to 30° to 40°, and elbow extension to 80° to 90°. Her wrists were immobilized in a 90° to 100° flexed position.

EMG revealed steady low-frequency firing of normal motor units that abruptly increased during spontaneous spasms, after somatosensory stimulation or on passive movements (figure 2). Evoked cortical responses to tibial nerve stimulation and the triceps surae H-reflex silent period were normal. Her general status did not allow magnetic brain stimulation or electrophysiologic testing for spasmodic reflex myoclonus, a physiologic type of myoclonic jerking characteristic of SMS.[14] Radiographs confirmed subluxation of the shoulders and disclosed recent multiple rib fractures on both sides thought to be caused by adduction spasms of the arms. MRI of the cervical spinal cord, albeit obscured by movement artifacts, showed no gross abnormalities; MRI of the brain was normal. Biopsy of the pectoralis muscle performed during mastectomy revealed mild and nonspecific chronic myopathic changes without increase of intramuscular connective tissue. Cerebrospinal fluid was normal and showed no oligoclonal banding. Routine laboratory investigations including tests for autoantibodies also yielded no abnormalities.

Histologic investigation of the mammary tissue revealed moderately differentiated ductal adenocarcinoma with metastatic invasion of 2 of the 11 excised axillary lymph nodes (tumor staging was pT1, N1, M0, GII; R0). Elevated levels of estrogen receptors were found in both tumor (472 fmol/mg) and metastatic tissue (791 fmol/mg). Progesterone receptors were normal. The patient was treated with anti-estrogenics, clonazepam (6 mg/d), and methylprednisolone 1,000 mg/d tapering off over the following 3 months. Within a few days, muscle tone normalized, and painful spasms disappeared. Subluxation of the shoulders and ankylosis of the wrists, however, did not significantly improve (figure 1B). Complex hand surgery involving wrist arthrodesis in the neutral position, multiple digital capsulotomies, and lengthening and transfer of various tendons enabled her to regain partial use of the hands so that she could care for herself without assistance. Clonazepam was tapered off gradually. The only permanent neurologic abnormality in follow-up examinations has been an increased biceps tendon jerk on the right side.

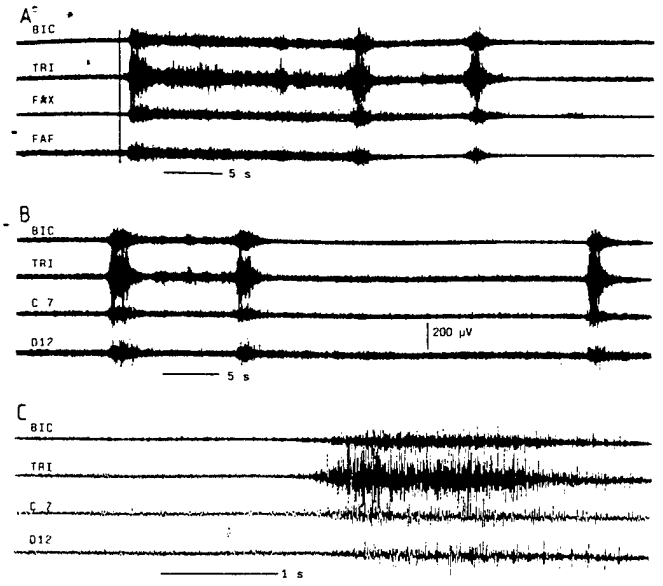

Figure 2. Polygraphic EMG recording (surface electrodes) of (A) reflex-induced and (B,C) spontaneous spasms from the right biceps (BIC), triceps (TRI), forearm extensor (FAX), and forearm flexor (FAF) muscles as well as paraspinal muscles at C-7 and TH (D) 12 levels. The vertical line in A marks the stimulus (electrical shock at motor threshold to the left median nerve at the wrist). Vertical calibration in B applies for all recordings. Note the stereotypical pattern of all spasms.

Methods. Western blot and immunoprecipitation techniques for identification of the 128-kd protein, amphiphysin, have been reported recently.[11,13] Rat tissues were fixed by transcardiac perfusion. Immunoperoxidase staining of frozen tissue sections was carried out as previously described.[15,16] Patient sera was diluted 1:10, and 4% formaldehyde was used as fixative.

Autoantibodies against GAD were determined with immunocytochemistry[5] and radioligand techniques. The GAD radioligand assay was performed with both the recombinant 65- and 67-kd isoforms of human GAD (GAD65 and GAD67) as recently reported.[17] In the second GAD Antibody Proficiency Program, the assay achieved 100% sensitivity and 100% specifity. As compared with immunocytochemistry testing, this radioligand assay identifies elevated GAD antibody levels in about 50% more patients with the clinical diagnosis SMS.[18]

Results. Although immunocytochemistry revealed no anti-GAD autoantibodies,[5,13] retrospective investigation of stored serum samples with the radioligand assay[17,18] yielded levels of autoantibodies directed against GAD65 that increased successively from 5 arbitrary units (AU) on second admission to 120 AU 2 years later (normal, <7 AU). In contrast, autoantibody levels against GAD67 constantly remained below the normal limit (6 AU).

With Western blot and immunoprecipitation techniques, autoantibodies against amphiphysin, a neuronal 128-kd protein, were detected in the patient's serum and CSF.[11,13] Using Western blots on rat brain homogenate, the serum of our patient recognized a band of 128 kd that precisely comigrated with a band recognized by both rabbit antibodies against chicken amphiphysin and rabbit serum raised against recombinant human amphiphysin. Furthermore, the 128-kd protein immunoprecipitated from rat brain extracts with the patient's serum was recognized in a Western blot assay by rabbit antibodies raised against amphiphysin. Western blots of two-dimensional gels of a soluble rat brain fraction probed with the patient's serum and with rabbit anti-amphiphysin serum revealed identical electrophoretic mobility of the 128-kd antigen and amphiphysin. Western blots of post-nuclear supernatants of rat tissues (brain, pituitary gland, testis, liver) and endocrine cell lines (PC12 cells [rat chromaffin cell line]), βTC3 cells (mouse insulinoma), and aTC9 cells (mouse glucagonoma) probed with either patient's or anti-amphiphysin serum showed a tissue distribution of the 128-kd protein identical to that of amphiphysin. Both proteins were expressed at high concentrations in brain and low concentrations in endocrine tissues.[13] Amphiphysin was, however, not detected in the patient's breast cancer tissue (see also reference 11). Using the patient's serum as a source of primary antibodies, indirect immunoperoxidase staining of cryostat rat brain sections demonstrated amphiphysin in a subset of neurons (figure 3, A and B) and concentrated at presynaptic nerve terminals surrounding neuronal perikarya (figure 3, C and D) and dendritic processes (figure 3D). Despite progressive clinical improvement, follow-ups revealed persistent autoimmunity directed against amphiphysin.

Discussion. The majority of SMS patients have autoantibodies directed against GAD, a neuronal antigen concentrated at presynaptic terminals.[5,18] In a few patients, including ours, autoantibodies are directed against amphiphysin.[11,13] Amphiphysin is a neuronal protein that is also concentrated in the presynaptic compartment of neurons.[19] Although the precise function of amphiphysin remains unclear, considerable evidence indicates that it may play a role in the endocytosis of synaptic vesicles.[20]

Several investigations of previous cases of SMS associated with malignant tumors suggested an autoimmune paraneoplastic pathogenesis but failed to demonstrate specific autoantibodies against neuronal antigens.[4,6-10] The triad of SMS, ductal adenocarcinoma of the breast, and anti-amphiphysin autoimmunity has been observed in three previous cases.[11] However, anti-amphiphysin autoimmunity does not appear to be present in either SMS patients without breast cancer or in breast cancer patients without SMS. Thus, this triad may well represent a new autoimmune paraneoplastic syndrome of the CNS. Hence, it may be advisable to search for occult breast cancer in SMS patients with anti-amphiphysin autoantibodies. Ours is the fourth patient reported to have autoantibodies directed against amphiphysin[11,13] and the first with autoantibodies directed against both amphiphysin and GAD65. However, the serum of patients with SMS and breast cancer has not been investigated with the novel radioligand assay. Whether anti-GAD65 or GAD67 autoantibodies also appear in other paraneoplastic SMS patients remains to be clarified.

Autoimmune paraneoplastic nervous system dis-

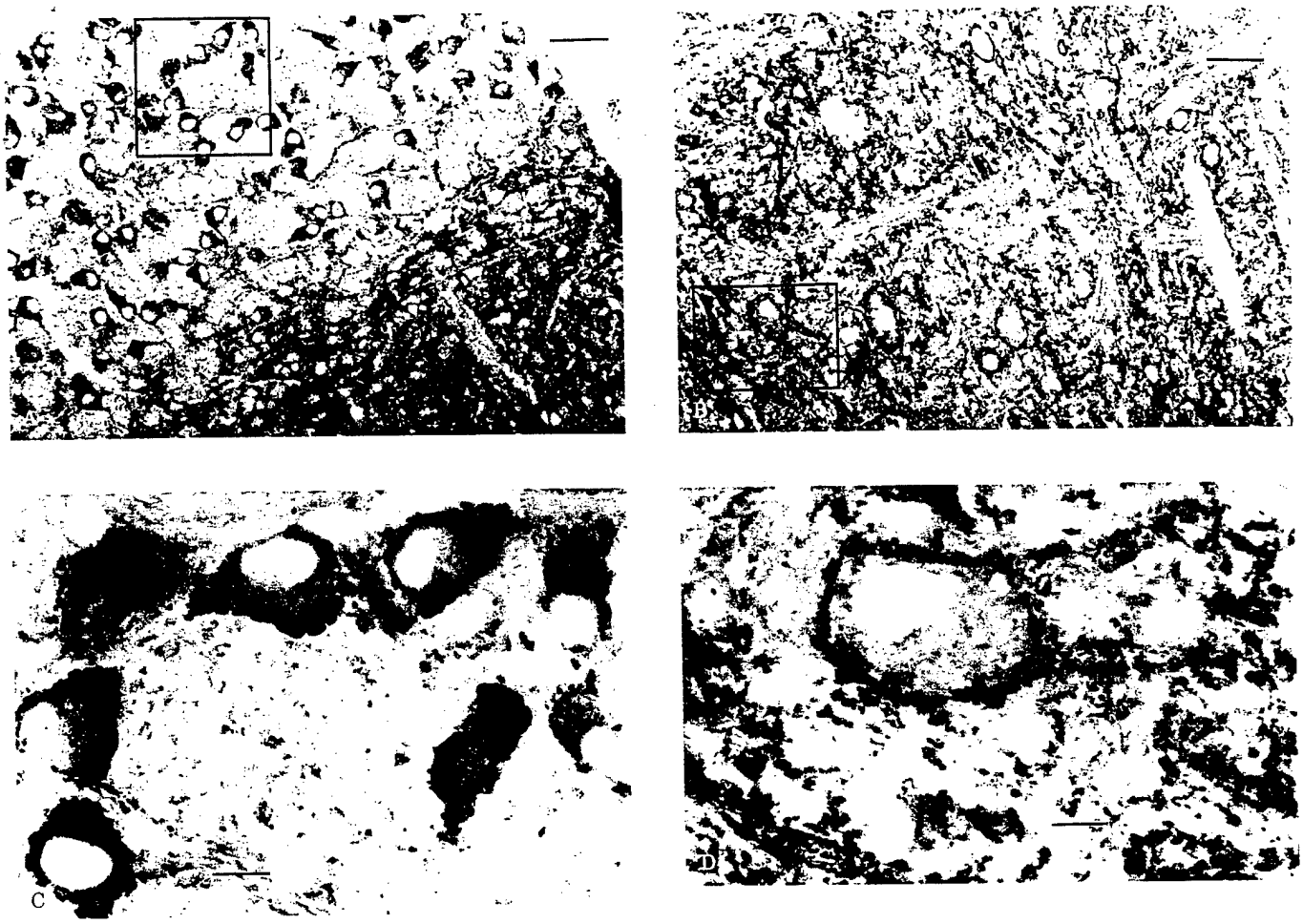

Figure 3. Indirect immunoperoxidase staining of cryostat rat brain regions (10 μm, sagittal sections) with patient's serum as a source of primary antibodies (1:100). (A and B) Low-magnification views of brainstem regions. (C) Higher magnification of the boxed field in panel A. (D) Higher magnification of the boxed field in panel B. The autoantigen recognized by the patient's autoantibodies, amphiphysin, is localized in the cytosol of a subset of neurons (A and B) showing dense distribution at the presynaptic nerve terminals surrounding neuronal perikarya (C and D) and dendritic processes (D). Immunostaining is not observed in glial cells or in the nuclei of immunolabeled neurons. Scale bar is 50 μm in panels A and B, and 10 μm in panels C and D.

orders are characterized by a distinct neurologic syndrome associated with specific humoral responses directed against cytoplasmic or nuclear neuronal antigens in the presence of certain types of neoplasm.[21-25] Autoantigens of most autoimmune paraneoplastic diseases of the nervous system are intracellular proteins, as are GAD and amphiphysin. The mechanisms underlying humoral or cellular autoimmunity directed against intracellular antigens remain unexplained, as do the links between autoimmunity directed against amphiphysin (or likewise GAD), neural damage, and clinical symptoms.[26] However, two observations made in our patient support the hypothesis that neurological symptoms in SMS are a result of functional rather than structural damage: (a) neurologic symptoms improved after treatment of cancer and introduction of steroid therapy (seen also in two previous cases[11]), and (b) cranial and cervical MRI lacked pathologic findings. Correspondingly, necropsy in cancer-associated SMS cases of brief duration revealed only perivascular lymphocyte cuffs in the brain and spinal cord[9] (see also reference 27), whereas loss of anterior horn neurons was observed only in long-standing cases.[6,7] Moreover, the persistence of strong autoimmunity directed against amphiphysin, as well as the delayed development of autoimmunity directed against GAD65 despite clinical remission, would suggest that autoantibodies against both antigens might be an epiphenomenon rather than a causative agent.

The locus of the suspected attack to the CNS remains speculative. In our patient, stiffness and spasms were confined to muscles of the C-6 through C-8 segments in an almost symmetric fashion, and brainstem or long tract signs were lacking. Hence, the disturbance might be tentatively located in the gray matter of the lower cervical spinal cord. This is consistent with prior necropsy findings in cases of SMS,[6,7,9,27] or with segmental rigidity and spasms caused by spinal cord ischemia[28-30] or tumors.[31-34]

In conclusion, the detection of amphiphysin-autoantibodies in a woman with SMS associated

with breast cancer has characteristics of a distinct paraneoplastic syndrome, although the pathogenesis of neuronal damage and of neurologic symptoms remains unexplained.

Acknowledgments

We thank W. Huttner, PhD, Heidelberg, Germany, for his kind cooperation and Dr. A. Lernmark, Seattle, WA, for kindly providing human cDNA for GAD65.

References

1. Moersch FP, Woltman HW. Progressive and fluctuating muscular rigidity and spasm (stiff-man syndrome): report of a case and some observations in 13 other cases. Mayo Clin Proc 1956; 31:421–427.
2. Gordon EE, Januszko DM, Kaufman L. A critical survey of stiff man syndrome. Am J Med 1967;42:582–599.
3. Lorish TR, Thorsteinsson G, Howard FM. Stiff-man syndrome updated. Mayo Clin Proc 1989;64:629–636.
4. Meinck HM, Ricker K, Hülser PJ, et al. Stiff man syndrome: clinical and laboratory findings in 8 patients. J Neurol 1994; 24:157–166.
5. Solimena M, De Camilli P. Autoimmunity to glutamic acid decarboxylase (GAD) in stiff man syndrome and insulin-dependent diabetes mellitus. Trends Neurosci 1991;14:452–457.
6. Roobol TH, Kazzaz BA, Vecht CJ. Segmental rigidity and spinal myoclonus as a paraneoplastic syndrome. J Neurol Neurosurg Psychiatry 1987;50:628–631.
7. Masson C, Prier S, Benoit C, et al. Amnésie, syndrome de l'homme raide. Ann Med Interne (Paris) 1987;138:502–505.
8. Piccolo G, Cosi V. Stiff man syndrome, dysimmune disorder, and cancer [letter]. Ann Neurol 1989;26:105.
9. Bateman DE, Weller RO, Kennedy P. Stiff man syndrome: a rare paraneoplastic disorder? J Neurol Neurosurg Psychiatry 1990;53:695–696.
10. Ferrari P, Federico M, Grimaldi LM, et al. Stiff man syndrome in a patient with Hodgkin's disease: an unusual paraneoplastic syndrome. Haematologica 1990;75:570–572.
11. Folli F, Solimena M, Cofiell R, et al. Autoantibodies to a 128 kD synaptic protein in stiff-man syndrome with breast cancer. N Engl J Med 1993;328:546–551.
12. Henningsen P, Clement U, KüchenhoffJ, et al. Psychological factors in the diagnosis and pathogenesis of stiff-man syndrome. Neurology 1996;47:38–42.
13. De Camilli P, Thomas A, Cofiell R, et al. The synaptic vesicle-associated protein amphiphysin is the autoantigen of stiff-man syndrome with breast cancer. J Exp Med 1993;178:2219–2223.
14. Meinck HM, Ricker K, Hülser PJ, et al. Stiff man syndrome: neurophysiological findings in eight patients. J Neurol 1995; 242:134–142.
15. De Camilli P, Cameron R, Greengard P. Synapsin I (protein I), a nerve terminal-specific phosphoprotein. I. Its general distribution in the synapses of the central and peripheral nervous system demonstrated by immunofluorescence in frozen and plastic sections. J Cell Biol 1983;96:1337–1354.
16. De Camilli P, Miller PE, Levitt P, et al. Anatomy of cerebellar Purkinje cells in the rat determined by a specific immunohistochemical marker. Neuroscience 1984;11:761–817.
17. Seissler J, Morgenthaler NG, Achenbach P, et al. Combined screening for antibodies to IA-2 and antibodies to glutamic acid decarboxylase in first-degree relatives of patients with IDDM. Diabetologia 1996;39:1351–1356.
18. Meinck HM, Maile S, Faber L, et al. Autoantibodies against glutamic acid decarboxylase 65 in stiff-man syndrome and in other neurological diseases: sensitivity and specifity of a novel radioligand assay [abstract]. Eur Neurol 1996;3(suppl 5):72.
19. Lichte B, Veh RW, Meyer H, et al. Amphiphysin, a novel protein associated with synaptic vesicles. EMBO J 1992;11: 2521–2530.
20. David C, McPherson PS, Mundigl O, et al. A role of amphiphysin in synaptic vesicle endocytosis suggested by its binding to dynamin in nerve terminals. Proc Natl Acad Sci USA 1996;93: 331–335.
21. Furneaux HM, Rosenblum MK, Dalmau J, et al. Selective expression of Purkinje-cell antigens in tumor tissue from patients with paraneoplastic cerebellar degeneration. N Engl J Med 1990;322:1844–1851.
22. Graus F, Elkon KB, Cordon-Cardo C, et al. Sensory neuronopathy and small cell lung cancer: antineuronal antibody that also reacts with the tumor. Am J Med 1986;80:45–52.
23. Hetzel DJ, Stanhope CR, O'Neil BP, et al. Gynecologic cancer in patients with subacute cerebellar degeneration predicted by anti-Purkinje cell antibodies and limited in metastatic volume. Mayo Clin Proc 1990;65:1558–1563.
24. Dropcho E, Payne R. Paraneoplastic opsoclonus myoclonus. Arch Neurol 1986;43:410–415.
25. Lambert EH, Lennon VA. Selected IgG rapidly induces Lambert-Eaton myasthenic syndrome in mice: complement independence and EMG abnormalities. Muscle Nerve 1988;11: 1133–1145.
26. Ellis TM, Atkinson MA. The clinical significance of an autoimmune response against glutamic acid decarboxylase. Nat Med 1996;2:148–153.
27. Mitsumoto H, Schwartzman MJ, Estes ML, et al. Sudden death and paroxysmal autonomic dysfunction in stiff-man syndrome. J Neurol 1991;238:91–96.
28. Gelfan S, Tarlov IM. Interneurones and rigidity of spinal origin. J Physiol 1959;146:594–617.
29. Murayama S, Smith CM. Rigidity of hind limbs of cats produced by occlusion of spinal cord blood supply. Neurology 1965;15:565–577.
30. Davis SM, Murray NMF, Diengdoh JV, et al. Stimulus-sensitive spinal myoclonus. J Neurol Neurosurg Psychiatry 1981;44:884–888.
31. Penry JK, Hoefnagel D, van den Noort S, et al. Muscle spasm and abnormal postures resulting from damage to interneurons in spinal cord. Arch Neurol 1960;3:500–512.
32. Rushworth G, Lishman WA, Hughes JT, et al. Intense rigidity of the arms due to isolation of motoneurones by a spinal tumour. J Neurol Neurosurg Psychiatry 1961;24:132–142.
33. Tarlov IM. Rigidity in man due to spinal interneuron loss. Arch Neurol 1967;16:536–543.
34. Tarlov IM. Deafferentation to relieve spasticity or rigidity: reasons for failure in some cases of paraplegia. J Neurosurg 1966;25:270–274.

J Neurol Neurosurg Psychiatry 1999;66:214–217

SHORT REPORT

Anti-amphiphysin I antibodies in patients with paraneoplastic neurological disorders associated with small cell lung carcinoma

A Saiz, J Dalmau, M Husta Butler, Q Chen, J Y Delattre, P De Camilli, F Graus

Abstract

Patients with stiff man syndrome and breast cancer develop anti-amphiphysin I antibodies that primarily recognise the C terminus of the protein. Anti-amphiphysin I antibodies have also been identified in a few patients with paraneoplastic neurological disorders (PND) and small cell lung cancer (SCLC). The frequency of anti-amphiphysin I antibodies in patients with SCLC and PND was analysed and the epitope specificity of these antibodies was characterised.

Anti-amphiphysin I antibodies were evaluated by immunohistochemistry on human and rat cerebellum and immunoblots of rat brain homogenates. Serum samples included 134 patients with PND and anti-Hu antibodies (83% had SCLC), 44 with SCLC and PND without anti-Hu-antibodies, 63 with PND and either Yo, Ri, or Tr antibodies, 146 with SCLC without PND, and 104 with non-PND. Positive serum samples were confirmed with immunoblots of recombinant human amphiphysin I and immunoreacted with five overlapping peptide fragments covering the full length of the molecule.

Serum samples positive for anti-amphiphysin I antibodies included those from seven (2.9%) patients with PND and two (1.4%) with SCLC without PND. Six of the seven anti-amphiphysin I antibody positive patients with PND had SCLC (three with Hu-antibodies), and one had anti-Hu-antibodies but no detectable tumour. The PND included encephalomyelitis/sensory neuropathy (five patients), cerebellar degeneration (one), and opsoclonus (one). All anti-amphiphysin I antibodies reacted with the C terminus of amphiphysin I, but seven also recognised other fragments of the molecule.

In conclusion, anti-amphiphysin I antibodies are present at low frequency in patients with SCLC irrespective of the presence of an associated PND. All anti-amphiphysin I antibody positive serum samples have in common reactivity with the C terminus of the protein.

(J Neurol Neurosurg Psychiatry 1999;66:214-217)

Service of Neurology and Institut d'Investigació Biomèdica August Pi i Sunyer (IDIBAPS), Hospital Clínic, University of Barcelona, Barcelona. Spain
A Saiz
F Graus

Department of Neurology, Memorial Sloan-Kettering Cancer Center, New York, USA
J Dalmau

Department of Cell Biology and Howard Hughes Medical Institute, Yale University School of Medicine, New Haven, Conn, USA
M Husta Butler
P De Camilli

Service of Neurology, Hôpital de la Pitié-Salpêtrière, INSERM U134, Paris, France
Q Chen
J Y Delattre

Correspondence to:
Dr Francesc Graus, Servei de Neurologia, Hospital Clínic, Villarroel 170, Barcelona 08036. Spain. Telephone 0034 3 2272213; fax 0034 3 2275414; email graus@medicina.ub.es

Received 9 March 1998 and in revised form 3 September 1998
Accepted 11 September 1998

Keywords: autoantibodies; amphiphysin I; paraneoplastic; small cell lung carcinoma; stiff man syndrome

Amphiphysin I, a nerve terminal protein with a putative role in endocytosis,[1] is recognised by autoantibodies present in the serum and CSF samples from female patients with paraneoplastic stiff man syndrome (SMS) and breast cancer.[2 3] The anti-amphiphysin I antibodies of these patients predominantly react with the C terminus of the protein.[1 4] A recent study[5] identified anti-amphiphysin I antibodies in the serum of three patients with small cell lung carcinoma (SCLC) and paraneoplastic encephalomyelitis and sensory neuronopathy (PEM/SN), a disorder usually associated with anti-Hu-antibodies.[6] The serum of one of these patients had anti-Hu antibodies but none of them developed typical SMS. Although this study suggested that PEM/SN in patients with SCLC may associate with several autoantibody specificities and that anti-amphiphysin I antibodies are not restricted to SMS, the frequency and specificity of these associations were not defined. A few additional cases of anti-amphiphysin I antibody positive patients with PND other than SMS associated with either breast or lung cancer were reported.[7] To clarify these clinical-serological associations is important because these antibodies are considered good markers of specific types of paraneoplastic syndromes and tumours.

In the present study, we analysed the frequency of anti-amphiphysin I antibodies in a large series of patients with PND other than SMS, to determine whether: (1) anti-amphiphysin I antibodies are associated with a particular type of PND or tumour and (2) whether amphiphysin I autoepitopes differ in patients with different clinical syndromes.

Materials and methods

Serum samples were obtained from 241 patients with PND, 146 with SCLC without PND or anti-Hu-antibodies, and 104 with non-paraneoplastic neurological disorders usually considered in the differential diagnosis of PND (cerebellar disorders 56, sensory neuropathy 41; opsoclonus seven). Among the 241 patients with PND, 134 had PEM/SN (83%

had SCLC), 44 had SCLC and PND without anti-Hu antibodies (paraneoplastic cerebellar degeneration 30; PEM/SN seven; opsoclonus seven), and 63 had PND and either Yo, Ri, or Tr antibodies. Serum samples were collected in three of the participant laboratories (Barcelona, Paris, and New York) and kept frozen at −70° C. Serum samples from two patients with paraneoplastic SMS and breast cancer were used as positive controls.

Immunohistochemistry on human and rat cerebellum (serum screening dilution 1:500) and immunoblot of rat brain homogeneate (serum dilution 1:10 000) were done as previously described in detail.[8,9] To make the anti-amphiphysin I antibody detection more uniform, all immunoblots were prepared in the same laboratory (Hospital Clinic, Barcelona) and nitrocellulose strips containing the same amount of immobilised antigen were sent to the other two participating laboratories (Paris and New York) that processed the strips with the same protocol.

CRITERIA FOR THE PRESENCE OF ANTI-AMPHIPHYSIN I ANTIBODIES

A serum was considered positive for anti-amphiphysin I antibodies when immunoblots of rat brain homogenate showed a reactive band of identical electrophoretic mobility (around 128 kDa) than that obtained with the positive control. All positive and seven randomly taken negative serum samples were subsequently evaluated by indirect immunofluorescence on formaldehyde fixed rat cerebellar tissue[2] and immunoblots of recombinant human amphiphysin I[4] at Yale University (MHB, PDC). Serum samples were tested at dilutions of 1:4 and 1:500 for the immunofluorescence and the immunoblot experiments respectively. Clinical information was blinded from investigators performing these immunoblots.

EPITOPE ANALYSIS

Glutathione S-transferase (GST) fusion proteins consisting of five overlapping fragments of amphiphysin I were prepared as described previously.[4] The five GST fusion proteins were subjected to SDS-PAGE (10% acrylamide) and western blotting as previously described.[10] Monoclonal antibodies directed to each fragment of amphiphysin I were used to identify the correct band. Positive and negative human serum samples were also used as controls.

Results

IMMUNOBLOT STUDIES

Nine serum samples immunoreacted with a band identical with that obtained with the positive control in immunoblots of rat brain homogenate (figure). In all of them, the presence of anti-amphiphysin I antibodies was confirmed in immunoblots of recombinant human amphiphysin I, whereas seven negative serum samples by the screening criteria, blindly examined with the positive ones, did not react with the recombinant protein. All nine positive samples reacted with fragment V of amphiphysin I that includes the C terminus of the molecule,[4] but the reactivity with the other four fragments of amphiphysin I was not uniform with seven samples recognising multiple fragments.

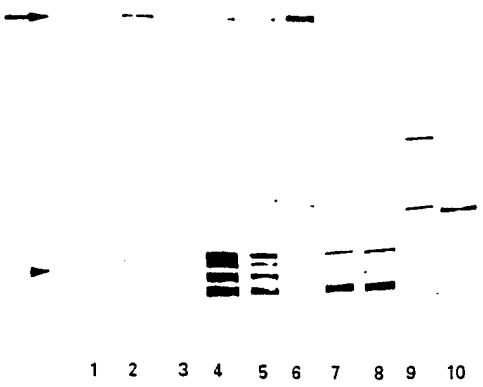

Immunoblots of rat brain homogenate probed with a normal human serum (lane 1), serum from paraneoplastic SMS and breast cancer with anti-amphiphysin I antibodies, as positive controls (lanes 2,3), PND and SCLC (lanes 4–8), and SCLC without PND (lanes 9–10). Three serum samples from patients with PND and SCLC (lanes 4–6) immunoreacted with a band (around 128 kDa) of the same electrophoretic mobility as that recognised by the positive anti-amphiphysin I antibody serum samples (arrow). Four serum samples also presented anti-Hu antibodies (arrowhead).

IMMUNOHISTOCHEMISTRY STUDIES

None of the nine positive anti-amphiphysin I antibody serum samples could be identified by immunohistochemistry on human cerebellum. In rat cerebellar sections evaluated by the avidin-biotin immunoperoxidase technique, the presence of anti-amphiphysin I antibodies was shown in only one serum sample, which corresponded to that with the strongest immunoreactivity in immunoblots. However, when the nine serum samples were evaluted by indirect immunofluorescence using a higher concentration,[2] all but one gave an immunoreactive pattern compatible with anti-amphiphysin I antibodies.

CLINICAL-IMMUNOLOGICAL CORRELATION

Seven anti-amphiphysin I antibody positive patients had PND(2.9%) and two had SCLC without neurological disorders (1.4%). Six of the seven patients with PND had SCLC that was diagnosed after onset of the neurological symptoms. In one patient, who also was anti-Hu-antibody positive, the tumour could not be found at necropsy. We include this patient in the PND group because the patient presented typical clinical and neuropathological features of PEM/SN with neuronal loss and inflammatory infiltrates in the dorsal root ganglia and spinal cord. None of the patients without PND or with PND associated with anti-Yo, Ri, or Tr antibodies had anti-amphiphysin I antibodies.

The clinical features of the seven patients with PND and anti-amphiphysin I antibodies are summarised in the table. Five of the seven patients developed symptoms of PEM/SN and four of them also had high titres of anti-Hu-antibodies. The other two patients had paraneoplastic cerebellar degeneration and

Clinical features of anti-amphiphysin positive patients with paraneoplastic neurological disorders

Patient	*Age/sex*	*Clinical syndrome*	*Hu-Ab*	*Time (months) PND/tumour*	*Cancer*	*Outcome*
1	60/F	Sensorimotor neuropathy	Yes	−23	SCLC	Necropsy: PEM/SN†
2	58/M	PEM/SN	Yes	−7	SCLC	Necropsy: PEM/SN†
3	71/M	PEM/SN and LEMS	Yes	−17	SCLC	Necropsy: PEM/SN†
4	64/M	Sensory neuropathy	No*	0	SCLC	Death: pulmonary embolus
5	64/M	Cerebellar syndrome	No	−18	SCLC	Alive for 7 years
6	74/M	Opsoclonus/myoclonus	No*	−1	SCLC	Necropsy: perivascular/meningeal inflammatory infiltrates. Moderate neuronal loss in dentate nucleus and Purkinje cells
7	80/F	Sensory neuropathy	Yes	n.a.	None	Necropsy: PEM/SN**

PEM/SN=Paraneoplastic encephalomyelitis/sensory neuronopathy; LEMS=Lambert-Eaton myasthenic syndrome; SCLC=small cell lung carcinoma; NA=not applicable.
*Patients had low titre of Hu-Ab similar to that found in 16% of SCLC without paraneoplastic neurological disorders.[11]
†Necropsy findings typical of PEM/SN with multifocal inflammatory infiltrates, reactive gliosis, and neuronal loss.

opsoclonus/myoclonus syndrome. The frequency of anti-amphiphysin I antibodies in patients with PND and SCLC (3.9%) with (2.7%) or without (6.8%) anti-Hu-antibodies was not statistically different from that in patients with SCLC without PND.

Discussion

The main finding of the present study is that the frequency of anti-amphiphysin I antibodies was low in patients with SCLC and PND. The group of patients with the highest frequency of anti-amphiphysin I antibodies (6.8%) corresponded with those with SCLC, PND, and negative anti-Hu-antibodies. However, even for this group the frequency of anti-amphiphysin I antibodies was not significantly different from that in patients with SCLC without PND.

The clinical range of anti-amphiphysin I antibody positive patients was not uniform. None developed clinical or neurophysiological features of SMS, five patients had PEM/SN and two developed other PND (see below). Four out of the five PEM/SN patients had anti-Hu-antibodies, a not surprising finding considering that the great majority of patients with PEM/SN, 95% in this series, had anti-Hu-antibodies.[6] Necropsy findings of the four patients with PEM/SN harbouring both anti-Hu-antibodies and anti-amphiphysin I antibodies were similar to those reported in anti-Hu-antibody positive patients with PEM/SN but without anti-amphiphysin I antibodies.[7] Although postmortem of one of our anti-amphiphysin I antibody positive patients did not show a tumour, this patient had anti-Hu-antibodies and typical clinical and postmortem features of PEM/SN raising the possibility that a small, tumour was overlooked.

The other two patients presented paraneoplastic cerebellar degeneration and the opsoclonus/myoclonus syndrome respectively. Patients with paraneoplastic cerebellar degeneration and SCLC, who do not develop other features of PEM/SN, usually lack anti-Hu-antibodies but 36% of them harbour P/Q type voltage gated calcium channel antibodies probably related to a higher than expected association with the Lambert-Eaton myasthenic syndrome.[12] Similarly, anti-Hu-antibodies are rarely identified in paraneoplastic opsoclonus-myoclonus associated with SCLC although a few patients have been reported.[13 14] Excluding these exceptions, when paraneoplastic cerebellar degeneration and opsoclonus/myoclonus develop as isolated syndromes in patients with SCLC, they are not generally associated with any specific antineuronal antibody. Our series supports this notion, because anti-amphiphysin I antibodies were identified in only 3% of paraneoplastic cerebellar degeneration and 14% of patients with opsoclonus-myoclonus and SCLC.

The low frequency of anti-amphiphysin I antibodies in patients with SCLC with PND, the lack of association with a particular neurological syndrome, and the similar frequency of anti-amphiphysin I antibodies in patients with SCLC without PND is by contrast with that described with anti-Hu-antibodies that are particularly associated with PEM/SN syndrome and SCLC.[6] This is also by contrast with the close link between anti-amphiphysin I antibodies and SMS associated with breast cancer.[2]

Our study suggests that the optimal immunohistochemical method to detect antineuronal antibodies depends on the type of antibody. In the current study, the use of recommended techniques and serum dilutions to detect antineuronal antibodies[15] failed to identify anti-amphiphysin I antibodies which, however, were readily demonstrated using higher serum concentrations and a different protocol.[2] In any case, immunoblot seems more sensitive than immunohistochemistry to detect anti-amphiphysin I antibodies.

The anti-amphiphysin I antibodies from all our patients recognised fragment V (C terminus) of human amphiphysin I, although many of them also recognised additional fragments. This finding is in agreement with that previously reported in patients with SCLC with PEM/SN and patients with SMS and breast cancer. Interestingly, in a series of 30 mouse monoclonal antibodies which were raised against human amphiphysin I, only three were directed against fragment V.[10] This indicates that the epitopes recognised by the human serum samples do not simply coincide with the most immunogenic portion of the molecule.

Anti-amphiphysin I antibodies may be useful in predicting the paraneoplastic origin of a neurological disorder in a given patient without known cancer because, in agreement with a previous report,[5] we did not find anti-amphiphysin I antibodies in a large series of patients without PND but whose symptoms were initially suspected to be paraneoplastic. However, the low incidence of anti-

amphiphysin I antibodies in patients with PND and SCLC represents a limitation for its use as a diagnostic marker of PND other than SMS.

We thank Dr M Solimena for many helpful discussions, Professor HM Meinck for providing one of the anti-amphiphysin I positive serum samples, and Mercé Bonastre for her excellent technical assistance. The work was supported in part by grantsSGR 9500027 Generalitat de Catalunya, FIS 97/2100 Madrid, Spain (FG), and NIH grant NS-26064, USA (JD).

1 David C, McPherson PS, Mundigl O, *et al.* The role of amphiphysin in synaptic vesicle endocytosis suggested by its binding to dynamin in nerve terminal. *Proc Natl Acad Sci USA* 1996;93:331–5.
2 Folli F, Solimena M, Cofiell R, *et al.* Autoantibodies to a 128-kd synaptic protein in three women with the stiff-man syndrome and breast cancer. *N Engl J Med* 1993;328:546–51.
3 De Camilli P, Thomas A, Cofiell R, *et al.* The synaptic vesicle-associated protein amphiphysin is the 128-kD autoantigen of stiff-man syndrome with breast cancer. *J Exp Med* 1993;178:2219–3.
4 David C, Solimena M, De Camilli P. Autoimmunity in stiff-man syndrome with breast cancer is targeted to the C-terminal region of human amphiphysin, a protein similar to the yeast proteins Rvs167 and Rvs161. *FEBS Lett* 1994; 351:73–9.
5 Dropcho EJ. Antiamphiphysin antibodies with small-cell lung carcinoma and paraneoplastic encephalomyelitis. *Ann Neurol* 1996;39:659–67.
6 Dalmau J, Graus F, Rosenblum MK, *et al.* Anti-Hu-associated paraneoplastic encephalomyelitis/sensory neuronopathy. A clinical study of 71 patients. *Medicine* 1992;71:59–72.
7 Lennon VA, Manley HA, Kim K, *et al.* Amphiphysin autoantibodies: a paraneoplastic serological marker of breast and lung cancer-related encephalomyeloradiculoneuritides but not classical stiff-man syndrome [abstract]. *Neurology* 1997;48:A434.
8 Graus F, Dalmau J, Valldeoriola F, *et al.* Immunological characterization of a neuronal antibody (anti-Tr) associated with paraneoplastic cerebellar degeneration and Hodgkin's disease. *J Neuroimmunol* 1997;74:55–61..
9 Saiz A, Arpa J, Sagasta A, *et al.* Autoantibodies to glutamic acid decarboxylase in three patients with cerebellar ataxia, late-onset insulin-dependent diabetes mellitus, and polyendocrine autoimmunity. *Neurology* 1997;49:1026–30.
10 Floyd S, Butler MH, Cremona O, *et al.* Expression of amphiphysin I, an autoantigen of paraneoplastic neurological syndromes, in breast cancer. *Molecular Med* 1998;4:29–39.
11 Graus F, Dalmau J, Reñé R, *et al.* Anti-Hu antibodies in patients with small-cell lung cancer: association with complete response to therapy and improved survival. *J Clin Oncol* 1997;15:2866–72.
12 Mason WP, Graus F, Lang B, *et al.* Small-cell lung cancer, paraneoplastic cerebellar degeneration and the Lambert-Eaton myasthenic syndrome. *Brain* 1997;120:1279–300.
13 Anderson NE, Budde-Steffen C, Rosenblum MK, *et al.* Opsoclonus, myoclonus, ataxia, and encephalopathy in adults with cancer: a distinct paraneoplastic syndrome. *Medicine* 1988;67:100–9.
14 Hersh B, Dangond F, Dalmau J, *et al.* Paraneoplastic opsoclonus-myoclonus associated with anti-Hu antibody. *Neurology* 1994;44:1754–5.
15 Moll JWB, Antoine JC, Brashear HR, *et al.* Guidelines on the detection of paraneoplastic anti-neuronal-specific antibodies. *Neurology* 1995;45:1937–41.

Brief Communications

A novel antineuronal antibody in a motor neuron syndrome associated with breast cancer

Article abstract—A 72-year-old woman developed a lower motor neuron syndrome (MNS) 4 months before the appearance of breast cancer. Monoparesis progressed to quadriparesis despite high-dose IV immunoglobulins, plasma exchange, and azathioprine, and high-dose IV methylprednisolone. The patient improved only after the removal of the tumor. MRI demonstrated hyperintensities in the cervical spinal cord. The patient had antibodies that reacted with axonal initial segments and nodes of Ranvier. The findings suggest that in this patient lower MNS may be a paraneoplastic condition associated with breast cancer. **Key words:** Antineuronal antibody—Motor neuron syndrome—Breast cancer.

NEUROLOGY 1999;53:852–855

F. Ferracci, MD; G. Fassetta, MD; M.H. Butler, PhD; S. Floyd; M. Solimena, MD; and P. De Camilli, MD

Whether motor neuron syndromes (MNSs) complicate cancer has long been debated. Their association with lymphoma and thymoma is well known.[1-4] A recent study[5] described 14 patients in whom MNSs preceded or followed the occurrence of various cancers and Hodgkin's lymphoma. Three patients were positive for the specific paraneoplastic antibody anti-Hu. We report a patient who developed a lower MNS 4 months before developing breast cancer. She had a new type of antineuronal antibody.

Case report. This 72-year-old woman was referred because of sudden weakness in her left upper limb. Arm abductors scored 3 points on the Medical Research Council scale; elbow flexors and extensors, wrist flexors and extensors, and finger abductors scored 2 points. Tendon reflexes were abolished. Sensory examination was normal. Plantar responses were flexor. T1-weighted MRI of the cervical spine demonstrated bulging of the intervertebral disk at C5-C6. Contrast enhanced brain CT was normal. After 20 days she complained of dizziness and had jerks of nystagmus in the primary position and when looking upward and laterally. These symptoms remitted in approximately 15 days. Gadolinium-enhanced MRI of the brain was normal. Muscle weakness progressed to areflexic quadriparesis in 2 months. Plantars were still flexor and sensory examination was normal. At 3 months all muscle groups in the upper limbs scored 1 point, and lower limb flexors and extensors scored 2 points. Furthermore the patient was hypophonic, dysphagic, and had paralysis of the upper and lower branches of the right facial nerve. The second contrast-enhanced MRI of the brain was normal. T2 sequences of the cervical spine revealed symmetric hyperintensities in the spinal cord (figure 1).

A ductal adenocarcinoma with metastatic extension to five of the seven excised lymph nodes was discovered 4 months after development of neurologic symptoms. Approximately 15 days after surgery the patient began to improve: Her swallowing and speaking were more efficacious. Thirty days later lower limb extensors scored 3 points proximally and distally, she could partially open and close her hands, and she could flex her forearms against gravity. Arm abductors scored 3 points on the right and 2 points on the left. At present she is still wheelchair bound and needs help throughout the day.

She did not respond to high-dose IV immunoglobulin, plasma exchange, and azathioprine, and IV methylprednisolone (1 g/day for 5 days).

Electrophysiologic findings. Repeated electromyographic examinations showed fibrillations and positive waves at rest in the affected muscles. Exertional activity was represented by decreased recruitment and isolated motor unit potentials. Motor and sensory conduction veloc-

Figure 1. T2 MRI of the cervical spine showing high-signal spots in the spinal cord. Axial view obtained at the C5-C6 level.

From the Department of Neurology (Drs. Ferracci and Fassetta), Ospedale di Belluno, Belluno, Italy; the Department of Cell Biology and Howard Hughes Medical Institute (Drs. Butler, Floyd, and De Camilli) and the Department of Internal Medicine, Section of Endocrinology (Dr. Solimena), Yale University, New Haven, CT.

Supported in part by grants from the NIH (CA46128) and the United States Army Medical Research and Development Command to P.D.C.

Received for publication November 20, 1998. Accepted in final form May 4, 1999.

Address correspondence and reprint requests to Dr. Franco Ferracci, Reparto di Neurologia, Ospedale di Belluno, Viale Europa, 32100 Belluno, Italy.

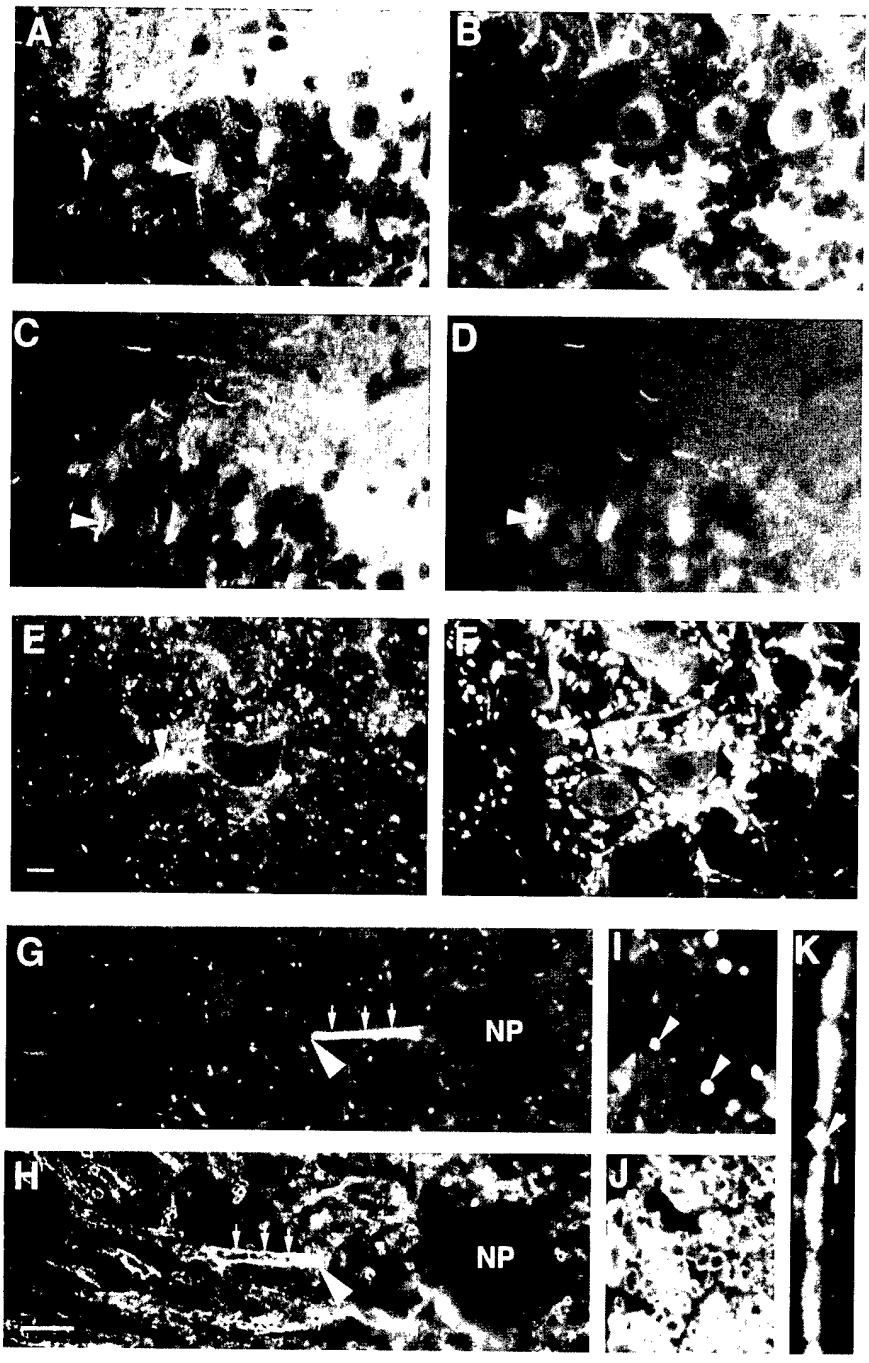

Figure 2. Immunofluorescent micrographs demonstrating the immunoreactivity recognized by the patient's autoantibodies. Rat brain sections were reacted with the serum of the patient (A, C, E, G, I, K) and counterstained for the perikaryal–dendritic marker microtubule-associated protein 2 (B, F), for the amphiphysin 2 immunoreactive epitope localized at axonal initial segments and nodes of Ranvier (D; antibody CD7), and for myelin basic protein (H, J). (A–D) Fields from the cerebellar cortex. Arrowheads point to initial segments of Purkinje's cell axons. (E, F) The anterior horn of the spinal cord (cross-section). The arrowhead points to the initial segment of a motor neuron. (G, H) The axon emerging from a neuronal perikaryon (NP) in the anterior horn is stained intensely by the autoantibodies (small arrows), and immunoreactivity stops at the site (arrowheads) where the myelin sheath begins (H). (I, J) Cross-sections of the white matter demonstrating cross-sectional nodes of Ranvier (arrowheads in I). (K) Immunoreactive node of Ranvier (arrowhead) in a longitudinally sectioned motor neuron axon in the anterior root of the spinal cord.

ities have always been normal. The compound motor action potential amplitude from the peroneal nerve was normal at onset and decreased as the disease progressed. Conduction blocks were not identified.

Normal brainstem auditory evoked potentials were recorded when the patient had nystagmus. Normal somatosensory evoked potentials to median and tibial nerve stimulation were obtained when she was quadriparetic.

Laboratory studies. CSF examination demonstrated increased protein and oligoclonal bands in three successive samples. Neoplastic cells or bacteria have never been found.

Routine blood studies, thyroid function tests, protein electrophoresis, urine porphyrin excretion, vitamin B_{12} and folate, muscle enzymes concentrations, and the screening for organ and nonorgan-specific antibodies and tumor markers were normal. Venereal disease research laboratory, Lyme serology, HIV, Epstein–Barr virus, cytomegalovirus, tick borne encephalitis, herpes virus 1 and 2, and poliovirus serologic tests were negative. Antibodies to gangliosides GM-1, asialio GM-1, GD-1b, and myelin-associated glycoprotein were absent. The search for herpesvirus 1 and 2, HIV, JC, varicella zoster, and polio viral genomic fractions in CSF by PCR gave negative results.

Antibodies directed against nervous system antigens were searched in serum by immunocytochemistry using methods already described.[6] We found antineuronal antibodies reacting with axonal initial segments and nodes of Ranvier. Examples of this immunoreactive pattern in the cerebellum and spinal cord are shown in figure 2, views A,

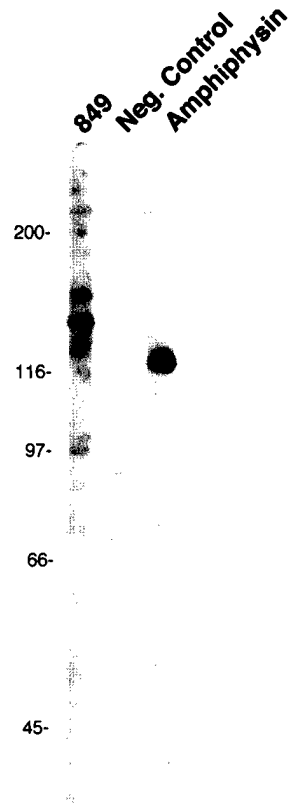

Figure 3. Western blot analysis of total rat brain homogenates reacted with the serum of the patient (849), a normal human serum (Neg. Control), and the serum of a patient with amphiphysin 1 autoimmunity (Amphiphysin).

C, E, G, I, and K. Counterstaining of the sections with antibodies directed against the perikaryal–dendritic marker microtubule-associated protein 2 (MAP-2)[7] (see figure 2, B and F) clearly demonstrated that the neuronal processes labeled by the autoantibodies were MAP-2 negative, confirming their identification as axonal initial segments. Furthermore, as shown by counterstaining with antimyelin basic protein antibodies (see figure 2, H and J), the bright immunoreactivity on axonal initial segments stops abruptly at the point where the myelin sheath starts (see figure 2, G and H). Immunoreactivity on both initial segments and nodes of Ranvier was restricted to the surface of the axon (see high-power micrographs in figure 2, G and I) and was indistinguishable from the pattern of immunoreactivity described previously[8] for an amphiphysin 2 immunoreactive epitope (antibody CD7; see figure 2D) and for ankyrin G.[9] No similar immunoreactivity, however, was seen in any of the hundreds of sera of patients with or without neurologic syndromes that we have examined. Western blot analysis of the patient's serum revealed a major immunoreactive band of approximately 148 kDa and additional minor bands (figure 3).

Discussion. In the absence of specific paraneoplastic markers, the co-occurrence of MNSs and cancer is considered coincidental. Therefore, should a patient with MNSs be investigated extensively for cancer? The study by Forsyth et al.[4] concerned 14 patients in whom MNSs preceded or followed the appearance of various cancers and Hodgkin's lymphoma. Anti-Hu antibodies were found in only three patients, two with small-cell lung cancer and one with prostate cancer. No autoantibodies were found in five women with breast cancer.

Our patient has an antineuronal immune reaction that has never been described previously. She has autoantibodies directed against an antigen concentrated at axonal initial segments and nodes of Ranvier. These regions of the axon are the sites where the action potential is generated and regenerated and, accordingly, have structural and biochemical similarities.[8,9] They are also intensely immunoreactive with two distinct rabbit sera (CD7 and CD8) raised against the COOH-terminal portion of amphiphysin 2.[8] This finding is of special interest because an amphiphysin isoform is the target of autoimmunity in stiff-man syndrome associated with breast cancer.[10] The autoantibodies of our patient, however, did not recognize amphiphysin 1 or 2 by Western blot analysis and immunoprecipitation. They recognized, instead, a novel 148-kDa band, which remains to be identified. Preliminary analysis suggests that this antigen is neuron specific.

Based on the presence of CSF oligoclonal bands and serum autoantibodies, we hypothesize that this syndrome is the result of an autoimmune reaction leading to a prominent degeneration of lower motor neurons and possibly to an encephalomyelitis. The presence of neuronal damage is suggested by the patient's limited recovery after surgery and by the abnormal findings of cervical MRI.

Another characteristic sets this patient apart from other patients with MNSs. In the series by Forsyth et al.,[4] all women with breast cancer had a predominant upper motor neuron syndrome. Our patient had a lower MNS of the brainstem and spinal cord. Because patients with lymphomas may exhibit both syndromes, it would be interesting to understand whether upper and lower MNSs in breast cancer patients mirror a different type of autoimmunity or not.

Lastly, spinal MRI findings deserve a a brief comment. A photographic report[11] showed that the cervical spinal cord of a patient with postpolio syndrome is hyperintense on T2 MRI. We looked for the same sign in our patient when she was quadriparetic and obtained T2-weighted sequences demonstrating hyperintensities in the cervical cord (see figure 1). This finding was not evident on T1 images. Without direct pathologic proof, the nature of these hyperintensities remains unknown.

Acknowledgment

The authors thank Elisa De Camilli for help with the immunofluorescence experiments and Dr. Rodolfo Muzzolon for his assistance and precious advice.

References

1. Walton JN, Tomlinson BE, Pearce GW. Subacute "poliomyelitis" and Hodgkin's disease. J Neurol Sci 1968;6:435–445.

2. Schold SC, Cho ES, Somasundaram M, Posner JP. Subacute motor neuronopathy: a remote effect of lymphoma. Ann Neurol 1979;5:271–287.
3. Younger DS, Rowland LP, Latov N, et al. Lymphoma, motor neuron diseases, and amyotrophic lateral sclerosis. Ann Neurol 1991;29:78–86.
4. Forsyth PA, Dalmau J, Graus F, et al. Motor neuron syndromes in cancer patients. Ann Neurol 1997;41:722–730.
5. Solimena M, Folli F, Denis–Donini S, et al. Autoantibodies to glutamic acid decarboxylase in a patient with stiff-man syndrome, epilepsy and type I diabetes mellitus. N Engl J Med 1988;318:1012–1020.
6. De Camilli P, Miller PE, Navone F, Theurkauf WE, Vallee RB. Distribution of microtubule-associated protein 2 in the nervous system of the rat studied by immunofluorescence. Neuroscience 1984;11:817–846.
7. Butler MH, David C, Ochoa GC, et al. Amphiphysin II (SH3P9; BIN1), a member of the amphiphysin/Rvs family, is concentrated in the cortical cytomatrix of axon initial segments and nodes of Ranvier in brain and around T tubules in skeletal muscle. J Cell Biol 1997;137:1355–1367.
8. Kordeli E, Lambert S, Bennet V. Ankyrin G. A new ankyrin gene with neural-specific isoforms localized at the axonal initial segment and node of Ranvier. Biol Chem 1995;270: 2352–2359.
9. De Camilli P, Thomas A, Cofiell R, et al. The synaptic vesicle associated protein amphiphysin is the autoantigen of stiff-man syndrome with breast cancer. J Exp Med 1993;178:2219–2223.
10. Rao DG, Bateman DE. Hyperintensities of the anterior horn cells on MRI due to poliomyelitis. J Neurol Neurosurg Psychiatry 1997;63:720.

Atypical stiff-person syndrome with spinal MRI findings, amphiphysin autoantibodies, and immunosuppression

Article abstract—In an atypical case of stiff-person syndrome (SPS), spinal T2-weighted MRI revealed a hyperintense lesion extending from C2 to C7 that corresponded with the clinical symptoms and signs. CSF showed lymphocytic pleocytosis and oligoclonal bands. Amphiphysin autoantibodies were detected In serum and CSF; however, unlike other reported cases, no malignancy occurred during a 3-year observation period. Methylprednisolone and cyclophosphamide pulse therapy led to a marked reduction of symptoms.

NEUROLOGY 1998;51:250–252

K. Schmierer, MD; J.M. Valdueza, MD; A. Bender, MD; P. DeCamilli, MD; C. David, MD; M. Solimena, MD; and R. Zschenderlein, MD

Stiff-person syndrome (SPS) is a rare disorder of motor function characterized by progressive involuntary stiffness of muscles and superimposed painful spasms, which are often precipitated by startle, emotional, and tactile stimuli and movements of affected or unaffected muscles. SPS predominantly affects the trunk and proximal limb muscles[1]; however, unusual symptoms and signs such as involvement of distal or faciobulbar muscles and autonomic disturbances have been reported.[2,3]

The pathogenesis of SPS is unclear. Evidence for a role of autoimmune mechanisms has been derived from the detection of autoantibodies against glutamic acid decarboxylase (GAD) in serum and CSF of 60% of SPS cases[4] as well as from the observation of SPS in patients with a variety of malignant tumors, suggesting a paraneoplastic nature of SPS in these cases.[5-7] Treatment of SPS has been mainly symptomatic. Several authors have reported beneficial effects from immunotherapeutic approaches.[3,5,7] We report an atypical case of SPS with spinal MRI findings and autoantibodies against amphiphysin but without development of a malignancy in a GAD antibody-negative patient who markedly improved with methylprednisolone and cyclophosphamide pulse therapy.

Case report. A healthy 53-year-old midwife developed progressive stiffness of her right upper arm and trunk 4 months before admission. She had been admitted to a district hospital, where she underwent Cloward's operation because of suspected disc prolapse between cervical vertebrae 6 and 7. As symptoms progressed, the patient was misdiagnosed as having Parkinson's disease or a psychogenic disorder. Medical history included a biopsy of the right breast without detection of a malignancy when she was 37 years old.

On admission, the woman presented with painful rigid muscles in her shoulder girdle, strongly pronounced on the right and spreading ipsilaterally to her upper trunk and distal arm. Muscle tone of the left upper limb was mildly increased. Mobility of the right upper extremity was massively reduced in all dimensions, whereas contralaterally there was mild impairment of upper limb function. Painful spasms of the affected region occurred spontaneously or were evoked by sudden loud noises or movements of either upper limb. Apart from Trömner's reflex, deep tendon jerks were absent in her right upper limb. Patellar tendon jerk was increased in the right leg (grade 3). Plantar response was flexor bilaterally. Coordination was normal. Vibration sense was decreased in the lower extremities. There was no further impairment of sensation. Examination of brainstem and psychic functions and general physical examination revealed no pathologic findings.

Electromyography (EMG) showed continuous low-frequency firing of normal motor units that subsided after intravenous injection of 10 mg diazepam. No spontaneous activity was observed. Results of nerve conduction studies and somatosensory and visual evoked potentials were normal. Routine laboratory investigations including tests for autoantibodies and infectious agents yielded no abnormalities. CSF examination revealed 50 mononuclear leukocytes/μL. Sediment analysis showed two plasma cells. CSF total protein (566 mg/L), albumin (308 mg/L), and immunoglobulin (Ig)M (1.6 mg/L) were elevated and oligoclonal bands (OCB) of IgG confined to the CSF were found. Serum and CSF were strongly positive for amphiphysin autoantibodies.[5]

On spinal MRI, we detected a hyperintense area in the right half of the spinal cord on T2-weighted scans, extending from C2 to C7 (figure 1 and 2). There was reduced signal intensity in the same region on T1-weighted images. Gadolinium-DTPA did not reveal pathologic enhancement. Cranial MRI was normal. Mammography and mammasonography revealed a small nodule (size: 1.5 × 1.5 cm) in the right breast. Further investigations consisting of gastroscopy, bronchoscopy, colonoscopy, ultrasound of the abdomen and thyroid gland, and CT scans of thorax and abdomen all had inconspicuous results.

The patient deteriorated for 3 weeks after admission despite treatment with oral diazepam up to 80 mg/d.

Figure 1. Sagittal T2-weighted MRI scan 18 weeks after onset of symptoms. Intramedullar hyperintense signal extends from C2 to C7.

Therefore, we added methylprednisolone (MP) 1,000 mg/d intravenously for 3 days, followed by 80 mg/d by mouth. Rigidity and pain were markedly reduced and spasms disappeared within a few days. However, reduction of MP below 60 mg/d led to a severe relapse. As intravenous immunoglobulins (IVIG; 30 g/d on 5 subsequent days) had no major effects until 9 days after the last infusion, an intravenous cyclophosphamide (CyP) pulse therapy was introduced (day 1: CyP 800 mg + MP 500 mg; days 2 and 3: MP 500 mg/d). This scheme, which began 8 months after onset of symptoms and was repeated seven times monthly, allowed subsequent reduction of oral MP and benzodiazepines. Three years after onset of symptoms, the patient reports minor blunt pain in her right arm during exercises on MP 8 mg/d and clonazepam 1 mg/d. Movements are minimally limited as rigidity has subsided.

On spinal MRI 6 weeks after introduction of MP, the lesion of the cervical cord had diminished; 8 weeks later, no abnormality could be detected. Using mammography, ultrasound, and MRI, the conspicuous nodule in the right breast could not be demonstrated 2 months after the initial finding or thereafter.

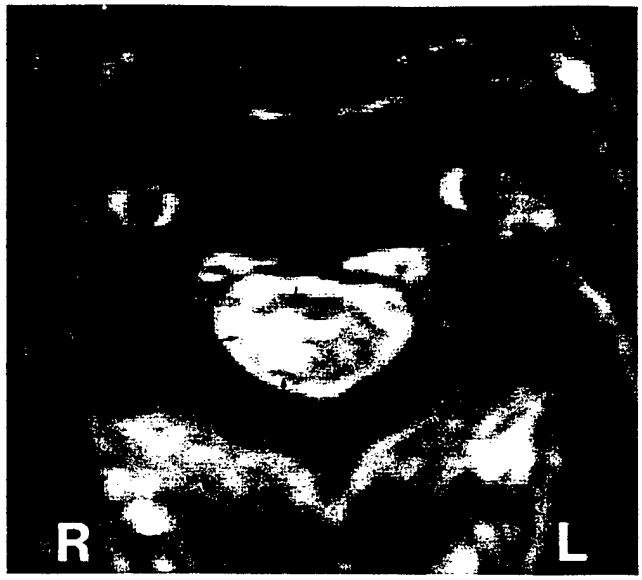

Figure 2. Axial T2-weighted MRI scan at C2/C3 level 18 weeks after onset of symptoms. Intramedullar hyperintense signal affects the anterior, lateral, and posterior column and the region of the pyramidal tract.

Discussion. Despite the putative involvement of the spinal cord in SPS,[2-5] there has been no previous report of MRI abnormalities in that region. This may be explained by the fact that our patient was studied 20 weeks after onset of symptoms, i.e., in an early stage of the disease. Other reports had MRI studies 1.5 years after onset or later.[2,3,7] The detection of an elevated cell count and OCB confined to CSF, the presence of amphiphysin autoantibodies, and the effectiveness of immunosuppression give strong evidence that SPS in this case was caused by an autoimmune mediated inflammation. Amphiphysin autoantibodies have been demonstrated in women with SPS and ductal breast adenocarcinoma, suggesting a distinct paraneoplastic variant of SPS.[5] These autoantibodies have also been reported with SPS related to colon carcinoma and Hodgkin's lymphoma as well as with paraneoplastic encephalomyelitis and sensory neuropathy related to small cell lung carcinoma.[6] Similar to GAD, amphiphysin is a cytoplasmic nerve terminal protein associated with the surface of synaptic vesicles.[5] Amphiphysin is an important binding partner for dynamin and synaptojanin, two proteins involved in the endocytosis of synaptic vesicles.[8]

The detection of a nodule in our patient's right breast could not be reaffirmed 2 months after the initial finding or thereafter. One explanation for the discrepancy in findings may be that the initial abnormality was an artifact, possibly due to biopsy of the right breast 18 years before development of SPS. Another possible explanation may be that this patient represents an example of tumor regression af-

Neuron, Vol. 24, 143–154, September, 1999, Copyright ©1999 by Cell Press

Endophilin/SH3p4 Is Required for the Transition from Early to Late Stages in Clathrin-Mediated Synaptic Vesicle Endocytosis

Niels Ringstad,* Helge Gad,† Peter Löw,† Gilbert Di Paolo,* Lennart Brodin,† Oleg Shupliakov,†‡ and Pietro De Camilli*‡
*Howard Hughes Medical Institute and
Department of Cell Biology
Yale University School of Medicine
New Haven, Connecticut 06510
†Nobel Institute for Neurophysiology
Department of Neuroscience
Karolinska Institute
S-171 77 Stockholm
Sweden

Summary

Endophilin/SH3p4 is a protein highly enriched in nerve terminals that binds the GTPase dynamin and the polyphosphoinositide phosphatase synaptojanin, two proteins implicated in synaptic vesicle endocytosis. We show here that antibody-mediated disruption of endophilin function in a tonically stimulated synapse leads to a block in the invagination of clathrin-coated pits adjacent to the active zone and therefore to a block of synaptic vesicle recycling. We also show that in a cell-free system, endophilin is not associated with clathrin coats and is a functional partner of dynamin. Our findings suggest that endophilin is part of a biochemical machinery that acts in *trans* to the clathrin coat from early stages to vesicle fission.

Introduction

Synaptic function requires that a pool of synaptic vesicles competent for neurotransmitter secretion is maintained in the presynaptic nerve terminal even during tonic activity. This goal is achieved by the rapid endocytosis and recycling of synaptic vesicle components after exocytosis. Several lines of evidence suggest that one pathway of synaptic vesicle recycling occurs via clathrin-mediated endocytosis and requires the large GTPase dynamin.

Heuser and Reese first described the role of clathrin in synaptic vesicle recycling by demonstrating a stimulation-dependent labeling of clathrin-coated vesicles in the nerve terminal with a fluid-phase endocytic marker (1973). Later studies demonstrated that clathrin-coated vesicles isolated from brain are enriched in synaptic vesicle proteins and that components of the AP2-clathrin endocytic machinery are concentrated in central synapses, further supporting the hypothesis that clathrin-coated vesicles are bona fide intermediates in synaptic vesicle recycling (Pfeffer and Kelly, 1985; Maycox et al., 1992; Ball et al., 1995; David et al., 1996). In a living nerve terminal, disruption of synaptic vesicle recycling by a variety of experimental conditions results in an accumulation of clathrin-coated structures at the presynaptic plasma membrane concomitant with a reduction in the number of synaptic vesicles in the nerve terminal (Shupliakov et al., 1997; Gad et al., 1998). Finally, genetic analysis of neurotransmission in *Drosophila melanogaster* has identified critical roles for the AP2-clathrin adaptor proteins and the clathrin accessory protein AP180 in synaptic vesicle recycling (González-Gaitán and Jäckle, 1997; Zhang et al., 1998). The presynaptic nerve terminal can therefore be a powerful system in which to study molecular mechanisms of clathrin-mediated endocytosis.

A widely accepted model of clathrin function posits that the clathrin coat assembles first on the donor membrane, forming a shallow coated pit, and then invaginates to generate a bud with a constricted neck and eventually a free clathrin-coated vesicle (Heuser, 1980). Clathrin coats alone can generate empty icosahedral cages; however, the formation of a clathrin-coated vesicle from a lipid bilayer is inherently more complex. In contrast to the assembly of a free clathrin cage, the invagination and fission of a patch of clathrin-coated membrane may require processive rearrangements of molecular interactions within the coat. Major changes are also likely to occur within the lipid bilayer itself to accommodate the high degree of membrane curvature required for vesicle formation. The clathrin-coated bud must finally undergo a fission reaction and be severed from the donor membrane. There is evidence that multiple proteins assist clathrin coat components in some or all stages of the generation of a clathrin-coated vesicle from a donor membrane.

The large GTPase dynamin has emerged as a key accessory protein in the process of clathrin-mediated endocytosis. Dynamin was first implicated as a critical component of the endocytic machinery through the discovery that the temperature-sensitive *shibire* mutation in *Drosophila* maps to a gene encoding a dynamin-like protein (Chen et al., 1991; van der Bliek and Meyerowitz, 1991). Upon a shift to the restrictive temperature, presynaptic nerve terminals of *shibire* flies are rapidly depleted of synaptic vesicles and accumulate collared pits at the presynaptic plasma membrane, presumably frustrated endocytic intermediates (Koenig and Ikeda, 1989). Subsequent studies in mammalian cells and cell-free systems have established a requirement for dynamin in clathrin-coated vesicle formation (Herskovits et al., 1993; Damke et al., 1994; Takei et al., 1995). Dynamin interacts directly or indirectly with a large number of proteins, many of which have been shown to be involved in clathrin-mediated endocytosis. These include amphiphysin, synaptojanin, eps15, epsin, Dap160/intersectin (reviewed in Cremona and De Camilli, 1997; Schmid et al., 1998), N-WASP, and syndapin (Qualmann et al., 1999). Previously, we have identified a family of three related proteins that are interacting partners of both the polyphosphoinositide phosphatase synaptojanin and dynamin: SH3p4/endophilin 1 (hereafter referred to as endophilin), SH3p8/endophilin 2, and SH3p13/endophilin 3 (Ringstad et al., 1997). Endophilin is the most

‡To whom correspondence should be addressed (e-mail: oleg.shupliakov@neuro.ki.se [O. S.], pietro.decamilli@yale.edu [P. D. C.]).

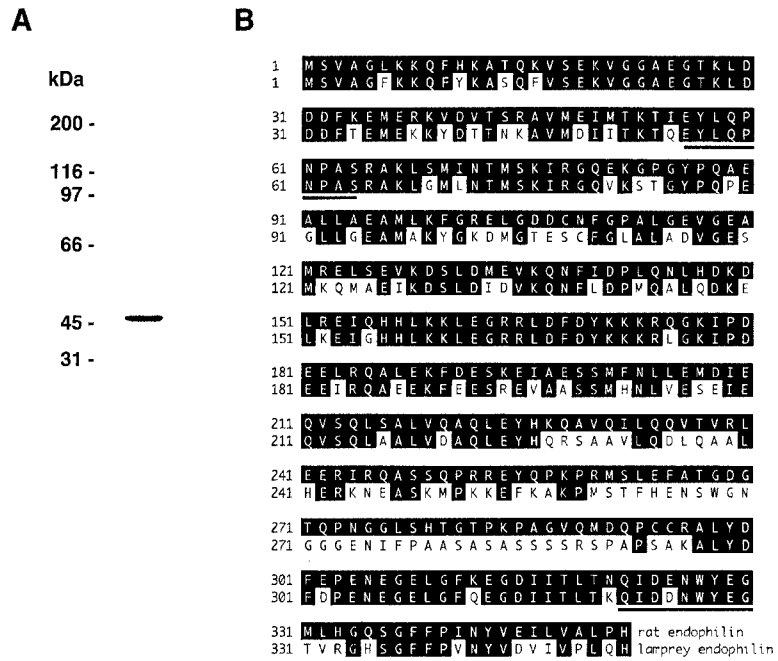

Figure 1. Identification of Lamprey Endophilin

(A) Fifty micrograms of lamprey spinal cord extract was analyzed by Western blotting using antibodies raised against the SH3 domain of rat endophilin.

(B) Alignment of mammalian and lamprey endophilin. Peptide sequences between rat endophilin and a nematode homolog used to design degenerate oligonucleotides for PCR cloning of lamprey endophilin are underlined. Boxed residues are identical in the sequences.

abundant member of this protein family in brain and is concentrated together with dynamin I and synaptojanin I in nerve terminals, where it is found in complexes with these two proteins (de Heuvel et al., 1997; Micheva et al., 1997; Ringstad et al., 1997). A preliminary report has also shown that endophilin is required for the in vitro generation of synaptic-like microvesicles in a cell-free assay (Schmidt and Huttner, 1998). In the present study, we sought to determine whether endophilin is a necessary factor for synaptic vesicle endocytosis and to define the stage at which endophilin is required. To investigate the role of endophilin in endocytosis in vivo, we have used the giant reticulospinal axon of lamprey, a synaptic preparation whose architecture allows for the microinjection of compounds or proteins directly into the presynaptic compartment. We have complemented these studies with an analysis of the localization of endophilin on endocytic coats generated in vitro.

Results

Identification and Characterization of Endophilin in Lamprey

As a first step toward the study of endophilin function in the lamprey reticulospinal synapse, we identified and characterized a lamprey endophilin ortholog. First, available anti-endophilin antibodies were screened by Western blotting of lamprey spinal cord extracts. Antibodies raised against the SH3 domain of rat endophilin recognized a prominent immunoreactivity of ~46 kDa, an appropriate size for an endophilin ortholog (Figure 1A). Second, a lamprey spinal cord cDNA library was screened by PCR using degenerate primers corresponding to highly conserved sequences between rat endophilin and a nematode homolog. Sequencing of the major product revealed that the library contained an endophilin-like sequence, and the entire open reading frame was subsequently cloned (Figure 1B). The cloned sequence encodes a protein highly similar to mammalian endophilins 1, 2, and 3. It comprises an NH2-terminal coiled-coil domain and a COOH-terminal SH3 domain connected by a variable region not conserved among endophilin family members (Ringstad et al., 1997). The NH_2-terminal and COOH-terminal domains are 72% and 75% identical between rat endophilin and the lamprey sequence, and the two sequences were 62% identical overall.

We next investigated whether the lamprey endophilin ortholog participates in a set of SH3 domain–mediated protein–protein interactions analogous to those described for mammalian endophilin (Ringstad et al., 1997). A sequence necessary and sufficient for endophilin binding had been identified by screening a panel of deletion mutants derived from the proline-rich COOH terminus of rat synaptojanin (N. R. and P. D. C., in preparation). A short peptide corresponding to the endophilin-binding site was used to affinity purify binding proteins from lamprey spinal cord extracts (Figure 2A). Bound material was analyzed by SDS-PAGE and either protein staining by Coomassie blue or Western blot using anti-endophilin antibodies. The major protein bound to the affinity matrix was a 46 kDa band that did not bind to a control column to which no peptide had been conjugated. Western blot analysis of the affinity-purified material demonstrated that this protein species was recognized by the anti-endophilin antibody and corresponded to the previously observed immunoreactivity (see Figure 1A). After enrichment on the peptide column, a minor immunoreactive band of slightly higher molecular weight was also detected. This band may represent a second endophilin-like protein present in lamprey spinal cord or a posttranslational modification of the major band.

Having determined that lamprey endophilin binds to the same sequences as mammalian endophilin, we next tested whether the interactions of endophilin with dynamin and synaptojanin were similarly conserved. We immunoprecipitated endophilin protein complexes from a detergent extract of lamprey spinal cord and analyzed the immunoprecipitated material by Western blot using

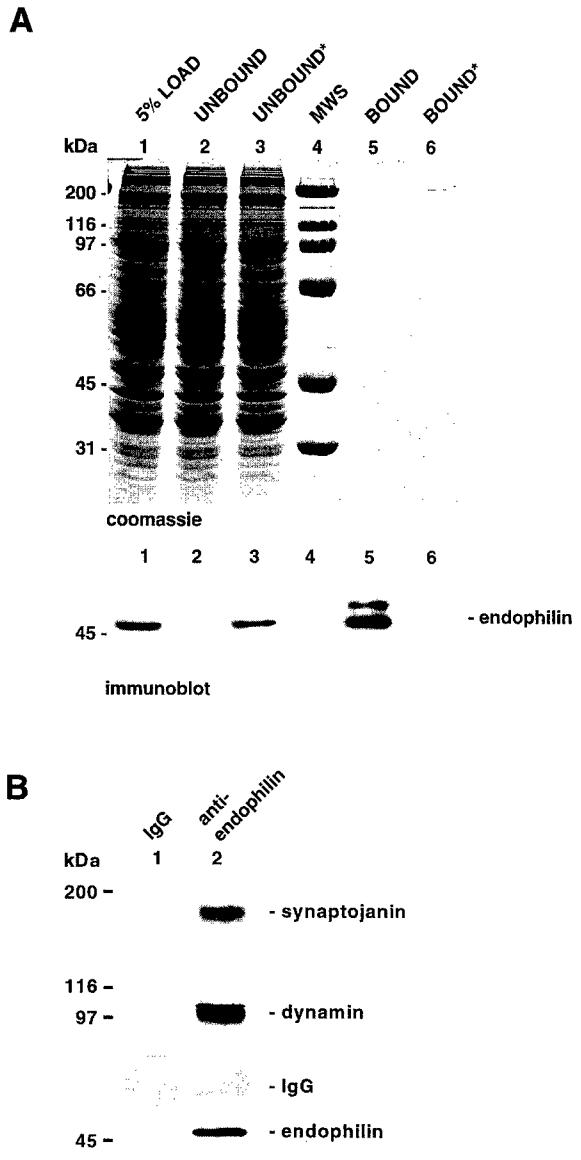

Figure 2. Lamprey Endophilin Binds the Same Proline-Rich Sequences as Mammalian Endophilin

(A) A peptide corresponding to the endophilin-binding site in rat synaptojanin 1 (see Experimental Procedures) was coupled to an affinity matrix and used to affinity purify interacting proteins from lamprey spinal cord extracts. Lamprey extracts were incubated with the immobilized endophilin-binding peptide or a control matrix coupled to no peptide. Bound proteins were eluted by SDS-PAGE sample buffer. Five percent of the starting material (lane 1) and unbound material from the columns (lanes 2 and 3), along with 50% of the material bound to the matrices (lanes 5 and 6), was separated by SDS-PAGE and analyzed by Coomassie blue stain (upper panel) and Western blot (lower panel). MWS, molecular weight standards. Asterisks indicate unbound and bound material from the control column (lanes 3 and 6, respectively).

(B) Immunoprecipitates from detergent extracts of lamprey spinal cord were prepared using either anti-endophilin antibodies (lane 2) or nonimmune rabbit IgGs (lane 1). The immune complexes were analyzed by Western blot using anti-endophilin antibodies, anti-synaptojanin antibodies, and anti-dynamin antibodies.

antibodies against dynamin (DG-1) or antibodies against a region in the catalytic 5-phosphatase domain of synaptojanin conserved across large phylogenetic distances (Figure 2B). As a control, we performed immunoprecipitations from lamprey spinal cord extracts using nonimmune rabbit immunoglobulins. Both dynamin and synaptojanin immunoreactivities were specifically present in anti-endophilin immunoprecipitates, demonstrating that endophilin's interactions with synaptojanin and dynamin are conserved in lamprey.

Endophilin Antibody Injection at the Lamprey Synapse Arrests Clathrin-Coated Pit Invagination at an Early Stage

Microinjection of endophilin antibodies into lamprey giant axons (n = 6) maintained at rest did not produce any evident changes in the ultrastructure of synaptic regions (Figure 3A). The number of synaptic vesicles did not differ significantly from uninjected synapses ($p > 0.05$) in adjacent axons, and we did not observe coated pits around release sites. Stimulation at 5 Hz for 30 min dramatically altered the morphology of the synapses in antibody-injected axons (n = 6). The synaptic vesicle pool was almost depleted (Figure 3B), and "pocket-like" expansions of the plasma membrane occurred (arrows in Figure 3B). A large number of clathrin-coated structures with a uniform shape accumulated in the plasma membrane area around the active zones (Figure 3B). These clathrin-coated structures were most similar to type I clathrin-coated pits as defined by Gad et al. (1998), that is, shallow pits without constricted necks (Figure 3B). The ultrastructure of synapses in adjacent stimulated axons from the same specimen showed only small changes (Figure 3C) that were similar to those described in our previous studies (Shupliakov et al., 1997). Large synaptic vesicle clusters were still present, and a limited number of coated pits of different shapes, including constricted coated pits (see Figure 3C), was observed at the margin of the synaptic area. Morphometric analysis showed that the number of both synaptic vesicles and coated pits at the margin of the active zone was significantly different in antibody-injected axons as compared to control axons (Figures 4A and 4B). Synapses in axons injected with GST (n = 5; for other injection controls, see Pieribone et al., 1995; Shupliakov et al., 1997) and stimulated at 5 Hz for 30 min displayed similar structural changes to the uninjected stimulated synapses (not shown).

To quantify the shape of the coated pits at the plasma membrane at the margins of active zones, the curvature index (see Experimental Procedures) of individual coated pits was calculated. This value is low for a shallow pit (1 = a flat membrane) and increases with the degree of invagination. The mean curvature index value for coated pits calculated in synapses at the injection site from three different injected axons was about 2.5 times lower than in control synapses (1.55 ± 0.39 /±SD/, n = 20, and 4.11 ± 1.79, n = 20, respectively; $p < 0.001$; t test). For comparison, we also subjected coated pits in axons injected with the amphiphysin SH3 domain from our previous study (Shupliakov et al., 1997) to the same analysis. This reagent has been shown to arrest clathrin-mediated endocytosis at the stage of deeply invaginated

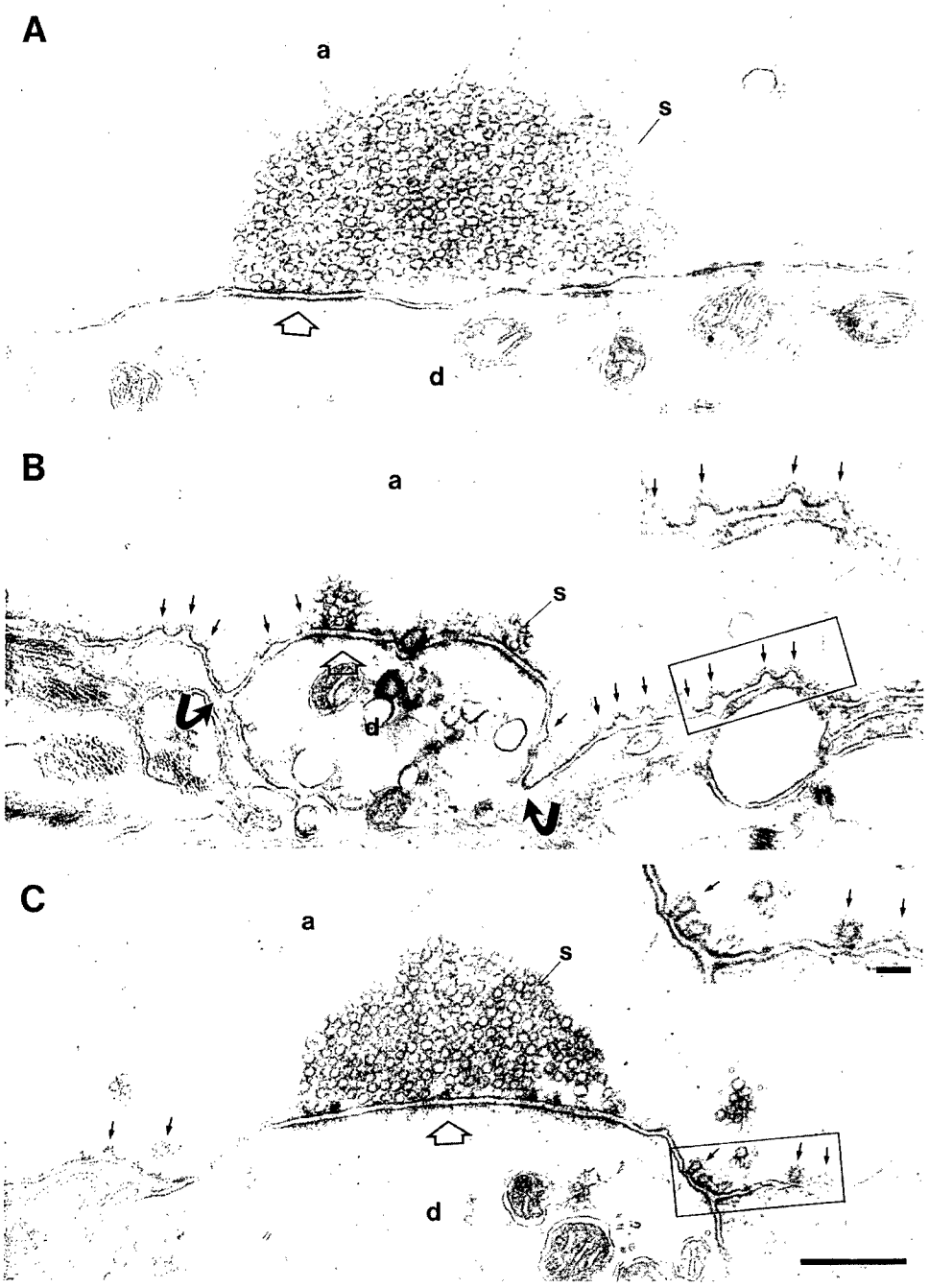

Figure 3. Inhibition of Synaptic Vesicle Recycling by Anti-Endophilin Antibodies

(A) Electron micrograph of a lamprey synapse injected with endophilin antibodies and maintained in a low calcium solution (0.1 mM Ca^{2+} and 4 mM Mg^{2+}) without stimulation for 60 min.

(B) A synapse in an axon that was stimulated in a normal Ringer's solution at 5 Hz for 30 min after the injection of endophilin antibodies. Note the "pocket-like" membrane expansions (arrows) at the margin of the synaptic area and the appearance of numerous "shallow" coated pits (small arrows). The inset shows the underlined area of the axonal membrane at higher magnification.

(C) Electron micrograph of a synapse from an uninjected adjacent axon to the one shown in (B). The inset shows coated pits (boxed area) at higher magnification. Compare the curvature of the coated pits with those in (B). a, axoplasmic matrix; s, synaptic vesicles; d, dendrite. Scale bar: 0.5 μm for (A–C) and 1.0 μm for the insets in (B) and (C).

coated pits. In these synapses, the mean curvature index was more than twice that in control synapses (9.63 ± 1.80, n = 20).

Coated pits in a given injected synapse possessed remarkably homogeneous curvatures. The mean curvature of the coats, however, varied among axons injected with different amounts of anti-endophilin antibodies. To determine the effect of different concentrations of the antibody, synapses located at different distances from the site of injection within a single axon were analyzed. The plot in Figure 4C shows the average curvature index as a function of the relative endophilin antibody concentration

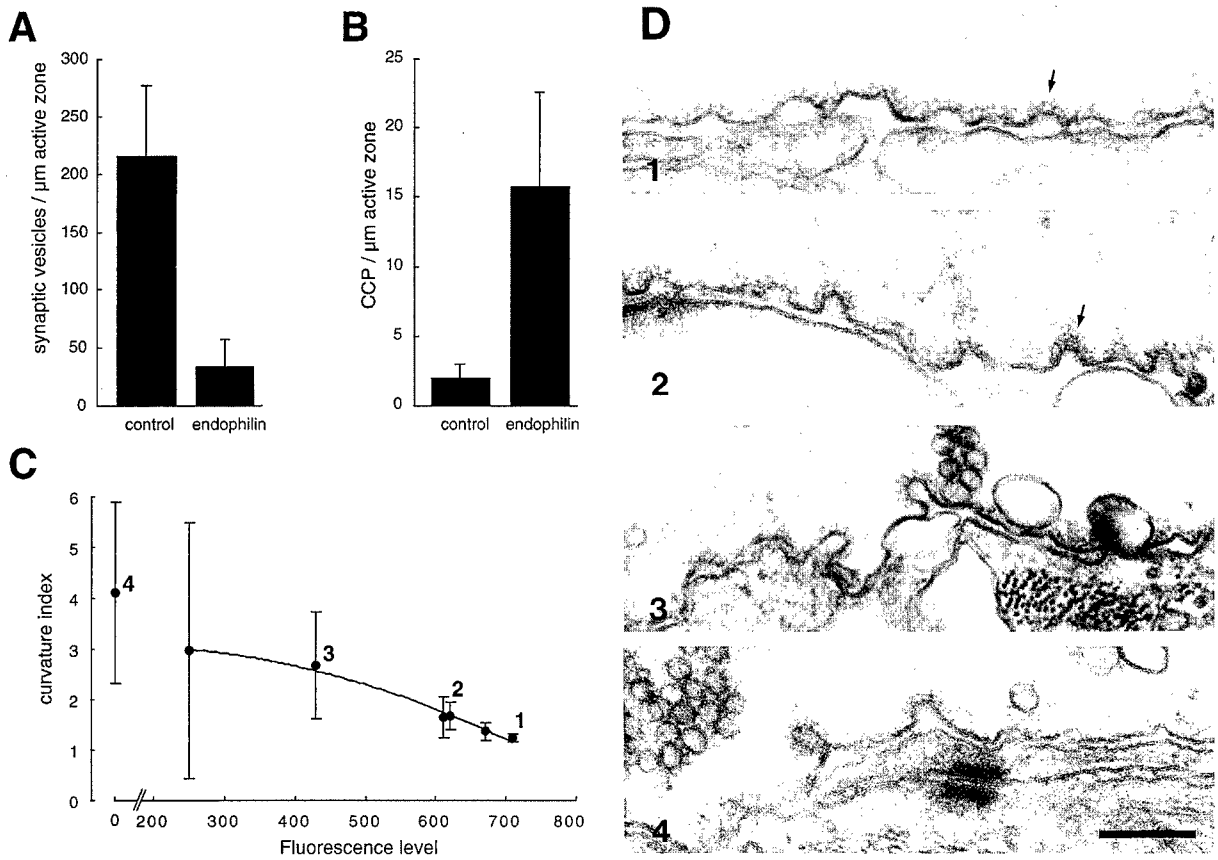

Figure 4. Quantitative Analysis of the Effects of Endophilin Antibodies in Stimulated Lamprey Synapses

(A) Reduction in the number of synaptic vesicles at active zones at the site of antibody injection. The values represent the number of synaptic vesicles in the center section of synapses normalized to the length of active zones (±SD; n = 5).

(B) Increase in number of coated pits at the plasma membrane at the margin of the synaptic area. The values represent averages of the total number of coated pits counted in the center section of five synapses in each group.

(C) Curvature index (see Experimental Procedures) of coated pits in the plasma membrane at the margin of active zones. All values are from synapses in a single axon located at different levels from the antibody injection site (1). "Fluorescence level" represents the fluorescence of the injection marker measured on a CCD image (arbitrary units). "0 fluorescence level" corresponds to the area outside the injection site (i.e., control). Each point in the plot represents an average of 20 coated pits (±SD) collected from serial sections.

(D) Electron micrographs of coated intermediates at the levels indicated as 1, 2, 3, and 4 on the plot shown in (C). Arrows in 1 and 2 indicate shallow coated pits with different curvatures. Scale bar: 0.2 µm.

(see Experimental Procedures), and Figure 4D shows representative fields corresponding to the data points in Figure 4C. The mean curvature of pits in a synapse increased as the antibody concentration decreased. Furthermore, the variability of the curvatures of coated pits in the synapse was also affected by the antibody concentration. In areas with high antibody concentrations (data points 1–2 in Figures 4C and 4D), the variability in the curvature indices of pits was low. At lower antibody concentrations, coated pits of different shapes began to occur (data points 3–4 in Figures 4C and 4D), and the overall number of coated pits per synapse also decreased.

Our previous studies in lamprey have shown that inhibition of synaptic vesicle endocytosis can be accompanied by the appearance of "endosome-like" structures in the synaptic area. Serial section analyses have shown that these membrane structures primarily represent infoldings of the plasma membrane (Shupliakov et al., 1997; Gad et al., 1998). In the present study, such infoldings were observed at the margins of synaptic regions in several synapses exposed to high antibody concentrations. In two synapses, these infoldings were analyzed in serial sections. Notably, they were found to exhibit coated pits that differed in shape from those located at the plasma membrane at the lateral edge of active zones (Figures 5A–5E). Occasional coated vesicles were also noted. Most of these coated pits were deeply invaginated with narrow necks, resembling those that accumulate after injection of the amphiphysin SH3 domain (Shupliakov et al., 1997). These results indicate that the requirement for endophilin in the invagination of coated pits depends on the site at which the coats are formed.

Endophilin Is Required In Vitro for the Formation of Dynamin Coats

To further investigate the requirement of endophilin in the formation of clathrin-coated pits, we tested whether depletion of endophilin from brain cytosol affected the formation of clathrin coats on synaptic membranes in a cell-free coating assay. Endophilin was removed from

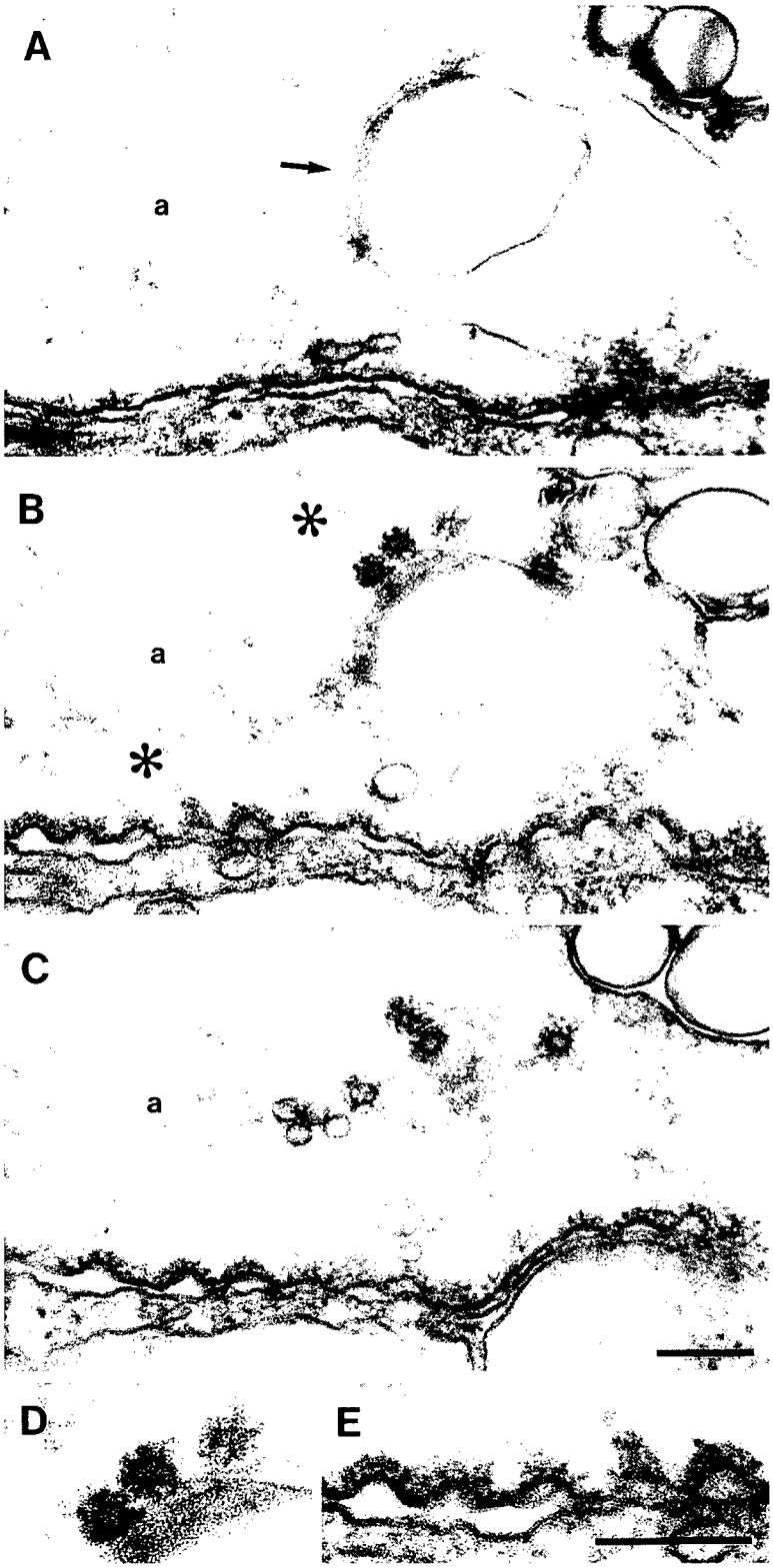

Figure 5. Plasma Membrane Infoldings Induced by Endophilin Antibodies

(A–C) Three consecutive serial sections from the margin of an active zone in a stimulated axon injected with endophilin antibodies. Tracing of the membrane structure (arrow) revealed that it had a complex, folded structure and was connected with the plasma membrane. (D) and (E) show the two areas marked with asterisks in (B) at high magnification. Note the presence of invaginated coated pits at the membrane infolding. Scale bars: 0.2 μm.

brain cytosol by immunoadsorption. Endophilin depletion did not result in a significant change in the amounts of the endophilin interacting partners synaptojanin and dynamin present in the treated cytosol (Figure 6A). Depleted or control cytosol was incubated with purified synaptic membranes in the presence of ATP and GTPγS, conditions previously shown to promote the formation of endocytic coats (Takei et al., 1996). After incubation, the membranes were fixed and processed for electron microscopy. Under both conditions, clathrin-coated pits were predominantly deeply invaginated (Figure 6B). Furthermore, addition of anti-endophilin antibodies to the

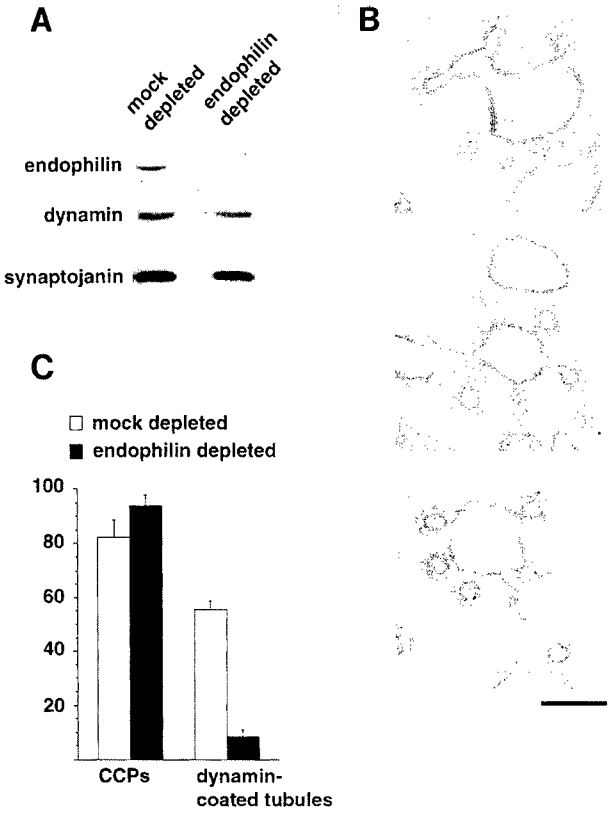

Figure 6. Depletion of Endophilin from Brain Cytosol Inhibits the Formation of Dynamin-Coated Structures on Synaptic Membranes

(A) Immobilized anti-endophilin antibodies or nonimmune rabbit immunoglobulins were used to generate endophilin- and mock-depleted cytosols. Depleted and mock-depleted cytosol was analyzed by Western blotting with ^{125}I protein A followed by autoradiography for the presence of endophilin and its interacting partners dynamin and synaptojanin.

(B) Representative clathrin-coated pits generated by mock-depleted cytosol, endophilin-depleted cytosol, or cytosol supplemented with anti-endophilin antibodies (15 $\mu g\ ml^{-1}$) on synaptic membranes in the presence of ATP and GTPγS. Note that in all cases, deeply invaginated pits are generated. Scale bar: 0.1 μm^2.

(C) The number of dynamin-coated tubules and clathrin-coated membrane profiles (CCPs) generated by mock- or endophilin-depleted cytosol was counted in fields corresponding to 1000 μm^2 of section area (n = 3). Data are presented as the mean of these countings with standard errors.

reaction had no effect on the morphology of the clathrin coats formed in vitro (Figure 6B). A morphometric analysis of membranes treated with depleted or control cytosol showed that the number of coated pits formed was not affected by endophilin depletion (Figure 6C). Strikingly, endophilin-depleted cytosol generated approximately 8-fold fewer dynamin-coated tubules (Takei et al., 1995) in comparison to control cytosol.

To determine whether endophilin associates with the endocytic coats generated in our cell-free system, we incubated synaptic membranes with control cytosol and processed this material for immunogold electron microscopy after labeling with anti-endophilin antibodies (Figure 7). Endophilin immunoreactivity was virtually absent from clathrin-coated profiles. On the other hand, dynamin-coated tubules formed in the same preparation were strongly and specifically stained with the antibody. A morphometric analysis of the immunostained material revealed that 52% of the immunogold particles was associated with dynamin-coated structures. The remaining signal was diffuse and associated with uncoated membranes or matrix found between membranes. Considering that dynamin tubules represent an extremely small fraction of the total membranes present in our cell-free assay, the enrichment of endophilin apparent on these structures is extremely high.

We therefore conclude that endophilin is required either for the formation or stabilization of dynamin-coated tubules in vitro but is not present on clathrin coats. Together with our observations in injected axons, these data suggest that the target of endophilin function is not the clathrin coat, but rather some factor extrinsic to the coat that affects coat invagination.

Discussion

In this study, we demonstrate an essential role for endophilin in clathrin-mediated synaptic vesicle recycling. Microinjection of anti-endophilin antibodies at the giant reticulospinal synapse of the lamprey resulted in a stimulation-dependent depletion of synaptic vesicles and the accumulation of clathrin-coated pits at the presynaptic plasma membrane. Disruption of endophilin function had a striking effect on the curvature of the clathrin lattice, but this effect depended on the location of the pits within the architecture of the synapse. The pits that accumulated around the active zone, that is, the site where clathrin-mediated endocytosis preferentially occurs in the synapse (Shupliakov et al., 1997; Gad et al., 1998), were shallow. Within a given axon, their mean curvature varied with the concentration of antibody present at that site. These shallow pits were clearly distinct from the deeply invaginated coated pits that accumulate in a stimulated synapse following the injection of the SH3 domain of amphiphysin or an amphiphysin-binding proline-rich peptide (Shupliakov et al., 1997). In contrast, coated pits that accumulated on deep infoldings of the plasma membrane represented more mature stages of the clathrin coat. Thus, the morphology of the coated pits in injected synapses seemed to depend on the membrane microenvironment at which these pits originate. Our study demonstrates that endophilin is a protein factor required for the acquisition of curvature by clathrin-coated pits in vivo. Furthermore, these data suggest that endophilin is required for this process at specific membrane domains within the nerve terminal.

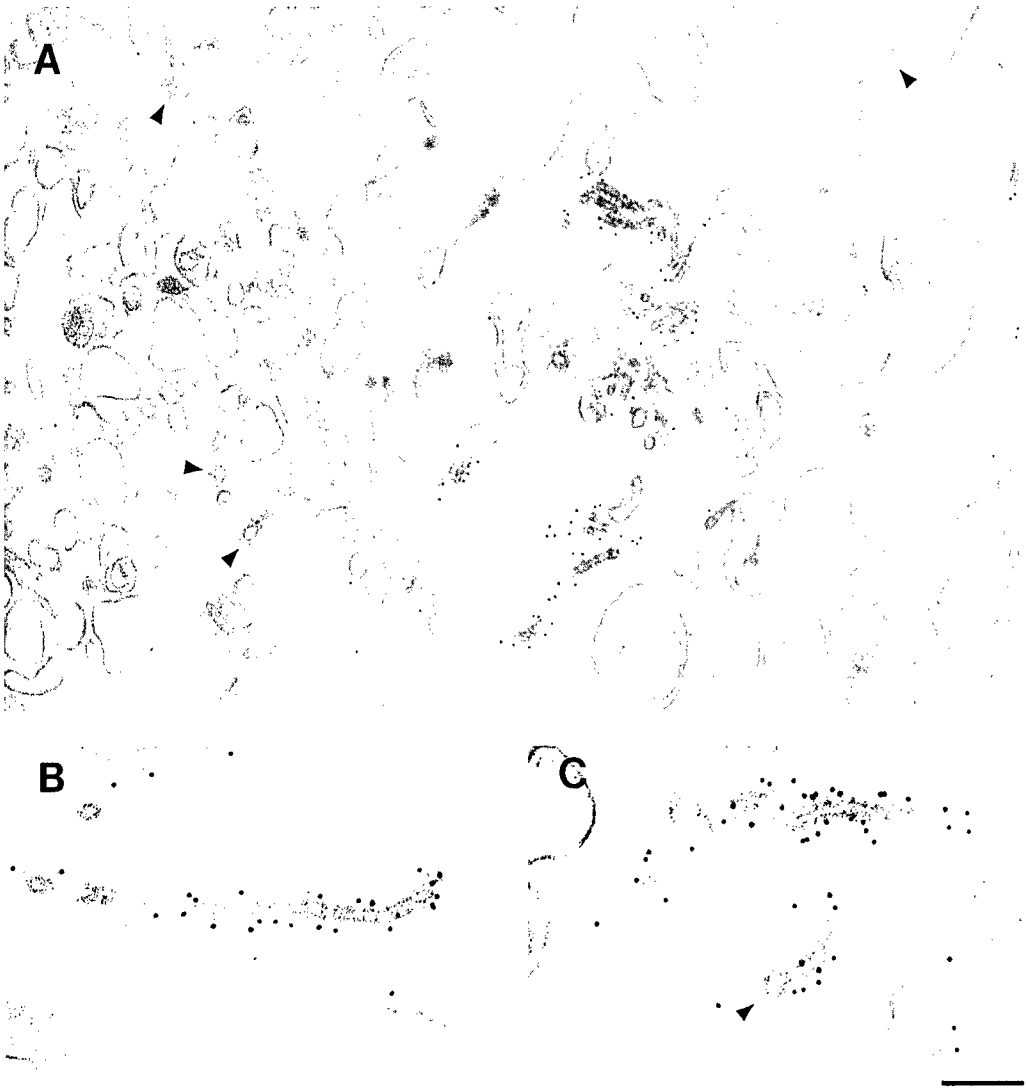

Figure 7. Immunolocalization of Endophilin on Endocytic Coats

Rat synaptic membranes (LP2 fraction) were incubated with brain cytosol, ATP, and GTPγS and then processed for immunogold electron microscopy. A low-power micrograph (A), as well as high-power views (B and C), shows the selective association of endophilin immunoreactivity with dynamin coats. In many cases, anti-endophilin labeling of dynamin tubules was uniformly intense along the tubule (B), and when a clathrin bud at the end of the tubule could be resolved, staining was restricted to the dynamin-coated segment of the tubule (C). Arrowheads indicate clathrin-coated membranes. Scale bar: 0.2 μm in (A) and 0.1 μm in (B) and (C).

Initiation of synaptic vesicle recycling during a regimen of tonic stimulation (as used in this study) is asynchronous, and one observes substantial variability in the curvature of the coated pits in an uninjected axon, reflecting their relative maturity. In axons injected with anti-endophilin antibodies, both the mean curvature of the coated pits localized around active zones and the variability of their curvatures were functions of antibody concentration. These observations are consistent with the hypothesis that anti-endophilin antibodies affect the rate at which nascent coated buds adopt curvature. At high antibody concentrations, the acquisition of curvature by coated pits may be extremely slow, even arrested, and therefore, most coated pits would appear shallow and homogeneous. As this rate of invagination increases at intermediate antibody concentrations, one would expect increased variability in the curvatures of the pits approaching the variability observed in an uninjected synapse.

The formation of deeply invaginated clathrin coats in vitro did not require the presence of endophilin, nor was endophilin immunoreactivity detected on these coats, consistent with observations in vivo that endophilin function is not generally required for the acquisition of curvature by coated pits. In contrast, endophilin immunoreactivity was highly enriched on dynamin-coated membrane tubules, structures that reflect the oligomerization of dynamin together with other endocytic proteins at the neck of clathrin-coated pits (Takei et al., 1999). Furthermore, brain cytosol depleted of endophilin was markedly less efficient at generating dynamin-coated tubules than control cytosol. These findings are in agreement with the reported biochemical interaction of endophilin with dynamin (Ringstad et al., 1997; Micheva

et al., 1997). Dynamin has been extensively characterized as a fission factor acting at a late stage in endocytosis. The requirement for endophilin in the formation of dynamin coats suggests a close functional relationship between endophilin and dynamin in the fission reaction; a similar functional relationship was proposed for amphiphysin that cooligomerizes with dynamin into the dynamin coat surrounding membrane tubules (Takei et al., 1999). In vivo, the early block imposed on coated pits surrounding the active zone by microinjection of anti-endophilin antibodies precludes the observation of a role for endophilin at later stages of endocytosis. However, the deeply invaginated pits observed on membrane infoldings may reflect such a role for endophilin in the fission reaction. In light of the early participation of endophilin in endocytosis demonstrated by this study, the partnership between endophilin and dynamin may also suggest a role for dynamin prior to the fission reaction in vivo. It is worth noting that several reports have demonstrated the presence of dynamin on clathrin-coated pits and even flat clathrin lattices (Damke et al., 1994; Takei et al., 1996; Baba et al., 1999).

Several models of endophilin function are consistent with our observations. One possibility is that endophilin may influence the invagination of coated buds by modulating membrane tension, as determined by the presence of a stabilizing cytoskeletal scaffold under the plasma membrane or by the anchoring of the presynaptic plasma membrane to the extracellular matrix. It has been previously shown that shallow coated pits are primarily observed in intact cells or membranes adsorbed to surfaces, while clathrin coats formed on membrane fragments in suspension adopt a more highly curved morphology (Moore et al., 1987; Heuser, 1989). An inverse relationship between clathrin-mediated endocytosis and membrane tension in intact cells has been demonstrated (Raucher and Sheetz, 1999). Both synaptojanin and dynamin, the two major binding partners of endophilin, have potential functional connections to the submembranous actin cytoskeleton. Dynamin has been shown to form protein complexes with profilin (Witke et al., 1998) and N-WASP (Qualmann et al., 1999), while synaptojanin catabolizes PtdIns(4,5)P_2 (McPherson et al., 1996; Guo et al., 1999), a potent regulator of the actin cytoskeleton. Endophilin may therefore regulate the membrane tension of the presynaptic plasma membrane by modifications of the actin-based cytoskeleton. This hypothesis may explain the lack of effect of the disruption of endophilin function on the invagination of clathrin-coated pits in cell-free systems or on plasmalemmal infolding in injected synapses. In our cell-free system, the physiological tension of the plasma membrane is clearly disrupted. Also, in injected synapses, the plasmalemmal infoldings that form after prolonged stimulation are the consequence of a massive expansion of the plasma membrane due to the incorporation of synaptic vesicle membranes. This addition of membrane may not be matched by the addition of new cytoskeletal scaffolding. The membranes of these deep infoldings are likely to possess different physical properties, and it is plausible that membrane tension is greatly reduced at these sites.

An alternative, and not necessarily exclusive, possibility is that the effects of endophilin on membrane curvature may reflect a role of this protein on membrane lipids. Recently, it has been shown that depletion of cholesterol from cells results in an accumulation of shallow coated pits strikingly similar to those we have observed in injected nerve terminals (Rodal et al., 1999). These experiments have demonstrated that the lipid composition of the donor membrane can strongly influence the invagination of a coated pit. Coated pit invagination implies the generation of membrane domains with increased curvature, which in turn may require the formation of microdomains with specific lipid composition. Endophilin and its interacting partner synaptojanin may be part of a protein–protein interaction network that participates in the modifications of the lipids in the donor membrane as clathrin coated pits invaginate. According to this model, the selective effect of endophilin disruption on the invagination of pits proximal to the active zone may reflect the specific organization of this enzymatic machinery at physiological endocytotic sites.

One final possibility is that endophilin function is required only for a subset of clathrin-mediated endocytosis. Both AP2 and AP3 adaptor complexes have been implicated in synaptic vesicle recycling (Ball et al., 1995; David et al., 1996; González-Gaitán and Jäckle, 1997; Faundez et al., 1998). The molecular composition of clathrin-coated buds that form around the active zone and on deep infoldings or in cell-free systems may differ in this respect.

The process of generating a clathrin-coated vesicle requires the formation of a clathrin coat on a patch of donor membrane, the maturation of the immature coat to form a deeply invaginated bud, and finally, scission of the bud to generate a free coated vesicle. It has been proposed that the generation of highly curved clathrin coats is accompanied by molecular rearrangements within the coat (Heuser, 1980). Other authors (Kirchhausen and Harrison, 1981) have proposed that such rearrangements would be opposed by a high number of interactions between clathrin triskelia (Smith et al., 1998; ter Haar et al., 1998). An alternative model has therefore been formulated in which clathrin coats are generated with predefined curvature and grow without rearrangements of the interactions between clathrin triskelia until a deeply invaginated bud is formed (ter Haar et al., 1998). Our studies do not allow us to discriminate between these two models. Our data, however, show that at least one protein extrinsic to the clathrin coat, endophilin, controls the acquisition of clathrin coat curvature in vivo.

Experimental Procedures

Antibodies

Anti-endophilin antibodies were generated by immunizing rabbits with a peptide (YQPKPRMSLEFATGDGTQPN) corresponding to amino acids 255–274 in the rat endophilin coding sequence or with a GST fusion protein of the COOH-terminal SH3 domain of endophilin, as previously described (Ringstad et al., 1997). Anti-peptide antibodies were specific for rat endophilin and were used to probe rat tissues, while antibodies raised against the fusion protein were used to probe lamprey tissues and in microinjection experiments. The anti-synaptojanin antibody CAT-1 was raised against a peptide (RRRKWPFDRSAEDLD) corresponding to amino acids 811–825 of

rat synaptojanin 1. The anti-dynamin antibody DG-1 has been previously described (Grabs et al., 1997).

Cloning of Lamprey Endophilin

A putative open reading frame from *Caenorhabditis elegans* genomic sequence with high homology to rat endophilin was found by database searches. An alignment of the predicted amino acid sequence of this open reading frame with that of rat endophilin revealed two stretches of identity within the endophilin peptide sequence: EYLQPNPA (amino acids 56 to 63 in the rat sequence) and QIDENWYEG (amino acids 322 to 330). Degenerate oligonucleotides were designed from these peptide sequences, and a lamprey cDNA library was screened by PCR using these oligonucleotides as primers. The 5′ and 3′ ends of the lamprey endophilin homolog were cloned by nested PCR using primer pairs derived from the known sequence of the endophilin homolog and sequences present in the library vector. Oligonucleotide synthesis and sequencing was performed in the Keck Biotechnology facility, Yale University School of Medicine. Endophilin sequences were aligned by the clustal method using the Lasergene software package.

Affinity Chromatography of Rat and Lamprey Tissue Extracts

Five grams of rat brain or lamprey spinal cord was minced and homogenized in 10 ml of buffer A (20 mM HEPES-KOH [pH 7.2], 100 mM KCl) plus protease inhibitors (complete protease inhibitor cocktail, Boehringer Mannheim). A postnuclear supernatant of the homogenate was prepared by centrifugation at 2600 rpm for 10 min at 4°C in an SS-34 rotor (Beckman). Triton X-100 was added to this supernatant to a final concentration of 1%, incubated at 4°C for 30 min, and then centrifuged for 60 min at 60,000 rpm in a Ti-70 rotor (Beckman). The resulting high-speed supernatant was saved as Triton X-100 extract of rat brain or lamprey spinal cord.

Detergent extracts of lamprey spinal cord or rat brain were incubated for 1 hr at 4°C with sulfolink resin (Pierce) charged with the endophilin-binding peptide CVAPPARPAPPQRPPPPSGA according to the manufacturer's instructions. Details of the identification and characterization of the endophilin-binding peptide will be presented elsewhere (N. R. and P. D. C., in preparation). After incubation, the affinity matrix was collected by centrifugation and washed three times with buffer A + 1% Triton X-100. Bound proteins were eluted with SDS-PAGE sample buffer and analyzed by SDS-PAGE.

Microinjection in the Lamprey Reticulospinal Synapse

The isolated lamprey spinal cord was placed in a recording chamber with Ringer solution maintained at 9°C (Shupliakov et al., 1995). The endophilin antibodies (2–3 mg/ml in 250 mM K acetate and 10 mM HEPES [pH 7.4]) were either mixed 10:1 with Cy5-labeled inactive antibodies (rabbit-anti-mouse IgG; Pieribone et al., 1995) or directly labeled with Cy5 (Amersham Pharmacia Biotech) according to the manufacturer's description. Similar results were obtained with the two protocols and will therefore be considered together. The antibodies were introduced in injection micropipettes (resistance 50–70 Mω) and injected into the axons with pressure pulses (5–15 psi) of 200 ms duration. The fluorescence was monitored with a CCD detector (Princeton Instruments, Trenton, NJ). To examine the effect of endophilin antibodies in resting axons, the specimen was left unstimulated in a low Ca^{2+} Ringer solution with 0.1 mM Ca^{2+} and 4 mM Mg^{2+} (Shupliakov et al., 1997) for 45–90 min after the antibody injection. To examine the effect following synaptic activity, electrical pulses were applied via an extracellular glass suction electrode applied at the caudal end of the spinal cord (Brodin et al., 1994). A second electrode, placed at the rostral end, was used to record the spike volley. After impaling an axon with the microinjection pipette, test stimuli were applied to verify that the axon was effectively stimulated. The microelectrode was removed after the antibody injection and after a period of 5–30 min stimulation was applied at 5 Hz. The effect of endophilin antibodies in stimulated axons was tested in three separate experiments. In each experiment, other axons in the same specimen were injected with other compounds that had different effects on the ultrastructure of synaptic regions, including that of coated intermediates (H. G., L. B., and O. S., unpublished observations). Control synapses were examined in uninjected axons adjacent to those injected with endophilin antibodies and in axons injected with Cy5-labeled GST, which has previously been shown not to affect synaptic vesicle recycling in this synapse (Shupliakov et al., 1997). The stimulation period (always 30 min) was ended by replacing the physiological solution with 3% glutaraldehyde with 0.5% p-formaldehyde in 0.1 M phosphate buffer (pH 7.4) or with 3% glutaraldehyde plus 4% tannic acid in 0.1 M cacodylate buffer (pH 7.4). In the latter case, specimens were maintained in this solution for 1 hr and then transferred to 3% glutaraldehyde in the same buffer (3 hr). The specimens were postfixed in 1% osmium tetroxide (1 hr), stained en bloc in 2% uranyl acetate, dehydrated in ethanol, and embedded in Durcupan ACM (Fluka). Ultrathin serial sections from the area of the injection were cut on an LKB ultrotome. After counterstaining with uranyl acetate and lead citrate, the sections were examined and photographed in a Philips CM12 electron microscope.

Quantitative Analysis of Injected Synapses

Complete series of sections of single synapses were collected for analysis. Electron micrographs were printed at magnifications from 17,000–45,000×. Coated pits were counted in complete series of sections. The number of synaptic vesicles was determined from the center section of serially cut synapses. In both cases, the values were normalized to the sectional length of the active zone (Shupliakov et al., 1995).

To quantify the effect of different concentrations of endophilin antibody, synapses in a single axon were collected at various distances from the injection site. At each distance, an estimate of the relative antibody concentration was obtained by measuring fluorescence levels in CCD images at the corresponding locations. These images had been taken just before the specimen was fixed. Twenty coated pits were randomly selected at each level. Their curvature index was calculated by dividing the perimeter length of the coated pit curvature with the distance between the edges of the coated pit.

In Vitro Generation of Endocytic Coats on Synaptic Membranes

Electron microscopy of agarose-embedded synaptic membranes was performed as previously described (De Camilli et al., 1983; Takei et al., 1996). Briefly, purified synaptic membranes (LP2) were incubated for 30 min at 30°C in the presence of dialyzed brain cytosol, an ATP-regenerating system, and 100 μM GTPγS (Sigma). The membranes were fixed in 4% paraformaldehyde (w/v), embedded in 1% agarose (w/v), and immunostained with anti-endophilin antibodies at a final concentration of 50 ng ml^{-1} followed by protein A conjugated to 5 nm colloidal gold. The embedded membranes were then osmicated, dehydrated, and embedded in epon as previously described (De Camilli et al., 1983). For morphometric analysis of clathrin- and dynamin-coated structures, three composite fields of 1000 square microns in area were photographed, and the number of clathrin-coated membrane profiles and dynamin-coated membrane tubules was counted in each field. Fields of comparable membrane density were selected at low magnification.

Miscellaneous Procedures

Immunodepletion of endophilin from rat brain cytosol was performed by incubating 7.5 mg of concentrated brain cytosol (Takei et al., 1996) overnight at 4°C with 20 μg of either affinity-purified anti-endophilin antibodies or purified rabbit IgG. Immune complexes were adsorbed to protein A–Sepharose for 1 hr at 4°C and removed by centrifugation. Immunoprecipitation of endophilin protein complexes from detergent extracts of lamprey spinal cord was performed as described (Ringstad et al., 1997). SDS-PAGE and Western blot analysis was performed as described (Laemmli, 1970; Towbin et al., 1979). Western blots were performed using ECL detection methods (Pierce) or iodinated protein A.

Acknowledgments

This work was supported in part by NIH grants NS36251 and CA46128, a grant from the United States Army Medical Research and Development Command (P. D. C.), grants from the Swedish Medical Research Council (project 112 87) and Hedlunds Stiftelse (L. B.), and grants and from Jeanssons Stittelse and Stiftelsen Sigurd

och Elsa Goljes Minne (O. S). N. R. is supported by an NIH predoctoral training grant (T32GM07527) to the Department of Cellular and Molecular Physiology, Yale University School of Medicine, and G. D. P. is supported by a long-term EMBO fellowship. The authors wish to thank Kohji Takei and Laurie Daniell for advice and technical assistance. N. R. especially wishes to thank Biff Forbush for long-term support and many helpful discussions.

Received June 23, 1999; revised August 2, 1999.

References

Baba, T., Ueda, H., Terada, N., Fujii, Y., and Ohno, S. (1999). Immunocytochemical study of endocytotic structures accumulated in HeLa cells transformed with a temperature-sensitive mutant of dynamin. J. Histochem. Cytochem. *47*, 637–648.

Ball, C.L., Hunt, S.P., and Robinson, M.S. (1995). Expression and localization of alpha-adaptin isoforms. J. Cell Sci. *108*, 2865–2875.

Brodin, L., Shupliakov, O., Hellgren, J., Pieribone, V., and Hill, R. (1994). The reticulospinal glutamate synapse in lamprey: plasticity and presynaptic variability. J. Neurophysiol. *72*, 592–604.

Chen, M.S., Obar, R.A., Schroeder, C.C., Austin, T.W., Poodry, C.A., Wadsworth, S.C., and Vallee, R.B. (1991). Multiple forms of dynamin are encoded by shibire, a Drosophila gene involved in endocytosis. Nature *351*, 583–586.

Cremona, O., and De Camilli, P. (1997). Synaptic vesicle exocytosis. Curr. Opin. Neurobiol. *7*, 323–330.

Damke, H., Baba, T., Warnock, D.E., and Schmid, S.L. (1994). Induction of mutant dynamin specifically blocks endocytic coated vesicle formation. J. Cell Biol. *127*, 915–934.

David, C., McPherson, P.S., Mundigl, O., and De Camilli, P. (1996). A role of amphiphysin in synaptic vesicle endocytosis suggested by its binding to dynamin in nerve terminals. Proc. Natl. Acad. Sci. USA *93*, 331–335.

De Camilli, P., Harris, S.M., Jr., Huttner, W.B., and Greengard, P. (1983). Synapsin I (Protein I), a nerve terminal-specific phosphoprotein. II. Its specific association with synaptic vesicles demonstrated by immunocytochemistry in agarose-embedded synaptosomes. J. Cell Biol. *96*, 1355–1373.

de Heuvel, E., Bell, A.W., Ramjaun, A.R., Wong, K., Sossin, W.S., and McPherson, P.S. (1997). Identification of the major synaptojanin-binding proteins in brain. J. Biol. Chem. *272*, 8710–8716.

Faundez, V., Horng, J.T., and Kelly, R.B. (1998). A function for the AP3 coat complex in synaptic vesicle formation from endosomes. Cell *93*, 423–432.

Gad, H., Löw, P., Zotova, E., Brodin, L., and Shupliakov, O. (1998). Dissociation between Ca^{2+}-triggered synaptic vesicle exocytosis and clathrin-mediated endocytosis at a central synapse. Neuron *21*, 607–616.

González-Gaitán, M., and Jäckle, H. (1997). Role of Drosophila α-adaptin in presynaptic vesicle recycling. Cell *88*, 767–776.

Grabs, D., Slepnev, V.I., Songyang, Z., David, C., Lynch, M., Cantley, L.C., and De Camilli, P. (1997). The SH3 domain of amphiphysin binds the proline-rich domain of dynamin at a single site that defines a new SH3 binding consensus sequence. J. Biol. Chem. *272*, 13419–13425.

Guo, S., Stolz, L.E., Lemrow, S.M., and York, J.D. (1999). SAC1-like domains of yeast SAC1, INP52, and INP53 and of human synaptojanin encode polyphosphoinositide phosphatases. J. Biol. Chem. *274*, 12990–12995.

Herskovits, J.S., Burgess, C.C., Obar, R.A., and Vallee, R.B. (1993). Effects of mutant rat dynamin on endocytosis. J. Cell Biol. *122*, 565–578.

Heuser, J.E. (1980). Three-dimensional visualization of coated vesicle formation in fibroblasts. J. Cell Biol. *84*, 560–583.

Heuser, J.E. (1989). Effects of cytoplasmic acidification on clathrin lattice morphology. J. Cell Biol. *108*, 401–411.

Heuser, J.E., and Reese, T.S. (1973). Evidence for recycling of synaptic vesicle membrane during transmitter release at the frog neuromuscular junction. J. Cell Biol. *57*, 315–344.

Kirchhausen, T., and Harrison, S.C. (1981). Protein organization in clathrin trimers. Cell *23*, 755–761.

Koenig, J.H., and Ikeda, K. (1989). Disappearance and reformation of synaptic vesicle membrane upon transmitter release observed under reversible blockage of membrane retrieval. J. Neurosci. *9*, 3844–3860.

Laemmli, U.K. (1970). Cleavage of structural proteins during the assembly of the head of bacteriophage T4. Nature *227*, 680–685.

Maycox, P.R., Link, E., Reetz, A., Morris, S.A., and Jahn, R. (1992). Clathrin-coated vesicles in nervous tissue are involved primarily in synaptic vesicle recycling. J. Cell Biol. *118*, 1379–1388.

McPherson, P.S., Garcia, E.P., Slepnev, V.I., David, C., Zhang, X., Grabs, D., Sossin, W.S., Bauerfeind, R., Nemoto, Y., and De Camilli, P. (1996). A presynaptic inositol-5-phosphatase. Nature *379*, 353–357.

Micheva, K.D., Kay, B.K., and McPherson, P.S. (1997). Synaptojanin forms two separate complexes in the nerve terminal. Interactions with endophilin and amphiphysin. J. Biol. Chem. *272*, 27239–27245.

Moore, M.S., Mahaffey, D.T., Brodsky, F.M., and Anderson, R.G. (1987). Assembly of clathrin-coated pits onto purified plasma membranes. Science *236*, 558–563.

Pfeffer, S.R., and Kelly, R.B. (1985). The subpopulation of brain coated vesicles that carries synaptic vesicle proteins contains two unique polypeptides. Cell *40*, 949–957.

Pieribone, V.A., Shupliakov, O., Brodin, L., Hilfiker-Rothenfluh, S., Czernik, A.J., and Greengard, P. (1995). Distinct pools of synaptic vesicles in neurotransmitter release. Nature *375*, 493–497.

Qualmann, B., Roos, J., DiGregorio, P.J., and Kelly, R.B. (1999). Syndapin I, a synaptic dynamin-binding protein that associates with the neural Wiskott-Aldrich syndrome protein. Mol. Biol. Cell *10*, 501–513.

Raucher, D., and Sheetz, M.P. (1999). Membrane expansion increases endocytosis rate during mitosis. J. Cell Biol. *144*, 497–506.

Ringstad, N., Nemoto, Y., and De Camilli, P. (1997). The SH3p4/Sh3p8/SH3p13 protein family: binding partners for synaptojanin and dynamin via a Grb2-like Src homology 3 domain. Proc. Natl. Acad. Sci. USA *94*, 8569–8574.

Rodal, S.K., Skretting, G., Garred, O., Vilhardt, F., van Deurs, B., and Sandvig, K. (1999). Extraction of cholesterol with methyl-beta-cyclodextrin perturbs formation of clathrin-coated endocytic vesicles. Mol. Biol. Cell *4*, 961–974.

Schmid, S.L., McNiven, M.A., and De Camilli, P. (1998). Dynamin and its partners: a progress report. Curr. Opin. Cell Biol. *10*, 504–512.

Schmidt, A., and Huttner, W.B. (1998). Biogenesis of synaptic-like microvesicles in perforated PC12 cells. Methods Enzymol. *16*, 160–169.

Shupliakov, O., Pieribone, V., Gad, H., and Brodin, L. (1995). Synaptic vesicle depletion in reticulospinal axons is reduced by 5-HT: direct evidence for presynaptic modulation of glutamatergic transmission. Eur. J. Neurosci. *7*, 1111–1116.

Shupliakov, O., Löw, P., Grabs, D., Gad, H., Chen, H., David, C., Takei, K., De Camilli, P., and Brodin, L. (1997). Synaptic vesicle endocytosis impaired by disruption of dynamin-SH3 domain interactions. Science *276*, 259–263.

Smith, C.J., Grigorieff, N., and Pearse, B.M. (1998). Clathrin coats at 21 Å resolution: a cellular assembly designed to recycle multiple membrane receptors. EMBO J. *17*, 4943–4953.

Takei, K., McPherson, P.S., Schmid, S.L., and De Camilli, P. (1995). Tubular membrane invaginations coated by dynamin rings are induced by GTP-gamma S in nerve terminals. Nature *374*, 186–190.

Takei, K., Mundigl, O., Daniell, L., and De Camilli, P. (1996). The synaptic vesicle cycle: a single vesicle budding step involving clathrin and dynamin. J. Cell Biol. *133*, 1237–1250.

Takei, K., Slepnev, V., Haucke, V., and De Camilli, P. (1999). Functional partnership between amphiphysin and dynamin in clathrin-mediated endocytosis. Nat. Cell Biol. *1*, 33–39.

ter Haar, E., Musacchio, A., Harrison, S.C., and Kirchhausen, T. (1998). Atomic structure of clathrin: a beta propeller terminal domain joins an alpha zigzag linker. Cell *95*, 563–573.

Towbin, H., Staehelin, T., and Gordon, J. (1979). Electrophoretic transfer of proteins from polyacrylamide gels to nitrocellulose sheets: procedure and some applications. Proc. Natl. Acad. Sci. USA *76*, 4350–4354.

van der Bliek, A.M., and Meyerowitz, E.M. (1991). Dynamin-like protein encoded by the Drosophila shibire gene associated with vesicular traffic. Nature *351*, 411–414.

Witke, W., Podtelejnikov, A.V., Di Nardo, A., Sutherland, J.D., Gurniak, C.B., Dotti, C., and Mann, M. (1998). In mouse brain profilin I and profilin II associate with regulators of the endocytic pathway and actin assembly. EMBO J. *17*, 967–976.

Zhang, B., Koh, Y.H., Beckstead, R.B., Budnik, V., Ganetzky, B., and Bellen, H.J. (1998). Synaptic vesicle size and number are regulated by a clathrin adaptor protein required for endocytosis. Neuron *21*, 1465–1475.

Functional partnership between amphiphysin and dynamin in clathrin-mediated endocytosis

Kohji Takei*†, Vladimir I. Slepnev*†, Volker Haucke* and Pietro De Camilli*‡

*Department of Cell Biology and Howard Hughes Medical Institute, Yale University School of Medicine, 295 Congress Avenue, New Haven, Connecticut 06510, USA
†These authors contributed equally to this work
‡e-mail: pietro.decamilli@yale.edu

Amphiphysin, a protein that is highly concentrated in nerve terminals, has been proposed to function as a linker between the clathrin coat and dynamin in the endocytosis of synaptic vesicles. Here, using a cell-free system, we provide direct morphological evidence in support of this hypothesis. Unexpectedly, we also find that amphiphysin-1, like dynamin-1, can transform spherical liposomes into narrow tubules. Moreover, amphiphysin-1 assembles with dynamin-1 into ring-like structures around the tubules and enhances the liposome-fragmenting activity of dynamin-1 in the presence of GTP. These results show that amphiphysin binds lipid bilayers, indicate a potential function for amphiphysin in the changes in bilayer curvature that accompany vesicle budding, and imply a close functional partnership between amphiphysin and dynamin in endocytosis.

Amphiphysin is the collective name given to two very similar proteins, amphiphysins 1 and 2, which may be involved in clathrin-mediated endocytosis, actin function and signalling pathways[1–9]. Isoforms of amphiphysin-1 and -2 form homodimers and heterodimers and are highly concentrated in the nerve terminal, where they have a putative role in the endocytosis of synaptic vesicles. Amphiphysin is composed of three main domains. The amino-terminal domain, which contains regions predicted to form coiled-coils, is involved in dimerization[3]. The central region binds, through distinct sites, the heavy chain of clathrin and the clathrin adaptor protein AP-2 (refs 3,10–12). The carboxy-terminal region comprises an Src-homology-3 (SH3) domain which binds the GTPase dynamin and the inositol-5′-phosphatase synaptojanin-1 (refs 2, 13–16). The interactions of both the SH3 domain and the central region are regulated by phosphorylation of amphiphysin and/or its binding partners[3]. Experimental manipulations of living cells that disrupt the interactions of amphiphysin with either dynamin or clathrin and AP-2 markedly inhibit clathrin-mediated endocytosis[3,17,18]. These findings indicate that amphiphysin may act as a regulated linker protein that couples clathrin-mediated budding of endocytotic vesicles to dynamin-mediated vesicle fission.

Our goal in this study was to provide a direct demonstration of this hypothesis, using purified components in a cell-free system. Protein-free liposomes composed of brain lipid extracts or synthetic lipid mixtures are fully competent to support the formation of several coated structures that have been implicated in vesicular membrane traffic, including clathrin-coated buds and dynamin-coated tubules[19–21]. In these cell-free systems, addition of GTP to dynamin-coated tubules produces tubule fragmentation and vesiculation[19,21]. As dynamin alone can tubulate liposomes, and clathrin coats alone can generate vesicular buds[19], we tested whether amphiphysin can mediate a coupling between these two processes. Our results not only confirm this hypothesis, but also demonstrate unexpected effects of amphiphysin on lipid curvature and on the liposome-fragmenting activity of dynamin.

Results

Amphiphysin-1 links clathrin coats and dynamin. Purified dynamin-1 can evaginate protein-free liposomes into narrow dynamin-coated tubules[19,21]. Likewise, a clathrin-coat fraction obtained by stripping bovine clathrin-coated vesicles can induce the formation of clathrin-coated buds on liposomes[19].

We incubated liposomes composed of a brain lipid extract with recombinant dynamin-1 and the coat fraction together. Negative staining of these preparations revealed both clathrin-coated buds and dynamin-coated tubules (Fig. 1a). The two types of structure, however, were largely independent of each other. A morphometric analysis revealed that only 24% of the dynamin-coated tubules were capped by a clathrin-coated bud (Fig. 1d, left bar). Addition of purified recombinant amphiphysin-1 to the lipid–protein mixture increased this association (Fig. 1b). Under these conditions, 72% of the dynamin tubules were capped with clathrin-coated buds (Fig. 1d, centre bar). This observation provides morphological evidence for the hypothesis that one of the functions of amphiphysin is to act as a linker between dynamin and the clathrin coat.

Amphiphysin-1 alone tubulates liposomes. In control experiments, we incubated liposomes with both amphiphysin-1 and the coat fraction in the absence of dynamin-1. To our surprise, we observed a massive tubulation of liposomes even under these conditions (Fig. 1c). Tubules were similar in diameter to those generated in the presence of dynamin-1 (compare Fig. 1a–c) and in about 95% of the cases the ends of the tubules were capped by clathrin-coated buds (Fig. 1d, right column).

As liposomes incubated with the coat fraction alone formed only clathrin-coated buds but not tubules[19], we tested the effect of amphiphysin-1 alone on the morphology of liposomes. Incubation of liposomes with amphiphysin-1 resulted in a tubulation of liposomes (Fig. 2b) that was even more massive than that produced by dynamin-1 at the same concentration. These results indicate that amphiphysin-1, like dynamin-1, has the ability to bind lipid bilayers and to evaginate them into high-curvature membranes. In addition to liposomes composed of the brain lipid extract, we tested liposomes composed of phosphatidylcholine and phosphatidylserine in several relative ratios. Tubulation by amphiphysin-1 increased in parallel with the ratio of phosphatidylserine to phosphatidylcholine, showing a preference of amphiphysin-1 for acidic phospholipids (data not shown). We used another lipid-binding protein, AP180 (ref. 22), as a control. AP180, a component of brain clathrin-coated vesicles with a putative role in controlling synaptic vesicle size[22,23], did not tubulate liposomes (data not shown), thus indicating that the effect of

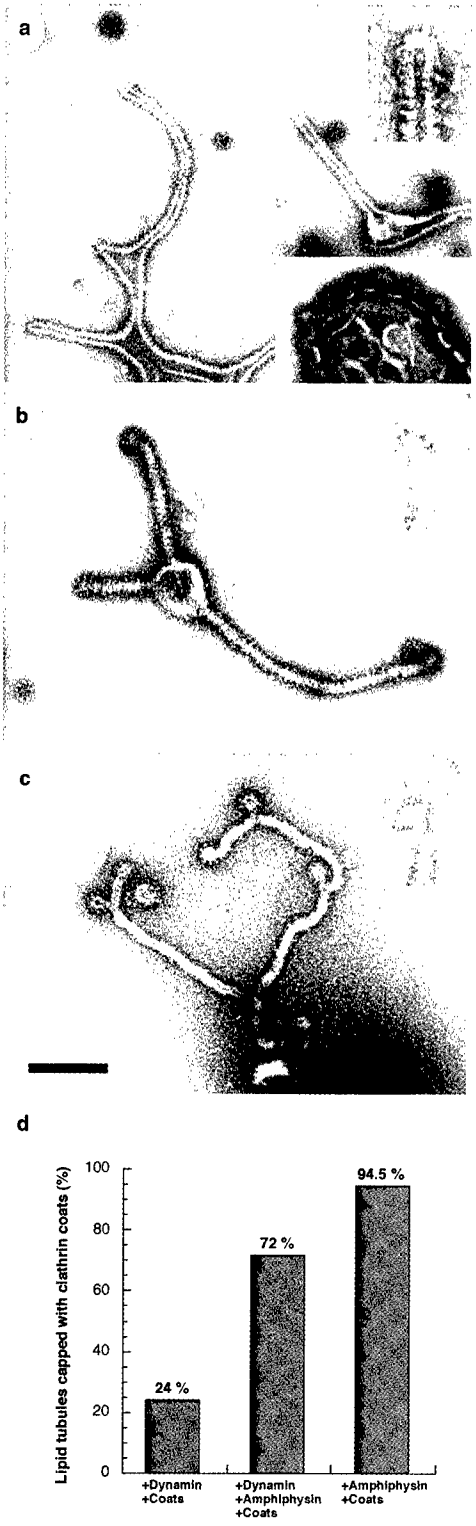

Figure 1 **Effect of amphiphysin-1 on the coupling between clathrin-coated budding and dynamin-mediated tubulation in protein-free liposomes composed of a brain lipid extract. a–c**, Negatively stained liposomes after incubation with the clathrin-coat fraction plus the following recombinant proteins: **a**, dynamin-1; **b**, dynamin-1 plus amphiphysin-1; **c**, amphiphysin-1. Top right insets show tubular ends at high magnification (**a**, negative staining; **b**, **c**, positive staining of thin sections). The bottom inset in **a** shows clathrin-coated buds. **d**, Morphometric analysis of the liposomes shown in **a–c**, showing the fraction of lipid tubules capped by a clathrin coat at their ends. Scale bar represents 300 nm in **a–c** and the bottom inset in **a** and 100 nm in the other insets.

amphiphysin-1 and dynamin-1 on the morphology of liposomes is specific.

To define the region of amphiphysin-1 that is required for lipid tubulation, we generated several fusion proteins containing different amphiphysin-1 fragments and glutathione-*S*-transferase (GST)[24] (Fig. 2a). Pilot experiments showed that GST did not alter

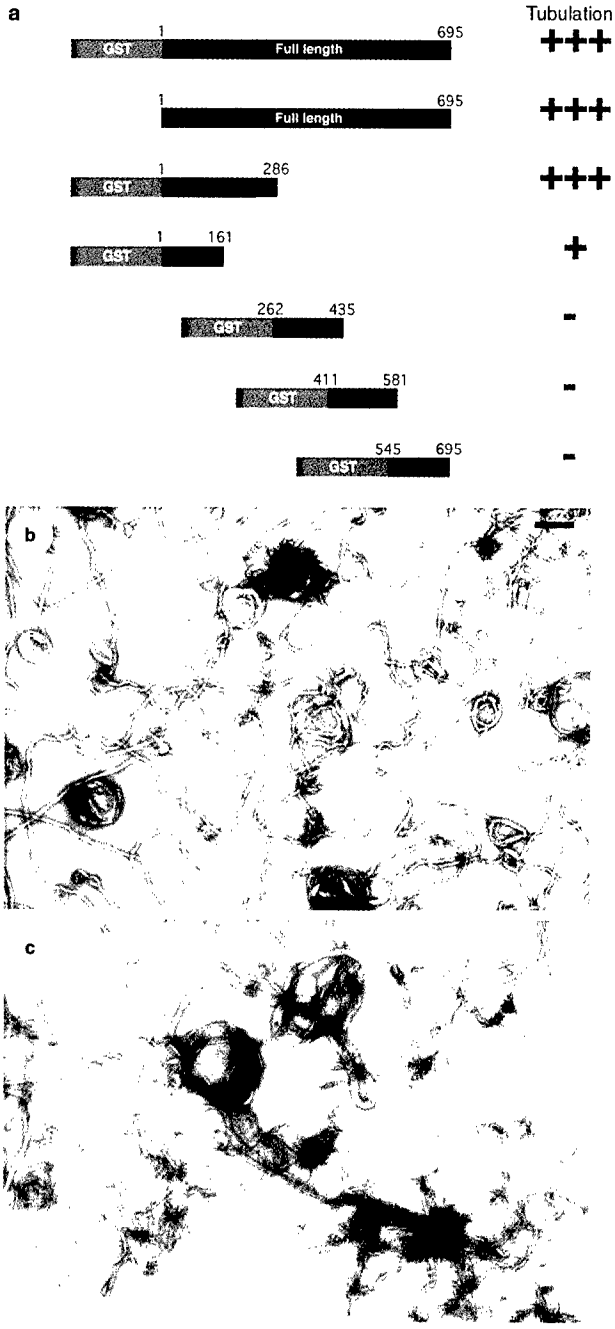

Figure 2 **Amphiphysin alone tubulates liposomes composed of a brain lipid extract. a**, Diagrams of the fusion proteins containing GST and amphiphysin-1 fragments that were tested for their effects on liposome morphology. Symbols at the right reflect a qualitative assessment of the membrane-tubulating activity of the GST fusion proteins. **b**, **c**, Negatively stained liposomes seen after incubation with full-length amphiphysin-1 cleaved from a GST–amphiphysin-1 fusion protein (**b**) or with the GST-fusion protein of the fragment encoding amphiphysin-1 amino acids 1–286 (**c**). Scale bar represents 500 nm.

the morphology of liposomes and that GST–amphiphysin-1 was as effective as amphiphysin-1 in liposome tubulation. We therefore used fragments of amphiphysin-1 fused to GST without cleaving off the GST. A fusion protein comprising amino acids 1–286 of amphiphysin-1 fully retained the tubulating activity of the full-length protein (Fig. 2c), whereas a further deletion at the C-terminal side of this fragment markedly decreased the tubulating activity. We therefore assign the lipid-tubulating activity of amphiphysin-1 to the N-terminal region, which is the portion of the molecule that is most conserved in evolution from yeast to humans.

A hybrid coat consisting of amphiphysin-1 and dynamin-1. High-power observation of negatively stained amphiphysin-1-coated tubules revealed a decoration by closely apposed rings (Fig. 3a). These rings were thinner and more tightly packed than those seen on dynamin-1-generated tubules produced from the same liposomes in either the absence (Fig. 3c) or the presence (data not shown) of the non-hydrolysable GTP analogue GTP-γS. In thin sections of conventionally processed material, the coats comprising amphiphysin-1 alone or dynamin-1 alone were hardly detectable (Fig. 3b, d). Thus, they were different from the thick, electron-dense, regularly spaced rings that are typically seen on tubules generated by incubation of liposomes or synaptic membranes with brain cytosol plus ATP and GTP-γS (Fig. 3g, h)[19,25]. These observations indicate that the rings generated in the presence of brain cytosol and GTP-γS may comprise other proteins in addition to dynamin.

We next studied the effect of recombinant amphiphysin-1 and dynamin-1 together on liposome morphology. A mixture of the two proteins, with or without GTP–γS, generated tubules whose coats were noticeably different from those generated by either one of the two proteins alone (Fig. 3e, f; see also below). Furthermore, whereas dynamin-1 alone decorated both the low-curvature and the tubular regions of liposomes (Fig. 3a), the presence of amphiphysin-1 appeared to segregate dynamin-1 to the liposomes' tubular portions (Fig. 3l). As seen by either negative or positive staining of plastic-embedded material, the coat produced by amphiphysin-1 and dynamin-1 together consisted of thick rings and was similar to that generated by brain cytosol in the presence of ATP and GTP-γS (Fig. 3g, h). A GST-fusion protein containing the amphiphysin SH3 domain, which did not tubulate liposomes, failed to generate this modified form of coats when incubated with liposomes and dynamin. Likewise, the amphiphysin-1 fragment comprising amino acids 1–286, which tubulates liposomes but lacks the SH3 domain, did not modify the dynamin coat. In the presence of this fragment, which does not bind dynamin, only amphiphysin-like or dynamin-like coats were generated, as if the two proteins segregated themselves into homogeneous coats (data not shown).

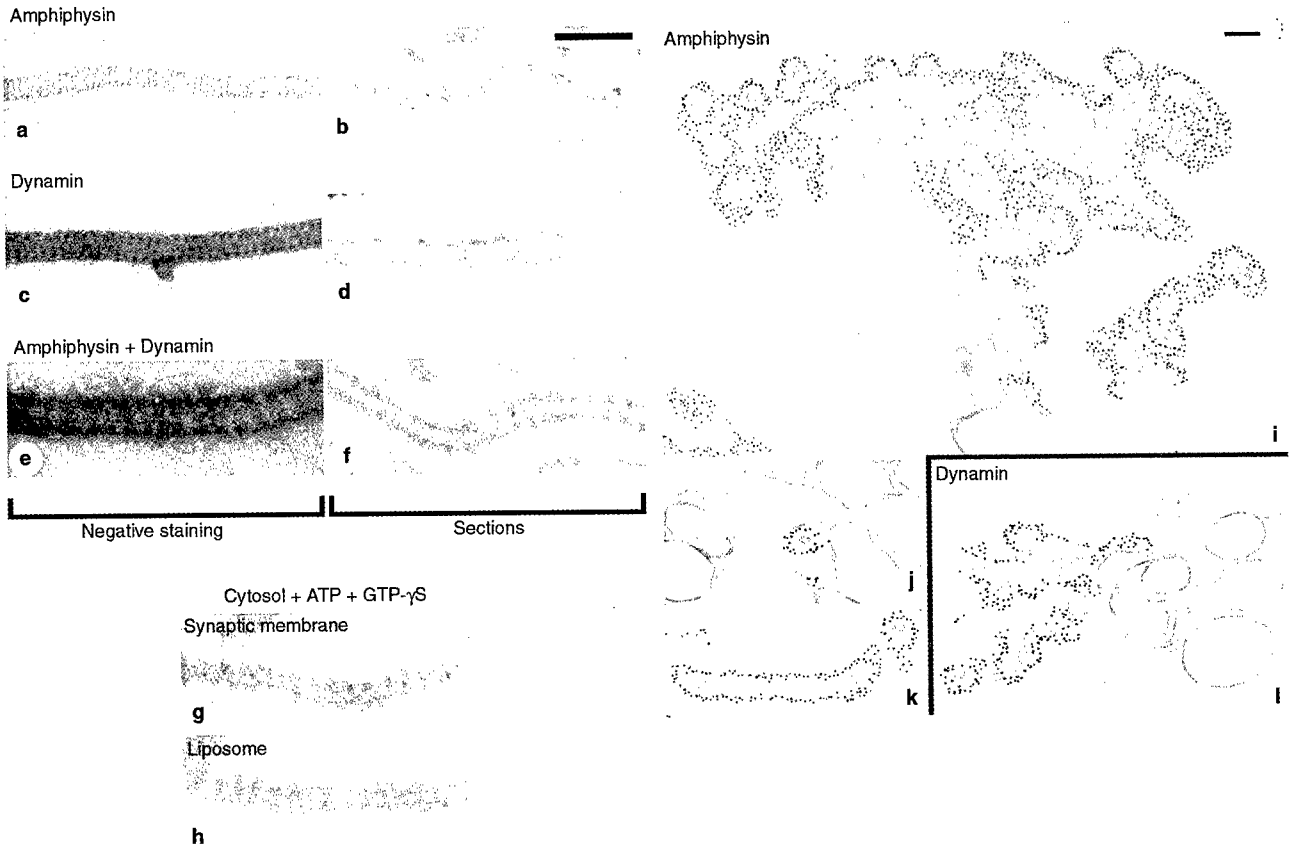

Figure 3 **Amphiphysin-1 and dynamin-1 co-assemble into a hybrid coat. a–h**, The tubular coat generated by a mixture of amphiphysin-1 and dynamin-1 (**e**, **f**) differs from those generated by either amphiphysin-1 (**a**, **b**) or dynamin-1 (**c**, **d**) alone. The hybrid coat resembles the coat generated from total brain cytosol on either liposomes (**h**) or synaptic membranes (**g**). **a**, **c**, **e**, Negative staining of liposomes; **b**, **d**, **f–h**, positive staining of liposomes or synaptic membranes that have been embedded in plastic and thin-sectioned. The amphiphysin-1 and the dynamin-1 coats are represented by tightly packed rings that are not easily visualized by conventional positive staining microscopy (**b**, **d**). Coats generated by amphiphysin-1 and dynamin-1 together or by total brain cytosol plus ATP and GTP-γS appear as thicker, less densely packed rings, which are electron-dense in conventional microscopy (**f–h**). **i–l**, Immunocytochemical demonstration that intense immunoreactivity for both amphiphysin-1 (**i–k**) and dynamin-1 (**l**) is present along the coated tubules generated by incubation of liposomes with amphiphysin-1 and dynamin-1. Note in **i**, **j**, **l** that vacuolar surfaces of liposomes are devoid of these proteins. Cross-sections and longitudinal sections of coated tubules are shown in **j**, **k**, respectively. Scale bars in **b** and **i** represent 100 nm in **a–h** and **i–l**, respectively.

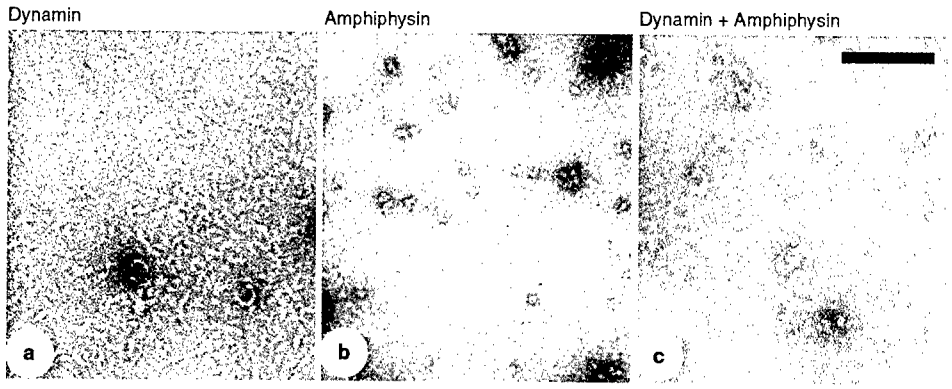

Figure 4 **Dynamin-1 and amphiphysin-1 co-polymerize into rings in a buffer of physiological ionic strength and pH.** Negative staining of the proteins incubated in the absence of liposomes. **a**, Dynamin-1 alone appears primarily as short rods. **b**, Amphiphysin-1 alone does not form rings. **c**, The two proteins together form numerous rings which are thicker than those formed by dynamin alone. Scale bar represents 200 nm.

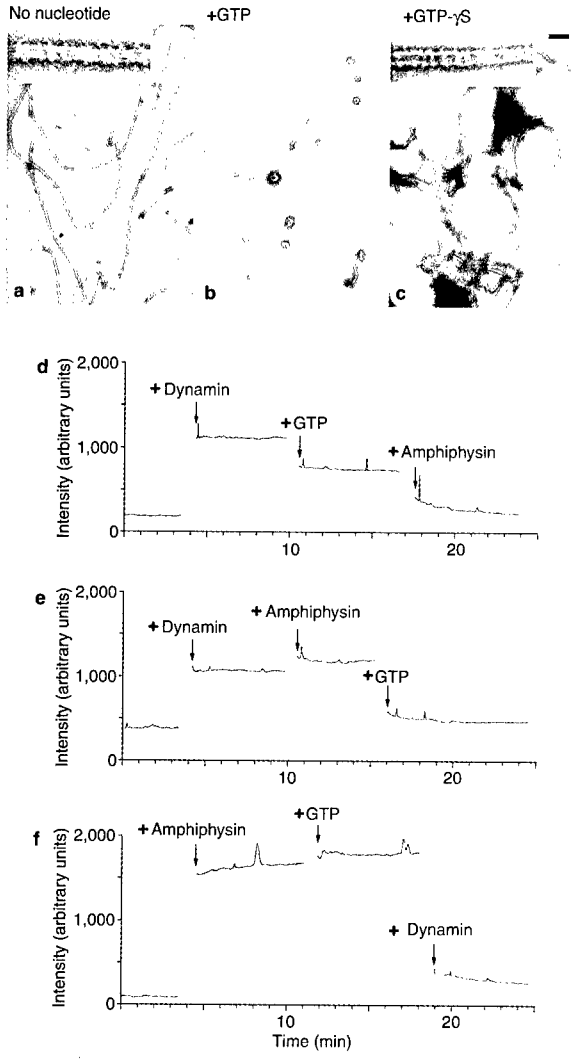

Figure 5 **GTP-dependent liposome fragmentation produced by dynamin-1 alone or by amphiphysin-1 and dynamin-1 together. a–c**, Negatively stained liposomes after incubation with the two proteins in the absence of nucleotides (**a**) or in the presence of GTP (**b**) or GTP-γS (**c**). The insets show high-power views of the tubular coat. Scale bar represents 500 nm in **a–c** and 55 nm in the insets. **d–f**, Time course of light scattering, showing that amphiphysin-1 enhances the fragmentation of liposomes. Liposomes were supplemented with dynamin, amphiphysin and GTP at the time points indicated by arrows.

Thus, both the lipid-binding N-terminal region and the SH3 domain of amphiphysin-1 are required for the generation of tubules coated with both amphiphysin-1 and dynamin-1.

Immunogold labelling of the coat generated by the dynamin–amphiphysin mixture revealed intense immunoreactivity towards both proteins along the entire tubule (Fig. 3i–l). This observation indicates that the thick, electron-dense ring generated under these conditions results from an interaction of the two proteins. After the same labelling protocol, tubules generated by cytosol, ATP and GTP-γS on synaptic membranes[26] were equally immunoreactive for dynamin-1, but much less intensely immunoreactive for amphiphysin-1[19,26]. It will be interesting to determine whether this discrepancy reflects masking of amphiphysin-1 epitopes by other cytosolic proteins or co-existence of amphiphysin-1 with other cytosolic SH3-domain-containing proteins, such as amphiphysin-2, in the dynamin coat.

Amphiphysin–dynamin rings in solution. One possible explanation for the morphology of the amphiphysin–dynamin hybrid coat is an intrinsic property of these two proteins to co-assemble into rings. To test this hypothesis, we studied the effect of amphiphysin-1 on the oligomerization of dynamin-1 in membrane-free solutions. Dynamin-1 has been shown previously to oligomerize into open rings spontaneously when incubated in buffers of low ionic strength[27]. Amphiphysin-1 alone never formed rings under several conditions tested (Fig. 4b and data not shown). Under conditions of physiological ionic strength, in which dynamin-1 alone formed only a very few rings (Fig. 4a), massive ring formation was produced by a mixture of amphiphysin-1 and dynamin-1 (Fig. 4c). These rings were similar in thickness and size to those formed by the amphiphysin-1–dynamin-1 mixture on lipid tubules. Together, these results indicate that amphiphysin-1 can co-assemble with dynamin-1 into ring-like structures and can cooperate with dynamin-1 in the formation of tubular coats.

Amphiphysin enhances dynamin's liposome-fragmenting activity. Addition of GTP to dynamin-1-coated lipid tubules results in their fragmentation, as shown by both negative-staining and light-scattering experiments[19,21]. This effect has been attributed to a conformational change in the dynamin ring that correlates with GTP hydrolysis. Addition of GTP, but not GTP-γS, to amphiphysin–dynamin-coated tubules had a similar effect, as shown by negative staining in Fig. 5. To test whether the presence of amphiphysin-1 affects the liposome-fragmenting activity of dynamin-1 in the presence of GTP, we performed light-scattering experiments. Addition of dynamin-1 to liposomes resulted in a steep increase in light scattering, reflecting the formation of tubules (Fig. 5d). GTP produced an immediate drop in light scattering (see also ref. 21) that persisted with time, indicating a new steady state. Subsequent addition of

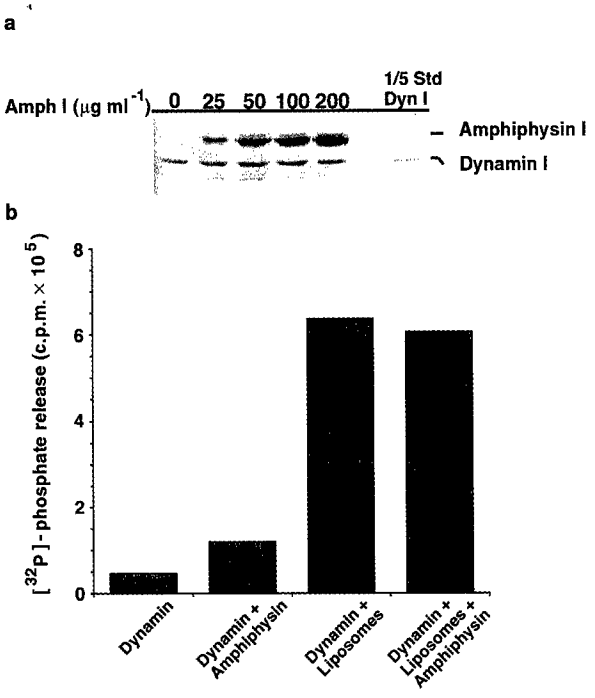

Figure 6 **Effect of amphiphysin-1 on the recruitment of dynamin-1 to liposomes and on its GTPase activity. a**, Recruitment of dynamin-1 to liposomes in the presence of increasing concentrations of amphiphysin-1. Liposome-associated proteins were analysed by SDS–PAGE, transferred to nitrocellulose membranes and stained with Ponceau S. 1/5 Std Dyn I: one-fifth of the total amount of dynamin-1 added to the assay. **b**, Effect of amphiphysin-1 on the GTPase activity of dynamin-1. The GTPase activity of dynamin-1 was measured in the presence or absence of liposomes and recombinant amphiphysin-1 as indicated.

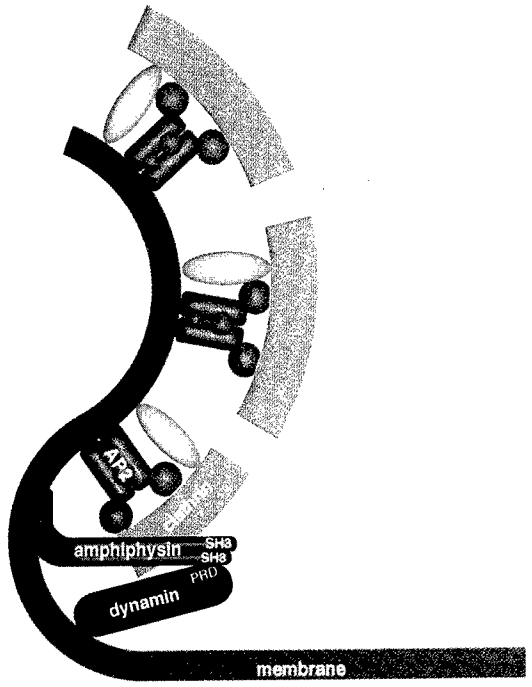

Figure 7 **Interactions of the amphiphysin dimer at a clathrin-coated endocytotic pit.** Amphiphysin dimerizes through its N-terminal region which also binds the lipid bilayer. It binds the heavy chain of clathrin and the clathrin adaptor AP-2 through its central region and binds dynamin through its C-terminal SH3 domain. As shown by our results, amphiphysin enhances membrane curvature and potentiates the liposome-fragmenting activity of dynamin in the presence of GTP. PRD, proline-rich domain.

amphiphysin produced an even greater drop in light scattering (Fig. 5d). Conversely, when amphiphysin-1 was added to dynamin-coated tubules in the absence of nucleotides, a small increase, rather than a decrease, in light scattering was observed, possibly reflecting enhanced tubulation. Addition of GTP to this mixture produced a drop in light scattering to the same values as those observed when amphiphysin-1 was added to the dynamin plus GTP mixture (Fig. 5e). Finally, tubules generated by amphiphysin-1 alone were resistant to GTP, but underwent rapid vesiculation when dynamin-1 was added to the mixture. All of the samples tested by light scattering were also analysed by negative staining. This morphological analysis confirmed that the potentiation of the GTP-dependent drop in light scattering produced by amphiphysin-1 resulted from enhanced liposome fragmentation (data not shown). At least a few short tubules, however, were seen in all conditions.

There may be several explanations for the enhancement by amphiphysin-1 of the liposome-fragmenting activity of dynamin-1. Amphiphysin-1 may potentiate the recruitment of dynamin-1 to liposomes. The results of sedimentation experiments, however, showed that, at least under our experimental conditions and with the ratio of reagents used, the amount of dynamin-1 recruited to liposomes was not affected by amphiphysin-1 (Fig. 6a). Another possibility is that amphiphysin-1 stimulates the GTPase activity of dynamin-1. However, when tested in solution amphiphysin produced only a very modest increase in dynamin's GTPase activity. Liposomes, in agreement with previous findings, had a powerful stimulatory effect on the activity, but amphiphysin-1 did not further stimulate this effect (Fig. 6b). Further possibilities are discussed below.

Discussion

In this study we have attempted to elucidate the physiological functions of some of the interactions that take place during synaptic-vesicle endocytosis by using a cell-free system and defined components. The process of clathrin-mediated endocytosis can be dissected into several major steps, which include recruitment of the clathrin coat, invagination of the coated membrane patch and fission of the coated bud in a process that requires dynamin[28]. A function of amphiphysin as a bridge between the AP-2/clathrin coat and dynamin-1 had been inferred from its biochemical properties[2,3,10,11,17]. In agreement with this prediction, we have shown here that a structural continuity between clathrin-coated and dynamin-coated membrane areas is enhanced by the presence of recombinant amphiphysin-1. Unexpectedly, these studies have also led us to discover new properties of amphiphysin-1. First, amphiphysin-1 binds lipid membranes. Second, amphiphysin-1, like dynamin-1, has a powerful ability to transform spherical liposomes into narrow tubules. Third, amphiphysin-1 co-assembles with dynamin and affects its function. Thus, amphiphysin may have multiple functions in the endocytotic reaction (Fig. 7).

The liposome-binding properties of amphiphysin-1 indicate that it may act as a multifunctional linker protein that anchors the clathrin coat, dynamin and the lipid bilayer to each other. Given its ability to bind both clathrin and the membrane, it may act as an accessory clathrin adaptor. A similar function has been proposed for arrestin[29]. It remains to be determined whether amphiphysin also assists dynamin in clathrin-independent endocytotic reactions[30,31].

Lipid tubulation by a protein reflects the ability of that protein to bind to, and to oligomerize at, the surface of a lipid bilayer. Sev-

eral proteins have been shown to tubulate liposomes and/or to form a helical array around lipid tubules[32,33]. In most cases reported, the protein and the lipid surface exhibit opposite charges and the process is presumably driven by electrostatic interactions. In contrast, amphiphysin-1, which is negatively charged, tubulates liposomes of the same charge, arguing against the involvement of nonspecific electrostatic effects. Moreover, the tubulation mediated by amphiphysin-1 and dynamin-1 takes place at a far higher rate and efficiency than tubulation mediated by the other proteins studied[32,33]. The generation of high-curvature membrane tubules by amphiphysin-1 and dynamin-1 is of special interest because the evagination of endocytotic buds requires deformation of the bilayer into high-curvature domains, at which amphiphysin-1 and dynamin-1 have been detected immunocytochemically. The membrane-tubulating activity of amphiphysin-1 resides in its N-terminal region. It has been mapped to a fragment (defined as domain A in ref. 24) that is the only one common to all amphiphysin-family members, including the yeast proteins Rvs161 and Rvs167 (ref. 24). It is therefore plausible that this activity may be shared by all amphiphysin-family members, and that the amphiphysin-1–amphiphysin-2 heterodimer functions in the same way as the amphiphysin-1 homodimer studied here.

The ability of amphiphysin to oligomerize with dynamin changes our view of the dynamin ring. Purified dynamin can spontaneously oligomerize into open rings and stacks of rings[27,34]. On the basis of this observation, the rings generated using total brain cytosol, ATP and GTP-γS on membrane templates *in vitro*[25], or by mutant dynamin *in situ*[35], were thought to represent dynamin alone. We have shown here that these structures are unlikely to consist of only dynamin. We have also shown that amphiphysin-1 and dynamin-1 together, both in solution and around lipid membranes, are sufficient to generate the thicker, electron-dense rings that are seen on membranes incubated with cytosol, ATP and GTP-γS. We conclude that the structures generated in the presence of cytosol, ATP and GTP-γS are likely to contain other proteins in addition to dynamin-1, and that amphiphysin-1 may be one such protein.

The liposome-fragmenting activity of dynamin-1 in our cell-free system was enhanced by addition of amphiphysin-1. However, the effect of amphiphysin-1 could not be explained by either enhanced recruitment of dynamin-1 to the membrane or stimulation of dynamin-1's GTPase activity. The effect of amphiphysin-1 on dynamin-1 in this assay may reflect the ability of amphiphysin to reorganize dynamin at the surface of the bilayer. The addition of amphiphysin-1 appeared to cause a more efficient segregation of dynamin-1 into the tubular portion of liposomes, which may be seen as equivalent to the neck of an endocytotic bud. Thus amphiphysin may have a physiological role in concentrating dynamin at the vesicle neck as vesicular buds are formed. Amphiphysin may also improve the coupling of dynamin action to membrane fission by other mechanisms. The ability of purified dynamin and amphiphysin to form highly ordered structures that undergo GTP-dependent changes provides a powerful experimental system with which to gain further insights into the structure–function relationship of these two proteins.

The precise relationship of the liposome-fragmenting activity of dynamin *in vitro* to the role of dynamin in endocytosis requires further clarification. Dynamin-1 alone can fragment liposomes *in vitro* in a GTP-dependent manner. However, dynamin-coated tubules may exist even in the presence of GTP, probably reflecting an equilibrium between tubule growth and tubule fragmentation under these conditions (see also ref. 19). In the living cell, dynamin may be only one component of a more complex machinery that drives the fission of a vesicle from the plasma membrane. As discussed previously[15], the main function of GTP-bound dynamin may be to recruit and/or activate other proteins at the neck of a vesicle bud. These other proteins may then act as the effectors in the fission reaction. Irrespective of the precise mechanism of action of dynamin in endocytosis, our findings indicate that the functions of amphiphysin and dynamin are closely interconnected and that the effects of amphiphysin rely not only on protein–protein interactions but also on a key interaction with membrane lipids. □

Methods

Reagents.

Mouse monoclonal antibodies against amphiphysin-1 have been described previously[36]. Monoclonal antibodies directed against dynamin (Hudy-1) were purchased from UBI (Lake Placid, NY). 6-nm protein-A–gold conjugates were prepared as described[37]. A bovine brain lipid extract (type I, Folch fraction I) was purchased from Sigma.

Liposomes.

Large liposomes were prepared as described[38] with some modifications. Lipids solubilized in a chloroform:methanol (1:2) mixture were dried in a glass tube by passing nitrogen through the tube, then lyophilized for 2h. The dried lipid film was hydrated by a stream of water-saturated nitrogen for 20 min. After gentle addition of degassed 0.3 M sucrose, the flask was flushed with nitrogen, sealed, and left undisturbed for 2h at 37 °C to allow spontaneous formation of liposomes. Large aggregates of lipids were removed by centrifugation.

Coat fraction.

Clathrin-coated vesicles were prepared from calf brains as described[39]. Coat proteins were extracted from the coated vesicles with a buffer containing 0.8 M Tris-Cl pH 7.4, 2 mM EGTA, 0.03% sodium azide, 0.5 mM dithiothreitol and 1 mM phenylmethylsulphonyl fluoride for 15 h at room temperature (modified from ref. 40). Solubilized coat proteins were separated from membranes by centrifugation at 100,000*g* for 1 h at room temperature. Coat proteins were either used directly or frozen in liquid nitrogen and stored at −70 °C.

Purified proteins.

Human dynamin-1aa was produced as a GST-fusion protein using a modified Bac-to-Bac baculovirus expression system (Gibco BRL) as described[19]. A complementary DNA encoding GST followed by a cleavage site for PreScission protease (Pharmacia) was inserted into the pFastBAC1 baculovirus transfer vector (Gibco BRL). The dynamin cDNA without the starting methionine was cloned into this vector downstream of the cleavage site. A recombinant virus was produced, amplified and used to infect insect Tn cells for 48 h in 1-l spinner cultures. The fusion protein was affinity purified on glutathione–Sepharose-4B and GST was removed by PreScission protease (Pharmacia) according to the manufacturer's protocols. The purity of dynamin in the final material was estimated to be more than 90% and its GTPase activity was confirmed using the EnzChek Phosphate Assay kit (Molecular Probes). A full-length human amphiphysin-1 (ref. 24) was inserted into the pGEX6-1 vector (Pharmacia), expressed in the bacterial strain DH5α and purified according to standard procedures. After removal of GST, amphiphysin was further purified by gel filtration on Superdex-200 to >90% purity. GST-fusion proteins containing amino acids 1–161, 1–286, 262–435, 411–581 or 545–695 of human amphiphysin were produced as described[24]. A GST cDNA fragment encoding amphiphysin amino acids 1–286 was amplified by the polymerase chain reaction, cloned into pGEX6-1 and purified as a GST-fusion protein as above.

Cell-free incubations.

Liposomes (final concentration 0.1 mg ml^{-1}) were incubated in 'cytosolic buffer' (25 mM HEPES-KOH, pH 7.4, 25 mM KCl, 2.5 mM magnesium acetate, 10 mM Ca^{2+}, 150 mM potassium glutamate) for 15 min at 37 °C with proteins and various nucleotides as indicated. The final concentration of proteins and nucleotides was as follows unless indicated otherwise: coat proteins, 0.5 mg ml^{-1}; purified amphiphysin-1 and dynamin-1, 0.1 mg ml^{-1}; ATP, 2 mM; GTP or GTP-γS, 200 μM. Samples containing ATP were also supplemented with an ATP-regenerating system consisting of 16.7 mM creatine phosphate and 16.7 IU ml^{-1} creatine phosphokinase. Samples with coat proteins and no nucleotides were supplemented with an ATP-depleting system consisting of 5 U ml^{-1} hexokinase and 10 mM glucose.

Electron microscopy.

For negative staining, samples were absorbed onto freshly glow-discharged Formvar- and carbon-coated electron-microscopy grids, stained with 2% uranyl acetate for 1 min, blotted and air dried. Some samples were fixed after absorption to electron microscopy grids with 3% glutaraldehyde. For standard electron microscopy, incubation mixtures were fixed in suspension with 3% formaldehyde and 2% glutaraldehyde in 50 mM HEPES-KOH buffer (pH 7.4) and pelleted in an Eppendorf centrifuge. Samples were postfixed in OsO_4, and then impregnated with 0.1% tannic acid to enhance the visualization of membrane coats. Immunoelectron microscopy was done as described[41].

Morphometry.

Association of lipid tubules with clathrin-coated buds was quantified by visually scanning negatively stained samples at the electron microscope. We observed 200 randomly chosen lipid tubules for each condition and scored them for the presence of clathrin-coated buds at their tips.

Light scattering.

Light scattering was measured on an Hitachi F-3010 fluorescence spectrophotometer at 350 nm. Excitation and emission slit widths were set at 3 nm. Liposomes (100 μg ml^{-1} lipid) were incubated in cytosolic buffer at room temperature and supplemented with the following reagents as indicated in Fig. 5: 20 μg ml^{-1} dynamin, 50 μg ml^{-1} amphiphysin-1 and 1 mM GTP.

GTPase-activity assay.

A GTPase-activity assay measuring $[^{32}P]PO_4$ release was performed as described[42] with the following modifications. Dynamin (20 μg ml^{-1}) was incubated in buffer containing 20 mM Tris (pH 7.5), 2.5 mM

$MgCl_2$, 20 mM NaCl, 200 μg ml^{-1} GST and 0.5 mM GTP (0.1 mCi mM^{-1}) in the absence or presence of amphiphysin-1 (50 μg ml^{-1}), a GST-fusion protein containing the SH3 domain (amino acids 545–695) of amphiphysin-1 (100 μg ml^{-1}) and liposomes (100 μg ml^{-1}) for 30–75 min at room temperature.

Assay of recruitment of amphiphysin-1 and dynamin-1.

Total brain liposomes (0.5 mg ml^{-1}) were incubated with 20 μg ml^{-1} purified dynamin-1 in the presence of increasing concentrations of amphiphysin-1 (up to 200 μg ml^{-1}) in cytosolic buffer for 15 min at 37°C. Liposomes were then re-isolated through a sucrose cushion (0.3 M sucrose in 20 mM HEPES-KOH, pH 7.4, 150 mM KCl). Samples were analysed by SDS–PAGE, transfered to nitrocellulose membranes and stained with Ponceau S.

RECEIVED 17 MARCH 1999; REVISED 29 MARCH 1999; ACCEPTED 30 MARCH 1999; PUBLISHED MAY 1999.

1. Mundigl, O. *et al.* Amphiphysin I antisense oligonucleotides inhibit neurite outgrowth in cultured hippocampal neurons. *J. Neurosci.* **18,** 93–103 (1998).
2. David, C., McPherson, P. S., Mundigl, O. & De Camilli, P. A role of amphiphysin in synaptic vesicle endocytosis suggested by its binding to dynamin in nerve terminals. *Proc. Natl Acad. Sci. USA* **93,** 331–335 (1996).
3. Slepnev, V. I., Ochoa, G. C., Butler, M. H., Grabs, D. & Camilli, P.D. Role of phosphorylation in regulation of the assembly of endocytic coat complexes. *Science* **281,** 821–824 (1998).
4. Wigge, P. & McMahon, H. T. The amphiphysin family of proteins and their role in endocytosis at the synapse. *Trends Neurosci.* **21,** 339–344 (1998).
5. Cremona, O. & De Camilli, P. Synaptic vesicle endocytosis. *Curr. Opin. Neurobiol.* **7,** 323–330 (1997).
6. Butler, M. H. *et al.* Amphiphysin II (SH3P9; BIN1), a member of the amphiphysin/Rvs family, is concentrated in the cortical cytomatrix of axon initial segments and nodes of ranvier in brain and around T tubules in skeletal muscle. *J. Cell Biol.* **137,** 1355–1367 (1997).
7. Leprince, C. *et al.* A new member of the amphiphysin family connecting endocytosis and signal transduction pathways. *J. Biol. Chem.* **272,** 15101–15105 (1997).
8. Ramjaun, A. R., Micheva, K. D., Bouchelet, I. & McPherson, P. S. Identification and characterization of a nerve terminal-enriched amphiphysin isoform. *J. Biol. Chem.* **272,** 16700–16706 (1997).
9. Wigge, P. *et al.* Amphiphysin heterodimers: potential role in clathrin-mediated endocytosis. *Mol. Biol. Cell* **8,** 2003–2015 (1997).
10. Wang, L. H., Südhof, T. C. & Anderson, R. G. W. The appendage domain of alpha-adaptin is a high affinity binding site for dynamin. *J. Biol. Chem.* **270,** 10079–10083 (1995).
11. McMahon, H. T., Wigge, P. & Smith, C. Clathrin interacts specifically with amphiphysin and is displaced by dynamin. *FEBS Lett.* **413,** 319–322 (1997).
12. Ramjaun, A. R. & McPherson, P. S. Multiple amphiphysin II splice variants display differential clathrin binding: identification of two distinct clathrin-binding sites. *J. Neurochem.* **70,** 2369–2376 (1998).
13. McPherson, P. S. *et al.* A presynaptic inositol-5-phosphatase. *Nature* **379,** 353–357 (1996).
14. Grabs, D. *et al.* The SH3 domain of amphiphysin binds the proline-rich domain of dynamin at a single site that defines a new SH3 binding consensus sequence. *J. Biol. Chem.* **272,** 13419–13425 (1997).
15. De Camilli, P. & Takei, K. Molecular mechanisms in synaptic vesicle endocytosis and recycling. *Neuron* **16,** 481–486 (1996).
16. Urrutia, R., Henley, J. R., Cook, T. & McNiven, M. A. The dynamins: redundant or distinct functions for an expanding family of related GTPases? *Proc. Natl Acad. Sci. USA* **94,** 377–384 (1997).
17. Shupliakov, O. *et al.* Synaptic vesicle endocytosis impaired by disruption of dynamin-SH3 domain interactions. *Science* **276,** 259–263 (1997).
18. Wigge, P., Vallis, Y. & McMahon, H. T. Inhibition of receptor-mediated endocytosis by the amphiphysin SH3 domain. *Curr. Biol.* **7,** 554–560 (1997).
19. Takei, K. *et al.* Generation of coated intermediates of clathrin-mediated endocytosis on protein-free liposomes. *Cell* **94,** 131–141 (1998).
20. Matsuoka, K. *et al.* COPII-coated vesicle formation reconstituted with purified coat proteins and chemically defined liposomes. *Cell* **93,** 263–275 (1998).
21. Sweitzer, S. M. & Hinshaw, J. E. Dynamin undergoes a GTP-dependent conformational change causing vesiculation. *Cell* **93,** 1021–1019 (1998).
22. Hao, W. *et al.* Regulation of AP-3 function by inositides. *J. Biol. Chem.* **272,** 6393–6398 (1997).
23. Zhang, B. *et al.* Synaptic vesicle size and number are regulated by a clathrin adaptor protein required for endocytosis. *Neuron* **21,** 1465–1475 (1998).
24. David, C., Solimena, M. & De Camilli, P. Autoimmunity in Stiff-Man syndrome with breast cancer is targeted to the C-terminal region of human amphiphysin, a protein similar to the yeast proteins, Rvs167 and Rvs161. *FEBS Lett.* **351,** 73–79 (1994).
25. Takei, K., McPherson, P. S., Schmid, S. L. & De Camilli, P. Tubular membrane invaginations coated by dynamin rings are induced by GTPγS in nerve terminals. *Nature* **374,** 186–190 (1995).
26. Bauerfeind, R., Takei, K. & De Camilli, P. Amphiphysin I is associated with coated endocytic intermediates and undergoes stimulation-dependent dephosphorylation in nerve terminals. *J. Biol. Chem.* **272,** 30984–30992 (1997).
27. Hinshaw, J. E. & Schmid, S. L. Dynamin self-assembles into rings suggesting a mechanism for coated vesicle budding. *Nature* **374,** 190–192 (1995).
28. Schmid, S. L. Clathrin-coated vesicle formation and protein sorting: an integrated process. *Annu. Rev. Biochem.* **66,** 511–548 (1997).
29. Gaidarov, I., Krupnick, J. G., Falck, J. R., Benovic, J. L. & Keen, J. H. Arrestin function in G protein-coupled receptor endocytosis requires phosphoinositide binding. *EMBO J.* **18,** 871–881 (1999).
30. Oh, P., McIntosh, D. P. & Schnitzer, J. E. Dynamin at the neck of caveolae mediates their budding to form transport vesicles by GTP-driven fission from the plasma membrane of endothelium. *J. Cell Biol.* **141,** 101–114 (1998).
31. Henley, J., Krueger, E., Oswald, B. & McNiven, M. Dynamin-mediated internalization of caveolae. *J. Cell Biol.* **141,** 85–99 (1998).
32. Polyakov, A., Severinova, E. & Darst, S. A. Three-dimensional structure of *E. coli* core RNA polymerase: promoter binding and elongation conformation of the enzyme. *Cell* **83,** 365–373 (1995).
33. Wilson-Kubalek, E. M., Brown, R. E., Celia, H. & Milligan, R. A. Lipid nanotubes as substrates for helical crystallization of macromolecules. *Proc. Natl Acad. Sci. USA* **95,** 8040–8045 (1998).
34. Carr, J. F. & Hinshaw, J. E. Dynamin assembles into spirals under physiological salt conditions upon the addition of GDP and gamma-phosphate analogues. *J. Biol. Chem.* **272,** 28030–28035 (1997).
35. Koenig, J. H. & Ikeda, K. Disappearance and reformation of synaptic vesicle membrane upon transmitter release observed under reversible blockage of membrane retrieval. *J. Neurosci.* **9,** 3844–3860 (1989).
36. Floyd, S. *et al.* Expression of amphiphysin I, an autoantigen of paraneoplastic neurological syndromes, in breast cancer. *Mol. Med.* **4,** 29–39 (1998).
37. Slot, J. W. & Geuze, H. J. A new method of preparing gold probes for multiple-labeling cytochemistry. *Eur. J. Cell Biol.* **38,** 87–93 (1985).
38. Reeves, J. P. & Dowben, R. M. Formation and properties of thin-walled phospholipid vesicles. *J. Cell Physiol.* **73,** 49–60 (1969).
39. Campbell, C., Squicciarini, J., Shia, M., Pilch, P. F. & Fine, R. E. Identification of a protein kinase as an intrinsic component of rat liver coated vesicles. *Biochemistry* **23,** 4420–4426 (1984).
40. Keen, J. H., Willingham, M. C. & Pastan, I. H. Clathrin-coated vesicles: isolation, dissociation and factor-dependent reassociation of clathrin baskets. *Cell* **16,** 303–312 (1979).
41. Takei, K., Mundigl, O., Daniell, L. & De Camilli, P. The synaptic vesicle cycle: a single vesicle budding step involving clathrin and dynamin. *J. Cell Biol.* **133,** 1237–1250 (1996).
42. Liu, J. P., Zhang, Q. X., Baldwin, G. & Robinson, P. J. Calcium binds dynamin I and inhibits its GTPase activity. *J. Neurochem.* **66,** 2074–2081 (1996).

ACKNOWLEDGEMENTS

This work was supported in part by grants from the NIH and the US Army Medical Research and Development Command (to P.D.C.), and a long-term fellowship from the Human Frontier Science Program (to V.H.).

Correspondence and requests for materials should be addressed to P.D.C.

Epsin is an EH-domain-binding protein implicated in clathrin-mediated endocytosis

Hong Chen*, Silvia Fre†, Vladimir I. Slepnev*, Maria Rosaria Capua†, Kohji Takei*, Margaret H. Butler*, Pier Paolo Di Fiore†‡ & Pietro De Camilli*

* *Howard Hughes Medical Institute and Department of Cell Biology, Yale University School of Medicine, 295 Congress Avenue, New Haven, Connecticut 06510, USA*
† *Department of Experimental Oncology, European Institute of Oncology, Milan 20141, Italy*
‡ *Istituto di Microbiologia, Universita' di Bari, Bari 70124, Italy*

During endocytosis, clathrin and the clathrin adaptor protein AP-2 (ref. 1), assisted by a variety of accessory factors, help to generate an invaginated bud at the cell membrane[2,3]. One of these factors is Eps15, a clathrin-coat-associated protein that binds the α-adaptin subunit of AP-2 (refs 4–8). Here we investigate the function of Eps15 by characterizing an important binding partner for its

region containing EH domains[9]; this protein, epsin, is closely related to the *Xenopus* mitotic phosphoprotein MP90 (ref. 10) and has a ubiquitous tissue distribution. It is concentrated together with Eps15 in presynaptic nerve terminals, which are sites specialized for the clathrin-mediated endocytosis of synaptic vesicles. The central region of epsin binds AP-2 and its carboxy-terminal region binds Eps15. Epsin is associated with clathrin coats *in situ*, can be co-precipitated with AP-2 and Eps15 from brain extracts, but does not co-purify with clathrin coat components in a clathrin-coated vesicle fraction. When epsin function is disrupted, clathrin-mediated endocytosis is blocked. We propose that epsin may participate, together with Eps15, in the molecular rearrangement of the clathrin coats that are required for coated-pit invagination and vesicle fission.

The core of the binding consensus of the EH domains of Eps15 is the sequence asparagine-proline-phenylalanine (NPF)[11]. This sequence is present in non-neuronal isoforms of proteins of the synaptojanin and AP180/CALM families, which have been implicated in clathrin-mediated endocytosis[12–14]. Members of these families interact with the EH domains of Eps15 and of the yeast protein Pan1[15,16]. Clathrin-mediated endocytosis of synaptic vesicles probably represents a specialization of the clathrin-mediated endocytosis typical of all cells[2], but the nerve-terminal isoforms of AP180 and synaptojanin do not contain NPF motifs[12,13,15,17], raising the possibility that Eps15 may be selectively involved in clathrin-mediated internalization of receptors and not in synaptic vesicle recycling. We therefore tested whether Eps15, and the homologous protein Eps15R (refs 6, 18), are concentrated in nerve endings, which would be expected for proteins that participate in synaptic vesicle endocytosis.

Immunofluorescence staining of frozen sections revealed differential expression of Eps15 and Eps15R in various rat brain regions, but produced in all regions a predominant nerve-terminal pattern of immunoreactivity, similar to that of synaptophysin, a synaptic-vesicle membrane protein[6,19] (Fig. 1a, and results not shown). There was an enrichment of Eps15 and Eps15R in brain relative to other tissues (Fig. 1b), consistent with an important role of clathrin-dependent synaptic vesicle recycling in this tissue.

We searched for nerve-terminal binding partners for the EH-domain-containing regions of Eps15 and Eps15R by reacting fusion proteins comprising glutathione-*S*-transferase (GST) and these regions (GST–EH_{eps15} and GST–EH_{eps15R}, respectively) with rat brain cytosol in a gel overlay assay. The two fusion proteins, but not GST alone (Fig. 2a), specifically recognized one predominant band corresponding to a relative molecular mass of ~94K (referred to here as epsin, for Eps15-interacting protein) and minor bands of smaller molecular masses. A protein band of 94K (p94) was identified previously by affinity chromatography as a binding partner for the appendage domain of α-adaptin, a subunit of the clathrin adaptor AP-2 (ref. 20), but was not characterized further. As shown by Fig. 2, antibodies raised against one of the three reported peptide sequences of bovine p94 specifically recognized in rat brain a protein band that co-migrated with epsin in SDS–PAGE (Fig. 2a) and which could be affinity-purified on immobilized GST–EH_{eps15} (Fig. 2b). The same antibodies immunodepleted epsin from rat brain cytosol (Fig. 2c).

Degenerate oligonucleotides designed from the reported peptide sequences of bovine p94 were used to clone by polymerase chain reaction (PCR) a fragment of rat epsin that was then used to screen a λZAPII rat brain complementary DNA library (from Stratagene). Clone 16 (accession no. AF018261) included a full-length 576-amino-acid open reading frame (Fig. 3) which contained stretches identical to the three peptides of bovine p94, except that there was an arginine-to-lysine substitution at residue 128. Searches of the databases revealed several related complete and partial sequences, including the yeast sequences YDL161w and YLR206w. The more closely related full-length sequence is that of MP90, a *Xenopus* mitotic phosphoprotein[10]. The domain comprising the first 165 amino acids of epsin is the most conserved phylogenetically and is present in proteins otherwise very divergent from epsin; it appears therefore to define a new protein module. The central 150-amino-acid region is strikingly characterized by the presence of several repeats of the triplet aspartate-proline-tryptophan (DPW), which are almost completely conserved from *Xenopus* to rat. The Cdc2 phosphorylation site of MP90 is localized in this region[10] and is conserved in epsin. The C-terminal region of epsin contains three NPF repeats (Fig. 3), consistent with the identification of epsin as a partner for the EH domains of Eps15 (ref. 11).

By northern blotting, a 2.6-kilobase (kb) epsin-specific band was labelled in all of several tissues tested, suggesting a housekeeping role for this protein; epsin immunoreactivity was also detectable in all tissues by western blotting. Like Eps15 and Eps15R, the highest

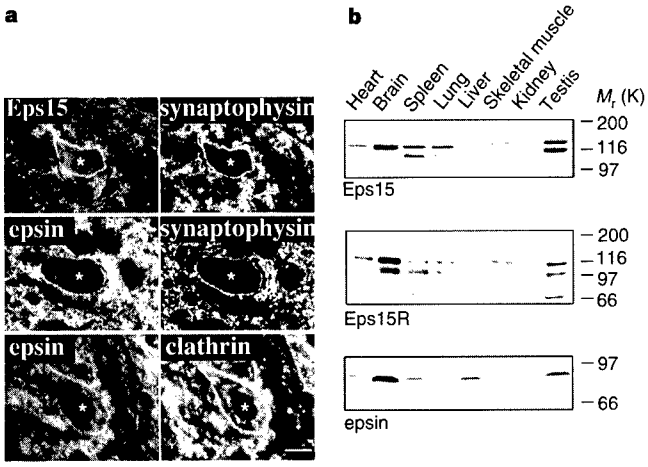

Figure 1 Eps15 and epsin are highly expressed in the brain and are concentrated in nerve terminals. **a**, Double-immunofluorescence micrographs of rat brain frozen sections showing the co-localization of Eps15 and epsin with synaptophysin and clathrin in nerve terminals. Epsin and clathrin are also localized in the Golgi complex, visible as perinuclear immunostaining. Asterisks, neuronal perikarya. Scale bar, 20 μm. **b**, Tissue distribution of Eps15, Eps15R and epsin, as determined by western blotting of total homogenates of rat tissues. The multiple bands stained by both anti-Eps15 and anti-Eps15R probably represent alternatively spliced isoforms of these two proteins[18].

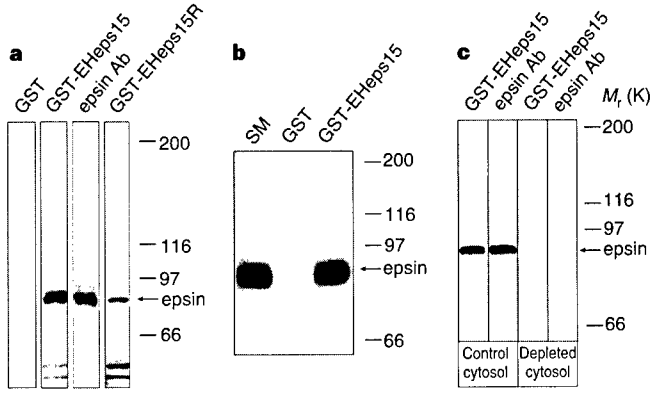

Figure 2 EH-domain-containing regions of Eps15 and Eps15R bind to a 94K protein (epsin) in rat brain. **a**, SDS–PAGE gels of rat brain cytosol were overlaid with GST fusion proteins comprising the three EH domains of Eps15 or Eps15R (GST–EH_{eps15} and GST–EH_{eps15R}) or antibodies raised against the p94 protein (ref. 20; epsin Ab). **b**, Affinity purification of rat brain Triton X-100 extract on either GST or GST–EH_{eps15}. The starting material (SM) and material bound to the beads were labelled by western blotting with antibodies directed against p94 (epsin). **c**, GST–EH_{eps15} overlay or anti-epsin western blotting of rat brain cytosol before or after immunodepletion with anti-p94 antibodies.

a

```
1    MSTSSLRRQMKNIVHNVSEAEIKVREATSNDPWGPSSSLMSEIADLTYNV
51   VAFSEIMSMIWKRLNDHGKNWRHVYKAMTLMEYLIKTGSERVSQQCKENM
101  YAVQTLKDFQYVDRDGKDQGVNVREKAKQLVALLRDEDRLREERAHALKT
151  KEKLAQTATASSAAVGSGPPPEAEQAWPQSSGEEELQLQLALAMSKEEAD
201  QPPSCGPEDDVQLQLALSLSREEHDKEERIRRGDDLRLQMAIEESKRETG
251  GKEESSLMDLADVFTTPALPQASDPWGGPASVPTAVPVAAAASDPWGAPA
301  VPPAADPWGGAAPTPASGDPWRPAAPTGPSVDPWGGTPAPAAGEGPTSDP
351  WGSADGGAPVSGPPSSDPWAPAPAFSDPWGGSPAKPSSNGTAAVGGFDTE
401  PDEFSDFDRLRTALPTSGSSTGELELLAGEVPARSPGAFDMSGVGGSLAE
451  SVGSPPPAATPTHTPPTRKTPESFLGPNAALVDLDSLVSRPGPTPPGAKA
501  SNPFLPSGAPATGPSVTNPFQPAPPATLTLNQLRLSPVPPVPGAPPTYIS
551  PLGGGPGLPPMMPPGPPAPNTNPFLL
```

b

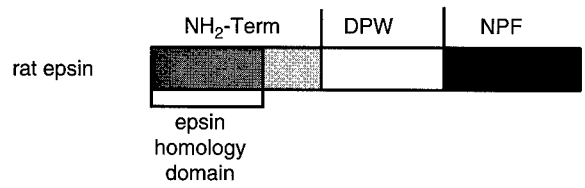

Figure 3 Primary sequence of rat epsin. **a**, Deduced amino-acid sequence of rat epsin. The three peptides sequences of bovine p94 obtained by Edman degradation[20] are underlined with thick grey bars. DPW sequences are in bold and NPF motifs are underlined. The putative Cdc2 phosphorylation site is indicated by an asterisk. **b**, Domain structure of epsin.

concentration of epsin was found in the brain (Fig. 1b). Epsin was concentrated in nerve terminals, where it co-localized with synaptophysin and with clathrin. It was also present, together with clathrin, in the Golgi complex (Fig. 1a). In subcellular fractions of rat brain, epsin and Eps15 were co-enriched in synaptosomes (P2 fraction) and had a roughly parallel distribution in other fractions (Fig. 4a). Epsin, like Eps15[21], was present but not enriched, in a clathrin-coated vesicle fraction prepared according to ref. 22, as was also found for other accessory proteins of clathrin-mediated endocytosis (amphiphysin I, dynamin I, and synaptojanin I; refs 23, 24 and 12, respectively). In contrast, intrinsic components of the clathrin coat (clathrin, AP-2 subunits and AP180)[2] were enriched in this fraction (Fig. 4a). Immunogold labelling of synaptic membranes confirmed a specific association of epsin with clathrin coats (Fig. 4b).

These results were supported by analysis of the subcellular distribution of epsin in transfected CHO cells briefly permeabilized before fixation. In cells with low-to-moderate expression, epsin immunofluorescence had a punctate pattern that was very similar to that of clathrin, AP-2 and Eps15 (Fig. 4c), and epsin immunogold labelled primarily clathrin-coated pits (Fig. 4b). In cells with high expression, there was additional labelling of the cytoplasmic face of the plasmalemma (not shown), indicating that epsin may interact with other molecules of the cortical cytoplasm besides clathrin-coated components.

To confirm the binding of epsin to α-adaptin and Eps15, and to identify binding regions for these proteins, brain cytosol was affinity-purified on GST fusion proteins of the three main domains of epsin. The NPF domain bound Eps15, as expected, whereas the DPW domain bound α-adaptin (both α_a and α_c subunits) (Fig. 5a).

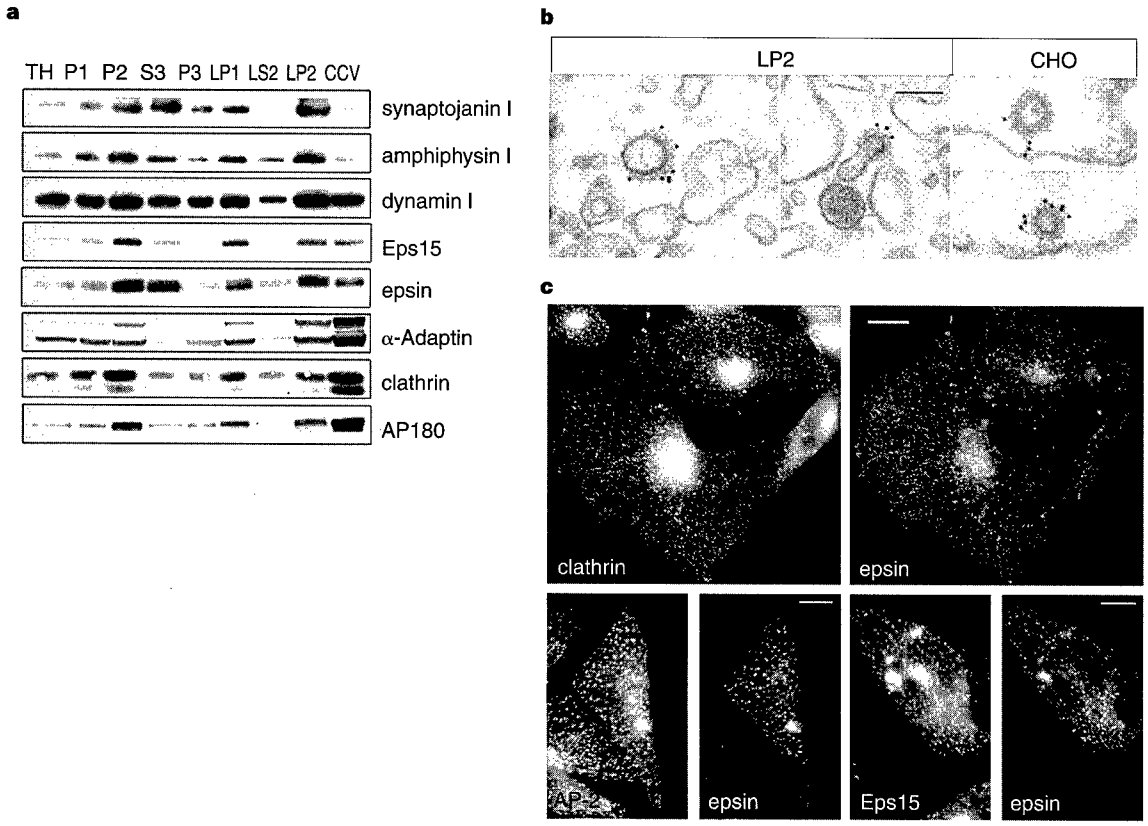

Figure 4 Subcellular localization of epsin. **a**, Distribution of epsin and other endocytic proteins in subcellular fractions of rat brain (TH to LP2) obtained according to ref. 28. A clathrin-coated vesicle fraction (CCV) was prepared as described[22]. **b**, Electron microscopy of immunogold labelling for epsin in an LP2 fraction of rat brain after incubation with brain cytosol, ATP and GTP-γS, and in transiently transfected CHO cells briefly lysed before fixation. Scale bar, 100 nm. **c**, Immunofluorescence of CHO cells transiently transfected with epsin cDNA and briefly permeabilized before fixation showing the co-localization of epsin with other endocytic proteins. Scale bar, 15 μm.

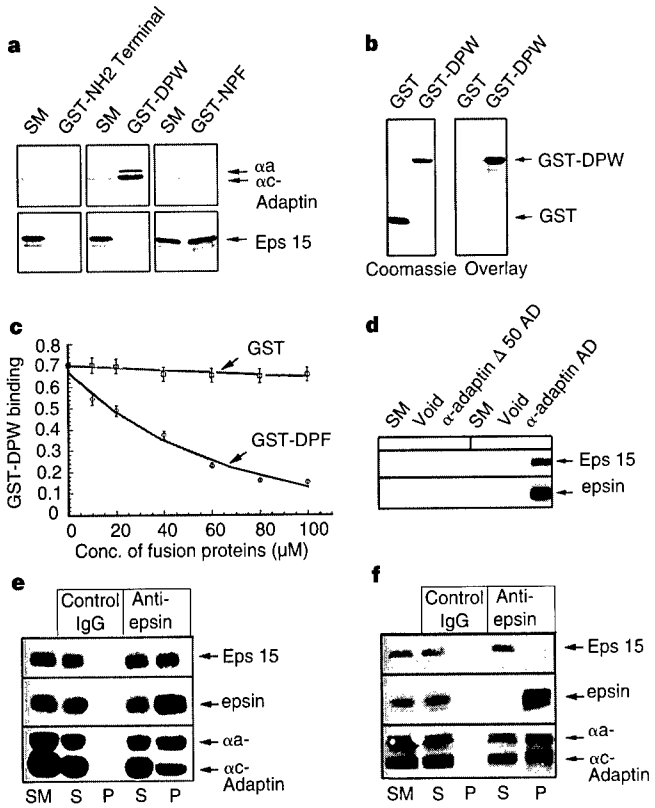

Figure 5 Interaction of epsin with α-adaptin and Eps15. **a**, A rat brain Triton X-100 extract was affinity-purified on GST fusion proteins comprising the three portions of epsin (see Fig. 3b). Starting material and bound material were probed by western blotting for α-adaptin or Eps15. **b**, Coomassie-blue staining and α-adaptin (appendage domain) overlay of GST and a GST–DPW fusion protein. **c**, ELISA assay showing that the DPF domain of Eps15 competes with the DPW domain of epsin for binding to the immobilized appendage domain of α-adaptin. **d**, Affinity purification of a rat brain Triton X-100 extract onto α-adaptin appendage domain (α-adaptin AD)[20] or a truncated appendage domain with a 50-amino-acid N-terminal deletion (α-adaptin Δ50 AD). Void, unbound material. **e**, **f**, Western blot analysis of immunoprecipitates from a Triton X-100 extract of a total homogenate of rat brain (**e**) or brain cytosol (**f**) with anti-epsin antibodies or control IgGs. SM, starting material; S, supernatant; P, pellet.

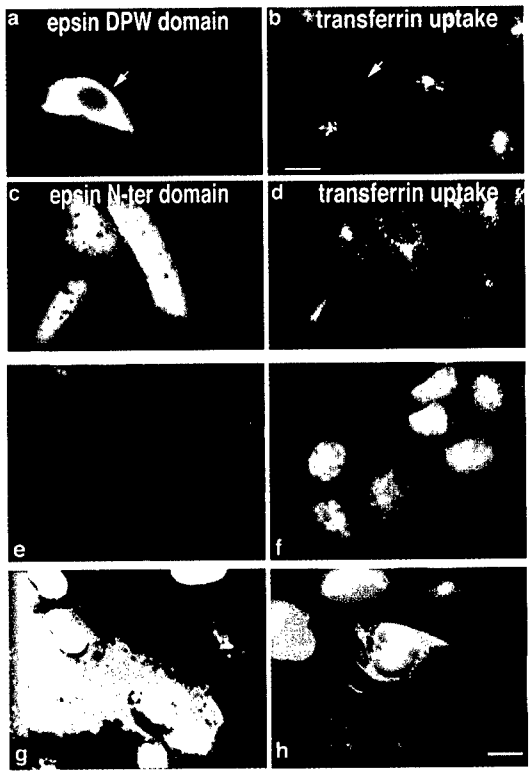

Figure 6 Perturbation of epsin function impairs receptor-mediated endocytosis. **a–d**, CHO cells were transiently transfected with the DPW domain (**a** and **b**, arrow) or the amino-terminal domain (**c**, **d**) of epsin and exposed to CY3-transferrin for 20 min before fixation and immunolabelling for the transfected proteins. Scale bar, 14 μm. **e–h**, Colour confocal micrographs demonstrating that microinjection of CV-1 cells with anti-epsin antibodies blocks EGF-receptor internalization. Cells were exposed to rhodamine-EGF for 1 h at 4 °C (**e**, note cell-surface-bound EGF) and then incubated for 15 min at 37 °C, briefly acid-washed and fixed (**f–h**). Cells in **g** and **h** were injected with control IgGs (**g**) or affinity-purified anti-epsin antibodies (**h**), respectively. Red, EGF; green, injected antibodies; blue, DAPI staining. Scale bar, 15 μm. Results are typical and representative of four experiments in which at least 100 cells were injected per experiment.

Further analysis by gel overlay revealed that there was direct interaction not only of the NPF domain with Eps15 (not shown, and Fig. 2a), but also of the DPW domain with the appendage domain of α-adaptin (Fig. 5b). As shown by an enzyme-linked immunosorbent assay (ELISA), the latter interaction was competitively inhibited by the α-adaptin binding domain of Eps15 (the so-called DPF domain)[4,7] (Fig. 5c, and results not shown). Consistent with a binding of epsin and Eps15 to the same region of α-adaptin, a 50-amino-acid N-terminal truncation of the appendage domain of α-adaptin abolished binding of both Eps15[4] and epsin (Fig. 5d). The occurrence of these interactions *in vivo* was confirmed by co-precipitation experiments, in which antibodies directed against epsin co-precipitated both α-adaptin and Eps15 from a Triton X-100 extract of a total brain homogenate (Fig. 5e). However, the same antibodies co-precipitated only α-adaptin from the cytosol (Fig. 5f), suggesting that the Eps15-epsin interaction occurs only at the membrane.

If epsin acts as a link protein between AP-2 and EH-domain-containing proteins, the overexpression of its AP-2-binding domain may have a dominant-negative effect on clathrin-mediated endocytosis. As shown by Fig. 6a–d, CY3-transferrin uptake[25] by CHO cells is inhibited by expression of the DPW domain of epsin but not by expression of its N-terminal domain. Likewise, microinjection of a GST–DPW construct in CV-1 cells blocked the clathrin-dependent internalization of receptors for epidermal growth factor (EGF) (results not shown). We also tested the effect of epsin disruption on clathrin-mediated endocytosis by injecting antibody into CV-1 cells. Injection of affinity-purified antibodies directed against epsin, but not of control antibodies, inhibited the internalization of both EGF (Fig. 6e–h) and transferrin (results not shown).

Collectively, our results indicated that epsin participates in clathrin-dependent endocytosis, including endocytosis at the synapse. Epsin, like Eps15 (ref. 21), is clearly not a major intrinsic component of the clathrin coat. As proposed for Eps15 (refs 8, 21), it may assist clathrin during oligomerization and during the progressive rearrangement of the clathrin lattice that leads to invagination and fission. As epsin and Eps15 can bind to each other at the membrane, they could form dynamic molecular bridges between neighbouring AP-2 complexes. This effect may be amplified by the property of Eps15, an elongated molecule, to form dimers and tetramers[26]. An entry in the GenBank database of a partial sequence that is likely to represent mouse epsin (AF057285) reveals that epsin binds intersectin (AF032118), another EH-domain-containing protein. Intersectin is homologous with DAP 160, a *Drosophila* dynamin-interacting protein[27]. Thus, epsin seems to participate in a network of protein–protein interactions that assists clathrin-mediated endocytosis and which may have additional functions in the cortical cytoplasm. As epsin is also localized in the Golgi

complex area, EH-domain-mediated interactions of epsin may have a general role in clathrin-mediated budding. □

Methods

Antibodies. Rabbit antibodies directed against epsin and Eps15 were obtained using the following immunogens: bovine epsin peptide ARQLVALLRDEDRLREE[20], GST fusion proteins of the DPW and NPF domains of epsin, and of the EH and DPF domains of Eps15. Antibodies directed against anti-Eps15R, dynamin I, amphiphysin I and synaptojanin I have been described[15,18,23]. A monoclonal antibody directed against the appendage domain of α-adaptin was from Sigma; antibodies directed against clathrin light chain, synaptophysin and synaptotagmin were gifts from R. Jahn.

Cloning and sequencing of epsin cDNA. Degenerate primers corresponding to two peptide sequences of bovine p94 (ref. 20; NIVHNY and FQYVDR) were used in PCR reactions with a rat brain cDNA library as template. A 300-bp PCR product was amplified, subcloned into a TA cloning vector (Invitrogen), radiolabelled and used to screen a rat brain cDNA library (Stratagene).

Production and affinity purification of fusion proteins. Portions of the coding region of rat epsin encoding amino-acid residues 1–248 (N-terminal domain), 249–401 (DPW domain), and 402–576 (NPF domain), were amplified by PCR using Vent polymerase (NEB, Beverly, MA). PCR fragments were digested by either *Eco*R1 and *Sal*1, or *Eco*R1 and *Xho*1, and subcloned into the pGEX4T series of vectors (Pharmacia). GST fusion proteins were produced and purified on a glutathione–Sepharose 4B column (Pharmacia) according to the manufacturer's protocol.

Cell transfection. Full-length epsin cDNA was subcloned into pcDNA3.1/His B (Invitrogen). Epsin fragments were subcloned into pcDNA3 with an N-terminal Flag tag. These constructs were transfected in CHO cells by the lipofectamine method (GIBCO) and cells were analysed 18–24 h after transfection. For CY3-transferrin (Molecular Probes) uptake[25], cells were incubated in the presence of the probe for 20 min at room temperature before fixation in 4% paraformaldehyde/120 mM sodium phosphate buffer, pH 7.4.

Cell microinjections. CV-1 cells were plated at a density of 5×10^4 cells on round glass gelatin-coated overslips. Injection pressure was set at 30–80 hPa and the injection time at 0.3–0.5 s. Affinity-purified anti-epsin polyclonal antibodies or rabbit IgG (Jackson Immunoresearch) were injected at 1.2 mg ml^{-1}. For EGF internalization assay, microinjected cells were incubated with 1 μg ml^{-1} rhodamine–EGF (Molecular Probes) in DMEM medium at 4 °C for 1 h. The EGF-containing medium was then replaced with warm DMEM and cells were further incubated at 37–C for 15 min, followed in some cases by an acid wash before fixation in order to remove cell-surface EGF. For transferrin internalization assay, microinjected cells were incubated with 50 μg ml^{-1} rhodamine–transferrin (Molecular Probes) in DMEM medium at 37 °C for 60 min. Following internalization, cells were fixed with 4% paraformaldehyde, and immunostained with FITC-conjugated goat anti-rabbit secondary antibodies (Jackson Immunoresearch) to identify injected cells. Nuclear counterstaining was done by incubating coverslips for 5 min at 25 °C with DAPI (Sigma).

Immunoprecipitation and immunodepletion. Rat brain cytosol or a Triton X-100 extract of a total brain homogenate (10 mg ml^{-1}) were incubated for 2 h at 4 °C with affinity-purified anti-epsin IgGs or control IgG bound to protein A–Sepharose beads. Immunoprecipitates were washed three times for 5 min with TBST buffer (20 mM Tris, pH 7.4, 150 mM NaCl, 1% Triton X-100, 1 mM PMSF), and analysed by SDS–PAGE and western blotting. For immunodepletion of the cytosol, a large excess of protein A–Sepharose precoated with IgGs directed against the bovine p94 peptide was added to the cytosol, incubated for 4 h at 4 °C and then separated by centrifugation.

Electron microscopy. Immunogold labelling of synaptic membrane (LP2 fractions)[28] was performed as described[24] after incubation of these membranes in the presence of brain cytosol, ATP and GTP-γ-S, to increase the number of clathrin-coated endocytic intermediates[24]. Transfected CHO cells were mechanically disrupted in cytosolic buffer by a nitrocellulose paper 'rip-off' method, then fixed in 3% formaldehyde and 0.1% glutaraldehyde, processed for immunogold labelling[24] while still attached on the Petri dish, and finally scraped and epon-embedded for ultrathin sectioning.

ELISA assay. 96-well microtitre plates were coated with α-adaptin appendage domain by overnight incubation at 4 °C with 20 μg ml^{-1} appendage domain in 100 mM borate buffer, pH 8.5, followed by blocking with 5% BSA. 2 μM biotinylated DPW domain was then added to each well in the presence of GST or GST fused to the DPF domain of Eps15, and incubated for 2 h at room temperature, followed by 1 h incubation with alkaline-phosphatase-conjugated streptavidin. Colorimetric reactions were quantified by a microplate reader.

Miscellaneous procedures. Rat brain homogenate was subcellular-fractionated as described[28]. SDS–PAGE, western blotting, gel overlays, protein assays and immunofluorescence were done as described[29]. For Fig. 4c, cells were exposed to 0.03% saponin in cytosolic buffer[24] for a minute before fixation to elute soluble proteins. Preparation of Triton X-100 rat brain extracts and affinity-purification methods from these extracts on immobilized GST fusion proteins were carried out as described[30].

Received 21 April; accepted 20 June 1998.

1. Robinson, M. S. The role of clathrin, adaptors and dynamin in endocytosis. *Curr. Opin. Cell Biol.* **6,** 538–544 (1994).
2. Cremona, O. & De Camilla, P. Synaptic vesicle endocytosis. *Curr. Opin. Neurobiol.* **7,** 323–330 (1997).
3. Kirchhausen, T., Bonifacino, J. S. & Riezman, H. Linking cargo to vesicle formation: receptor tail interactions with coat proteins. *Curr. Opin. Cell Biol.* **9,** 488–495 (1997).
4. Benmerah, A., Begue, B., Dautry-Varsat, A. & Cerf-Bensussan, N. The ear of alpha-adaptin interacts with the COOH-terminal domain of the Eps 15 protein. *J. Biol. Chem.* **271,** 12111–12116 (1996).
5. Benmerah, A. *et al.* AP-2/Eps15 interactions is required for receptor-mediated endocytosis. *J. Cell. Biol.* **140,** 1055–1062 (1998).
6. Carbone, R. *et al.* eps15 and eps15R are essential components of the endocytic pathway. *Cancer Res.* **57,** 5498–5504 (1997).
7. Iannolo, G. *et al.* Mapping of the molecular determinants involved in the interaction between eps15 and AP-2. *Cancer Res.* **57,** 240–245 (1997).
8. Tebar, F., Sorkina, T., Sorkin, A., Ericsson, M. & Kirchhausen, T. Eps15 is a component of clathrin-coated pits and vesicles and is located at the rim of coated pits. *J. Biol. Chem.* **271,** 28727–28730 (1996).
9. Wong, W. T. *et al.* A protein-binding domain, EH, identified in the receptor tyrosine kinase substrate Eps15 and conserved in evolution. *Proc. Natl Acad. Sci. USA* **92,** 9530–9534 (1995).
10. Stukenberg, P. T. *et al.* Systematic identification of mitotic phosphoproteins. *Curr. Biol.* **7,** 338–348 (1997).
11. Salcini, A. E. *et al.* Binding specificity and *in vivo* targets of the EH domain, a novel protein–protein interaction module. *Genes Dev.* **11,** 2239–2249 (1997).
12. McPherson, P. S. *et al.* A presynaptic inositol-5-phosphatase. *Nature* **379,** 353–357 (1996).
13. Dreyling, M. H. *et al.* The t(10;11)(p13;q14) in the U937 cell line results in the fusion of the AF10 gene and CALM, encoding a new member of the AP-3 clathrin assembly protein family. *Proc. Natl Acad. Sci. USA* **93,** 4804–4809 (1996).
14. Srinivasan, S. *et al.* Disruption of three phosphatidylinositol-polyphosphate 5-phosphatase genes from *Saccharomyces cerevisiae* results in pleiotropic abnormalities of vacuole morphology, cell shape, and osmohomeostasis. *Eur. J. Cell Biol.* **74,** 350–360 (1997).
15. Haffner, C. *et al.* Synaptojanin 1: localization on coated endocytic intermediates in nerve terminals and interaction of its 170 kDa isoform with Eps15. *FEBS Lett.* **419,** 175–180 (1997).
16. Wendland, B. & Emr, S. D. Pan1p, Yeast eps15, Functions as a multivalent adaptor that coordinates protein–protein interactions essential for endocytosis. *J. Cell Biol.* **141,** 71–84 (1998).
17. Zhou, S., Sousa, R., Tannery, N. H. & Lafer, E. M. Characterization of a novel synapse-specific protein. *J. Neurosci.* **12,** 2144–2155 (1992).
18. Coda, L. *et al.* Eps15R is a tyrosine kinase substrate with characteristics of a docking protein possibly involved in coated pits-mediated internalization. *J. Biol. Chem.* **273,** 3003–3012 (1998).
19. Navone, F. *et al.* Protein p38: an integral membrane protein specific for small vesicles of neurons and neuroendocrine cells. *J. Cell Biol.* **103,** 2511–2527 (1986).
20. Wang, L. H., Sudhof, T. C. & Anderson, R. G. The appendage domain of alpha-adaptin is a high affinity binding site for dynamin. *J. Biol. Chem.* **270,** 10079–10083 (1995).
21. Cupers, P., Jadhav, A. P. & Kirchhausen, T. Assembly of clathrin coats disrupts the association between Eps15 and AP-2 adaptors. *J. Biol. Chem.* **273,** 1847–1850 (1998).
22. Maycox, P. R., Link, E., Reetz, A., Morris, S. A. & Jahn, R. Clathrin-coated vesicles in nervous tissue are involved primarily in synaptic vesicle recycling. *J. Cell Biol.* **118,** 1379–1388 (1992).
23. Bauerfeind, R., Takei, K. & De Camilli, P. Amphiphysin I is associated with coated endocytic intermediates and undergoes stimulation-dependent dephosphorylation in nerve terminals. *J. Biol. Chem.* **272,** 30984–30992 (1997).
24. Takei, K., McPherson, P. S., Schmid, S. L. & De Camilli, P. Tubular membrane invaginations coated by dynamin rings are induced by GTP-gamma S in nerve terminals. *Nature* **374,** 186–190 (1995).
25. Cameron, P. L., Sudhof, T. C., Jahn, R. & De Camilli, P. Localization of synaptophysin with transferrin receptors: implications for synaptic vesicle biogenesis. *J. Cell Biol.* **115,** 151–164 (1991).
26. Cupers, P., ter Haar, E., Boll, W. & Kirchhausen, T. Parallel dimers and antiparallel tetramers formed by epidermal growth factor receptor pathway substrate clone 15. *J. Biol. Chem.* **272,** 33430–33434 (1997).
27. Roos, J. & Kelly, R. B. Dap160, a neural-specific EH- and multiple SH3-domain containing protein that interacts with Drosophila dynamin. *J. Biol. Chem.* (in the press).
28. Huttner, W. B., Schiebler, W., Greengard, P. & De Camilli, P. Synapsin I (protein I), a nerve terminal-specific phosphoprotein. *J. Cell Biol.* **96,** 1374–1388 (1983).
29. David, C., McPherson, P. S., Mundigl, O. & de Camilli, P. A role of amphiphysin in synaptic vesicle endocytosis suggested by its binding to dynamin in nerve terminals. *Proc. Natl Acad. Sci. USA* **93,** 331–335 (1996).
30. Ringstad, N., Nemoto, Y. & De Camilli, P. The SH3p4/Sh3p8/SH3p13 protein family: binding partners for synaptojanin and dynamin via a Grb2-like Src homology 3 domain. *Proc. Natl Acad. Sci. USA* **94,** 8569–8574 (1997).

Acknowledgements. We thank Y. Nemoto for help in preliminary experiments, R. Bauerfeind and O. Cremona for advice, L. Daniell and M. Salazar for help with electron microscopy, X. Zhang for technical assistance and support, and M. M. Zhou for discussion. This work was supported in part by grants from the NIH, the HFSP and the US Army Medical Research and Development Command (to P.D.C.), and from the Associazione Italiana Ricerca sul Cancro, the Consiglio Nazionale delle Ricerche, the European Community (BIOMED-2 Programme), the Armenise-Harvard Foundation and the Ferrero Foundation (to P.P.D.F.).

Correspondence and requests for materials should be addressed to P.D.C. (e-mail: pietro.decamilli@yale.edu). The accession number for the rat epsin nucleotide and amino-acid sequences is AF018261 in GenBank.

Cell, Vol. 94, 131–141, July 10, 1998, Copyright ©1998 by Cell Press

Generation of Coated Intermediates of Clathrin-Mediated Endocytosis on Protein-Free Liposomes

Kohji Takei, Volker Haucke, Vladimir Slepnev, Khashayar Farsad, Marco Salazar, Hong Chen, and Pietro De Camilli*
Department of Cell Biology and Howard Hughes Medical Institute
Yale University School of Medicine
New Haven, Connecticut 06510

Summary

Clathrin-coated buds and dynamin-coated tubules morphologically similar to corresponding structures observed in synaptic membranes can be generated on protein-free liposomes by incubation with cytosol, or with clathrin coat proteins and purified dynamin, respectively. Dynamin- and clathrin-coated intermediates may form independently of each other, despite the coupling between the two processes typically observed in synaptic membranes. Formation of both structures on liposomes can occur in the absence of nucleotides. These findings indicate that interfaces between lipids and cytosolic proteins are fully sufficient to deform lipids bilayers into buds and tubules. They suggest that a main function of membrane proteins is to act as positive and negative regulators of coat assembly, therefore controlling these processes in time and space.

Introduction

In eukaryotic cells, anatomically distinct membranes are functionally connected to each other via vesicular transport. A fundamental basis for these processes is the property of intracellular membranes to generate vesicular buds enriched in selected cargo proteins, which then separate as free vesicles. Vesicle formation starts with the assembly on the donor membrane of a "coat," which acts as a scaffold both to bend the membrane and to select cargo membrane proteins (Pearse and Robinson, 1990; Rothman, 1994; Schekman and Orci, 1996). Several coats have been characterized. They include the COPI coat (Rothman, 1994), the COPII coat (Schekman and Orci, 1996), and the clathrin coats (Pearse and Robinson, 1990).

One of the most thoroughly investigated budding reactions is the formation of clathrin-coated vesicles from the plasmalemma. This process is implicated in a variety of cellular functions, including the internalization of receptors, the uptake of viruses (Mellman, 1996), and the recycling of synaptic vesicle membranes in nerve terminals (Heuser and Reese, 1973; Takei et al., 1996). While some of the protein isoforms that participate in clathrin-mediated endocytosis in nerve terminals are unique, the fundamental aspects of clathrin-mediated endocytosis appear to be highly conserved (De Camilli and Takei, 1996). Thus, clathrin-mediated recycling at the synapse has been a very useful model system to study molecular mechanisms in clathrin-mediated endocytosis.

Nerve terminal clathrin coats comprise, besides clathrin, the clathrin adaptor AP-2 (Robinson, 1994) and the protein AP180 (Ye and Lafer, 1991; Morris et al., 1993). Following formation of a deeply invaginated bud, the generation of a free vesicle is completed when oligomerization of dynamin I at the neck of the coated pit drives the fission reaction (Hinshaw and Schmid, 1995; Takei et al., 1995). A variety of other accessory cytosolic proteins have also been implicated in these processes. These include amphiphysin, synaptojanin I (Wang et al., 1995; David et al., 1996; McPherson et al., 1996; Bauerfeind et al., 1997; Ramjaun et al., 1997; Wigge et al., 1997), Eps15 (Benmerah et al., 1996; Di Fiore et al., 1997), and epsin (Chen et al., 1998). Several potential membrane binding proteins for AP-2–containing clathrin coats have been identified (Kirchhausen et al., 1997). Some of these proteins are nonobligatory passengers of clathrin-coated vesicles. However, a high affinity docking apparatus that plays an essential role in coat formation and contains a trypsin-sensitive site has also been postulated (Kirchhausen et al., 1997). The protein synaptotagmin was proposed to represent this site (Zhang et al., 1994).

In addition to protein–protein interactions, recent studies have suggested an important role of lipids in the recruitment of coats, including the clathrin coat. Both AP-2 and the protein AP180, which has the property of an accessory clathrin adaptor (Ye and Lafer, 1991; Morris et al., 1993), were found to bind phosphoinositides (Ye et al., 1995; Gaidarov et al., 1996). Furthermore, dynamin was shown to interact with membrane acidic phospholipids (Tuma et al., 1993; Liu et al., 1994) and to bind phosphoinositides via its PH domain (Lin et al., 1997). Together with results of other studies implicating lipids in vesicular traffic, these findings have raised the possibility that phospholipids may contribute to the membrane anchoring of "coats" either directly or via allosteric regulation of protein–protein interactions (De Camilli et al., 1996; Kirchhausen et al., 1997; Rapaport et al., 1997).

We have previously established a cell-free system that allows for the visualization of transient endocytic intermediates which participate in the clathrin-dependent reformation of synaptic vesicles (Takei et al., 1995, 1996). These intermediates consist of clathrin-coated pits that are often connected to donor membranes by a narrow tubular stalk decorated with dynamin rings (Takei et al., 1995). The goal of the present study was to determine whether specific synaptic membrane proteins play an essential role in the recruitment of the nerve terminal cytosolic endocytic apparatus. To this aim, we have tested the ability of brain cytosolic proteins to generate endocytic intermediates on a variety of non-neuronal membrane templates and have found that lipids alone can support the formation of clathrin-coated buds and dynamin-coated tubules.

*To whom correspondence should be addressed.

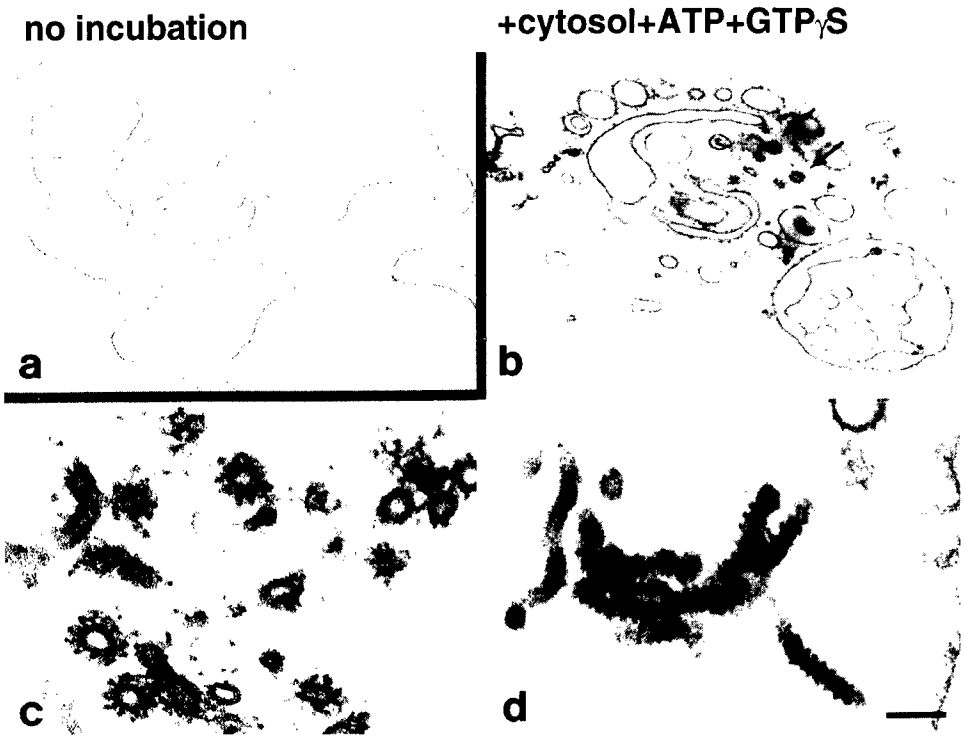

Figure 1. Electron Micrographs Demonstrating the Effects of Various Incubations on the Morphology of Inside-Out Erythrocyte Vesicles

Inside-out resealed vesicles are characterized by the presence of a submembranous cytomatrix at their external surface (a). Incubation of the membranes with rat brain cytosol, ATP, and GTPγS generated clathrin-coated buds ([b] [arrows] and [c]) and dynamin-coated tubules (d). Calibration bar, 400 nm in (a) and (b); 100 nm in (c) and (d).

Results

Brain Cytosol Generates Coated Endocytic Intermediates on Nonneuronal Plasma Membranes

We have previously shown that incubation of synaptic membranes with brain cytosol, ATP, and GTPγS (200 μM) results in the formation of numerous clathrin buds and dynamin-coated tubules (Takei et al., 1995, 1996). These endocytic structures are also positive for other nerve terminal proteins thought to have an accessory role in clathrin-mediated endocytosis, such as amphiphysin and synaptojanin (Bauerfeind et al., 1997; Haffner et al., 1997). When the same cell-free incubations were performed using CHO cell plasma membranes as templates, similar coated intermediates, positive for all of several cytosolic nerve terminal endocytic proteins tested, were generated (data not shown). We next used as templates plasma membranes that do not normally have any endocytic function and that are not expected therefore to contain intrinsic membrane proteins specialized for endocytosis: the plasma membrane of erythrocytes.

Erythrocyte membrane ghosts were processed under conditions that enhance formation of inside-out resealed plasmalemmal vesicles (Sulpice et al., 1994). These vesicles, which were recognizable by EM due to the presence of a residual submembranous cytoskeleton at their external surface, had a smooth profile (Figure 1a). Incubation with brain cytosol plus ATP and GTPγS produced a major morphological change, including the formation of numerous clathrin-coated pits and dynamin-coated tubules (Figures 1b–1d). Consistent with previous studies, ATP alone was sufficient to deform inside-out vesicles (data not shown), probably due to a rearrangement of the submembranous cytoskeleton (Morris et al., 1992). However, the presence of clathrin-coated pits and dynamin-coated tubules did not occur under these conditions.

These findings raised the possibility that specific docking proteins in the membrane may not be essential for the formation of clathrin- and dynamin-coated intermediates. They prompted us to perform similar experiments with protein-free liposomes.

Cytosol Generates Endocytic-like Coated Tubules and Buds on Liposomes

Liposomes prepared from a brain total lipid extract had smooth profiles and large diameters, some exceeding 1 μm (Figure 2a). Incubation with brain cytosol, ATP, and GTPγS resulted in a drastic morphological change with the massive formation of high curvature membrane profiles as seen by both thin sectioning and whole-mount preparations (Figures 2c and 2d). The more prominent change was the formation of dynamin-coated tubules (Figures 2d and 2e), but clathrin-coated buds were also observed (Figures 2d and 2f). At the level of resolution of thin section electron microscopy, these structures were morphologically identical to corresponding

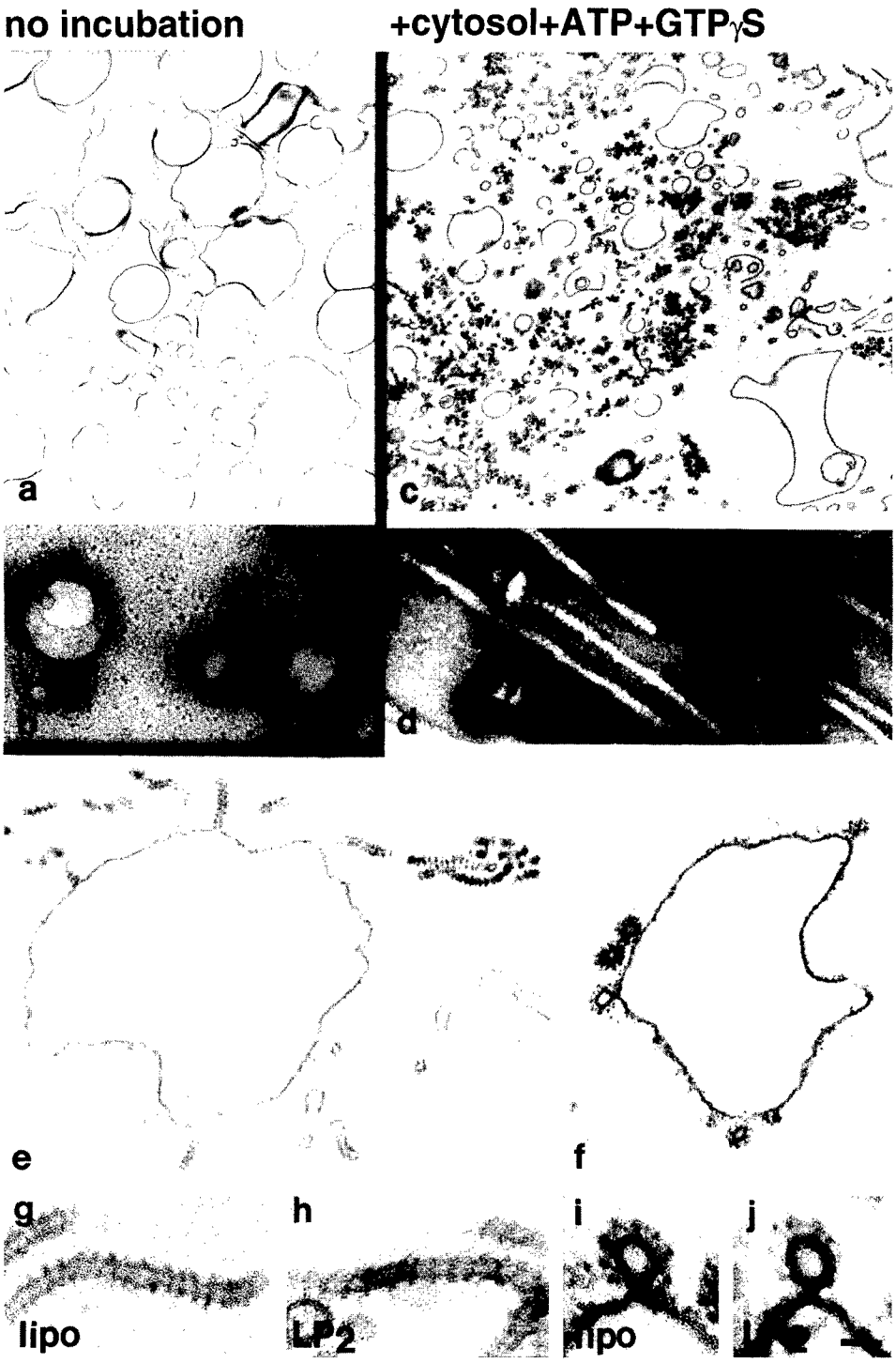

Figure 2. Electron Micrographs Demonstrating the Effect of Brain Cytosol on Liposomes Composed of Total Brain Lipids

Preparations were observed after plastic embedding and thin sectioning with the exception of fields (b) and (d), which show negative staining of whole-mount preparations. (a and b) Control liposomes not incubated with brain cytosol. (c–f) Liposomes incubated with ATP, GTPγS, and brain cytosol. High power observation reveals presence of dynamin-like rings and clathrin coats. Fields (g)–(j) demonstrate the similarity of dynamin-coated tubules and clathrin-coated pits observed on liposomes (lipo) and synaptic membranes (LP2 fraction) incubated with brain cytosol, ATP, and GTPγS. Calibration bar, 500 nm in (a) and (c); 140 nm in (b) and (d); 150 nm in (e) and (f); and 50 nm in (g)–(j).

endocytic intermediates observed in synaptic membranes (LP2 subfractions) incubated under the same conditions (Figures 2g–2j). However, tubules were much more abundant in liposomes, while the number of clathrin-coated pits in these preparations was lower than in synaptic membranes (data not shown). Furthermore, negative staining observations revealed that the majority of the dynamin-coated tubules present in the

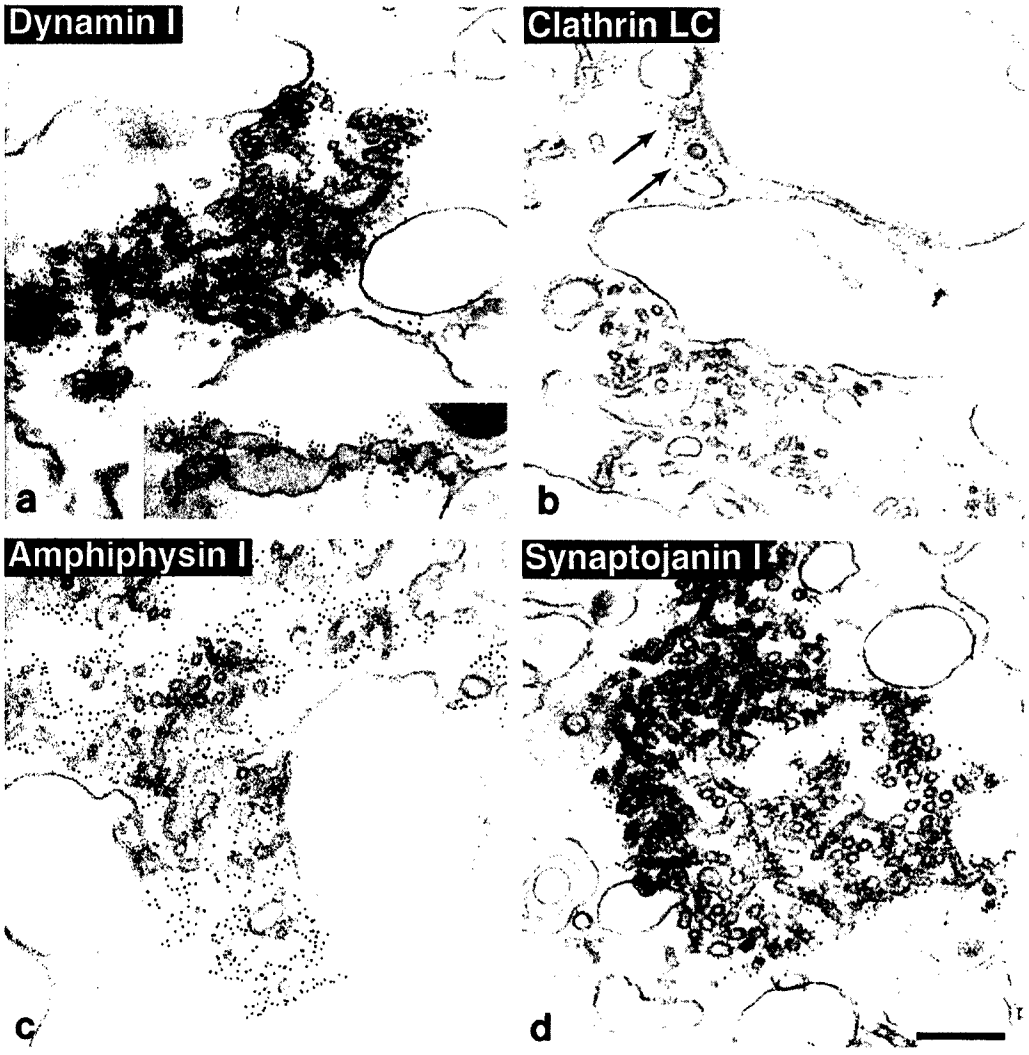

Figure 3. Immunogold Localization of Cytosolic Endocytic Proteins on Liposomes of Total Brain Lipids Incubated with Cytosol, ATP, and GTPγS

Dynamin I and clathrin are concentrated at tubules and buds (arrows in [b]), respectively. Note the concentration of dynamin at sites of liposome constriction in the inset of field (a). Amphiphysin I (c) and synaptojanin I (d) are also concentrated on the coated evaginations. Calibration bar, 200 nm.

liposomes were not capped by a clathrin coat (for example, see Figure 2d). Interestingly, clathrin-coated buds occurred in clusters as though assembly of these buds was a cooperative process.

To confirm that the coats were represented by dynamin and clathrin, we performed electron microscopy immunogold cytochemistry. As shown in Figures 3a and 3b, coated tubules and pits were intensely positive for dynamin I and clathrin immunoreactivity, respectively. Amphiphysin I and synaptojanin I were also concentrated on coated liposomal surfaces (Figures 3c and 3d), consistent with their accessory role in dynamin I action (Bauerfeind et al., 1997; Haffner et al., 1997).

Given the relatively low number of clathrin-coated pits visible in these preparations, we tested the effect of a brain protein extract highly enriched in clathrin coats, which we obtained by stripping purified bovine brain clathrin-coated vesicles (Figure 4a and 4b). Addition of the coat protein fraction to liposomes in the presence of ATP plus GTPγS resulted in a massive formation of clathrin-coated membrane profiles, most of which (and possibly all) were represented by coated pits (Figure 4c, field i). The number of clathrin-coated profiles in these preparations was more than 100-fold higher than on liposomes incubated with total brain cytosol. No dynamin-coated tubules were visible after these incubations, consistent with the very low amount of dynamin present in the coat fraction (see Figure 4b). However, several dynamin-coated tubules capped by clathrin-coated pits were observed when unfractionated brain cytosol, which contains endogenous dynamin, was added to the coat fraction (Figure 4c, field ii). Under these conditions a lower number of clathrin-coated pits was observed, as if dynamin tubulation competed with clathrin-coated pit formation.

To gain some initial insight into the lipid requirement

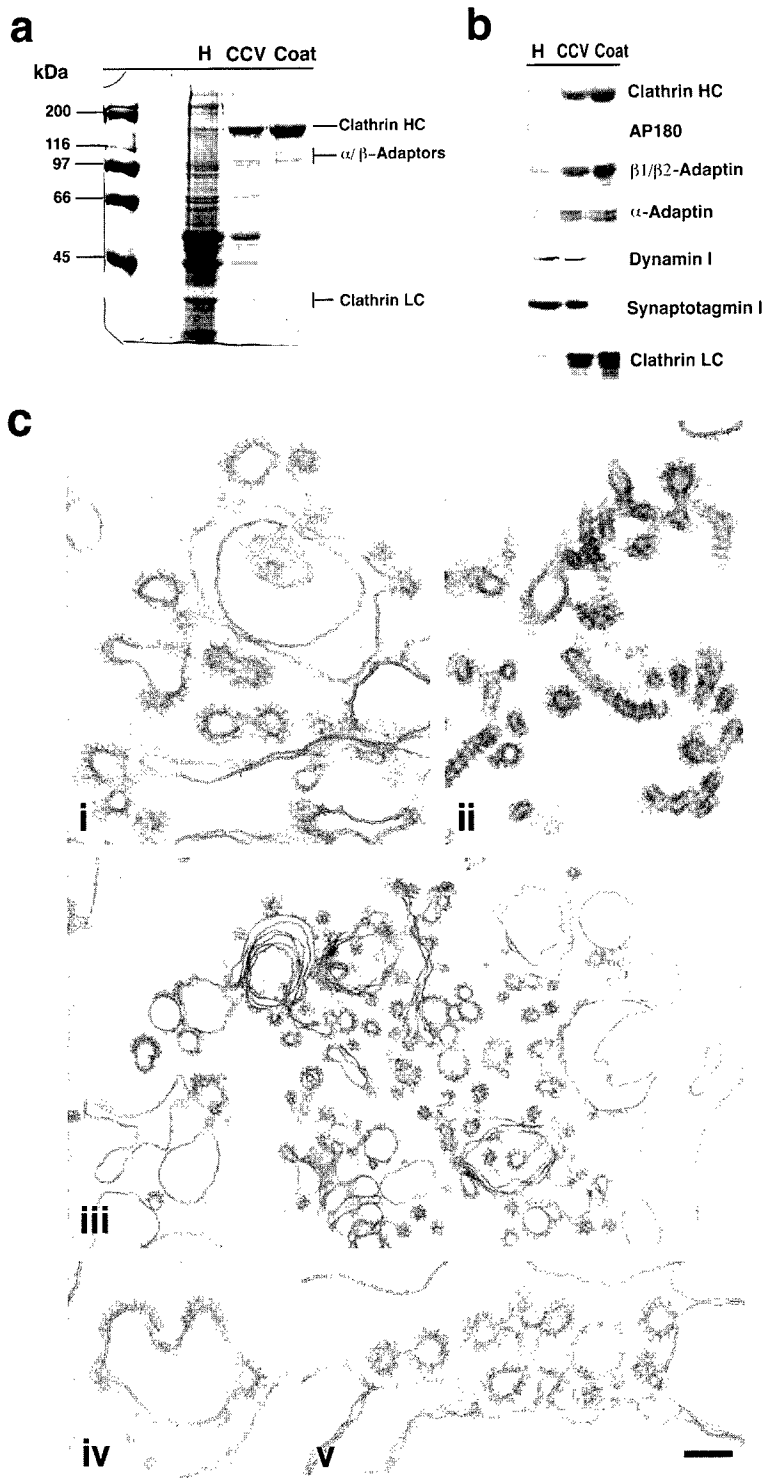

Figure 4. A Clathrin Coat Fraction Induces Massive Formation of Clathrin Coats on Liposomes Irrespective of the Presence of Nucleotides

(a) Preparation of a highly enriched clathrin coat fraction from bovine brain. Total brain homogenate (H; 50 μg protein), clathrin-coated vesicles (CCV), and the final coat protein fraction (coat; 30 μg protein each) were analyzed by SDS-PAGE followed by Coomassie blue staining.

(b) Western blot analysis of the samples shown in (a). Fifty micrograms of proteins were loaded in each lane. Blots were developed by ^{125}I-based autoradiography. Note the absence of synaptotagmin, a membrane marker, in the coat fraction.

(c) Electron micrographs of liposomes of total brain lipids after incubation with the coat fraction. (i) Liposomes incubated in the presence of coat fraction, ATP, and GTPγS. (ii) Liposomes incubated with total brain cytosol supplemented by the coat fraction in the presence of ATP and GTPγS. (iii–v) Liposomes incubated with the coat fraction without added nucleotides and in the presence of an ATP-depleting system. Calibration bar, 100 nm in (i), (ii), (iv), and (v); 180 nm in (iii).

of these coating reactions, total brain cytosol was incubated in the presence of ATP plus GTPγS with liposomes of defined lipid composition. These liposomes contained a basic mixture comprising 20% each of cholesterol, phosphatidylcholine, phosphatidylethanolamine (PE), and phosphatidylserine (PS), and an additional 20% of one of the following phospholipids: phosphatidylinositol (PI), a phosphoinositide mixture (PIs), PE, PS, phosphatidyl glycerol (PG), or phosphatidic acid (PA) (Figure 5a). Dynamin-coated tubule formation, as detected by electron microscopic observation and morphometry, was the highest in PA supplemented liposomes followed, in order of decreasing abundance, by PG, PIs, PI, PS, and PE (Figure 5b). In contrast, the highest number of clathrin-coated pits was observed in PE supplemented liposomes (Figure 5c). Biochemical

a. Compositions of defined liposomes

components \ liposomes	PI	PIs	PE	PS	PG	PA
cholesterol	20 %	20 %	20 %	20 %	20 %	20 %
phosphatidylchorine	20 %	20 %	20 %	20 %	20 %	20 %
Phosphatidylethanolamine	20 %	20 %	40 %	20 %	20 %	20 %
Phosphatidylserine	20 %	20 %	20 %	40 %	20 %	20 %
phosphatidylinositol	20 %					
phosphoinositide mixture		20 %				
Phosphatidylglycerol					20 %	
Phosphatidic acid						20 %

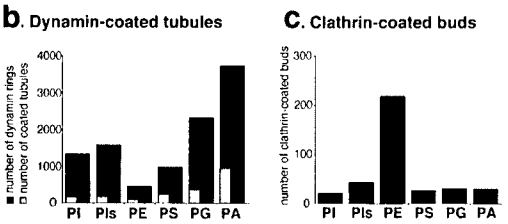

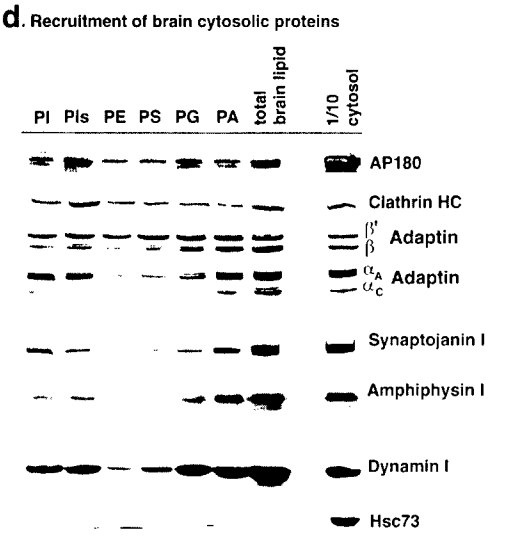

Figure 5. Effect of Phospholipids on Coat Recruitment

(a) Compositions of the lipid mixtures used for the following morphometric (b and c) and biochemical analysis (d).

(b and c) Morphometric analysis of the formation of dynamin-coated tubules and clathrin-coated pits in liposomes of defined compositions incubated with brain cytosol, ATP, and GTPγS. (b) Total number of longitudinal tubular profiles as well as total number of dynamin rings in a total thin section area of 6×10^4 μm². The total number of rings represents an estimate derived by multiplying the number of tubules by the average number of rings. (c) Total number of coated pits counted over the same area analyzed for dynamin-coated tubules.

(d) Western blots illustrating the recruitment of endocytic proteins onto liposomes. After incubation of liposomes with brain cytosol, ATP, and GTPγS, bound protein was analyzed. One-tenth of the amount of cytosol added to the liposomes was run in the right lane.

analysis of the property of various liposomes to recruit dynamin was in good agreement with the electron microscopic results (Figure 5d). Dynamin recruitment was the highest with total brain liposomes, lower in PA, PG, PI, and PIs supplemented liposomes, and even lower in PS and PE supplemented liposomes. Qualitatively similar results were observed for synaptojanin I and amphiphysin I. In contrast, no correlation was found between lipid binding of intrinsic components of the clathrin coat (AP180, the AP-2 subunit α-adaptin and clathrin) and the presence of clathrin-coated pits, suggesting that at least a fraction of these proteins bind to membranes (either directly or indirectly) independently and irrespective of coat assembly (Figure 5d).

Coated Tubules and Buds Can Form in the Absence of Nucleotides

Brain cytosol produced a massive tubulation of liposomes even in the absence of nucleotides. Tubules formed under these conditions were somewhat different from those formed in the presence of ATP and GTPγS (Figure 6, compare fields [a] and [d]). They were slightly variable in diameter, and their wall was only sparsely decorated by dynamin rings. A morphology similar to that produced by cytosol alone was observed with liposomes incubated with cytosol plus ATP (data not shown). Surprisingly, tubules with a patchy irregular coat were observed even in the presence of ATP plus GTP (200 μM) (Figure 6c) or in liposomes that had been incubated for 10 min with brain cytosol, ATP, and 200 μM GTPγS, and then supplemented with an excess of GTP (10-fold molar excess to GTPγS) for an additional 10 min to reverse the effect of GTPγS (data not shown). Previous studies of synaptic membranes had shown that tubules did not form if 200 μM GTPγS was replaced with 200 μM GTP (Takei et al., 1996). However, tubules that resemble in morphology the tubules generated by brain cytosol on liposomes in the presence of GTP were previously described at synapses fixed in situ (Heuser and Miledi, 1971; Lovas, 1971; Hama and Saito, 1977), and a few examples of such tubules can be observed in intact synaptosomes (Figure 6e). The connection of these tubules to clathrin had suggested their endocytic nature (Heuser and Miledi, 1971; Lovas, 1971; Hama and Saito, 1977). Thus, tubule formation in the presence of GTP may reflect a phenomenon that occurs physiologically at least under certain conditions.

Despite their different morphology, the tubules observed after all the various incubation conditions were positive for dynamin I, synaptojanin I, and amphiphysin I (Figure 6b and data not shown). Likewise, tubules occasionally observed at synapses in situ were also positive for these proteins (Figures 6f and 6g).

As in the case of dynamin-coated tubules, generation of clathrin-coated buds on liposomes did not require nucleotides. The massive formation of clathrin-coated buds on liposomes incubated with the coat fraction and in the presence of an ATP-depleting system is shown in Figure 4c (fields iii–v).

Dynamin-Coated Tubules Can Form Independently of Clathrin-Coated Buds

It has been speculated that dynamin-coated tubules may result from the progressive polymerization of dynamin at the neck of clathrin-coated buds (De Camilli

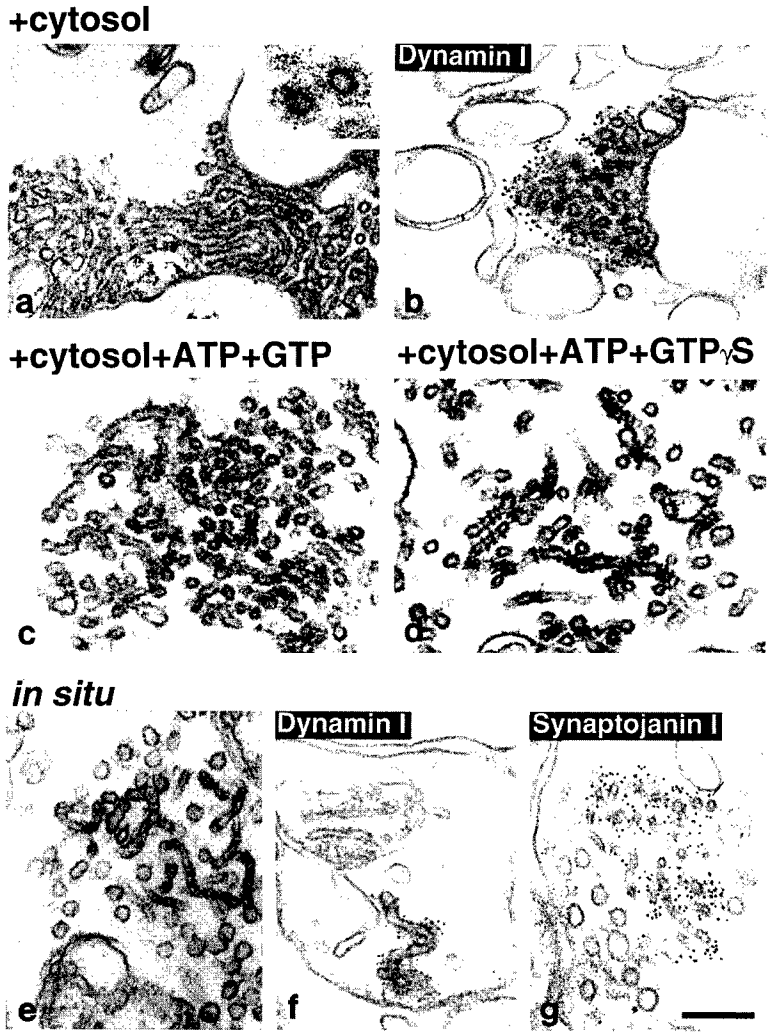

Figure 6. Brain Cytosol Tubulates Liposomes Irrespective of the Presence of Nucleotides

Liposomes of total brain lipids were incubated with cytosol in the absence of nucleotides (fields [a] and [b]), with cytosol plus ATP and GTP (field [c]), or with cytosol plus ATP and GTPγS (field [d]). The inset of field (a) shows clathrin-coated vesicular profiles. Field (b) shows liposomes immunolabeled for dynamin I and demonstrates that the surfaces of the tubules accessible to gold are heavily labeled. Tubules generated in the absence or presence of GTPγS have a similar diameter but regularly spaced dynamin rings are visible only in GTPγS reacted preparations. (e–g) Electron micrographs demonstrating that dynamin-coated tubular structures can occasionally be seen in synaptosomes not subjected to any cell-free incubation. (e) Freshly prepared intact synaptosome. (f and g) Broken synaptosomes immunolabeled for dynamin I (f) and synaptojanin I (g). Calibration bars, 200 nm; 100 nm, inset of (a).

and Takei, 1996). As mentioned above (Figure 2), however, many of the dynamin-coated tubules generated by total brain cytosol on liposomes (irrespective of the nucleotide condition) were not capped by clathrin coats. This finding can be explained either by clathrin-independent tubule formation or by dissociation of the clathrin coat after tubules have started to grow. We therefore tested the effect of purified recombinant dynamin I on liposomes in the absence of other cytosolic proteins and found that purified dynamin alone could tubulate liposomes both in the absence or in the presence of guanylnucleotides (200 μM GTP or GTPγS) (Figure 7). We conclude that the generation of a vesicular bud is not an essential prerequisite for tubule formation. As observed for total brain cytosol (see above), tubules generated in the presence of GTP were shorter, with a less regular diameter. Furthermore, they were often interspersed with small vesicular structures (Figure 7b). These observations suggest the occurrence of both tubule growth and tubule fragmentation under these conditions.

Discussion

Our results demonstrate that the cytosolic endocytic apparatus responsible for clathrin- and dynamin-mediated endocytosis can assemble on liposomes. Thus, the deformation of a lipid membrane by coat proteins does not require the presence of protein anchors within the lipid bilayer. Molecular interfaces between cytosolic proteins and lipids appear to be fully sufficient to generate both clathrin-coated pits and dynamin-coated tubules morphologically identical to corresponding structures observed in situ.

Specific membrane proteins have been implicated in the recruitment of clathrin coats to membranes (Moore et al., 1987; Kirchhausen et al., 1997). Our results imply that protein binding sites do not play an essential role in the formation of endocytic structures but act only as facilitators of coat recruitment. The much higher abundance of clathrin-coated pits generated by total brain cytosol on synaptic membrane fractions (LP2 fractions) (Takei et al., 1995, 1996) than on liposomes is consistent

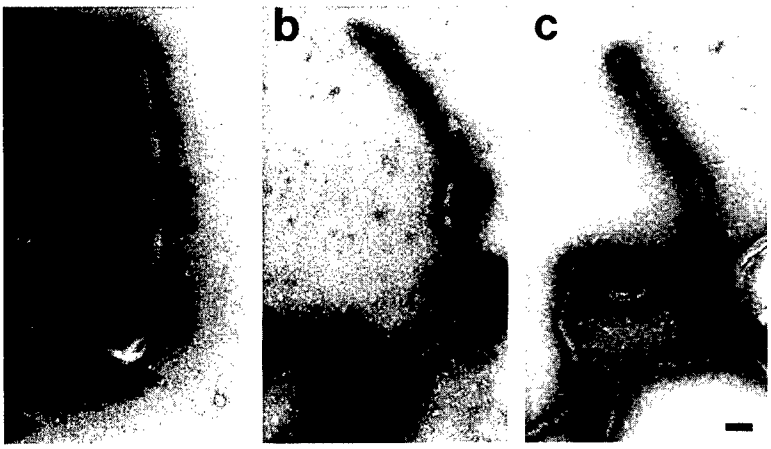

Figure 7. Electron Micrographs Demonstrating Tubulation of Liposomes by Purified Dynamin

Liposomes of total brain lipids were incubated with purified dynamin in the absence of nucleotides (a) or in the presence of either 200 μM GTP (b) or 200 μM GTPγS (c). Tubulation is visible in all conditions. Note in the GTP condition the less regular profile of the tubule and the presence of small liposomal fragments. Calibration bar, 100 nm.

with the possibility that the abundant synaptic protein synaptotagmin (Zhang et al., 1994) acts as a major facilitator in clathrin coat recruitment at the synapse.

Dynamin-mediated tubulation was strikingly more prominent in liposomes than in synaptic membranes. A scaffold of membrane proteins may inhibit dynamin binding or hinder tubulation in biological membranes. Unexpectedly, dynamin-mediated tubulation of lipid bilayers neither requires any cofactor nor the previous formation of a bud neck. Thus, dynamin alone is sufficient to evaginate a low curvature membrane into a tubule. Similar findings were reported by Sweitzer and Hinshaw (1998). Thus, the direct and indirect interactions between dynamin and components of the clathrin coat (Wang et al., 1995; David et al., 1996; McMahon et al., 1997; Ramjaun et al., 1997), which may account for the efficient coupling between clathrin coat formation and dynamin ring oligomerization, do not preclude independent actions of dynamin. Accordingly, it was recently shown that dynamin is implicated in the internalization of caveolae, a clathrin-independent process (Henley et al., 1998; Oh et al., 1998).

Experiments with brain cytosol demonstrated a striking preference of dynamin for acidic phospholipids, in agreement with previously reported biochemical studies of dynamin–phospholipid interactions (Tuma et al., 1993). Furthermore, they showed that phosphoinositides were not required for tubulation despite the presence of a PH domain in dynamin (Lin et al., 1997). Tubule formation appeared to have an antagonistic effect on clathrin-coated pit formation (possibly by sequestering acidic phospholipids or protein factors), and the relative abundance of clathrin-coated pits in PE enriched liposomes compared to other liposomes may reflect this effect.

The formation of clathrin- and dynamin-coated structures on liposomes did not require ATP. ATP independence was previously shown for the self-assembly of clathrin cages, of clathrin-adaptor coats, and of dynamin rings in the absence of membrane templates (Zaremba and Keen, 1983; Keen, 1987; Morris et al., 1989; Pearse and Robinson, 1990). However, studies of the ATP dependence of clathrin-coated pit formation have yielded conflicting results (Moore et al., 1987; Schmid and Carter, 1990; Schmid, 1993). Our findings suggest that oligomerization of clathrin coats and dynamin rings are energy-independent processes, at least under cell-free conditions, irrespective of whether they occur in solution or on a protein-free lipid bilayer. An ATP requirement of clathrin coat assembly on cell membranes could be explained by ATP-dependent reactions that play an accessory role in clathrin coat assembly, such as the release of membrane-associated proteins or the modification of membrane lipids.

Finally, we have shown that liposomes can be tubulated by purified dynamin or cytosol in vitro irrespective of the nucleotide condition. No tubules were previously observed in synaptic membranes reacted with 200 μM GTP (Takei et al., 1996). Tubules, however, could be formed at the same GTP concentration on liposomes. In the presence of 200 μM GTP, tubules were shorter than in other nucleotide conditions, had an irregular profile, and, as shown by experiments with purified dynamin I, coexisted with vesicular fragments, suggesting a coexistence of tubular growth and fragmentation. A direct demonstration that dynamin can act as a GTP-dependent mechanochemical enzyme that cleaves lipid tubules is reported in the independent study by Sweitzer and Hinshaw (1998). These authors show that the tubule-severing activity of dynamin increases in parallel with the concentration of GTP, with a massive effect at 1 mM GTP. The fission reaction is likely to be dependent upon a synchronous conformational change of all dynamin subunits within a ring. Accessory factors present in cell membranes may assist the synchronous disassembly of dynamin rings at physiological concentrations of GTP. At least in some cases, however, dynamin-coated tubules appear to represent physiologically occurring endocytic intermediates (Heuser and Miledi, 1971; Lovas, 1971; Hama and Saito, 1977; Willingham and Pastan, 1983).

The massive predominance of structures coated by clathrin and dynamin in liposomes reacted with total brain cytosol most likely reflects the extremely high concentration in brain of cytosolic components implicated in synaptic vesicle endocytosis. It is possible, however, that some of the clathrin-coated buds visible in our preparations may be generated by Golgi complex– or endosome-derived clathrin coats. Furthermore, some vesicle buds decorated by nonclathrin coats were present in liposomes incubated with total cytosol and nucleotides (data not shown), suggesting that the property of coats

to assemble on liposomes may be general. This is consistent with the report that COPII-mediated budding can be reconstituted in vitro with purified coat proteins, liposomes, and nucleotides (Matsuoka et al., 1998).

Clearly, coat assembly in vivo occurs with a high degree of spatial and temporal specificity. This layer of specificity must be mediated by intrinsic membrane proteins either via protein–protein interactions or via short range modifications of the lipid environment.

Experimental Procedures

Reagents

Polyclonal and monoclonal antibodies against amphiphysin I and synaptojanin I were raised in our laboratory (David et al., 1994; Butler et al., 1997; Haffner et al., 1997). Other monoclonal antibodies were obtained from the following sources: anti-neuronal clathrin light chain (CI 57.1) and anti-β/β'-adaptin (C420 10A) from Dr. Reinhard Jahn (Göttingen, Germany) and Dr. Thomas Kirchhausen (Boston, MA), respectively; anti-clathrin heavy chain (TD.1) from ATCC (Nathke et al., 1992); anti-dynamin (Hudy-1) from UBI (Lake Placid, NY); anti-α-adaptin (AC1-MC11) from Affinity BioReagents Inc. (Golden, CO); anti-HSC73 (715) from StressGen Biotechnologies Corp. (Victria, BC, Canada); and anti-AP180 from Sigma (St. Louis, MO). Six nanometer protein A-gold conjugates were prepared as described (Slot and Geuze, 1985). Bovine brain lipid extract and phosphoinositides were purchased from Sigma (St. Louis, MO); the remaining lipids were acquired from Avanti Polar Lipids (Alabaster, AL).

Inside-Out Erythrocyte Vesicles

Erythrocyte membrane vesicles were prepared from human blood as described (Sulpice et al., 1994).

Liposomes

Large liposomes were prepared as described (Reeves and Dowben, 1969) with some modifications. Lipids solubilized in a chloroform/methanol (1:2) mixture were dried in a rotary evaporator and then hydrated by a stream of water-saturated nitrogen for 20 min. After gently adding degassed 0.3 M sucrose, the flask was flushed with nitrogen, sealed, and left undisturbed for 2 hr at 37°C to allow spontaneous formation of liposomes. The liposomes were recovered by centrifugation at 12,000 × g for 10 min and resuspended in cytosolic buffer (see below) prior to cell-free incubation.

Brain Cytosol

A fraction containing diluted cytosol was prepared from fresh or frozen rat brain by high speed centrifugation as described (Huttner et al., 1983; Takei et al., 1996). The fraction was desalted and concentrated by amonium sulfate precipitation and dialysis as described (Malhotra et al., 1989).

Coat Proteins

Clathrin-coated vesicles were prepared from four fresh calf brains as described (Campbell et al., 1984; Heilker et al., 1996). Coat proteins were extracted from the coated vesicles with a buffer containing 0.8 M Tris-Cl (pH 7.4), 2 mM EGTA, 0.03% sodium azide, 0.5 mM DTT, 1 mM PMSF for 15 hr at room temperature (modified from Keen et al., 1979). The soluble coat protein containing supernatant was separated from stripped vesicles and other membrane contaminants by centrifugation at 100,000 × g for 1 hr at room temperature. Coat proteins were either used directly or frozen in liquid nitrogen and stored at −70°C.

Preparation of Purified Dynamin

Human dynamin (Urrutia et al., 1997) was produced as a GST fusion protein using a modified Bac-to-Bac baculovirus expression system (GIBCO BRL). A cDNA encoding GST followed by a cleavage site for PreScission protease (Pharmacia) was inserted into pFastBAC1 baculovirus transfer vector (GIBCO BRL). Dynamin 1aa cDNA without the starting methionine was cloned into this vector downstream to the cleavage site. A recombinant virus was produced, amplified, and used to infect insect Tn cells for 48 hr in 1 l spinner cultures. Glutathione-Sepharose 4B affinity-purification of the fusion protein from cell lysates and removal of GST by PreScission protease (Pharmacia) were performed according to manufacturer's protocols. The purity of dynamin in the final material was estimated to be more than 90%, and its GTPase activity was validated using the EnzChek phosphate assay kit (Molecular Probes).

Cell-Free Incubations

Morphological Experiments

Erythrocyte vesicles at a protein concentration of 5 mg/ml or liposomes at a concentration of 1 mg of lipid/ml were incubated in 1 ml of cytosolic buffer (25 mM HEPES-KOH [pH 7.4], 25 mM KCl, 2.5 mM magnesium acetate, 150 mM K-glutamate) with or without "cytosol" (6 mg/ml), coat fraction (0.5 mg/ml), purified dynamin (0.1 mg/ml), various nucleotides as indicated, and either 10 μM Ca^{2+} or 2 mM EGTA (no obvious morphological differences were observed in number or type of coat structures obtained in the absence or presence of Ca^{2+}). Final concentrations of nucleotides were 2 mM ATP, 200 μM GTP, and 200 μM GTPγS. Samples containing ATP were also supplemented with an ATP regenerating system consisting of 16.7 mM creatine phosphate and 16.7 IU/ml creatine phosphokinase. In some of the no-nucleotides samples, an ATP-depleting system consisting of 5 U/ml of hexokinase and 10 mM glucose was used. These mixtures were incubated for 15 min at 37°C, and incubations were stopped by the addition of 1 ml 2× concentrated fixative (see below).

Biochemical Experiments

Liposomes were tagged with the lipophilic dye 1,6 diphenyl-1,3,5-hexatriene (DPH) and incubated under the same conditions described above with the exception that only 1/5 of the material was used for each sample in a total volume of 0.2 ml. At the end of the incubation, liposomes were loaded on 0.5 M sucrose and centrifuged at 120,000 × g in a Beckman TLA100.2 rotor for 30 min at 4°C to separate bound proteins from unbound proteins. Liposomes were recovered in the pellet, and the recovery was assessed using an Hitachi F-3010 fluorescence spectrophotometer by monitoring the emitted fluorescence at 430 nm upon excitation at 360 nm. Equal amounts of the recovered liposomes were analyzed by SDS-PAGE and Western blotting as described (Bauerfeind et al., 1997). Western blots were performed with ^{125}I-protein A for amphiphysin I and dynamin I, and with horseradish peroxidase followed by visualization with 4-chloro-1-naphthol for the other proteins.

Electron Microscopy

For standard electron microscopy, incubation mixtures were fixed in suspension with 3% formaldehyde, 2% glutaraldehyde in 50 mM HEPES-KOH buffer (pH 7.4), pelleted in an Eppendorf centrifuge, and postfixed in OsO_4. In some samples, OsO_4 postfixation was followed by impregnation with 0.2% tannic acid to enhance visualization of membrane coats (Orci et al., 1986). For immunoelectron microscopy, liposomes or synaptic membranes were fixed and labeled as described (Takei et al., 1996). For whole-mount observation, liposomes were first incubated with proteins or cytosol in suspension and then absorbed onto Formvar-coated EM grids pretreated with poly-L-lysine. The samples were fixed with 3% formaldehyde, 2% glutaraldehyde and negatively stained with 2% uranyl acetate.

Morphometry

The number of dynamin- and clathrin-coated profiles on liposomes of defined lipid composition was determined by visually scanning a large area of ultrathin sections (6×10^4 μm^2) at the electron microscope for the presence of longitudinal profiles of dynamin-coated tubules and clathrin-coated pits, respectively. The average number of dynamin rings on the entire length of a continuous tubular profile was calculated by counting the number of rings on 100 tubular profiles for each sample. Considering the regular periodic arrangements of the dynamin rings, this value reflects very closely the length of the tubular profile in the plane of section. The total number of dynamin rings present in the area examined was estimated by multiplying the number of the coated tubules by the average number of dynamin rings.

Acknowledgments

We thank Laurie Daniell for technical assistance, Dr. Thomas Kirchhausen for helpful discussion and advice, Dr. Sandra Schmid for the human dynamin I clone, and Dr. Ruth Collins for the gift of Tn cells. This work was supported in part by grants from the National Institutes of Health (NS36251 and CA46128) and the United States Army Medical Research and Development Command to P. D. C. and fellowships from the European Molecular Biology Organization and the Human Frontier Science Program to V. H.

Received March 12, 1998; revised June 3, 1998.

References

Bauerfeind, R., Takei, K., and De Camilli, P. (1997). Amphiphysin I is associated with coated endocytic intermediates and undergoes stimulation-dependent dephosphorylation in nerve terminals. J. Biol. Chem. *272*, 30984–30992.

Benmerah, A., Begue, B., Dautry-Varsat, A., and Cerf-Bensussan, N. (1996). The ear of alpha-adaptin interacts with the COOH-terminal domain of the Eps 15 protein. J. Biol. Chem. *271*, 12111–12116.

Butler, M.H., David, C., Ochoa, G.C., Freyberg, Z., Daniell, L., Grabs, D., Cremona, O., and De Camilli, P. (1997). Amphiphysin II (SH3P9; BIN1), a member of the amphiphysin/Rvs family, is concentrated in the cortical cytomatrix of axon initial segments and nodes of ranvier in brain and around T tubules in skeletal muscle. J. Cell Biol. *137*, 1355–1367.

Campbell, C., Squicciarini, J., Shia, M., Pilch, P.F., and Fine, R.E. (1984). Identification of a protein kinase as an intrinsic component of rat liver coated vesicles. Biochemistry *23*, 4420–4426.

Chen, H., Fre, S., Slepnev, V.I., Capua, M.R., Takei, K., Butler, M.H., Di Fiore, P.P., and De Camilli, P. (1998). Epsin, an EH domain binding protein implicated in clathrin-mediated endocytosis. Nature, in press.

David, C., Solimena, M., and De Camilli, P. (1994). Autoimmunity in stiff-Man syndrome with breast cancer is targeted to the C-terminal region of human amphiphysin, a protein similar to the yeast proteins, Rvs167 and Rvs161. FEBS Lett. *351*, 73–79.

David, C., McPherson, P.S., Mundigl, O., and de Camilli, P. (1996). A role of amphiphysin in synaptic vesicle endocytosis suggested by its binding to dynamin in nerve terminals. Proc. Natl. Acad. Sci. USA *93*, 331–335.

De Camilli, P., and Takei, K. (1996). Molecular mechanisms in synaptic vesicle endocytosis and recycling. Neuron *16*, 481–486.

De Camilli, P., Emr, S.D., McPherson, P.S., and Novick, P. (1996). Phosphoinositides as regulators in membrane traffic. Science *271*, 1533–1539.

Di Fiore, P.P., Pelicci, P.G., and Sorkin, A. (1997). EH: a novel protein-protein interaction domain potentially involved in intracellular sorting. Trends Biochem. Sci. *22*, 411–413.

Gaidarov, I., Chen, Q., Falck, J.R., Reddy, K.K., and Keen, J.H. (1996). A functional phosphatidylinositol 3,4,5-trisphosphate/phosphoinositide binding domain in the clathrin adaptor AP-2 alpha subunit. J. Biol. Chem. *271*, 20922–20929.

Haffner, C., Takei, K., Chen, H., Ringstad, N., Hudson, A., Butler, M.H., Salcini, A.E., Di Fiore, P.P., and De Camilli, P. (1997). Synaptojanin 1: localization on coated endocytic intermediates in nerve terminals and interaction of its 170 kDa isoform with Eps15. FEBS Lett. *419*, 175–180.

Hama, K., and Saito, K. (1977). Fine structure of the afferent synapse of the hair cells in the saccular macula of the goldfish, with special reference to the anastomosing tubules. J. Neurocytol. *6*, 361–373.

Heilker, R., Manning-Krieg, U., Zuber, J.F., and Spiess, M. (1996). In vitro binding of clathrin adaptors to sorting signals correlates with endocytosis and basolateral sorting. EMBO J. *15*, 2893–2899.

Henley, J.R., Krueger, E.W.A., Oswald, B.J., and McNiven, M.A. (1998). Dynamin-mediated internalization of caveolae. J. Cell Biol. *141*, 85–99.

Heuser, J., and Miledi, R. (1971). Effects of lanthanum ions on function and structure of frog neuromuscular junctions. Proc. R Soc. Lond. B Biol. Sci. *179*, 247–260.

Heuser, J.E., and Reese, T.S. (1973). Evidence for recycling of synaptic vesicle membrane during transmitter release at the frog neuromuscular junction. J. Cell Biol. *57*, 315–344.

Hinshaw, J.E., and Schmid, S.L. (1995). Dynamin self-assembles into rings suggesting a mechanism for coated vesicle budding. Nature *374*, 190–192.

Huttner, W.B., Schiebler, W., Greengard, P., and De Camilli, P. (1983). Synapsin I (protein I), a nerve terminal-specific phosphoprotein. J. Cell Biol. *96*, 1374–1388.

Keen, J.H. (1987). Clathrin assembly proteins: affinity purification and a model for coat assembly. J. Cell Biol. *105*, 1989–1998.

Keen, J.H., Willingham, M.C., and Pastan, I.H. (1979). Clathrin-coated vesicles: isolation, dissociation and factor-dependent reassociation of clathrin baskets. Cell *16*, 303–312.

Kirchhausen, T., Bonifacino, J.S., and Riezman, H. (1997). Linking cargo to vesicle formation: receptor tail interactions with coat proteins. Curr. Opin. Cell Biol. *9*, 488–495.

Lin, H.C., Barylko, B., Achiriloaie, M., and Albanesi, J.P. (1997). Phosphatidylinositol (4,5)-bisphosphate-dependent activation of dynamins I and II lacking the proline/arginine-rich domains. J. Biol. Chem. *272*, 25999–26004.

Liu, J.P., Powell, K.A., Sudhof, T.C., and Robinson, P.J. (1994). Dynamin I is a Ca(2+)-sensitive phospholipid-binding protein with very high affinity for protein kinase C. J. Biol. Chem. *269*, 21043–21050.

Lovas, B. (1971). Tubular networks in the terminal endings of the visual receptor cells in the human, the monkey, the cat and dog. Z. Zellforsch *121*, 341–357.

Malhotra, V., Serafini, T., Orci, L., Shepherd, J.C., and Rothman, J.E. (1989). Purification of a novel class of coated vesicles mediating biosynthetic protein transport through the Golgi stack. Cell *58*, 329–336.

Matsuoka, K., Orci, L., Amherdt, M., Bednarek, S.Y., Hamamoto, S., Schekman, R., and Yeung, T. (1998). COPII-coated vesicle formation reconstituted with purified coat proteins and chemically defined liposomes. Cell *93*, 263–275.

McMahon, H.T., Wigge, P., and Smith, C. (1997). Clathrin interacts specifically with amphiphysin and is displaced by dynamin. FEBS Lett. *413*, 319–322.

McPherson, P.S., Garcia, E.P., Slepnev, V.I., David, C., Zhang, X., Grabs, D., Sossin, W.S., Bauerfeind, R., Nemoto, Y., and De Camilli, P. (1996). A presynaptic inositol-5-phosphatase. Nature *379*, 353–357.

Mellman, I. (1996). Endocytosis and molecular sorting. Annu. Rev. Cell Dev. Biol. *12*, 575–625.

Moore, M.S., Mahaffey, D.T., Brodsky, F.M., and Anderson, R.G. (1987). Assembly of clathrin-coated pits onto purified plasma membranes. Science *236*, 558–563.

Morris, S.A., Ahle, S., and Ungewickell, E. (1989). Clathrin-coated vesicles. Curr. Opin. Cell Biol. *1*, 684–690.

Morris, M.B., Monteith, G., and Roufogalis, B.D. (1992). The inhibition of ATP-dependent shape change of human erythrocyte ghosts correlates with an inhibition of Mg(2+)-ATPase activity by fluoride and aluminofluoride complexes. J. Cell. Biochem. *48*, 356–366.

Morris, S.A., Schroder, S., Plessmann, U., Weber, K., and Ungewickell, E. (1993). Clathrin assembly protein AP180: primary structure, domain organization and identification of a clathrin binding site. EMBO J. *12*, 667–675.

Nathke, I.S., Heuser, J., Lupas, A., Stock, J., Turck, C.W., and Brodsky, F.M. (1992). Folding and trimerization of clathrin subunits at the triskelion hub. Cell *68*, 899–910.

Oh, P., McIntosh, D.P., and Schnitzer, J.E. (1998). Dynamin at the neck of caveolae mediates their budding to form transport vesicles by GTP-driven fission from the plasma membrane of endothelium. J. Cell Biol. *141*, 101–114.

Orci, L., Glick, B.S., and Rothman, J.E. (1986). A new type of coated vesicular carrier that appears not to contain clathrin: its possible role in protein transport within the Golgi stack. Cell *46*, 171–184.

Pearse, B.M., and Robinson, M.S. (1990). Clathrin, adaptors, and sorting. Annu. Rev. Cell. Biol. *6*, 151–171.

Ramjaun, A.R., Micheva, K.D., Bouchelet, I., and McPherson, P.S. (1997). Identification and characterization of a nerve terminal-enriched amphiphysin isoform. J. Biol. Chem. *272*, 16700–16706.

Rapaport, I., Miyazaki, M., Boll, W., Duckworth, B., Cantley, L.C., Shoelson, S., and Kirchhausen, T. (1997). Regulatory interactions in the recognition of endocytic sorting signals by AP-2 complexes. EMBO J. *16*, 2240–2250.

Reeves, J.P., and Dowben, R.M. (1969). Formation and properties of thin-walled phospholipid vesicles. J. Cell. Physiol. *73*, 49–60.

Robinson, M.S. (1994). The role of clathrin, adaptors and dynamin in endocytosis. Curr. Opin. Cell Biol. *6*, 538–544.

Rothman, J.E. (1994). Mechanisms of intracellular protein transport. Nature *372*, 55–63.

Schekman, R., and Orci, L. (1996). Coat proteins and vesicle budding. Science *271*, 1526–1533.

Schmid, S.L. (1993). Coated-vesicle formation in-vitro conflicting results using defferent assays. Trends Cell Biol. *3*, 145–148.

Schmid, S.L., and Carter, L.L. (1990). ATP is required for receptor-mediated endocytosis in intact cells. J. Cell Biol. *111*, 2307–2318.

Slot, J.W., and Geuze, H.J. (1985). A new method of preparing gold probes for multiple-labeling cytochemistry. Eur. J. Cell Biol. *38*, 87–93.

Sulpice, J.C., Zachowski, A., Devaux, P.F., and Giraud, F. (1994). Requirement for phosphatidylinositol 4,5-bisphosphate in the Ca(2+)- induced phospholipid redistribution in the human erythrocyte membrane. J. Biol. Chem. *269*, 6347–6354.

Sweitzer, S.M., and Hinshaw, J.E. (1998). Dynamin undergoes a GTP-dependent conformational change causing vesiculation. Cell *93*, 1021–1029.

Takei, K., McPherson, P.S., Schmid, S.L., and De Camilli, P. (1995). Tubular membrane invaginations coated by dynamin rings are induced by GTP-gamma S in nerve terminals. Nature *374*, 186–190.

Takei, K., Mundigl, O., Daniell, L., and De Camilli, P. (1996). The synaptic vesicle cycle: a single vesicle budding step involving clathrin and dynamin. J. Cell Biol. *133*, 1237–1250.

Tuma, P.L., Stachniak, M.C., and Collins, C.A. (1993). Activation of dynamin GTPase by acidic phospholipids and endogenous rat brain vesicles. J. Biol. Chem. *268*, 17240–17246.

Urrutia, R., Henley, J.R., Cook, T., and McNiven, M.A. (1997). The dynamins: redundant or distinct functions for an expanding family of related GTPases? Proc. Natl. Acad. Sci. USA *94*, 377–384.

Wang, L.H., Sudhof, T.C., and Anderson, R.G. (1995). The appendage domain of alpha-adaptin is a high affinity binding site for dynamin. J. Biol. Chem. *270*, 10079–10083.

Wigge, P., Kohler, K., Vallis, Y., Doyle, C.A., Owen, D., Hunt, S.P., and McMahon, H.T. (1997). Amphiphysin heterodimers: potential role in clathrin-mediated endocytosis. Mol. Biol. Cell *8*, 2003–2015.

Willingham, M.C., and Pastan, I. (1983). Formation of receptosomes from plasma membrane coated pits during endocytosis: analysis by serial sections with improved membrane labeling and preservation techniques. Proc. Natl. Acad. Sci. USA *80*, 5617–5621.

Ye, W., and Lafer, E.M. (1991). Clathrin binding and assembly activities of expressed domains of the synapse-specific clathrin assembly protein AP-3. J. Biol. Chem. *266*, 4442–4447.

Ye, W., Ali, N., Bembenek, M.E., Shears, S.B., and Lafer, E.M. (1995). Inhibition of clathrin assembly by high affinity binding of specific inositol polyphosphates to the synapse-specific clathrin assembly protein AP-3. J. Biol. Chem. *270*, 1564–1568.

Zaremba, S., and Keen, J.H. (1983). Assembly polypeptides from coated vesicles mediate reassembly of unique clathrin coats. J. Cell Biol. *97*, 1339–1347.

Zhang, J.Z., Davletov, B.A., Sudhof, T.C., and Anderson, R.G. (1994). Synaptotagmin I is a high affinity receptor for clathrin AP-2: implications for membrane recycling. Cell *78*, 751–760.

The American Society for Cell Biology

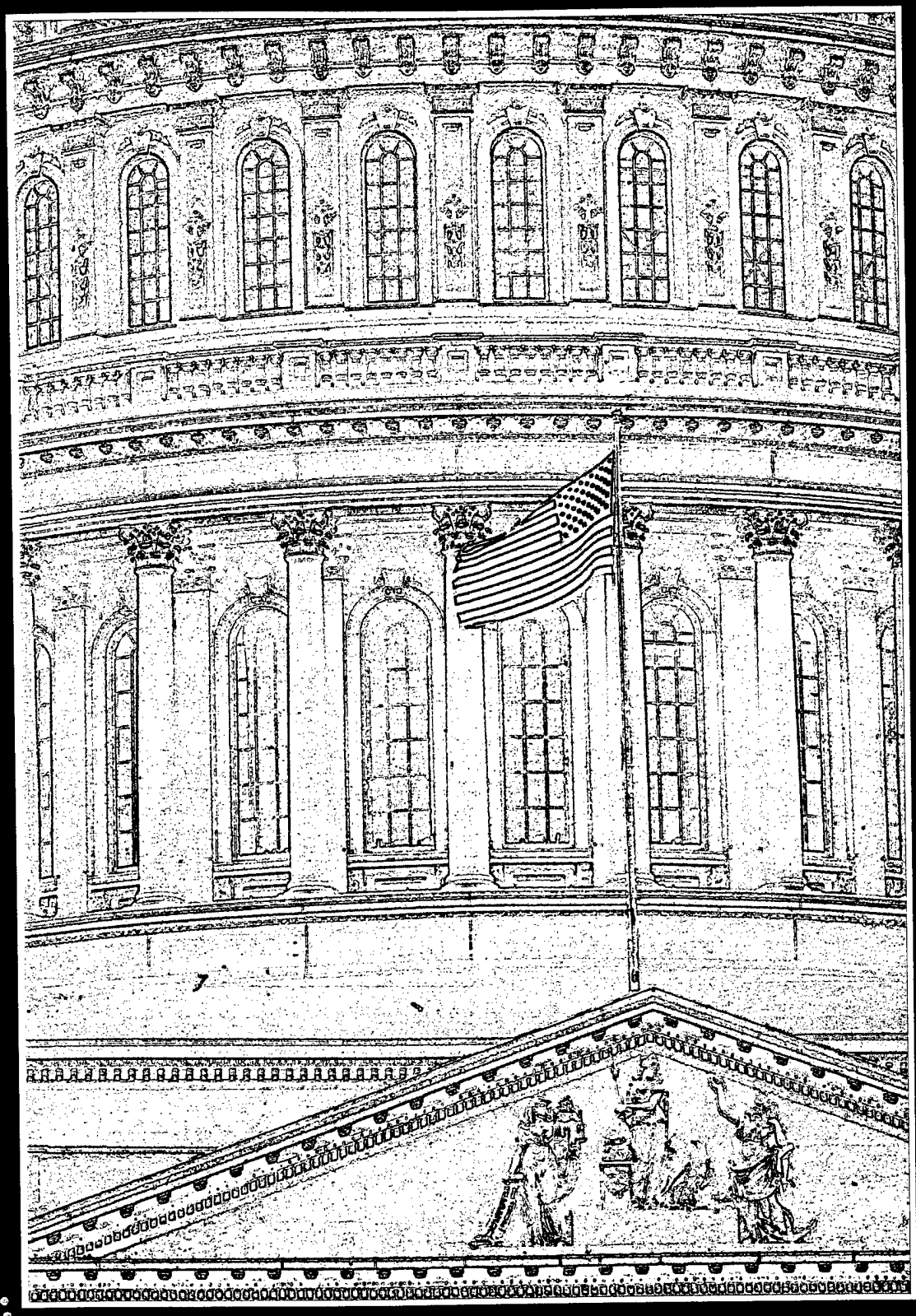

37th Annual Meeting

DECEMBER 13-17, 1997 ■ WASHINGTON, D.C.

Program

774 *

INDUCTION OF TYROSINE PHOSPHORYLATION AND Na+/H+ EXCHANGER ACTIVATION DURING SHRINKAGE OF HUMAN NEUTROPHILS ((E. Krump, K. Nikitas, and S. Grinstein.)) Division of Cell Biology, Research Institute, the Hospital for Sick Children, Toronto, On., Canada.

The Na+/H+ exchanger (NHE1) is essential for the regulation of cell volume. The underlying molecular mechanism is poorly understood and was studied in polymorphonuclear leukocytes (PMN). Suspension of PMN in hypertonic media induced rapid cellular shrinkage and activation of NHE1. Hypertonicity also induced extensive tyrosine phosphorylation of several proteins. Pretreatment of PMN with genistein, a tyrosine kinase inhibitor, prevented the tyrosine phosphorylation and also the activation of NHE1. The signal elicited by hyperosmolarity that induces activation of tyrosine kinases and NHE1 was investigated. Methods were devised to change medium osmolarity without altering cell volume and vice versa. Increasing medium and intracellular osmolarity in normovolemic cells failed to activate tyrosine kinases or NHE1. However, shrinkage of cells under isoosmotic conditions stimulated both tyrosine phosphorylation and NHE1 activity. These findings imply that cells detect alterations in cell size, but not changes in osmolarity or ionic strength. The proteins that were tyrosine phosphorylated in response to cell shrinkage were also investigated and found not to be the mitogen-activated protein kinases SAPK, p38, erk1, and erk2. In contrast, the tyrosine kinases $p59^{fgr}$ and $p56/59^{hck}$ were phosphorylated and activated upon hypertonic challenge. We propose that cells respond to alterations in cell size, but not to changes in osmolarity, with increased tyrosine phosphorylation, which in turn leads to the activation of NHE1. The resulting changes in ion content and pH contribute to the restoration of cell volume.

Oncogenes and Tumor Suppressors (775-778)

775

REDUCTION AND LOSS OF EXPRESSION OF THE TIGHT JUNCTION MAGUK ZO-1 IN BREAST CANCER ((Kevin Hoover[1], Dean Stathakis[1] Hoda Anton-Culver [2], Peter J. Bryant[1].)) [1]Department of Developmental and Cell Biology and [2]Department of Medicine, University of California, Irvine, CA 92697. (Sponsored by KB Hoover)

Membrane-associated guanylate kinase homologs (MAGUKs) may play a role in cellular functions required to prevent tumorigenesis, as indicated by the neoplastic phenotype caused by loss of the Drosophila MAGUK Dlg. We examined expression of the tight-junction MAGUK ZO-1 in paraffin-embedded breast cancer samples, using immunohistochemistry and confocal microscopy. Over 66% of the tumors analysed (n=30) showed a reduction or loss of ZO-1 expression. Expression was reduced or lost in 40% of well differentiated tumors (n=5), 100% of moderately differentiated tumors (n=7), and 87.5% of poorly differentiated tumors (n=8). Expression of ZO-1 was closely correlated with glandular differentiation of the tumors. Loss of heterozygosity of the polymorphic marker D15S1019, within 1.0 Mb of ZO-1, in 3 of 7 informative tumors suggests that a genetic mechanism may be responsible for at least some cases of lost ZO-1 expression.

776

A SUBSET OF BREAST CANCERS EXHIBITS ENHANCED EXPRESSION OF AMPHIPHYSIN I, AN AUTOANTIGEN OF PARANEOPLASTIC NEUROLOGICAL SYNDROMES. (([1]Scott Floyd, [1]Margaret H. Butler, [1]Ottavio Cremona, [1]Carol David, [1]Zachary Freyberg, [1]Anna Zhang, [2]Michele Solimena, [3]Akira Tokunaga, [3]Hideki Ishizu, [3]Kimiko Tsutsui , and [1]Pietro De Camilli)) [1]Howard Hughes Medical Institute and Department of Cell Biology and [2]Department of Medicine, Yale University School of Medicine, 295 Congress Ave., New Haven CT, 06510; [3] Third Department of Anatomy, Okayama University Medical School, 2-5-1 Shikata-cho, Okayama 700, Japan.

Amphiphysin I is the dominant autoantigen in patients with breast cancer and neurological symptoms characteristic of Stiff-Man syndrome as well as in other paraneoplastic autoimmune disorders. Amphiphysin I is an SH3 domain containing protein expressed at high levels in neurons and concentrated in nerve terminals where it has a putative role in the clathrin dependent endocytosis of synaptic vesicles via its interactions with dynamin, synaptojanin, and AP2. We have now found that low levels of amphiphysin I are expressed in all of a variety of tissues tested, including normal breast tissue. Furthermore, we report that expression of amphiphysin I was enhanced in several human breast tumors including the tumor of a patient with paraneoplastic sensory neuropathy and anti-amphiphysin I autoimmunity. Amphiphysin I expression was also enhanced in 2/8 human breast cell lines. The isoform of amphiphysin I most frequently observed in breast cancer migrates at 108 kDa in SDS-PAGE and corresponds to a band present in a number of non-neuronal tissues. The expression of this band correlates with the expression of an alternatively spliced variant of amphiphysin I mRNA missing a 126 base pair insert. Although human autoantibodies are primarily directed against the COOH-terminal region of the amphiphysin I, only 3 of 28 monoclonal antibodies raised against amphiphysin I recognize this region, demonstrating that this is not the immunodominant region. These findings provide a direct link between amphiphysin I expression and autoimmunity and raise the possibility that amphiphysin I may be implicated in the biology of breast cancer.

777

IDENTIFICATION OF AN ADHESION-ASSOCIATED TYROSINE KINASE THAT IS TIGHTLY REGULATED IN BREAST CANCER ((Nicole Dodge Zantek and Michael S. Kinch.)) Department of Basic Medical Sciences, Purdue University, West Lafayette, IN 47907-1246

Changes in protein tyrosine phosphorylation and cell adhesion play an important role in cancer progression. While sites of cell adhesion are the primary localization of tyrosine phosphorylated proteins, only a few of these proteins have been identified to date. To identify new proteins, we utilized an innovative new approach to generate monoclonal antibodies. We selected for tyrosine phosphorylated proteins enriched within sites of cell adhesion in human breast cancer cells. This allowed us to generated as many as 430 different antibodies for specific proteins within focal adhesions or adherens junctions. One antibody, D7, recognizes a 130kDa tyrosine phosphorylated protein found in cell-cell junctions. *In vitro* kinase assays with immunoprecipitated material reveal potent tyrosine kinase activity. D7 is not found within cell-cell junctions of Ras-transformed cells and is not tyrosine phsophorylated. Moreover, expression of the D7 protein is completely absent in breast cancer cells, but is expressed in some other carcinomas. The function of D7 thus can be regulated by changes in its phosphorylation, localization or expression. This suggests that D7 is a tumor suppressor and a sensitive new marker for breast cancer progression. *This work was supported by grants from the American Cancer Society (MSK) and Howard Hughes Medical Institute (NDZ).*

778

A NOVEL GENE LOST WHEN HUMAN BREAST CELLS BECOME MALIGNANT IS REEXPRESSED IN REVERTED CELLS ((H-M Chen[1], OW Petersen[2] and MJ Bissell[1].)) [1]Berkeley Lab, Berkeley, CA [2]The Panum Institute, Copenhagen, Denmark

A human breast cancer progression series HMT3522 was developed by Briand et al. (Can. Res.56:2039,1996) from nonmalignant epithelial (S1) cells by EGF deprivation giving rise to premalignant (S2) and tumor (T4) cells. To isolate possible "oncogenes" or "suppressor genes", expression patterns of S2 and T4 cells were compared with differential display-PCR technique. A novel gene tentatively named AZ-1 was isolated. The level of a predominant 4.4-kb AZ-1 transcript was significantly lowered in T4 compared to S2 cells cultured either on tissue culture plastic or embedded in 3-dimensional (3-D) basement membrane matrix. AZ-1 was present in S1 cells, secondary human breast epithelial cells and organoids, and various tissues including brain, lung, and kidney. In contrast, expression of AZ-1 gene was drastically repressed in ten human breast epithelial cancer cell lines. Modulation of AZ-1 gene expression by phenotypic alteration of tumor cells was examined in a tumor reversion system described recently in our laboratory (Weaver et al., JCB 137:231, 1997). Briefly, when T4 cells were cultured in the presence of inhibitory β1-integrin antibody in a 3-D assay system, they reverted morphologically to S1-like cells. AZ-1 gene was up-regulated in the reverted T4 cells to a level reminiscent of that seen in the S1 cells. While the function of the AZ-1 gene remains to be determined, based on the inverse relationship of the expression of AZ-1 and tumor phenotype, AZ-1 gene may serve as a molecular marker to detect early oncogenesis of human breast cancer (Supported by DOE contract DE-AC03-76SF00098, DOD grant MM4558G9E and NIH grant CA64786)

***Author(s) and/or presenter(s) have noted that there is a potential conflict of interest.**

Specificity in Signal Transduction

Organizers: Norbert Perrimon and Tony J. Pawson

Sponsored by The Director's Sponsor Fund

Oncogene Networks in Signal Transduction

Organizers: Jacalyn H. Pierce, George F. Vande Woude and J. Silvio Gutkind

Sponsored by Parke-Davis/Warner-Lambert and The Director's Sponsor Fund

Keystone, Colorado • April 9 - 14, 1999

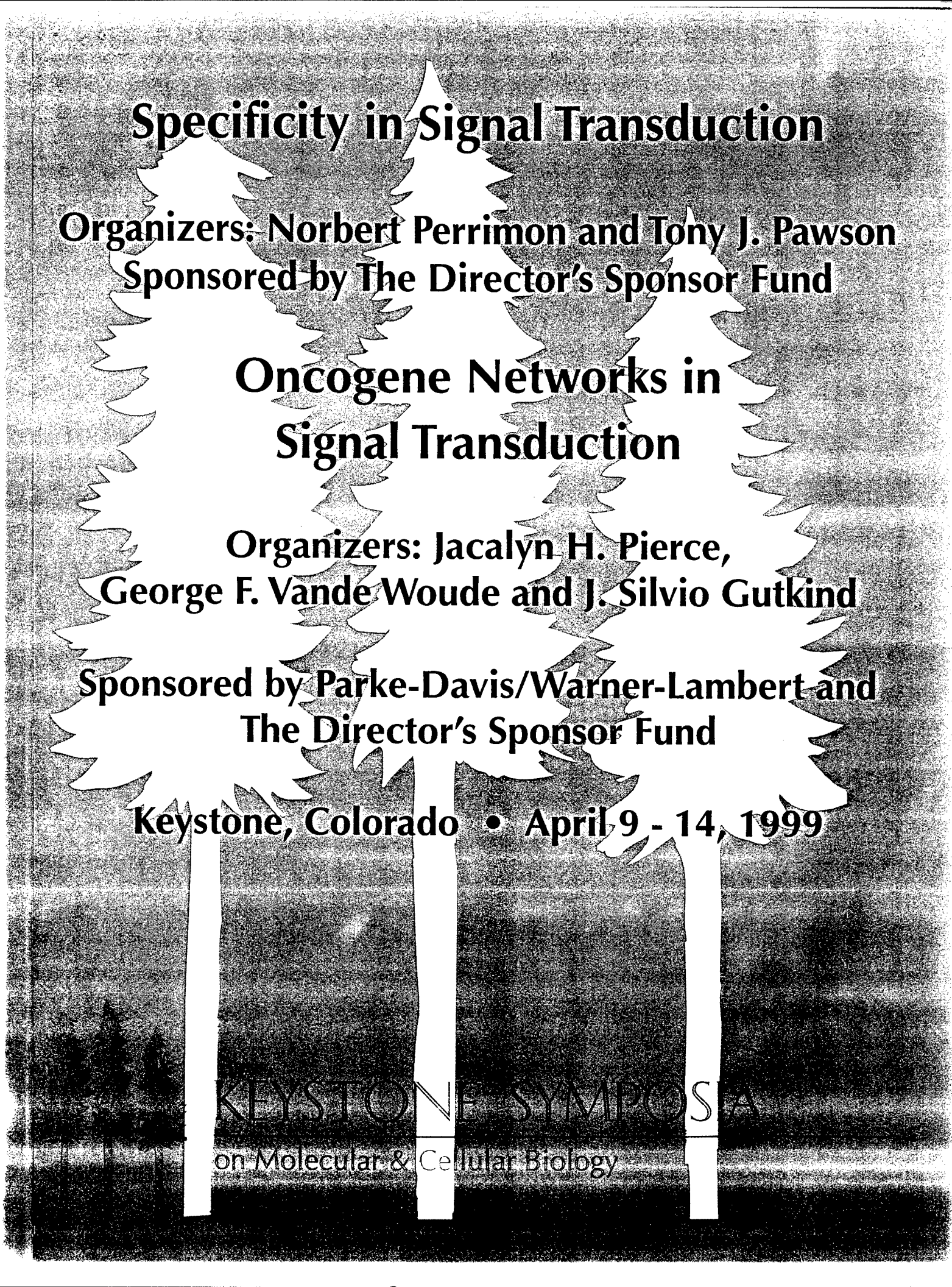

KEYSTONE SYMPOSIA

on Molecular & Cellular Biology

1009 Ceramide Participates in Endothelial Anoikis

A. Erdreich-Epstein[†], H. Shimada[‡], S. Groshen[§], L.S. Metelitsa[#], R.C. Seeger[#], and D.L. Durden[†]. From the Neil Bogart Memorial Laboratories, Div. Hematology-Oncology[†], Dept. Pediatrics and Dept. Pathology[‡], Childrens Hospital Los Angeles, USC School of Medicine, LA, CA 90027, Dept. Preventive Medicine[§], USC School of Medicine, and Children's Cancer Group, Arcadia, CA 91066.

Integrins $\alpha_v\beta_3$ and $\alpha_v\beta_5$ are crucial to angiogenesis. Their inhibition leads to endothelial detachment and apoptosis (anoikis), and to disruption of tumor vasculature and its growth. When bovine brain endothelial cells (BBEC) were suspended on a BSA-coated surface, ceramide, a lipid second messenger which increases following several apoptotic signals, was elevated by up to 50% compared to control cells allowed to attach and spread on vitronectin or fibronectin. Ceramide also increased in BBEC exposed to the RGD-blocking peptide, RGDfV, which inhibited attachment to vitronectin and fibronectin by specific inhibition of integrins $\alpha_v\beta_3$ and $\alpha_v\beta_5$, but did not increase with the control peptide, RADfV. Furthermore, C_2-ceramide, a cell-permeable synthetic ceramide, induced dose-dependent cell death in BBEC, with apoptotic features as determined by Annexin-V staining and DNA laddering. During this process, JNK, a MAPK involved in apoptosis signaling pathways, was activated in response to C_2-ceramide. These data indicate that ceramide may play a key role in endothelial cell anoikis resulting from inhibition of integrin $\alpha_v\beta_3/\alpha_v\beta_5$ signaling. Finally, a total 39 cases of human neuroblastoma (NB), a retinoid responsive pediatric tumor, was examined immunohistochemically for expression of these integrins: $\alpha_v\beta_3$ was expressed on 60% of the angiogenic vessels in high-risk NB (stage IV & MYCN-amplified stage III, n=27), but only on 18% of vessels in the low-risk tumors (stage I, II & MYCN non-amplified stage III, n=12). Integrin $\alpha_v\beta_5$ was also expressed on the angiogenic endothelium of the high-risk NB. This suggests that integrins $\alpha_v\beta_3$ and $\alpha_v\beta_5$ function in angiogenesis in human NB. These data provide the first evidence that ceramide functions in signaling pathways regulating integrin-dependent endothelial cell survival and apoptosis, and may thus provide a target for anti-angiogenic treatment.

Supported in part by NIH grants CA75637, CA60104, CA02649, and CA14089, grants from the Childrens Cancer Research Fund and the Concern Foundation, and the Neil Bogart Memorial Fund of the T.J. Martell Foundation for Leukemia, Cancer, and AIDS Research.

1010 Amphiphysin I is a Substrate for the p35/cdk5 Complex and Associates with p35 in Vitro and in Vivo.

Scott Floyd*, Vladimir Slepnev* , Li-Huei Tsai** and *Pietro De Camilli. *Department of Cell Biology, Yale University School of Medicine, New Haven, CT 06511, USA and **Department of Pathology, Harvard Medical School, Boston, MA 02115, USA.

Amphiphysin I is an SH3 domain containing phospho-protein which undergoes stimulation dependent dephosphorylation and is implicated in endocytosis of synaptic vesicles in neurons. Antisense knock-out of amphiphysin I in rat hippocampal neurons in culture showed a defect in neurite outgrowth. A yeast homologue of amphiphysin, Rvs167p, has been reported to associate with Pcl2p, an activator of the yeast cyclin dependent kinase Pho85p. Cdk5 is the mammalian homologue of Pho85p, but is active in post-mitotic neurons where it associates with the brain specific activator p35. Knockout mouse studies of cdk5 and p35 revealed a defect in neuron migration as well as neurite outgrowth.

Here, we show that amphiphysin I associates with p35 in vitro, and that amphiphysin I and p35 are present in the growth cones of rat hippocampal neurons in culture. We also show that amphiphysin I is a substrate for the kinase activity of the p35/cdk5 complex in vitro. We propose that the activity of cdk5 on amphiphysin I may be important for neurite outgrowth.

1011 Synthesis of D-4-phosphorylated-phosphoinositides by p85/p110 type PI-kinase

Makoto Funaki, Hideki Katagiri, Hiraku Ono, Masatoshi Kikuchi and Tomoichiro Asano, Tokyo, Japan

p85/p110 type PI-kinase, an enzye the activity of which is apparently enhanced by association with tyrosine-phosphorylated protein, is assumed to phosphorylate the D-3-position of the inositol ring of phosphoinositides. This PI-kinase phosphorylates the D-4 position with a similar or higher efficiency than the D-3 position when TCA-treated cell membrane is used as a substrate, although it phosphorylates almost exclusively the D-3 when purified phosphatidylinositol (PI) is used as a substrate. In fact, overexpression of p110 in Sf-9 or 3T3-L1 cells induced marked phosphorylation of the D-4 position to a level comparable to or much greater than that of D-3, while inhibition of endogenous p85/p110 type PI-kinase via overexpression of dominant negative p85α (Δp85α) in 3T3-L1 adipocytes abolished insulin-induced synthesis of both. Furthermore, overexpression of chimeric p110, whose lipid kinase domain is substituted with that of VPS34 or p170, another subfamily of PI 3-kinase, increased D-3- but not D-4-phosphorylated phosphoinositides, excluding the possibility that D-3-phosphorylated phosphoinositide produced by p110 activated unknown PI 4-kinases. Thus, p85/p110 type PI-kinase phosphorylates the D-4 position of phosphoinositides more efficiently than the D-3 position *in vivo*, and each of D-3- or D-4-phosphorylated phosphoinositides may transmit the signals to the downstream.

1012 A TrkA-selective, Fast Internalizing Nerve Growth Factor-Antibody Complex Induces Trophic but Not Neuritogenic Signals

M. Gagnon[†], H.U. Saragovi[†,¶], W. Zheng[†], S. Maliartchouk[†], G.M. DiGugliemo[§], Y.R. Mawal[†], S.B. Woo[*] and K.E. Neet[*]. †Department of Pharmacology and Therapeutics, ¶Oncology/Cancer Center and §Department of Cell Biology, McGill University, Montreal, PQ and *Department of Biological Chemistry, Finch University of Health Sciences/The Chicago Medical School, North Chicago, IL

Association of nerve growth factor (NGF) with an anti-NGF monoclonal antibody (mAb NGF30) targeted at the C termini of NGF creates a complex with binding and biological activity different of NGF. NGF•mAb retains high binding affinity to the TrkA receptor but does not interact with the $p75^{LNTR}$, indicating that the C termini of NGF may dock onto $p75^{LNTR}$ but not TrkA. Binding of NGF•mAb to TrkA leads to faster, more extensive internalization and transient kinetics of phosphorylation of TrkA and downstream signaling components (Shc and MAPK). There was no detectable SNT tyrosine phosphorylation or activation. Therefore, the altered signaling of NGF•mAb does not reduce the trophic functions of NGF in cell survival assays but abolishes its neuritogenic capabilities in differentiation assays. These results suggest that biological response modifiers of neurotrophins can afford ligands with selected activities. Supported by an MRCC grant to H.U.S.

APPENDIX B

Figures

FIGURE LEGENDS

Fig. 1. A pool of amphiphysin I exists in a complex with p35 in rat brain. Immunoprecipitate using anti-p35 antibodies (p35) or non-specific rabbit immunoglobulin (IgG) from rat brain extract Western blotted with anti-p35 (panel A) or anti-amphiphysin I antibodies (Panel B).

Fig. 2. Association of amphiphysin I with p35 is modulated by phosphorylation. Rat brain extract was either untreated (lanes a, d, e, h), treated under phosphorylating conditions (lanes b, f) or dephosphorylating conditions (lanes c, g) amphiphysin I and II were co-immunoprecipitated using anti-amphiphysin (mab3) or control (cdc2) antibodies. Material was then probed for co-immunoprecipitation of amphiphysin I and II (panel A) or p35 (panel B). Note molecular weight shift of amphiphysin I, II and p35 under phosphorylating conditions. Lane a: starting material, lanes b-d, unbound material, lanes e-h, bound material.

Fig. 3. The first 161 amino acids of Amphiphysin associate directly with p35 in-vitro. GST tagged fragments of overlapping fragments of amphiphysin I corresponding to the indicated amino acid numbers were incubated with radio labeled in-vitro translated p35 then isolated on glutathione sepharose beads. Panel A: the N-terminal 306 amino acids of amphiphysin were able to affinity purify p35 while neither the remaining C-terminal 600 amino acids nor GST alone purified p35. Panel B: Using the same technique, deletion constructs of the N-terminus of amphiphysin I were able to refine the binding site to the first 161 amino acids.

Fig. 4. Amphiphysin I colocalizes with p35 in ttransfected fibroblasts. CHO fibroblasts were stably transfected with the amphiphysin I gene in mammalian expression vector pcDNA3. These cells were then transfected with p35 also in pcDNA3, fixed with 4% paraformaldehyde and immuno stained for amphiphysin I and p35. Images were obtained by laser scanning confocal microscopy.

Fig. 5. Amphiphysin I is a substrate for the cdk5 kinase complex in vitro. Panel A: Immunoprecipitates from rat brain extract using non-specific rabbit IgG (lanes a, b) or anti-p35 antibodies (lanes c-h) were combined with purified recombinant histone H1 or amphiphysin I. These mixtures were combined with radiolabeled ATP, incubated, separated by SDS-PAGE and exposed to film. Histone H1 (lane c), full length amphiphysin I (lane d), and fragments corresponding to amino acids 1-306 (lane e) and 262-435 (lane f) show incorporation of radiolabeled phosphate. Panel B: Amino acid sequence of phosphorylated region from Panel A with arrows to indicate consensus sequences for cdk5.

Fig. 6. Generation of amphiphysin I knock-out mice. The exon containing the first codon for the amphiphysin I gene was isolated by screening a mouse genomic library with sequential rounds of hybridization with amphiphysin specific DNA probes. A neomycin cassette was inserted in this exon and assembled into a vector for transfection into mouse embryonic stem cells. These cells were then screened for homologous recombination by Southern blotting of an Eco RI digest of genomic DNA with an amphiphysin specific probe as shown in left hand panel. Chimeric mice were generated by injecting recombinant cells into mouse embryos at the blastocyst stage and implantation in pseudo-pregnant foster females. Chimeric mice were then crossed with C57 black 6 mice to obtain heterozygous (F1) and homozygous (F2) knock-out mice. Presence of the mutant allele in homozygous and heterozygous mice is demonstrated by Southern blot of an Eco RI digest of genomic DNA with an amphiphysin specific probe.

Fig. 7. Amphiphysin is not expressed in knock-out mice. Western blot of homogenates of brain and muscle tissue from amphiphysin homozygous knock-out and litter-matched wild type controls with anti-amphiphysin I and amphiphysin II antibodies.

Fig. 1

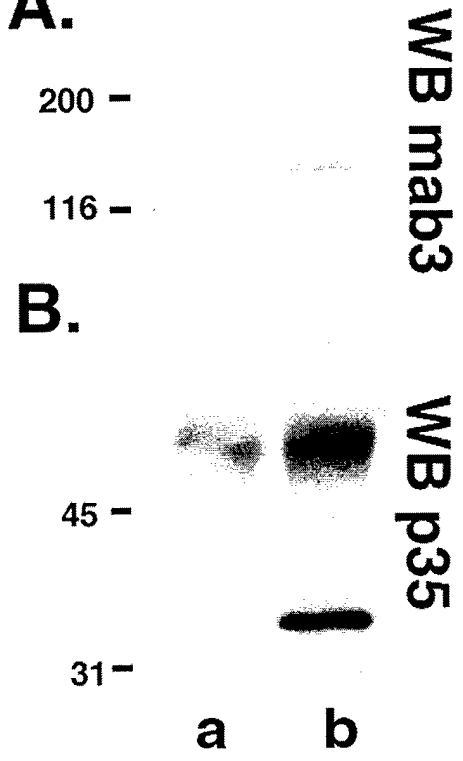

Fig. 2

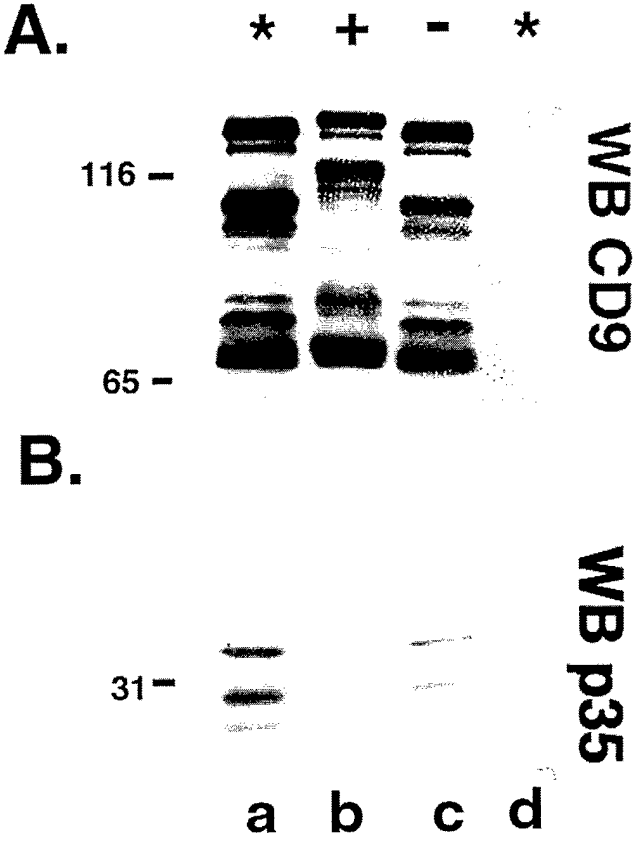

Fig. 3

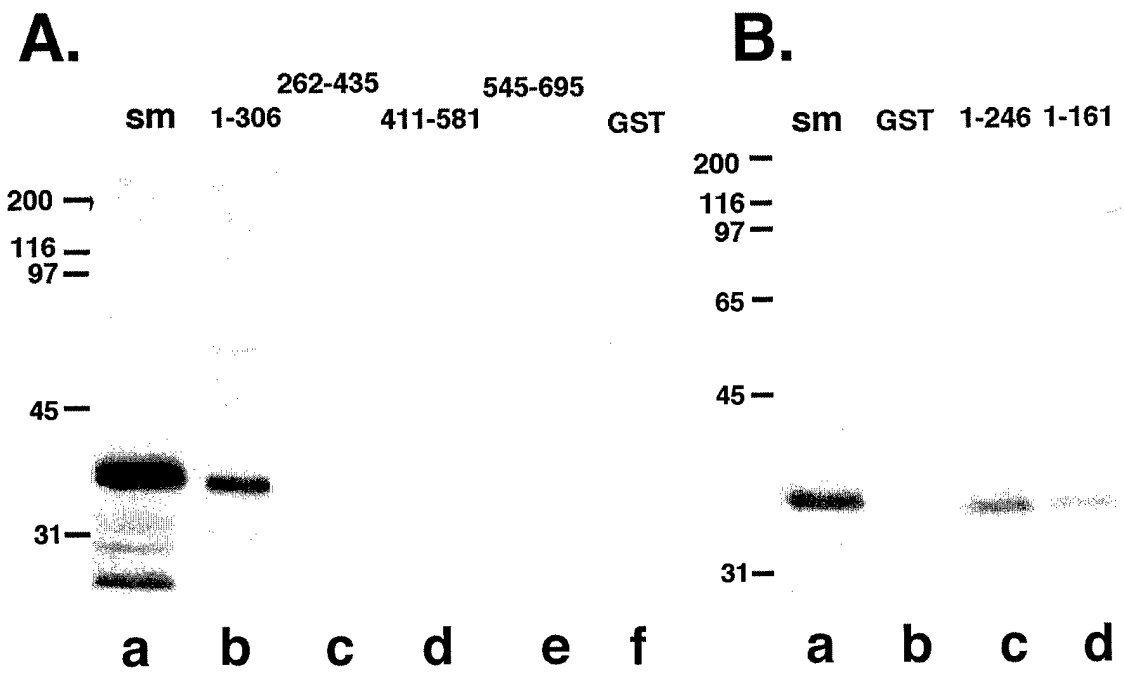
A.
sm
1-306
262-435
411-581
545-695
GST
200
116
97
45
31
a
b
c
d
e
f
B.
sm
GST
1-246
1-161
200
116
97
65
45
31
a
b
c
d

Fig. 4

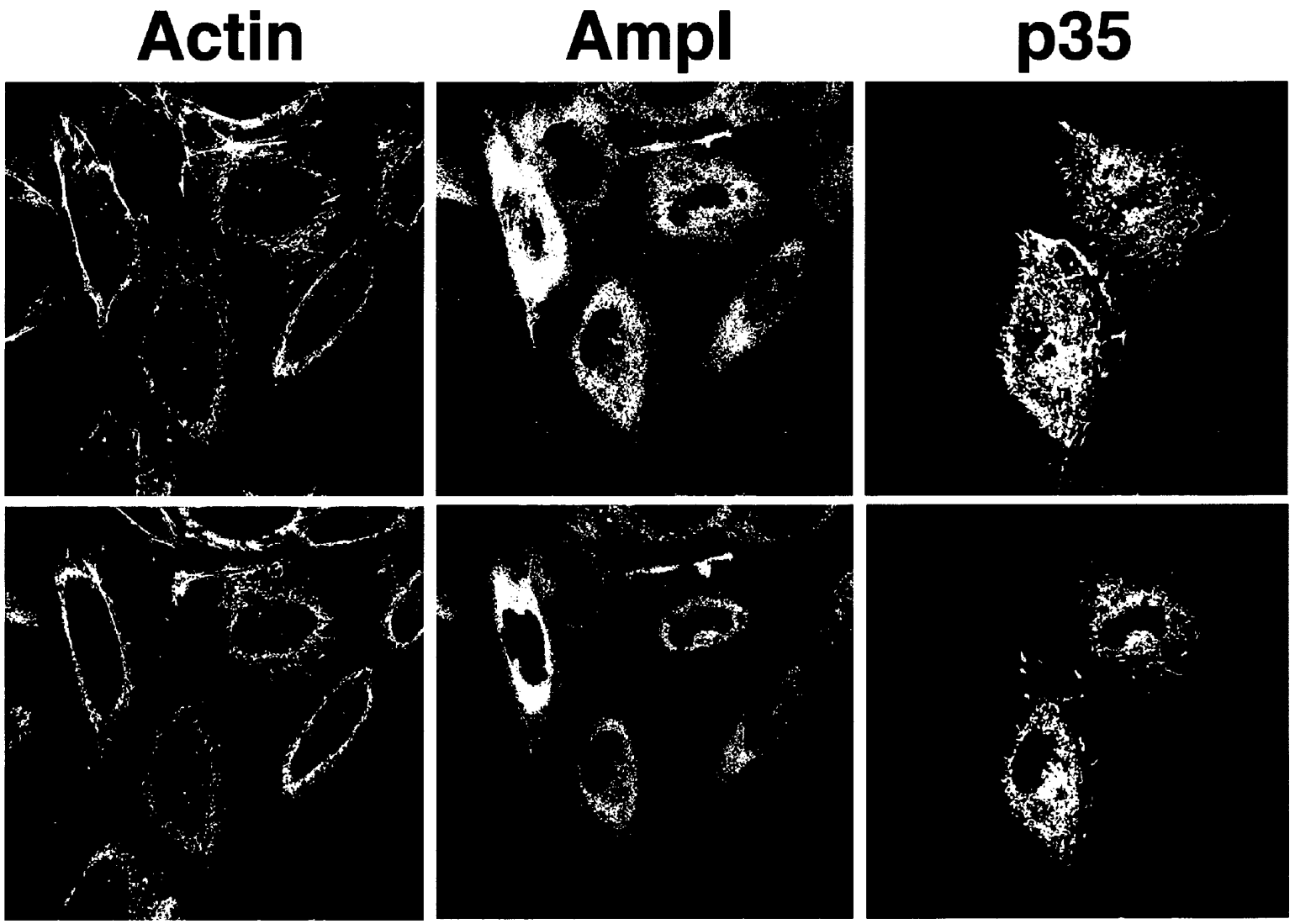

Fig. 5

A.

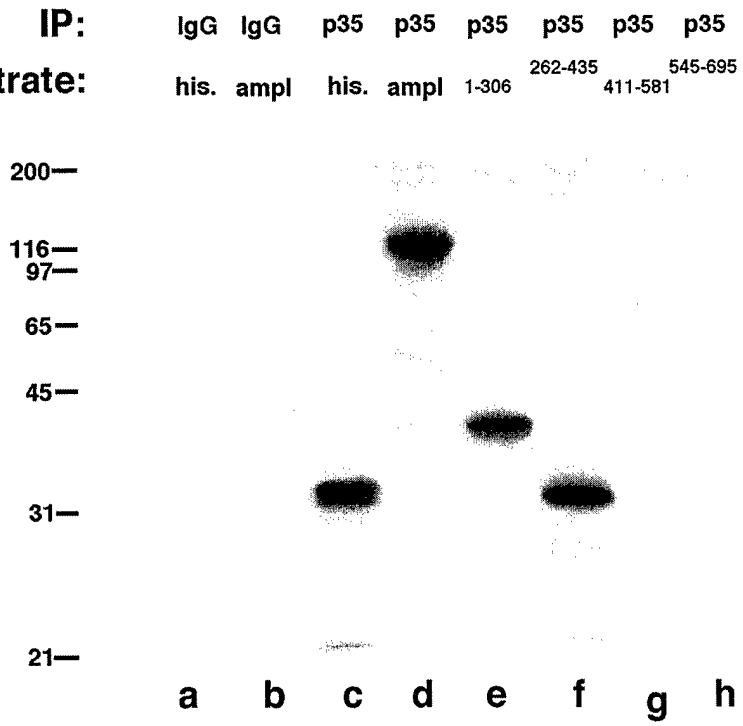
IP:
IgG IgG p35 p35 p35 p35 p35 p35
Substrate:
his. ampl his. ampl 1-306 262-435 411-581 545-695
200
116
97
65
45
31
21
a b c d e f g h

B.


PLRIAKTPSPPEEPSPLPSPTASPNHTLAPASPAPARPRSPSQTRKGPPVPPLPKVTPTKELQQENI
a.a. 254
a.a. 320

Fig. 7

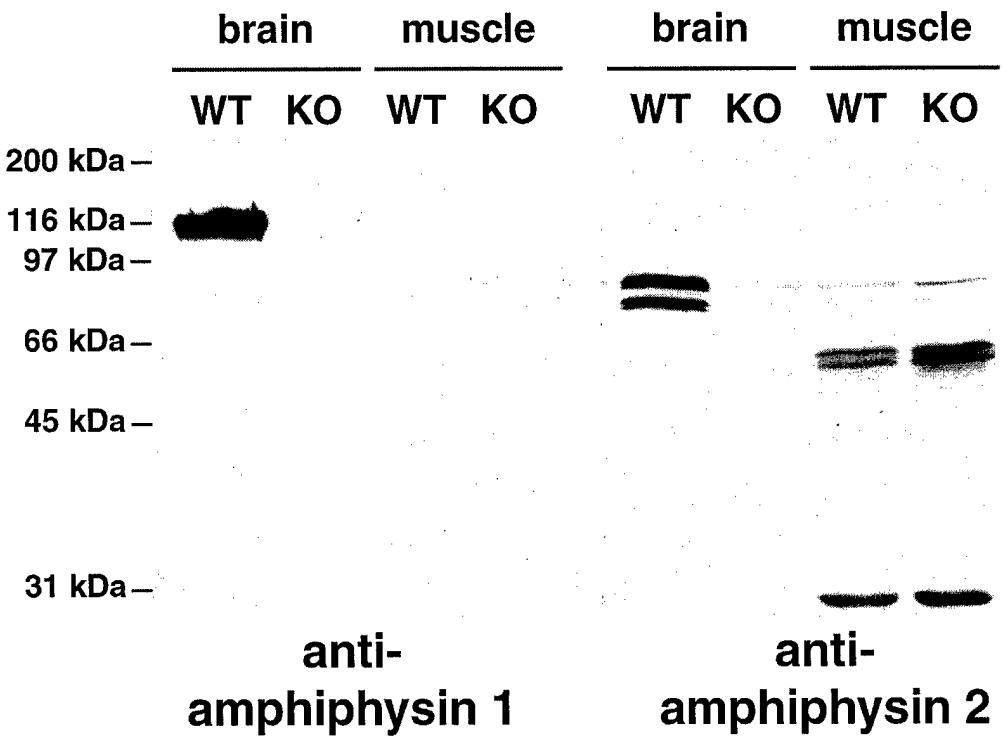
brain
muscle
brain
muscle
WT KO WT KO WT KO WT KO
200 kDa
116 kDa
97 kDa
66 kDa
45 kDa
31 kDa
anti-
amphiphysin 1
anti-
amphiphysin 2

Fig. 6